

Synthesis, Spectroscopic Characterization, X-ray
Structure and Preliminary Evaluation of DNA Binding
Parameters of Organotin(IV) Dithiocarboxylates



A Thesis Submitted to the Department of Chemistry,
Quaid-i-Azam University, Islamabad, in partial fulfillment of
the requirement for the degree of

Doctor of Philosophy

in

Inorganic/Analytical Chemistry

by

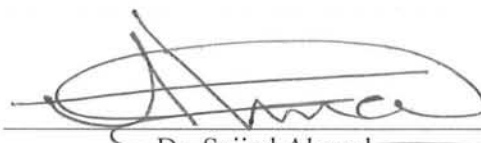
Zia-ur-Rehman

Department of Chemistry
Quaid-i-Azam University
Islamabad, Pakistan
(2009)

DECLARATION

This is to certify that this dissertation entitled "*Synthesis, Spectroscopic Characterization, X-ray Structure and Preliminary Evaluation of DNA Binding Parameters of Organic(IV) Dithiocarbonylates*" submitted by Mr. Zia-ur-Rehman is accepted in its present form by the Department of Chemistry, Quaid-i-Azam University, Islamabad, Pakistan, as satisfying the partial requirement for the degree of *Doctor of Philosophy* in *Inorganic/Analytical Chemistry*.

External Examiner(1):



Dr. Sajjad Ahmad
PSO, Metallurgy Division
Dr. A.Q. Khan Research Labs
P.O. Box 502, Islamabad

External Examiner(2):



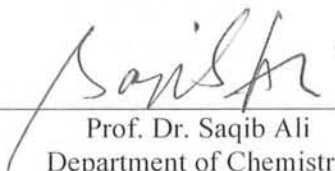
Dr. M. Aziz Chaudhary
Associate Professor
Department of Chemistry
AJK University, Muzaffarabad

Head of Section:



Prof. Dr. M. Mazhar
Department of Chemistry
Quaid-i-Azam University
Islamabad

Supervisor:



Prof. Dr. Saqib Ali
Department of Chemistry
Quaid-i-Azam University
Islamabad

Chairman:



Prof. Dr. S. Sakawat Shah
Department of Chemistry
Quaid-i-Azam University
Islamabad



Dedicated

to

Humanity

CONTENTS

<i>Acknowledgements</i>	i
<i>Abstract</i>	iii
<i>List of Tables</i>	v
<i>List of Figures</i>	ix
Chapter 1 Introduction	1-39
1.1 Tin-Metal	1
1.1.1 General Description	1
1.1.2 Properties of Tin	2
1.2 Organotin Compounds	3
1.3 Principal coordination geometries at the tin centre in organotin compounds	4
1.4 Organotin(IV) dithiocarboxylates	5
1.4.1 Methods of preparation	5
1.5 Structural chemistry of Organotin(IV) dithiocarboxylates	6
1.5.1 Triorganotin(IV) dithiocarboxylates structures	6
1.5.2 Chlorodiorganotin(IV) dithiocarboxylates structures	11
1.5.3 Diorganotin(IV) dithiocarboxylates structures	15
1.6 Biological activities of organotin(IV) dithiocarboxylates	27
1.6.1 Anti-tumor activity	27
1.6.2 Antifungal and antibacterial activities	29
1.6.3 Insecticidal activity	30
1.7 Organotin(IV) dithiocarboxylates as synthetic precursors for Tin-Sulfides	30
References	32-38

Chapter 2	Experimental	39-61
2.1	Chemicals	39
2.2	Instrumentation	39
2.3	General procedure for the synthesis of ligand salts	40
2.4	General procedure for the synthesis of triorganotin(IV) dithio-carboxylates	41
2.5	General procedure for the synthesis of chlorodiorganotin(IV) dithiocarboxylates	42
2.6	General procedure for the synthesis of diorganotin(IV) dithio-carboxylates	43
2.7	Biological Studies	59
	2.7.1 DNA binding studies	59
	2.7.2 Antibacterial Activity	59
	2.7.3 Antifungal Activity	59
	References	61
Chapter 3	Results and Discussion	62-131
3.1	Synthesis of organotin(IV) dithiocarboxylates	62
3.2	Raman spectra	62
3.3	Infrared spectra	63
3.4	¹ H-NMR spectra	63
3.5	¹³ C-NMR spectra	71
3.6	¹¹⁹ Sn-NMR spectra	71
3.7	Mass spectrometry	81
3.8	Evaluation of DNA binding parameters	86
	3.8.1 Evaluation of DNA binding parameters of triorganotin(IV) dithiocarboxylates	86

3.8.1.1	Cyclic voltammetry of compounds 1, 2 and 4 and their DNA adduct	86
3.8.1.2	Electronic absorption spectra of compounds 1, 2 and 4 and their DNA adduct	88
3.8.2	Evaluation of DNA binding parameters of chlorodiorganotin(IV) and diorganotin (IV) dithiocarboxylates	102
3.8.2.1	Cyclic voltammetry of compounds 5, 7 and 12 and their DNA adduct	102
3.8.2.2	UV-Vis spectroscopy of compounds 5, 7 and 12 and their DNA adduct	107
3.9	Antibacterial activity	117
3.10	Antifungal activity	117
	References	130,131
Chapter 4	Crystallographic analysis	132-196
4.1	X-ray structure of Ph_3SnL (4)	132
4.2	X-ray structure of $n\text{-Bu}_2\text{SnCIL}$ (5)	136
4.3	X-ray structure of Et_2SnCIL (7)	140
4.4	X-ray structure of $\text{Ph}_3\text{SnL}^{\text{a}}$ (16)	144
4.5	X-ray structure of $n\text{-Bu}_2\text{SnL}_2^{\text{a}}$ (18)	148
4.6	X-ray structure of $\text{Et}_2\text{SnCIL}^{\text{a}}$ (19)	152
4.7	X-ray structure of $\text{Me}_2\text{SnCIL}^{\text{a}}$ (21)	156
4.8	X-ray structure of $\text{Ph}_3\text{SnL}^{\text{b}}$ (28)	160
4.9	X-ray structure of $n\text{-Bu}_2\text{SnL}_2^{\text{b}}$ (30)	164
4.10	X-ray structure of $n\text{-Bu}_2\text{SnCIL}^{\text{c}}$ (41)	168
4.11	X-ray structure of $\text{Et}_2\text{SnCIL}^{\text{c}}$ (43)	172
4.12	X-ray structure of $\text{Cy}_3\text{SnL}^{\text{d}}$ (50)	176
4.13	X-ray structure of $\text{Ph}_3\text{SnL}^{\text{d}}$ (52)	180
4.14	X-ray structure of $n\text{-Bu}_2\text{SnL}_2^{\text{d}}$ (54)	184

4.15	X-ray structure of $\text{Me}_2\text{SnCIL}^{\text{d}}$ (57)	188
4.16	X-ray structure of $\text{Me}_2\text{SnL}_2^{\text{d}}$ (58)	192
	References	196
	Conclusions	197, 198
	Publications list	199, 200

ACKNOWLEDGEMENTS

I owe my profound thanks and deepest sense of gratitude to Almighty **ALLAH**, Who blessed me with fortitude, potential and capability to complete my Ph. D work.

I wish to express fervent sense of thankfulness to my affectionate supervisor, **Prof. Saqib Ali**, Department of Chemistry, Quaid-i-Azam University, Islamabad, for his wholehearted interest and dedicated supervision. His inspiring guidance, valuable suggestions, energizing encouragement, generous help, good manners and friendly behavior make me possible to accomplish this tough task.

I am highly indebted to pay my cordial gratitude to **Prof. Ian S Butler** of Department of chemistry, University of McGill, Canada, for his mammoth help, cooperation and for accommodating me in his Lab. for the span of six months. I also acknowledge the valuable discussion of **Prof. Ivor Wharf** (retired) of the same department. Many thanks to crystallographer, **Dr. A. Meetsma**, of Crystal Structure Centre, Chemical Physics Zernike Institute for Advance Material, University of Groningen, The Netherlands for single crystal analysis (data collection, structure solution and structure analysis) and fruitful collaboration.

I am highly appreciated **Prof. Dr. S. Sakhawat Shah**, Chairman, Department of Chemistry, Quaid-i-Azam University, Islamabad, for providing Lab. facilities during research work. **Prof. Amin Badshah** and **Prof. M. Mazhar**, from the same Department are highly acknowledged due to their friendly behavior, cheering attitude and fruitful discussion.

Mrs. Mirela M. Barsan, **Mr. Ezzat Khan** and **Mr. Muhammad Altaf** are appreciated for lend a hand in Raman, NMR and single crystal analysis, respectively. For covering the biological aspects of present study, the cooperation of **Mr. Afzal shah**, **Dr. Rumana Qureshi** for DNA interaction study and **Mr. Momin Khan** for antimicrobial activities is praiseworthy. I am thankful to **Dr. Din Mohammad** for thesis corrections.

A special word of gratitude is due to **Mr. Shaukat Shuja**, **Mr. Aziz-ur-Rehman**, **Mr. M. Hanif**, **Mr. Hafiz Niaz Muhammad**, **Mr. Mukhtiar Hussain** and to all my friends specially **Mr. Hazir Ullah**, **Mr. Gul Shahzada** and **Mr. Tasfeen Akhtar** for their guidance, countless assistance and nice company. I would like to express my deepest appreciation to all Lab. fellows whom in one way or the other assisted me, mentioning them individually by name are rather impossible.

I am greatly honored to mention the nice cooperation of all employees of the department, especially Mr. Sharif Chohan and Muhammad Ilyas.

Last but not least, no words to portray my feelings of admiration about my affectionate parents, the prayers of whom enable me to achieve this target. I am also grateful to my brothers, **Principal Saifullah, Dr. Atta-ur-Rehman (Oral & Maxillofacial Surgeon) and Dr. Muneeb-ur-Rehman (Physicist)** and to my two sisters for their prayers, love and care.

Countless thanks to my nephews, **Mr. Iftikhar Ahmad, Mr. Tariq Ahmad, Mr. Asadullah, Mr. Hafiz Irfanullah and Mr. Hafiz Farooq Ahmad**, whose supplications enabled me to achieve what I longed for.

Many thanks to **Higher Education Commission of Pakistan** for financial support.

Zia-ur-Rehman

ABSTRACT

In the present study, a series of tri- chlorodi- and diorganotin(IV) dithiocarboxylates have been synthesized by the metathesis reaction of tri- and diorganotin(IV) chlorides with aryl substituted piperazinium/piperidinium salts of various dithiocarboxylates in dry methanol. The ligands used were 4-(4-nitrophenyl)piperazine-1-carbodithioate (**L**), 4-(2-methoxyphenyl)piperazine-1-carbodithioate (**L^a**), 4-(4-methoxyphenyl)piperazine-1-carbodithioate (**L^b**), 4-Benzhydrylpiperazine-1-carbodithioate (**L^c**) and 4-Benzylpiperidine-1-carbodithioate (**L^d**). The coordination mode of ligands, structural confirmation and geometry assignment of the complexes in solid and in solution states were made, using different analytical techniques such as elemental analysis, Raman, FT-IR, multinuclear (^1H , ^{13}C and ^{119}Sn) NMR, mass spectrometry and X-ray single crystal analysis. Based on results, the ligand appeared to coordinate the Sn atom through CSS moiety. The triorganotin(IV) derivatives mostly demonstrate trigonal bipyramidal geometry both in solid and solution state with few exceptions with tetrahedral geometry in solution. For all chlorodiorganotin(IV) complexes, the ligands retain their solid state bidentate mode of chelation even in solution. Octahedral geometry was exhibited by all diorganotin(IV) dithiocarboxylates in solid state, however, the coordination around Sn alter from six to five in solution, in most cases.

The interaction of R_3SnL (where $\text{R} = n\text{-C}_4\text{H}_9$, C_6H_{11} and C_6H_5), R_2SnCIL ($\text{R} = n\text{-C}_4\text{H}_9$ and C_2H_5) and Ph_2SnL_2 with DNA were investigated by cyclic voltammetry (CV) and UV-Vis spectroscopy. The diffusion coefficient of the free and DNA bound complexes were determined by Randles-Sevcik equation. The positive peak potential shift in CV and hypochromic effect in spectroscopy evidenced intercalative mode of interaction of these complexes with DNA except for $(n\text{-C}_4\text{H}_9)_2\text{SnCIL}$ where electrostatic interaction was observed. The CV results revealed the following increasing order of binding strength: $(\text{C}_6\text{H}_{11})_3\text{SnL}$ (2.4×10^3) < $(\text{C}_6\text{H}_5)_3\text{SnL}$ (3.6×10^3) < $(n\text{-C}_4\text{H}_9)_2\text{SnCIL}$ (5.4×10^3) < $(n\text{-C}_4\text{H}_9)_3\text{SnL}$ (6.9×10^3) < $(\text{C}_6\text{H}_5)_2\text{SnL}$ (8.4×10^3) < $(\text{C}_2\text{H}_5)_2\text{SnCIL}$ (1.24×10^4) M^{-1} . The UV-Vis spectroscopic data also indicated the same order of binding strength. The negative values of ΔG designate the spontaneity of complex-DNA binding.

Some of the synthesized complexes were also screened for their antibacterial and antifungal activities against various medically important bacteria and fungi. The triorganotin(IV) derivatives have strong bactericidal and fungicidal action than chlorodi- and diorganotin(IV) complexes. Most of the compounds were found to have biological activity comparable to the reference drugs and some were found even more active. These observations suggest that these compounds may be used as bactericides and fungicides in future.

Tables List

Table	Title	Page
1.1	Selected geometric parameters (Å, deg) for $R_3Sn(S_2CNR'_2)$	10,11
1.2	Selected geometric parameters (Å, deg) for $R_2Sn(S_2CNR'_2)Cl$	14,15
1.3	Selected geometric parameters (Å, deg) for $R_2Sn(S_2CNR'_2)_2$	24-26
3.1	1H -NMR data of ligands-salt	65
3.2	1H -NMR data of organotin(IV) derivatives of 4-(4-nitro-phenyl)piperazine-1-carbodithioate	66
3.3	1H -NMR data of organotin(IV) derivatives of 4-(2-methoxy-phenyl)piperazine-1-carbodithioate	67
3.4	1H -NMR data of organotin(IV) derivatives of 4-(4-methoxy-phenyl)piperazine-1-carbodithioate	68
3.5	1H -NMR data of organotin(IV) derivatives of 4-benzhydryl-piperazine-1-carbodithioate	69
3.6	1H -NMR data of organotin(IV) derivatives of 4-benzyl-piperidine-1-carbodithioate	70
3.7	^{13}C -NMR data of ligands-salt	73
3.8	^{13}C -NMR data of organotin(IV) derivatives of 4-(4-nitro-phenyl)piperazine-1-carbodithioate	74
3.9	^{13}C -NMR data of organotin(IV) derivatives of 4-(2-methoxy-phenyl)piperazine-1-carbodithioate	75
3.10	^{13}C -NMR data of organotin(IV) derivatives of 4-(4-methoxy-phenyl)piperazine-1-carbodithioate	76
3.11	^{13}C -NMR data of organotin(IV) derivatives of 4-benzhydryl-piperazine-1-carbodithioate	77
3.12	^{13}C -NMR data of organotin(IV) derivatives of 4-benzyl-piperidine-1-carbodithioate	78
3.13	(C-Sn-C) angles (°) based on NMR parameters of selected organotin(IV) derivatives of 4-(4-nitrophenyl)piperazine-1-carbodithioate	79
3.14	(C-Sn-C) angles (°) based on NMR parameters of selected organo- tin(IV) derivatives of 4-(2-methoxyphenyl)piperazine-1-	

	carbodithioate	79
3.15	(C-Sn-C) angles (°) based on NMR parameters of selected organotin(IV) derivatives of 4-(4-methoxyphenyl)piperazine-1-carbodithioate	80
3.16	(C-Sn-C) angles (°) based on NMR parameters of selected organotin(IV) derivatives of 4-benzhydrylpiperazine-1-carbodithioate	80
3.17	(C-Sn-C) angles (°) based on NMR parameters of selected organotin(IV) derivatives of 4-benzylpiperidine-1-carbodithioate	80
3.18	Voltammetric parameters of compound 1, 2 and 4 in the absence and presence of DNA	89
3.19	The association constants and Gibbs free energies of 1-DNA, 2-DNA and 4-DNA complexes as determined by voltammetry and UV-Vis spectroscopy	89
3.20	CV data of compounds 5, 7 and 12	106
3.21	Summary of kinetic and binding parameters of compounds 5, 7 and 12., as obtained from electrochemical measurements	106
3.22	Antibacterial activity data of organotin(IV) derivatives of 4-(2-methoxyphenyl)piperazine-1-carbodithioate	119,120
3.23	Antibacterial activity data of organotin(IV) derivatives of 4-benzhydrylpiperazine-1-carbodithioate	121,122
3.24	Antibacterial activity data of organotin(IV) derivatives of 4-benzylpiperidine-1-carbodithioate	123,124
3.25	Antifungal activity of organotin(IV) 4-(2-methoxy phenyl) piperazine-1-carbodithioate.	125
3.26	Antifungal activity of organotin(IV) derivatives of 4-benzhydrylpiperazine-1-carbodithioate	126
3.27	Antifungal activity of organotin(IV) derivatives of 4-benzyl piperidine-1-carbodithioate.	127
4.1	Crystal data and structure refinement parameters for Ph ₃ SnL (4)	134
4.2	Selected bond lengths (Å) and bond angles (°) for Ph ₃ SnL (4)	135

4.3	Crystal data and structure refinement parameters for n-Bu ₂ SnCIL (5)	138
4.4	Selected bond lengths (Å) and bond angles (°) for n-Bu ₂ SnCIL (5)	139
4.5	Crystal data and structure refinement parameters for Et ₂ SnCIL (7)	142
4.6	Selected bond lengths (Å) and bond angles (°) for Et ₂ SnCIL (7)	143
4.7	Crystal data and structure refinement parameters for Ph ₃ SnL ^a (16)	146
4.8	Selected bond lengths (Å) and bond angles (°) for Ph ₃ SnL ^a (16)	147
4.9	Crystal data and structure refinement parameters for n-Bu ₂ SnL ^a ₂ (18)	150
4.10	Selected bond lengths (Å) and bond angles (°) for n-Bu ₂ SnL ^a ₂ (18)	151
4.11	Crystal data and structure refinement parameters for Et ₂ SnCIL ^a (19)	154
4.12	Selected bond lengths (Å) and bond angles (°) for Et ₂ SnCIL ^a (19)	155
4.13	Crystal data and structure refinement parameters for Me ₂ SnCIL ^a (21)	158
4.14	Selected bond lengths (Å) and bond angles (°) for Me ₂ SnCIL ^a (21)	159
4.15	Crystal data and structure refinement parameters for Ph ₃ SnL ^b (28)	162
4.16	Selected bond lengths (Å) and bond angles (°) for Ph ₃ SnL ^b (28)	163
4.17	Crystal data and structure refinement parameters for n-Bu ₂ SnL ^b ₂ (30)	166
4.18	Selected bond lengths (Å) and bond angles (°) for n-Bu ₂ SnL ^b ₂ (30)	167
4.19	Crystal data and structure refinement parameters for n-Bu ₂ Sn CIL ^c (41)	170
4.20	Selected bond lengths (Å) and bond angles (°) for n-Bu ₂ SnCIL ^c (41)	171

4.21	Crystal data and structure refinement parameters for $\text{Et}_2\text{SnCIL}^c$ (43)	174
4.22	Selected bond lengths (\AA) and bond angles ($^\circ$) for $\text{Et}_2\text{SnCIL}^c$ (43)	175
4.23	Crystal data and structure refinement parameters for Cy_3SnL^d (50)	178
4.24	Selected bond lengths (\AA) and bond angles ($^\circ$) for Cy_3SnL^d (50)	179
4.25	Crystal data and structure refinement parameters for Ph_3SnL^d (52)	182
4.26	Selected bond lengths (\AA) and bond angles ($^\circ$) for Ph_3SnL^d (52)	183
4.27	Crystal data and structure refinement parameters for $n\text{-Bu}_2\text{SnCl}$ L^d_2 (54)	186
4.28	Selected bond lengths (\AA) and bond angles ($^\circ$) for $n\text{-Bu}_2\text{SnL}^d_2$ (54)	187
4.29	Crystal data and structure refinement parameters for $\text{Me}_2\text{SnCIL}^d$ (57)	190
4.30	Selected bond lengths (\AA) and bond angles ($^\circ$) for $\text{Me}_2\text{SnCIL}^d$ (57)	191
4.31	Crystal data and structure refinement parameters for $\text{Me}_2\text{SnL}^d_2$ (58)	194
4.32	Selected bond lengths (\AA) and bond angles ($^\circ$) for $\text{Me}_2\text{SnL}^d_2$ (58)	195

Figure	Title	Page
1.1	Tin metal	1
1.2	Principle coordination geometries for di- and tetra-valent tin	5
1.3	Molecular structure of $\text{Ph}_3\text{Sn}[\text{S}_2\text{CN}(\text{CH}_2\text{CH}_2)_2\text{O}]$, Serving as an example for structures of the general formula $\text{R}_3\text{Sn}[\text{S}_2\text{CNR}'_2]$	7
1.4	Molecular structure of $\text{Me}_2[2-(4,4\text{-dimethyl-2-oxazolinyl})\text{-3-thienyl}]\text{Sn}(\text{S}_2\text{CNMe}_2)$, highlighting the skewed trapezoidal bipyramidal geometry for tin	8
1.5	Molecular structure of $\text{Ph}_2(2\text{-NC}_5\text{H}_4\text{CH}_2\text{CH}_2)\text{Sn}(\text{S}_2\text{CNMe}_2)$, highlighting the trigonal bipyramidal geometry for tin	8
1.6	Molecular structure of centrosymmetric $\text{Ph}_3\text{Sn}[\text{S}_2\text{CN}(\text{CH}_2\text{CH}_2)_2\text{NCS}_2]_2\text{SNPh}_3$, highlighting the distorted trigonal bipyramidal geometry for tin	9
1.7	Molecular structure of $\text{Me}_2\text{Sn}(\text{S}_2\text{CNEt}_2)\text{Cl}$, serving as an exemplar for structures of the general formula $\text{R}_2\text{Sn}(\text{S}_2\text{CNR}'_2)\text{X}$	12
1.8	Molecular structure of $[\text{MeO}(\text{O}=\text{C})\text{CH}_2\text{CH}_2]_2\text{Sn}(\text{S}_2\text{CNMe}_2)\text{Cl}$, showing the presence of intramolecular $\text{Sn}\cdots\text{O}$ interactions that are responsible for the deviation of the C_2ClS_2 donor set toward a square pyramidal geometry	13
1.9	Supramolecular zig-zag chain in the structure of $\text{Me}_2\text{Sn}(\text{S}_2\text{Cpiperidine})\text{Cl}$ mediated by secondary $\text{Sn}\cdots\text{S}$ interactions	13
1.10	Molecular structure of $\text{Me}_2\text{Sn}(\text{S}_2\text{CNEt}_2)_2$, serving as an exemplar of motif I for structures of the general formula $\text{R}_2\text{Sn}(\text{S}_2\text{CNR}'_2)_2$	19
1.11	Molecular structure of $\text{Ph}_2\text{Sn}(\text{S}_2\text{CNEt}_2)_2$, serving as an exemplar of motif II for structures of the general formula $\text{R}_2\text{Sn}(\text{S}_2\text{CNR}'_2)_2$	19
1.12	Molecular structure of $(t\text{-Bu})_2\text{Sn}(\text{S}_2\text{CNMe}_2)_2$, the sole example for motif III for structures of the general formula $\text{R}_2\text{Sn}(\text{S}_2\text{CNR}'_2)_2$	20
1.13	Molecular structure of $[\text{MeO}(\text{O}=\text{C})\text{CH}_2\text{CH}_2]_2\text{Sn}(\text{S}_2\text{CNMe}_2)_2$, the sole example for motif IV for structures of the general formula	

	$R_2Sn(S_2CNR'_2)_2$	20
1.14	Dimer formation in the structure of $[H_2C=(H)C]_2Sn[S_2CNCy_2]_2$, via secondary Sn---S interactions	21
1.15	Supramolecular zig-zag chain formation via O-H---O hydrogen (orange-dashed lines) in the structure of $Me_2Sn[S_2CN(CH_2CH_2$ $OH)_2]_2$	21
1.16	Molecular structure of dinuclear $[PhSn(S_2CNEt_2)(S)(CH_2CH_2$ $CH_2)SnPh(S_2CNEt_2)]$	22
1.17	Molecular structure of centrosymmetric $(t-Bu)_2Sn[S_2CN(H)CH_2$ $CH_2N(H)CS_2]_2Sn(t-Bu)_2 \cdot 2(tetrahydrofuran)$, featuring a bi- functional dithiocarboxylate ligand. Orange dashed bonds represent N-H---O and N-H---S hydrogen bonds	23
3.1	Cyclic voltammograms of 3.00 mM of compound 1 in 10 % aqueous DMSO with 0.1 M TBAP as supporting electrolyte in the absence (a) and presence of 3.0×10^{-5} , (b) 6.5×10^{-5} (c) and 1.05×10^{-4} M DNA (d) at 25°C temperature. Glassy carbon electrode (0.071 cm^2) was used as working electrode and all potentials were reported vs. SCE at 100 mV/s scan rate	90
3.2	Plot of $1/(1-i/i_0)$ vs. $1/[DNA]$ used to calculate the binding constant of 1-DNA adduct	91
3.3	Absorption spectra of 3mM of compound 1 in the absence (a) and presence of 2.0×10^{-5} , (b) 3.0×10^{-5} , (c) 4.5×10^{-5} , (d) $6.0 \times$ 10^{-5} , (e) 7.0×10^{-5} , (f) 9.0×10^{-5} , (g) 1.0×10^{-4} , (h) 1.15×10^{-4} (i) and 1.25×10^{-4} M DNA (j). The arrow direction indicates increasing concentrations of DNA	92
3.4	Plot of $A_0/(A-A_0)$ vs. $1/[DNA]$ for the determination of binding constant of 1-DNA adduct	93
3.5	Cyclic voltammograms of 3.00 mM of compound 2 in 10 % aqueous DMSO with 0.1 M TBAP as supporting electrolyte in the absence (a) and presence of 3.2×10^{-5} M DNA (b) at 25°C temperature. Glassy carbon electrode (0.071 cm^2) was used as working electrode and all potentials were reported vs. SCE at 100 mV/s scan rate	94

3.6	Plot of $1/(1-i/i_0)$ vs. $1/[DNA]$ used to calculate the binding constant of 2-DNA adduct	95
3.7	Absorption spectra of 3mM of compound 2 in the absence (a) and presence of 2.0×10^{-5} , (b) 2.5×10^{-5} , (c) 3.5×10^{-5} , (d) 4.5×10^{-5} , (e) 5.5×10^{-5} , (f) 6.5×10^{-5} , (g) 7.5×10^{-4} , (h) 8.5×10^{-4} (i) and 9.5×10^{-4} M DNA (j). The arrow direction indicates increasing concentrations of DNA	96
3.8	Plot of $A_0/(A-A_0)$ vs. $1/[DNA]$ for the determination of binding constant of 2-DNA adduct	97
3.9	Cyclic voltammograms of 3.00 mM of compound 4 in 10 % aqueous DMSO with 0.1 M TBAP as supporting electrolyte in the absence (a) and presence of 5.0×10^{-5} M DNA (b) at 25°C temperature. Glassy carbon electrode (0.071 cm^2) was used as working electrode and all potentials were reported vs. SCE at 100 mV/s scan rate	98
3.10	Plot of $1/(1-i/i_0)$ vs. $1/[DNA]$ used to calculate the binding constant of 4-DNA adduct	99
3.11	Absorption spectra of 3mM of compound 4 in the absence (a) and presence of 2.0×10^{-5} , (b) 3.5×10^{-5} , (c) 4.5×10^{-5} , (d) 5.5×10^{-5} , (e) 6.5×10^{-5} , (f) 7.5×10^{-5} , (g) 9.5×10^{-4} (h) and 1.15×10^{-4} M DNA (i) The arrow direction indicates increasing concentrations of DNA	100
3.12	Plot of $A_0/(A-A_0)$ vs. $1/[DNA]$ for the determination of binding constant of 4-DNA adduct	101
3.13	CV behavior of 3 mM of compound 5 at clean GC electrode in the absence (a) and presence of 60 μM DNA (b) in 10 % aqueous DMSO using 0.1 M TBAFB as supporting electrolyte at 0.1 V/s scan rate	108
3.14	CV behavior of 3 mM of compound 7 at clean GC electrode in the absence (a) and presence of 60 μM DNA (b) in 10 % aqueous DMSO using 0.1 M TBAFB as supporting electrolyte at 0.1 V/s	109

	scan rate	
3.15	Plots of I vs. $\nu^{1/2}$, for the determination of the diffusion coefficients of 3 mM of compounds 5, 7 and 12. Scan rates: 0.1, 0.2, 0.3, 0.4 and 0.5 Vs ⁻¹	110
3.16	Plots of I vs. $\nu^{1/2}$, for the determination of the diffusion coefficients of 3 mM of compounds 5, 7 and 12 in the presence of 60 μ M DNA. Scan rates: 0.1, 0.2, 0.3, 0.4 and 0.5 Vs ⁻¹	111
3.17	Plots of $\log (I_{H-G}/(I_G-I_{H-G}))$ vs. $\log (1/[DNA])$ used to calculate the binding constants of complexes 5, 7 and 12 with DNA	112
3.18	$I-I_{DNA}/I_{DNA}$ vs $[DNA]$ for the determination of binding site size	113
3.19	Absorption spectra of 30 μ M of compound 5 in the absence (a) and presence of 20 μ M, (b) 30 μ M, (c) 40 μ M, (d) 50 μ M, (e), 60 μ M (f), 70 μ M (g) and 80 μ M DNA (h) in 10 % aqueous DMSO at 25 °C	114
3.20	Absorption spectra of 30 μ M of compound 7 in the absence (a) and presence of 20 μ M, (b) 30 μ M, (c) 40 μ M, (d) 50 μ M, (e), 60 μ M (f), 70 μ M (g) and 80 μ M DNA (h) in 10 % aqueous DMSO at 25 °C	115
3.21	Absorption spectra of 30 μ M of compound 12 in the absence (a) and presence of 20 μ M, (b) 30 μ M, (c) 40 μ M, (d) 50 μ M, (e), 60 μ M (f), and 80 μ M DNA (g) in 10 % aqueous DMSO at 25 °C	116
3.22	Numbering scheme for ¹ H and ¹³ C-NMR of ligands	128
3.23	Numbering scheme of organic moiety attached to Sn atom	129
4.1	ORTEP drawing of Ph ₃ SnL (4) with atomic numbering scheme	133
4.2	The ORTEP drawing of molecule 1 (top) and molecule 2 (lower) of the n-Bu ₂ SnCIL (5). Displacement ellipsoids for non-H atoms are drawn at the 50% probability level. H atoms have been omitted to improve clarity	137
4.3	ORTEP drawing of Et ₂ SnCIL (7) with atomic numbering scheme	141
4.4	ORTEP drawing of Ph ₃ SnL ^a (16) with atomic numbering scheme	145
4.5	ORTEP drawing of n-Bu ₂ SnL ^a ₂ (18) with atomic numbering scheme	149

4.6	ORTEP drawing of one of the three independent molecules of $\text{Et}_2\text{SnCIL}^{\text{a}}$ (19) with atomic numbering scheme	153
4.7	ORTEP drawing of $\text{Me}_2\text{SnCIL}^{\text{a}}$ (21) with atomic numbering scheme	157
4.8	ORTEP drawing of $\text{Ph}_3\text{SnL}^{\text{b}}$ (28) with atomic numbering scheme	161
4.9	ORTEP drawing of $\text{n-Bu}_2\text{SnL}^{\text{b}}_2$ (30) with atomic numbering scheme	165
4.10	ORTEP drawing of molecule 1 (top) and molecule 2 (lower) of the $\text{n-Bu}_2\text{SnCIL}^{\text{c}}$ (41) with atomic numbering scheme	169
4.11	ORTEP drawing of $\text{Et}_2\text{SnCIL}^{\text{c}}$ (43) with atomic numbering scheme	173
4.12	ORTEP drawing of $\text{Cy}_3\text{SnL}^{\text{d}}$ (50) with atomic numbering scheme	177
4.13	ORTEP drawing of $\text{Ph}_3\text{SnL}^{\text{d}}$ (52) with atomic numbering scheme	181
4.14	ORTEP drawing of $\text{n-Bu}_2\text{SnL}^{\text{d}}_2$ (54) with atomic numbering scheme	185
4.15	ORTEP drawing of one of the two independent molecules of $\text{Me}_2\text{SnCIL}^{\text{d}}$ (57) with atomic numbering scheme	189
4.16	ORTEP drawing of $\text{Me}_2\text{SnL}^{\text{d}}_2$ (58) with atomic numbering scheme	193

INTRODUCTION

1.1 Tin-Metal

1.1.1 General Description

Ordinary tin is a silvery-white metal, is malleable, somewhat ductile, and has a highly crystalline structure. Due to the breaking of these crystals, a "tin cry" is heard when a bar is bent. The element has two allotropic forms. On warming, grey, or α -tin, with a cubic structure, changes at 13.2°C into white, or β -tin, the ordinary form of the metal.

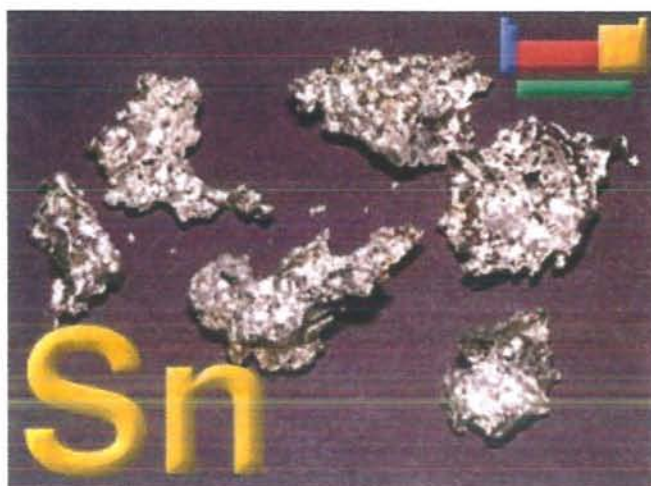


Fig. 1.1 Tin metal

White tin has a tetragonal structure. When tin is cooled below 13.2°C, it changes slowly from white to grey. This change is affected by impurities such as aluminium and zinc, and can be prevented by small additions of antimony or bismuth. The conversion was first noted as growths on organ pipes in European cathedrals, where it was thought to be the devils work. This conversion was also speculated to be caused by microorganisms and was called "tin plague" or "tin disease".

There is normally little need to isolate tin metal in the laboratory as it is readily available commercially. Tin is commonly available as the mineral cassiterite, SnO_2 . Reduction of this dioxide with burning coal results in tin metal and was probably how tin was made by the ancients.



Tin is a 4th member of group 14 elements (C, Si, Ge, Sn and Pb) of the periodic table with atomic number 50. The electronic configuration is [Kr] 4d¹⁰5s²5p² and the four valence electrons in the low level of orbitals are non-equivalent. The ground state term is ³P and for four-covalent states the s-electrons are uncoupled, which results sp³ hybridization and ⁵S term is obtained.

Elements of the group 14 are playing vital role in the life of human being and have wide applications. Due to the specific significance, these elements have been placed in 'Main Group Metal Elements' in the periodic table.

1.1.2 Properties of Tin

Tin has four electrons in the outer electronic shell in common with the other group 14 elements, C, Si, Ge and Pb. Thus, tin exists in two oxidation states II and IV. The oxidation number II is always positive whereas IV has amphoteric properties showing +IV or -IV behavior, depending on the nature of its reaction partner.

Tin is inert to react with oxygen, nitrogen, hydrogen, water and ammonia at ambient temperatures. However, at elevated temperature both the oxygen and water vapors give thin oxide films on the tin surface. Similarly, when tin is heated in the presence of oxygen, at white heat it burns with a pale white flame to form tin(IV) oxide. Chlorine and bromine show greater affinity to tin than their counterparts fluorine and iodine. The reaction of tin with sulfur, selenium or tellurium is reported to be vigorous only on heating [1]. Due to the amphoteric nature, metallic tin is vulnerable to hydrogen halides and also dissolves in a hot aqueous solution of alkali hydroxide to form an alkaline stannite and hydrogen. Dry hydrogen sulfide reacts with tin at 100-400°C to yield stannous sulfide. Phosphorous pentachloride reduces into phosphorous trichloride on treating with fine powdered tin at 170 °C, which yields in turn stannic chloride [1].

Tin has ten naturally occurring stable isotopes more than any other element, in addition to several radioactive isotopes with half-lives varying from 2.2 min to ~10⁵ years. A consequence of which is that there are a variety of analytical techniques, which can be used for structural studies of tin and its derivatives [2, 3]. For example, there are three magnetically active ($I = 1/2$) tin isotopes suitable for NMR studies i.e., ¹¹⁵Sn, ¹¹⁷Sn and ¹¹⁹Sn of relative abundances 0.35, 7.67 and 8.68%, respectively [4].

Furthermore, the isotope $^{119\text{m}}\text{Sn}$, obtained by the (n, γ) reaction of ^{118}Sn is an excellent source of the gamma rays for Mössbauer spectroscopy [5].

1.2 Organotin Compounds

Organotin compounds are those containing at least one carbon to tin bond ($\text{Sn}-\text{C}$) forming a compound of the formula $\text{R}_n\text{SnX}_{4-n}$, where n is 1 to 4. X may be hydrogen, a metal, or a group attached to tin through oxygen, sulfur, nitrogen, halogen, etc. The first description dates back to 1849, when Frankland synthesized diethyltin diiodide, Et_2SnI_2 [6]. But the commercial application of organotins for use as PVC stabilizer in the 1940's marks the real takeoff of organotin chemistry and extensive studies in the area.



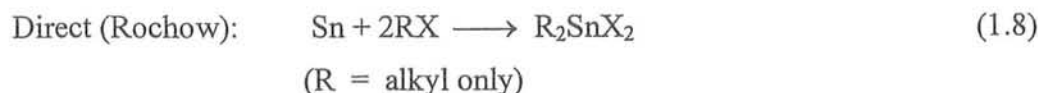
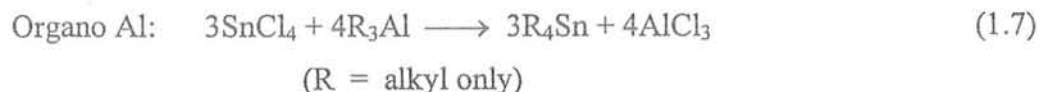
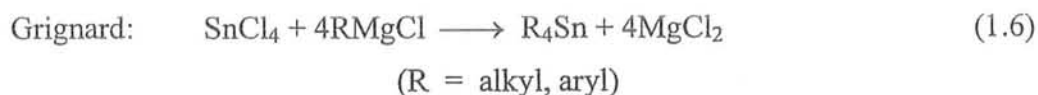
Although the carbon to tin bond ($\text{Sn}-\text{C}$) is weaker than the $\text{C}-\text{C}$ or $\text{Si}-\text{C}$ bond, it is relatively non-polar and is therefore, stable in the presence of air and moisture as well as many nucleophilic species. However, cleavage of $\text{Sn}-\text{C}$ bond occurs with different agents, including halogens, metal halides, mineral acids, alkali, etc.



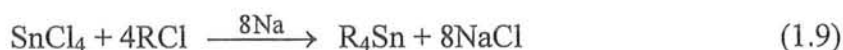
Cleavage of aryl, allyl or vinyl groups occur more readily than alkyl groups and lower alkyl groups are cleaved more readily than the higher alkyl groups. Because, of the large size of the tin atom and availability of low-lying empty $5d^0$ atomic orbitals, coordination numbers greater than four are frequently encountered in organotin structures.

The organotin compounds have found a variety of applications in industry [7, 8, 9] which depend upon the stability of the $\text{Sn}-\text{C}$ bond, the lability of the anion X , and the possibility of expansion to coordination numbers greater than four. These characteristics, largely account for its applications in different chemical transformations including transmetalation reactions, addition to unsaturated compounds, catalysts and PVC stabilizers.

Organotin compounds can be synthesized by standard methods of which following are typical:



All these routes are used on an industrial scale and in addition the Grignard method (or the equivalent organolithium reagent) is convenient for laboratory scale. Rather less used is the modified Wurtz-type reaction.



Conversion of R_4Sn to the partially halogenated species is readily achieved by scrambling reaction with SnCl_4 . Reduction of $\text{R}_n\text{SnX}_{4-n}$ with LiAlH_4 affords the corresponding hydrides and hydrostannation (addition of Sn-H) to C–C double bond and triple bonds is an attractive route to unsymmetrical or heterocyclic organotin compounds.

1.3 Principal Coordination Geometries at the Tin Centre in Organotin Compounds

Since the empty 5d orbitals of suitable energy may also be involved in the hybridization in divalent as well as in tetravalent tin higher coordination numbers at tin are possible. Reactions of alkyltin chloride with the appropriate nucleophiles give the alkyltin, alkoxides, carboxylates, amides, thioalkoxides, etc. The presence of these electronegative groups on tin renders the metal susceptibility for the coordination by Lewis bases, simple tetrahedral coordination is the exception rather than the rule. Hydrolysis of organotin halides gives the organotin oxides and in the case of dihalides and trihalides, the reaction proceeds through a series of well characterized intermediate hydrolysis products. In Figure 1.2 the principal coordination geometries for both divalent and tetravalent tin are given, while it is assumed that in the case of divalent tin, the lone pair is also involved in the hybridization.

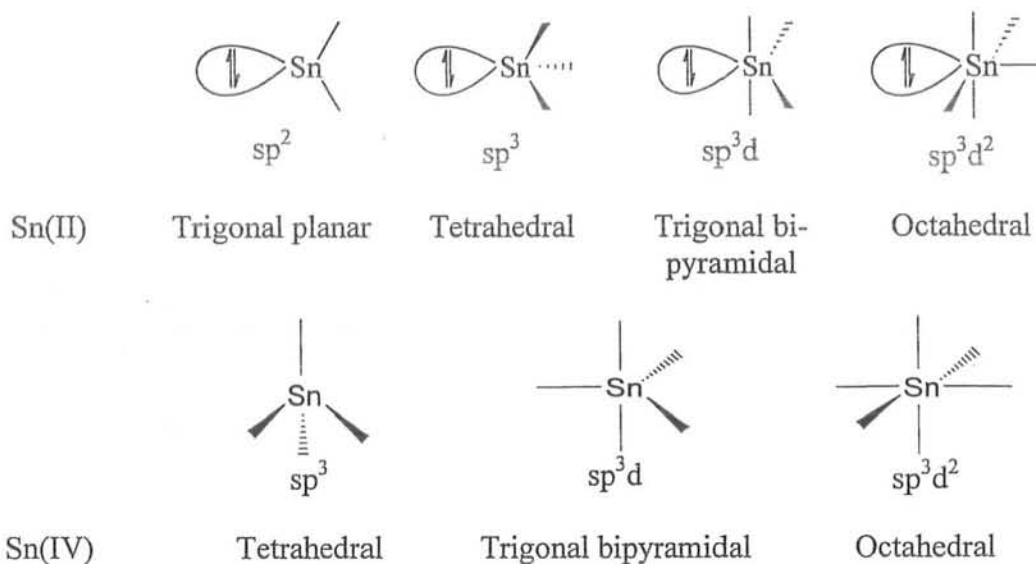


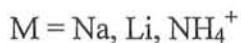
Figure 1.2: Principle coordination geometries for di- and tetra-valent tin.

1.4 Organotin(IV) dithiocarboxylates

This class of compounds comprises organotin compounds containing a Sn-S bond formed via the CSS^- group. Di and triorganotin dithiocarboxylates have been widely studied due to their wide range of applications in industry and agriculture on one hand and structural diversity leading to further developments on the other side.

1.4.1 Methods of preparation

Organotin dithiocarbamates are commonly prepared by treating organotin halides with metal dithiocarbamates or with ammonium dithiocarbamates.



Some alternate methods are also available for the synthesis of organotin dithiocarboxylate. For instance, the reaction of organotin halides with dithiocarboxylic acids in the presence of suitable base like triethylamine gives the corresponding organotin dithiocarboxylates.



1.5 Structural chemistry of organotin(IV) dithiocarboxylates

Based on the available crystal structures organotin(IV) dithiocarboxylates can be categorized into four classes.

- (i) Triorganotin(IV) dithiocarboxylates
- (ii) Chlorodiorganotin(IV) dithiocarboxylates
- (iii) Diorganotin(IV) dithiocarboxylates
- (iv) Monoorganotin(IV) dithiocarboxylates

As per our interest, the structure diversity related to the first three groups, will be discussed here.

1.5.1 Triorganotin(IV) dithiocarboxylates structures

The prototype structure for the majority of structures in this category, i.e. with general formula $R_3Sn(S_2CNR'_2)$, is shown in Fig. 1.3 for the structure of $Ph_3Sn[S_2CN(CH_2CH_2)_2O]$ [10]. Here, the tin atom is coordinated by an asymmetrically coordinating dithiocarboxylate ligand and three carbon atoms from the organic substituents. In the more precisely determined structures, the $Sn-S_{short}$ bond distances fall in the narrow range 2.45–2.48 Å. Similarly, the $Sn-S_{long}$ bond distances fall in the range 2.92–3.24 Å. The longer $Sn-S_{long}$ bond distances are generally found with bulky tin-bound substituents, e.g. cyclohexyl, indicating a possible steric influence upon these distances. The coordination geometry is best described as being based on a distorted trigonal bipyramidal geometry with the sulfur atom involved in forming the longer $Sn\cdots S$ bonds occupying one of the axial positions. Based on the values of τ [11], all but one structure has a coordination environment for tin more closely resembling a trigonal bipyramidal geometry. The exceptional structure is that of $Ph_3Sn[S_2CN(CH_2CH_2)_2NCH_2Ph]$ [12] for which $\tau = 0.41$. This probably arises as a result of a wide $S-Sn-C$ angle, i.e. $126.5(1)^\circ$, involving the more tightly bound sulfur atom, which, in turn, comes about by the relatively close approach of the less tightly bound sulfur atom, i.e. 2.9223(15) Å.

There are two $R_3Sn(S_2CNR'_2)$ structures in which one of the tin-bound R groups carries additional donor atoms capable of coordination to tin. One example, namely $Me_2[2-(4,4\text{-dimethyl-2-oxazolinyl})\text{-3-thienyl}]Sn(S_2CNMe_2)$ [13] is illustrated in Fig.

1.4. Here, the 2-(4,4-dimethyl-2-oxazolinyl)-3-thienyl group provides an additional nitrogen donor atom, Sn---N is 2.723(3) Å, so that the coordination number of the tin atom is increased to six, based on a skewed trapezoidal bipyramidal geometry. The second structure conforming to this type is that of $\text{Ph}_2(2\text{-NC}_5\text{H}_4\text{CH}_2\text{CH}_2)\text{Sn}(\text{S}_2\text{CNMe}_2)$ [14] shown in Fig. 1.5. Here, the dithiocarboxylate ligand is monodentate and the Sn–N bond distance is considerably shorter, i.e. 2.486(7) Å, compared with the previous structure. The coordination geometry is based on a trigonal bipyramid with the axial positions being occupied by the more tightly bound sulfur and the nitrogen atoms, the axial S–Sn–N angle is 169.6(2)°.

The four remaining structures to be described are each dinuclear and centrosymmetric [15–18]. The structure of $\text{Ph}_3\text{Sn}[\text{S}_2\text{CN}(\text{CH}_2\text{CH}_2)_2\text{NCS}_2]_2\text{SnPh}_3$, representative of the four, is shown in Fig. 1.6. Each of the structures features the bi-functional, dinegative dithiocarboxylate ligand, $^-\text{S}_2\text{CN}(\text{CH}_2\text{CH}_2)_2\text{NCS}_2^-$, and these bridge the triorganotin centers, defining coordination geometries almost indistinguishable from those described above for mononuclear $\text{R}_3\text{Sn}(\text{S}_2\text{CNR}'_2)$, with asymmetrically coordinating dithiocarboxylate ligands and approximate trigonal bipyramidal coordination geometries.

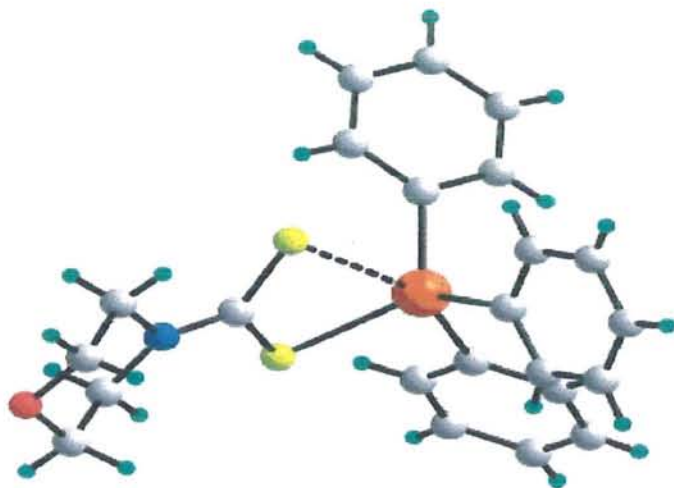


Fig. 1.3 Molecular structure of $\text{Ph}_3\text{Sn}[\text{S}_2\text{CN}(\text{CH}_2\text{CH}_2)_2\text{O}]$, Serving as an example for structures of the general formula $\text{R}_3\text{Sn}[\text{S}_2\text{CNR}'_2]$.

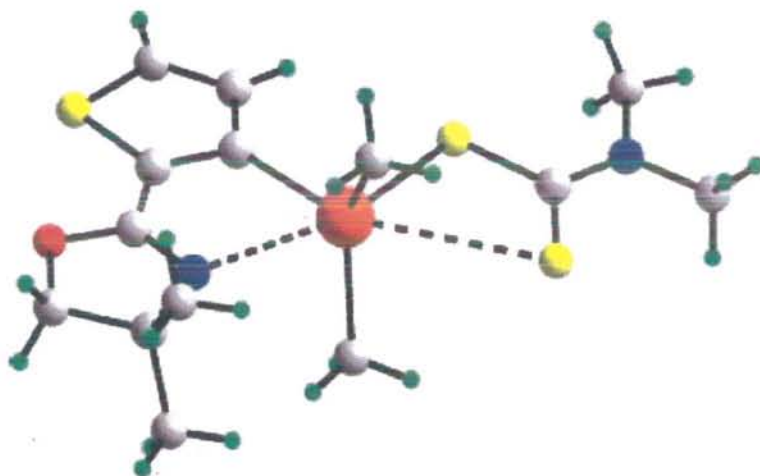


Fig. 1.4 Molecular structure of $\text{Me}_2[2-(4,4\text{-dimethyl-2-oxazoliny})\text{-3-thienyl}]\text{Sn}(\text{S}_2\text{CNMe}_2)$, highlighting the skewed trapezoidal bipyramidal geometry for tin.

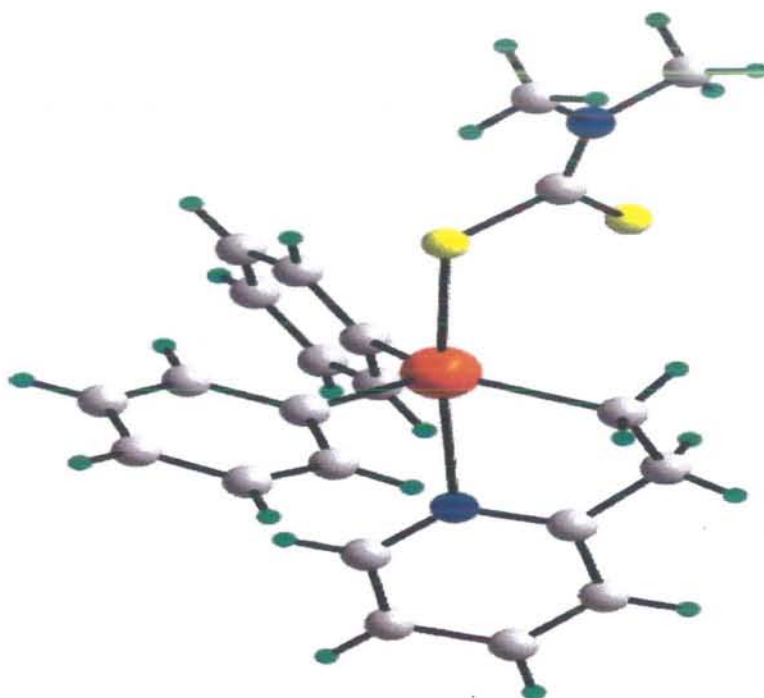


Fig. 1.5 Molecular structure of $\text{Ph}_2(2\text{-NC}_5\text{H}_4\text{CH}_2\text{CH}_2)\text{Sn}(\text{S}_2\text{CNMe}_2)$, highlighting the trigonal bipyramidal geometry for tin.

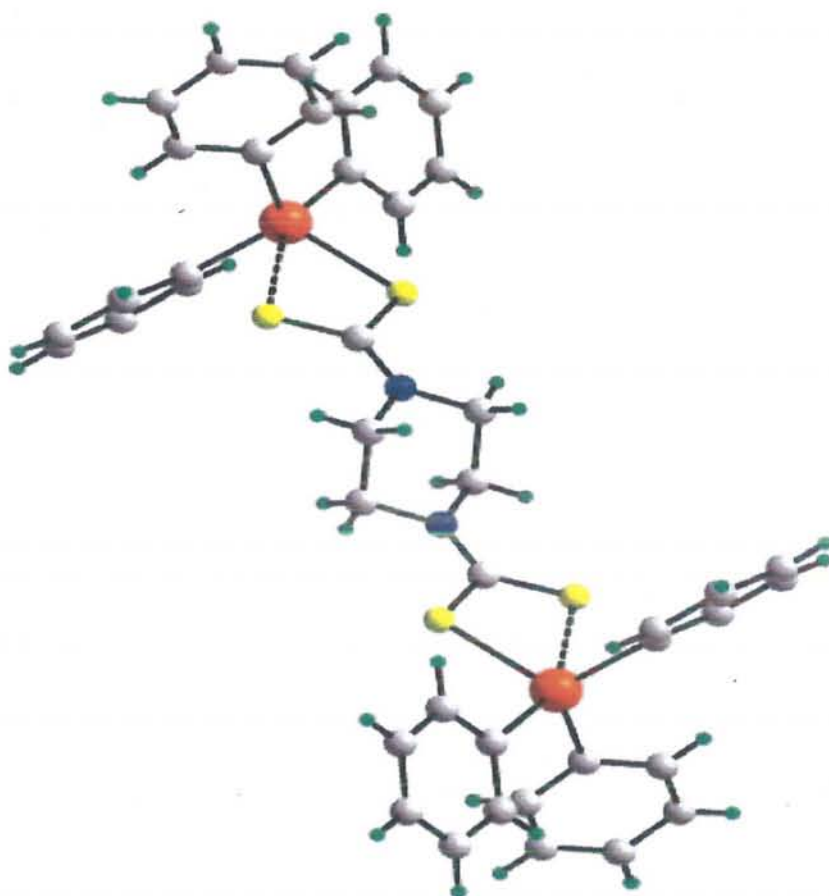


Fig. 1.6 Molecular structure of centrosymmetric $\text{Ph}_3\text{Sn}[\text{S}_2\text{CN}(\text{CH}_2\text{CH}_2)_2\text{NCS}_2]_2$ SNPh_3 , highlighting the distorted trigonal bipyramidal geometry for tin.

Table 1.1: Selected geometric parameters (Å, deg) for $R_3Sn(S_2CNR'_2)$

Compound	Sn-S _{chelate}	C-Sn---S	τ	Reference
$Me_3Sn(S_2CNMe_2)^{a,b}$	2.47(1), 3.33(3)	154(1)	0.56	[19]
	2.47(4), 3.16(3)	153(1)	0.56	
$Me_3Sn(S_2CNMe_2)^c$	2.47(1), 3.17(1)	156(1)	0.62	[20]
$Cy_3Sn[S_2CNH(iBu)]$	2.473(3), 3.239(3)	156.7(3)	0.61	[21]
$Cy_3Sn[S_2CN(n-Bu)_2]$	2.4679(5), 3.1343(6)	159.36(5)	0.72	[22]
$Ph_3Sn(S_2CNMe_2)^{b,d}$	2.460(2), 3.154(2)	155.2(2)	0.61	[23]
	2.4682(18), 3.050(3)	155.4(2)	0.58	
$Ph_3Sn(S_2CNEt_2)$	2.4543(12), 3.1315(11)	155.9(1)	0.58	[24, 25]
$Ph_3Sn[S_2CN(n-Bu)_2]^b$	2.482(2), 2.945(2)	158.9(2)	0.62	[26]
$Ph_3Sn[S_2CNMe(n-Bu)]$	2.4631(10), 3.0840(12)	152.13(6)	0.55	[27]
$Ph_3Sn[S_2CN(Me)(Cy)]$	2.4558(6), 3.0134(7)	158.43(6)	0.70	[28]
$Ph_3Sn[S_2CN(Me)Ph]$	2.4783(14), 3.0161(19)	158.3(2)	0.63	[29]
$Ph_3Sn[S_2CNEt(nPr)]$	2.460(1), 3.095(1)	156.50(6)	0.60	[30]
$Ph_3Sn[S_2CNEt(Cy)]$	2.4758(6), 2.9426(8)	157.11(6)	0.64	[31]
$Ph_3Sn(S_2CNR^1)^e$	2.4651(15), 3.1059(12)	156.32(9)	0.60	[32]
$Ph_3Sn(S_2CNR^2)^{f,g}$	2.482(3), 2.919(2)	156.5(1)	0.59	[33]
$Ph_3Sn(S_2CNR^2)^{f,h}$	2.4713(11), 2.9454(10)	158.57(7)	0.65	[25]
$Ph_3Sn(S_2CNR^3)^i$	2.4649(9), 3.0316(9)	157.25(7)	0.65	[29]
$Ph_3Sn(S_2CNR^4)^j$	2.4700(11), 3.0124(8)	155.49(9)	0.50	[34]
$Ph_3Sn(S_2CNR^5)^k$	2.4858(16), 2.9223(15)	154.3(1)	0.41	[12]
$Ph_3Sn(S_2CNR^6)^l$	2.4635(8), 3.0328(8)	157.10(7)	0.65	[10]
$Ph_2(n-Bu)Sn(S_2CNMe_2)$	2.467(3), 3.079(3)	158.8(2)	0.71	[35]
$(C_6H_5CH_2)_3Sn(S_2CNR^7)^m$	2.4808(19), 3.0275(18)	159.4(1)	0.67	[36]
$(C_6H_5CH_2)_3Sn(S_2CNR^8)^n$	2.4875(7), 3.0527(7)	156.21(8)	0.68	[37]
$(o-FC_6H_4CH_2)_3Sn(S_2CNR^7)^m$	2.461(4), 3.035(4)	158.3(2)	0.64	[38]
$(o-FC_6H_4CH_2)_3Sn(S_2CNR^8)^{b,n}$	2.465(4), 3.122(5)	158.6(2)	0.74	[39]
	2.464(4), 3.054(4)	159.9(2)	0.74	
$(o-ClC_6H_4CH_2)_3Sn(S_2CNR^7)^m$	2.4664(12), 3.0797(13)	156.90(8)	0.65	[38]
$(o-ClC_6H_4CH_2)_3Sn(S_2CNR^2)^f$	2.4519(16), 3.0624(17)	157.4(1)	0.67	[40]
$(o-ClC_6H_4CH_2)_3Sn(S_2CNR^3)^i$	2.471(2), 3.0999(17)	156.7(1)	0.61	[40]

$(p\text{-FC}_6\text{H}_4\text{CH}_2)_3\text{Sn}(\text{S}_2\text{CNR}^7)^m$	2.470(3), 3.183(4)	156.3(2)	0.66	[41]
$(p\text{-FC}_6\text{H}_4\text{CH}_2)_3\text{Sn}(\text{S}_2\text{CNR}^4)^j$	2.4719(10), 3.1262(10)	157.08(9)	0.67	[42]
$\text{Me}_2(\text{R}^1)\text{Sn}(\text{S}_2\text{CNMe}_2)^o$	2.5274(11), 3.2678(10)	-	-	[12]
$\text{Ph}_2(\text{R}^2)\text{Sn}(\text{S}_2\text{CNMe}_2)^p$	2.560(2), 3.466(3)	-	0.68	[14]
$\text{Ph}_3\text{Sn}[\text{S}_2\text{CN}(\text{CH}_2\text{CH}_2)_2\text{NCS}_2]_2\text{SNPh}_3^{q,r}$	2.4717(17), 3.0659(17)	156.0(1)	0.66	[15]
$(o\text{-FC}_6\text{H}_4\text{CH}_2)_3\text{Sn}[\text{S}_2\text{CN}(\text{CH}_2\text{CH}_2)_2\text{NC}$ $\text{S}_2]_2\text{Sn}(\text{CH}_2\text{C}_6\text{H}_4\text{F-}o)_3^q$	2.457(3), 3.085(2)	156.2(2)	0.64	[16]
$(o\text{-ClC}_6\text{H}_4\text{CH}_2)_3\text{Sn}[\text{S}_2\text{CN}(\text{CH}_2\text{CH}_2)_2\text{NC}$ $\text{S}_2]_2\text{Sn}(\text{CH}_2\text{C}_6\text{H}_4\text{Cl-}o)_3^q$	2.436(4), 3.045(5)	157.8(3)	0.63	[17]
$(\text{PhC}(\text{Me})_2\text{CH}_2)_3\text{Sn}[\text{S}_2\text{CN}(\text{CH}_2\text{CH}_2)_2\text{NC}$ $\text{S}_2]_2\text{Sn}(\text{CH}_2\text{C}(\text{Me})_2\text{Ph})_3^q$	2.4588(11), 3.3289(10)	158.20(8)	0.71	[18]

^aOrthorhombic form. ^bTwo independent molecules in the asymmetric unit. ^cMonoclinic form. ^dCompound crystallizes as a methanol hemisolvate. ^e NR^1 = pyrrolidine. ^f NR^2 = piperidine. ^gMonoclinic form I. ^hMonoclinic form II. ⁱ NR^3 = piperazine. ^j NR^4 = 4-methylpiperazine. ^k NR^5 = 4-benzylpiperazine. ^l NR^6 = morpholine. ^m NR^7 = pyrrolidine. ⁿ NR^8 = morpholine. ^oFor structure of R^1 = 2-(4,4-dimethyl-2-oxazoliny)-3-thienyl, $\text{C}_9\text{H}_{10}\text{NOS}$, see Fig. 1.4. ^p R_2 = $\text{CH}_2\text{CH}_2(2\text{-NC}_5\text{H}_4)$. ^qMolecule is centrosymmetric. ^rCompound crystallizes as a methanol solvate.

1.5.2 Chlorodiorganotin(IV) dithiocarboxylates structures

The first class of mononuclear diorganotin dithiocarboxylate structures conform to the general formula $\text{R}_2\text{Sn}(\text{S}_2\text{CNR}'_2)\text{X}$, where X is usually chloride [39, 43, 44a, 45-71]. By contrast to the $\text{R}_2\text{Sn}(\text{S}_2\text{CNR}'_2)_2$ structures with four distinct structural motifs (see section 1.5.3), the $\text{R}_2\text{Sn}(\text{S}_2\text{CNR}'_2)\text{X}$ compounds are decidedly more homogeneous in their structural chemistry. The coordination geometries to be described here for $\text{R}_2\text{Sn}(\text{S}_2\text{CNR}'_2)\text{X}$ closely resemble that observed for $(t\text{-Bu})_2\text{Sn}(\text{S}_2\text{CNMe}_2)_2$ motif III for the $\text{R}_2\text{Sn}(\text{S}_2\text{CNR}'_2)_2$ structures (Fig. 1.12), in which one of the dithiocarboxylate ligands is monodentate. Table 1.2 summarizes the pertinent structural information for these structures and the prototype structure, namely, $\text{Me}_2\text{Sn}(\text{S}_2\text{CNEt}_2)\text{Cl}$, is illustrated in Fig. 1.7. The tin atom is five-coordinated, being chelated by an asymmetrically coordinating dithiocarboxylate ligand, a halide and two organic substituents. The Sn–S bond distance approximately *trans*- to the halide atom is always longer than the other Sn–S bond distance. The coordination geometry is almost intermediate between square pyramidal and trigonal bipyramidal with the majority of the structures having a

that generally lie in the range 0.40–0.60. However, there are several structures with values of τ [11] less than 0.40, Table 1.2. In the structure of $\text{Ph}_2\text{Sn}(\text{S}_2\text{CNMe}_2)\text{Br}$ [57], $\tau = 0.38$, which contrasts with $\tau = 0.59$ and 0.57 in the structures of $\text{Ph}_2\text{Sn}(\text{S}_2\text{CNEt}_2)\text{X}$ for $\text{X} = \text{Cl}$ [52] and I [58], respectively; however, the different R' substituents in the dithiocarboxylate ligands are noted. Further work is clearly required to elucidate the variations in τ for this series of structures. More tangible explanations are available for the deviation of the coordination geometries towards square pyramidal in each of $[\text{MeO}(\text{O}=\text{CCH}_2\text{CH}_2)_2\text{Sn}(\text{S}_2\text{CNMe}_2)\text{Cl}]$ [69], $(o\text{-FC}_6\text{H}_4\text{CH}_2)_2\text{Sn}[\text{S}_2\text{C}(\text{N}(\text{CH}_2\text{CH}_2)_2\text{NEt})]\text{Cl}$ [63] and $\text{Me}_2\text{Sn}(\text{S}_2\text{Cpiperidine})\text{Cl}$ [47]. In $[\text{MeO}(\text{O}=\text{CCH}_2\text{CH}_2)_2\text{Sn}(\text{S}_2\text{CNMe}_2)\text{Cl}]$ [69], with $\tau = 0.29$, there are two intramolecular $\text{Sn}\cdots\text{O}$ contacts formed by the carbonyl-oxygen atoms, i.e. $2.949(5)$ and $3.147(5)$ Å, Fig. 1.8, and in the case of $(o\text{-FC}_6\text{H}_4\text{CH}_2)_2\text{Sn}[\text{S}_2\text{C}(\text{N}(\text{CH}_2\text{CH}_2)_2\text{NEt})]\text{Cl}$ [63] with $\tau = 0.35$, the lower value of τ is due to the presence of an intramolecular $\text{Sn}\cdots\text{F}$ interaction of $3.518(15)$ Å. Finally, in the structure of $\text{Me}_2\text{Sn}(\text{S}_2\text{Cpiperidine})\text{Cl}$ [47], the presence of intermolecular secondary $\text{Sn}\cdots\text{S}$ interactions, that lead to the formation of a supramolecular zig-zag chain, Fig. 1.9, accounts for the variation in coordination geometry. The above notwithstanding, it is likely that it is the more symmetric mode of coordination for the dithiocarboxylate ligands in the $\text{R}_2\text{Sn}(\text{S}_2\text{CNR}'_2)\text{X}$ structures, Table 1.2, that accounts for the essentially molecular nature of these compounds.

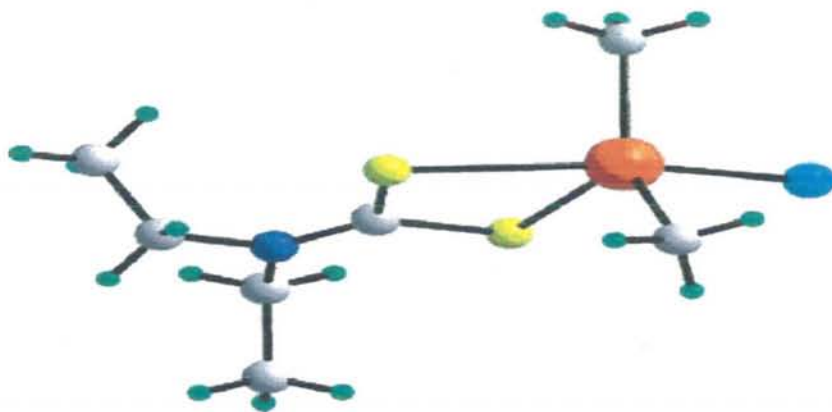


Fig. 1.7 Molecular structure of $\text{Me}_2\text{Sn}(\text{S}_2\text{CNEt}_2)\text{Cl}$, serving as an exemplar for structures of the general formula $\text{R}_2\text{Sn}(\text{S}_2\text{CNR}'_2)\text{X}$.

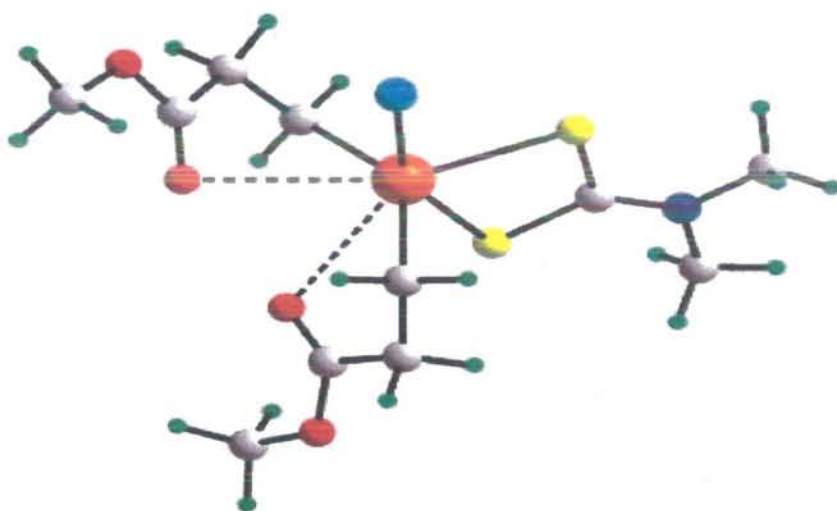


Fig. 1.8 Molecular structure of $[\text{MeO}(\text{O}=\text{CCH}_2\text{CH}_2)]_2\text{Sn}(\text{S}_2\text{CNMe}_2)\text{Cl}$, showing the presence of intramolecular $\text{Sn}\cdots\text{O}$ interactions that are responsible for the deviation of the C_2ClS_2 donor set toward a square pyramidal geometry.

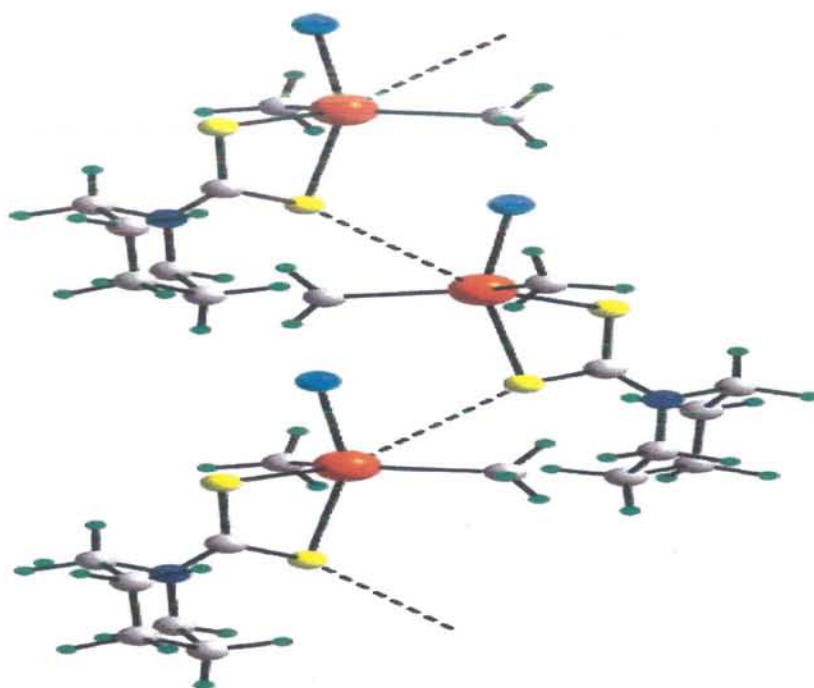


Fig. 1.9 Supramolecular zig-zag chain in the structure of $\text{Me}_2\text{Sn}(\text{S}_2\text{Cpiperidine})\text{Cl}$ mediated by secondary $\text{Sn}\cdots\text{S}$ interactions.

Table 1.2: Selected geometric parameters (Å, deg) for $R_2Sn(S_2CNR'_2)Cl$

Compound	Sn-S _{chelate}	C-Sn---S	τ	Reference
$Me_2Sn(S_2CNMe_2)Cl$	2.482(14), 2.805(14)	154.59(4)	0.45	[43]
$Me_2Sn(S_2CNEt_2)Cl$	2.463(2), 2.703(2)	157.53(8)	0.50	[44a]
$Me_2Sn[S_2CN(c-Hex)_2]Cl$	2.464(2), 2.659(2)	156.79(7)	0.52	[44a]
$Me_2Sn(S_2CNR^1)Cl^a$	2.4826(13), 2.7555(12)	154.49(4)	0.48	[45]
$Me_2Sn(S_2CNR^2)Cl^b$	2.4667(9), 2.7398(14)	154.19(3)	0.46	[46]
$Me_2Sn(S_2CNR^3)Cl^c$	2.4838(9), 2.7114(8)	154.57(2)	0.39	[47]
$Et_2Sn(S_2CNR^4)Cl^d$	2.4758(6), 2.6959(6)	156.58(2)	0.55	[48]
$(n-Bu)PhSn(S_2CNEt_2)Cl$	2.5452(12), 2.7446(17)	156.86(3)	0.49	[48]
$(n-Bu)_2Sn(S_2CNR^4)Cl^{d,e}$	2.4720(5), 2.7315(5)	155.11(2)	0.46	[50]
	2.4690(5), 2.7088(5)	155.67(2)	0.45	
$(t-Bu)_2Sn(S_2CNMe_2)Cl$	2.4866(11), 2.7418(13)	153.06(4)	0.45	[51]
$(t-Bu)_2Sn(S_2CNEt_2)Cl^e$	2.4794(18), 2.7318(18)	153.19(7)	0.41	[52]
	2.4824(19), 2.7340(19)	154.16(7)	0.42	
$(t-Bu)_2Sn(S_2CN(c-Hex)_2)Cl^e$	2.477(3), 2.744(4)	152.3(1)	0.47	[44b]
	2.471(3), 2.722(4)	152.0(1)	0.45	
$(t-Bu)_2Sn(S_2CNR^5)Cl^f$	2.492(2), 2.767(2)	150.01(6)	0.45	[53]
$(t-Bu)_2Sn(S_2CNR^6)Cl^g$	2.483(2), 2.751(2)	152.19(8)	0.46	[53]
$(t-Bu)_2Sn(S_2CN(Et)c-Hex)Cl$	2.479(3), 2.756(3)	152.58(9)	0.45	[44a]
$(c-Hex)_2Sn(S_2CNEt_2)Cl$	2.471(3), 2.768(2)	155.55(7)	0.45	[44a]
$(c-Hex)_2Sn[S_2CN(c-Hex)_2]Cl$	2.471(3), 2.680(2)	154.44(6)	0.51	[44a]
$Ph_2Sn(S_2CNEt_2)Cl$	2.4449(13), 2.7156(15)	157.82(6)	0.59	[52]
$Ph_2Sn[S_2CN(c-Hex)_2]Cl$	2.440(2), 2.657(2)	153.57(5)	0.47	[54]
$Ph_2Sn(S_2CNR^3)Cl^c$	2.4737(7), 2.6287(7)	154.68(2)	0.51	[55]
$Ph_2Sn(S_2CNR^2)Cl^b$	2.4614(6), 2.6570(6)	153.55(2)	0.51	[46]
$Ph_2Sn[S_2CN(Et)(c-Hex)]Cl$	2.459(3), 2.681(3)	157.3(1)	0.55	[56]
$Ph_2Sn(S_2CNMe_2)Br$	2.454(2), 2.668(2)	156.05(4)	0.38	[57]
$Ph_2Sn(S_2CNEt_2)I$	2.4504(12), 2.6699(10)	155.48(3)	0.57	[58]
$(C_6H_5CH_2)_2Sn(S_2CNMe_2)Cl$	2.4637(19), 2.707(2)	154.03(6)	0.48	[59]
$(C_6H_5CH_2)_2Sn(S_2CNR^3)Cl^c$	2.469(2), 2.666(2)	155.95(6)	0.52	[60]
$(C_6H_5CH_2)_2Sn(S_2CNR^7)Cl^h$	2.4738(11), 2.6716(12)	156.06(4)	0.52	[61]
$(C_6H_5CH_2)_2Sn(S_2CNR^8)Cl^i$	2.466(2), 2.724(3)	159.45(7)	0.58	[62]

$(o\text{-FC}_6\text{H}_4\text{CH}_2)_2\text{Sn}(\text{S}_2\text{CNR}^5)\text{Cl}^f$	2.4568(15), 2.659(2)	154.53(7)	0.35	[63]
$(p\text{-FC}_6\text{H}_4\text{CH}_2)_2\text{Sn}(\text{S}_2\text{CNR}^8)\text{Cl}^i$	2.466(2); 2.684(2)	157.30(6)	0.46	[39]
$(o\text{-ClC}_6\text{H}_4\text{CH}_2)_2\text{Sn}(\text{S}_2\text{CNR}^9)\text{Cl}^j$	2.4668(14), 2.6981(14)	156.66(4)	0.47	[66]
$(o\text{-ClC}_6\text{H}_4\text{CH}_2)_2\text{Sn}(\text{S}_2\text{CNR}^5)\text{Cl}^f$	2.4695(16), 2.6614(15)	155.83(5)	0.46	[65]
$(m\text{-ClC}_6\text{H}_4\text{CH}_2)_2\text{Sn}(\text{S}_2\text{CNBen}_2)\text{Cl}$	2.4694(15), 2.6573(14)	158.44(5)	0.53	[66]
$(p\text{-ClC}_6\text{H}_4\text{CH}_2)_2\text{Sn}(\text{S}_2\text{CNEt}_2)\text{Cl}$	2.455(2), 2.672(2)	156.86(2)	0.52	[67]
$(p\text{-ClC}_6\text{H}_4\text{CH}_2)_2\text{Sn}(\text{S}_2\text{CNR}^1)\text{Cl}^{a,k}$	2.471(3), 2.697(3)	158.52(7)	0.49	[68]
$\text{R}_2\text{Sn}(\text{S}_2\text{CNMe}_2)\text{Cl}^l$	2.5131(17), 2.6729(13)	153.91(5)	0.29	[69]
$[\text{PhSn}(\text{S}_2\text{CNEt}_2)(\text{S})(\text{CH}_2\text{CH}_2\text{CH}_2)\text{SnPh}(\text{S}_2\text{CNEt}_2)]$	2.4596(18), 2.894(2)	160.42(5)	0.68	[70]
	2.4658(17), 2.9573(18)	160.60(5)	0.70	
$(t\text{-Bu})_2\text{Sn}[\text{S}_2\text{CN}(\text{H})\text{CH}_2\text{CH}_2\text{N}(\text{H})\text{CS}_2]_2\text{Sn}(t\text{-Bu})_2^m$	2.459(3), 2.878(3)	155.79(7)	0.48	[71]

^aNR¹ = pyrrolidine. ^bNR² = 4-methylpiperidine. ^cNR³ = piperidine. ^dNR⁴ = 4-(*p*-nitrophenyl)piperazine. ^eTwo independent molecules in the asymmetric unit. ^fNR⁵ = 4-ethylpiperazine. ^gNR⁶ = 4-benzylpiperazine. ^hNR⁷ = piperazine. ⁱNR⁸ = morpholine. ^jNR⁹ = 4-methylpiperazine. ^kCompound crystallizes as a water solvate. ^lR¹ = CH₂CH₂C(=O)OMe. ^mCompound crystallizes as a tetrahydrofuran di-solvate.

1.5.3 Diorganotin(IV) dithiocarboxylates

In terms of crystallographic analyses, the diorganotin dithiocarboxylates, $\text{R}_2\text{Sn}(\text{S}_2\text{CNR}'_2)_2$, are the best studied and arguably the most interesting in terms of the observed structural diversity. There are two dinuclear diorganotin dithiocarboxylates available in the literature. There are 42 $\text{R}_2\text{Sn}(\text{S}_2\text{CNR}'_2)_2$ compounds in the literature that have been structurally characterized and when taking into account polymorphism, there are about 50 individual structure determinations [24, 66, 72-111]. A systematic analysis of these structures shows that there are four distinct structural motifs. The most prevalent motif is illustrated in Fig. 1.10 for $\text{Me}_2\text{Sn}(\text{S}_2\text{CNEt}_2)_2$ [73-75] Motif I features two asymmetrically coordinating dithiocarboxylates ligands that define a skewed trapezoidal plane and two tin-bound methyl groups that lie over the weaker Sn---S interactions so that the coordination geometry is best described as being skewed trapezoidal bipyramidal. There is a great deal of homogeneity in the geometric parameters describing these structures, Table 1.3. The short Sn-S bond

distances lie in the relatively narrow range 2.48–2.57 Å with the longer distances found in the structures with the more bulky tin-bound groups, e.g. *t*-butyl, cyclohexyl and *o*-ClC₆H₄CH₂. The longer distances fall in the range 2.81–3.08 Å. The structures uniformly have the sulfur atoms forming the shorter Sn–S bonds to one side of the SnS₄ plane and hence the skewed-trapezoidal planar description. With one exceptional structure, the S_{short}–Sn–S_{short} bond angles always lie in the range 78–88° and the S_{long}–Sn–S_{long} angles are always in the range 140–154°; normally the values are midway between these extremes. The exceptional structure is that of (*o*-ClC₆H₄CH₂)₂Sn[S₂C(4-methylpiperidine)]₂ [99], for which the S_{short}–Sn–S_{short} and S_{long}–Sn–S_{long} angles are 95.33(4) and 131.37(4)°, respectively. The presence of an intramolecular Sn---Cl interactions of 3.901(2) Å may be responsible for the widening of the S_{short}–Sn–S_{short} angle and concomitant narrowing of the S_{long}–Sn–S_{long} angle in this structure. However, it should be noted that discerning systematic trends from this class of compound is well known to be fraught with danger [111]. To illustrate this point, an examination of the trimorphic Me₂Sn(S₂CNEt₂)₂ [73–75] system shows that the Sn–S_{short} bond distances lie in the range 2.4877(10)–2.5307(8) Å, Sn–S_{long} 2.916(3)–3.0121(9) Å, S_{short}–Sn–S_{short} angles 81.95(3)–84.29(3)°, S_{long}–Sn–S_{long} 146.62(3)–149.49(3)°, and even the C–Sn–C angle 135.7(2)–142.62(5)°. These variations go well beyond experimental error and point to the influence of crystal packing upon their geometric parameters. Indeed, comparative investigations on organotin compounds, including organotin dithiocarboxylates, where experimental, i.e. crystallographic, structures are compared with geometry optimized structures obtained from *abinitio* molecular orbital calculations, i.e. theoretical, showed that molecules crystallizing in polymorphs optimize to the same energy minimized structure, and structures with multiple molecules in the asymmetric unit similarly optimize to a single energy minimized structure [112]. The generally applicable conclusion from these studies was that molecular structures were syntactic with their crystalline manifold and adjustments in bond distances and angles were made to accommodate the dictates of crystal packing. In the absence of crystal packing effects, chemically equivalent geometric parameters are equal and, whenever chemically possible, the molecular structures became symmetric [112]. The second motif for the R₂Sn(S₂CNR'₂)₂ compounds is adopted exclusively by the R = Ph derivatives, Table 1.3. This observation supports the notion that, relative to their alkyl (and vinyl)

counterparts, phenyl substituents are less electropositive/more electronegative so that the resulting $\text{Ph}_2\text{Sn}(\text{S}_2\text{CNR}'_2)_2$ structures are octahedral. The exemplar structure for motif II is $\text{Ph}_2\text{Sn}(\text{S}_2\text{CNEt}_2)_2$, shown in Fig. 1.11, which highlights the distorted octahedral geometry and the *cis*-disposition of the tin-bound phenyl groups. In fact, this compound crystallizes in two polymorphs, a monoclinic polymorph with no crystallographically imposed molecular symmetry [104], and a tetragonal polymorph with crystallographic two-fold symmetry [24]. Unrestricted geometry optimization calculations showed that both experimental structures converged to the same energy minimized structure, with two-fold symmetry, so that experimentally distinct geometric parameters observed in the crystal structures were artifacts of the crystal packing and not due to any inherent chemical reason [44b]. While an electronic reason can be discerned for the appearance of motif II, no obvious reason can be proffered for the appearance of motif III, adopted by one example, namely $(t\text{-Bu})_2\text{Sn}(\text{S}_2\text{CNMe}_2)_2$ [109], shown in Fig. 1.12. This structure is quite readily related to the skewed trapezoidal bipyramidal geometry for motif I. As a starting point, the structure of the diethyldithiocarboxylate analogue, i.e. $(t\text{-Bu})_2\text{Sn}(\text{S}_2\text{CNEt}_2)_2$ [90], is considered. Simply, there is a twist about one of the short Sn–S bonds so that the weakly coordinated dithiocarboxylate-sulfur atom is moved to a position approximately orthogonal to the original SnS_4 plane. In so doing, the Sn---S distance expands to 3.5319(11) Å, clearly non-bonding. Both Sn–S bond distances of the remaining chelating dithiocarboxylate ligand decrease significantly and the C–Sn–C angle contracts to 119.1(1)°. The resulting coordination geometry is intermediate between square pyramidal and trigonal bipyramidal as seen in the value of $\tau = 0.47$ [11]. There are several examples in the literature, where the difference between structures is found solely in the nature of the nitrogen-bound substituent but the structures of $(t\text{-Bu})_2\text{Sn}(\text{S}_2\text{CNR}_2)_2$, R = Me [91] and Et [109], are the only examples where such a profound difference in the molecular structure is observed. The fourth and final motif for the $\text{R}_2\text{Sn}(\text{S}_2\text{CNR}'_2)_2$ structures is also readily related to motif I. The molecular structure of $[\text{MeO}(\text{O}=\text{C})\text{CH}_2\text{CH}_2]_2\text{Sn}(\text{S}_2\text{CNMe}_2)_2$ [110], is represented in Fig. 1.15. Here, the tin-bound groups carry additional donor atoms for coordination to tin and one of these in fact forms an intramolecular Sn---O interaction. To a first approximation, the coordination geometry can be thought of as skewed trapezoidal bipyramidal as for motif I. As noted in Fig. 1.13, the carbonyl-oxygen atom of one of

the $\text{MeO}(\text{O}=\text{C})\text{CH}_2\text{CH}_2$ groups approaches the tin atom in the SnS_4 plane. The $\text{Sn}\cdots\text{O}$ separation is $2.75(2)$ Å and this association results in the formation of a five-membered SnC_3O chelate ring. As expected, there are some geometric consequences of the close association of the carbonyl-oxygen atom. The $\text{S}_{\text{long}}\text{---Sn}\text{---S}_{\text{long}}$ angle opens up by about 5° compared with the motif I structures but, interestingly, the $\text{S}_{\text{short}}\text{---Sn}\text{---S}_{\text{short}}$ angle of $81.91(9)^\circ$ falls in the range of $\text{S}_{\text{short}}\text{---Sn}\text{---S}_{\text{short}}$ angles, albeit the lower end. This suggests that the sulfur atoms forming $\text{Sn}\text{---S}_{\text{short}}$ bond distances cannot get any closer, no doubt for steric reasons. In order to accommodate the incoming oxygen atom, these sulfur atoms have elongated their $\text{Sn}\text{---S}$ bonds compared with those of motif I and, concomitantly, one of the $\text{Sn}\text{---S}_{\text{long}}$ distances has contracted [$2.847(4)$ Å] and the other is at the lower end of the $\text{Sn}\text{---S}_{\text{long}}$ range [$2.914(5)$ Å]. The presence of an $\text{Sn}\cdots\text{O}$ intramolecular interaction in the structure of $[\text{MeO}(\text{O}=\text{C})\text{CH}_2\text{CH}_2]_2\text{Sn}(\text{S}_2\text{CNMe}_2)_2$ [110], raises the question whether any other of the $\text{R}_2\text{Sn}(\text{S}_2\text{CNR}'_2)_2$ structures associate in the solid-state via secondary $\text{Sn}\cdots\text{S}$ interactions [113]. An analysis of the crystal packing for these compounds showed that, in fact, seven out of the 36 structures adopting motif I do in fact form $\text{Sn}\cdots\text{S}$ contacts with centrosymmetrically related mates. The magnitude of the $\text{Sn}\cdots\text{S}$ distances vary from long $3.9071(13)$ Å in $(o\text{-ClC}_6\text{H}_4\text{CH}_2)_2\text{Sn}[\text{S}_2\text{C}(4\text{-methylpiperidine})]_2$ [101] $3.853(3)$ Å in $\text{Me}_2\text{Sn}(\text{S}_2\text{CNEt}_2)_2$ [75], $3.821(3)$ Å in $(p\text{-NCC}_6\text{H}_4\text{CH}_2)_2\text{Sn}(\text{S}_2\text{CNEt}_2)_2$ [66] $3.8162(10)$ Å in $(\text{PhCH}_2)_2\text{Sn}(\text{S}_2\text{CNEt}_2)_2$ [94] $3.765(3)$ Å in $(p\text{-ClC}_6\text{H}_4\text{CH}_2)_2\text{Sn}[\text{S}_2\text{C}(4\text{-methylpiperidine})]_2$ [103] $3.662(5)$ Å in $[\text{H}_2\text{C}=\text{(H)C}]_2\text{Sn}[\text{S}_2\text{CN}(\text{c-Hex})]_2$ [83] illustrated in Fig. 1.14, and $3.638(3)$ Å in $(m\text{-ClC}_6\text{H}_4\text{CH}_2)_2\text{Sn}[\text{S}_2\text{C}(4\text{-ethylpiperazine})]_2$ [101]. While these interactions are weak they fall within the sum of the van der Waals radii of tin and sulfur, taken as 4.0 Å [114]. While there is a dominance of dibenzyl derivatives in this listing, the lack of systematic trends for such $\text{Sn}\cdots\text{S}$ secondary interactions is highlighted by the fact that they are observed in the triclinic form of $\text{Me}_2\text{Sn}(\text{S}_2\text{CNEt}_2)_2$ [75] but not in the orthorhombic [73] nor monoclinic forms [74, 75]. As noted in Table 1.3, some of the dithiocarboxylate ligands carry hydrogen-bonding functionality so that, while the sulfur atoms of the dithiocarboxylate ligands rarely engage in supramolecular aggregation, certainly not to form extended arrays, the substituents might [115] This is illustrated in Fig. 1.15 for the structure of $\text{Me}_2\text{Sn}[\text{S}_2\text{CN}(\text{CH}_2\text{CH}_2\text{OH})]_2$ [76], where

cooperative hydrogen bonding links the molecules into a supramolecular zig-zag chain.

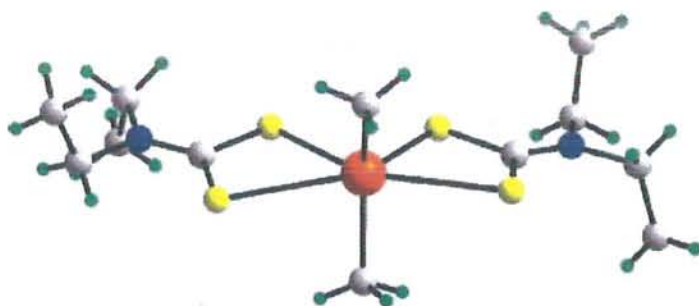


Fig. 1.10 Molecular structure of $\text{Me}_2\text{Sn}(\text{S}_2\text{CNEt}_2)_2$, serving as an exemplar of motif I for structures of the general formula $\text{R}_2\text{Sn}(\text{S}_2\text{CNR}'_2)_2$.

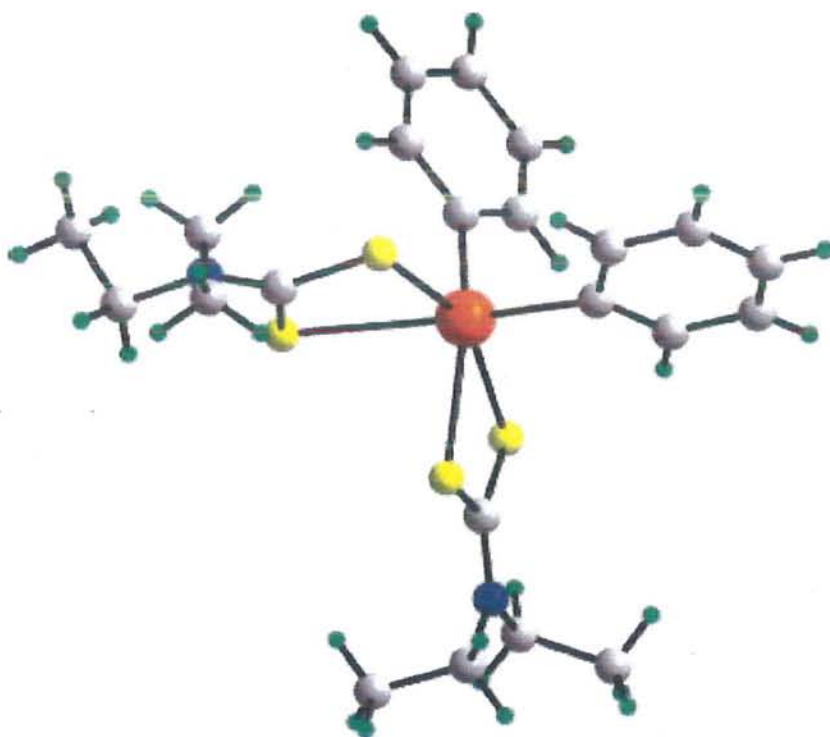


Fig. 1.11 Molecular structure of $\text{Ph}_2\text{Sn}(\text{S}_2\text{CNEt}_2)_2$, serving as an exemplar of motif II for structures of the general formula $\text{R}_2\text{Sn}(\text{S}_2\text{CNR}'_2)_2$.

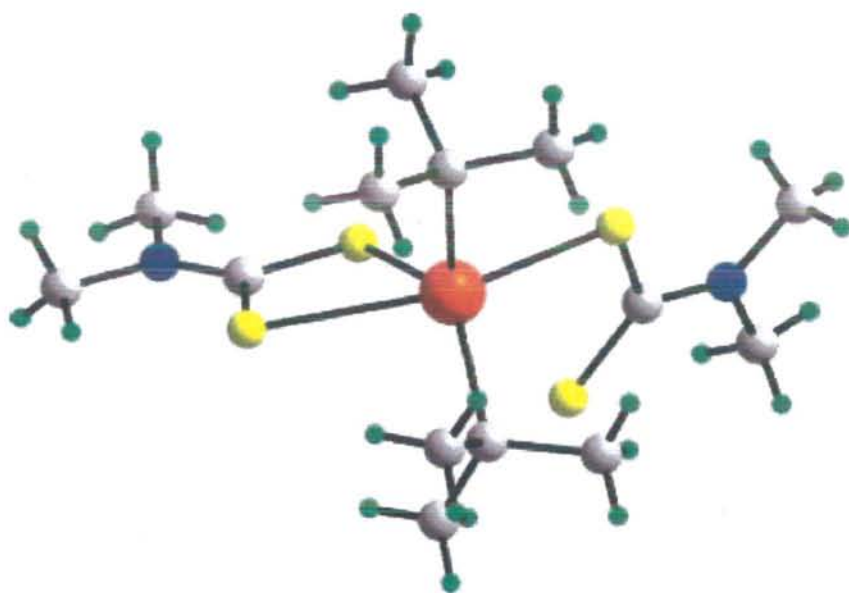


Fig. 1.12 Molecular structure of $(t\text{-Bu})_2\text{Sn}(\text{S}_2\text{CNMe}_2)_2$, the sole example for motif III for structures of the general formula $\text{R}_2\text{Sn}(\text{S}_2\text{CNR}'_2)_2$.

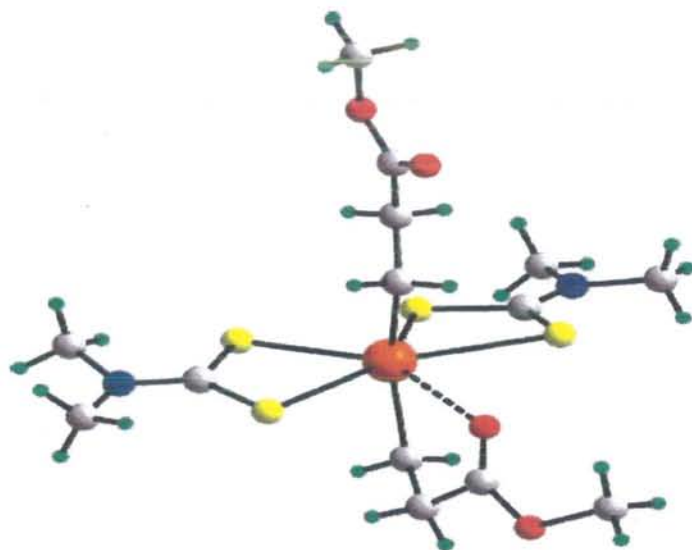


Fig. 1.13 Molecular structure of $[\text{MeO}(\text{O}=\text{C})\text{CH}_2\text{CH}_2]_2\text{Sn}(\text{S}_2\text{CNMe}_2)_2$, the sole example for motif IV for structures of the general formula $\text{R}_2\text{Sn}(\text{S}_2\text{CNR}'_2)_2$.

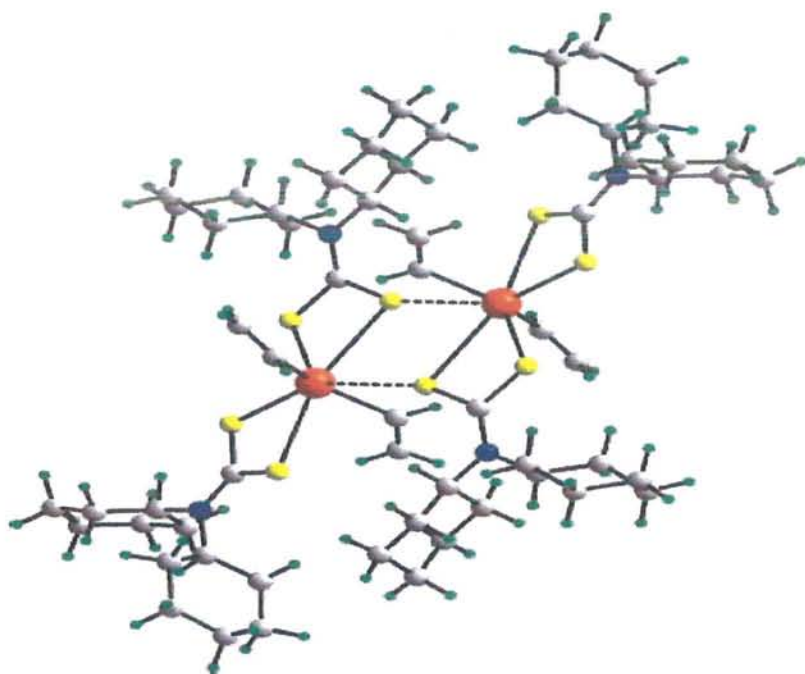


Fig. 1.14 Dimer formation in the structure of $[\text{H}_2\text{C}=\text{(H)C}]_2\text{Sn}[\text{S}_2\text{CNCy}_2]_2$, via secondary Sn---S interactions.

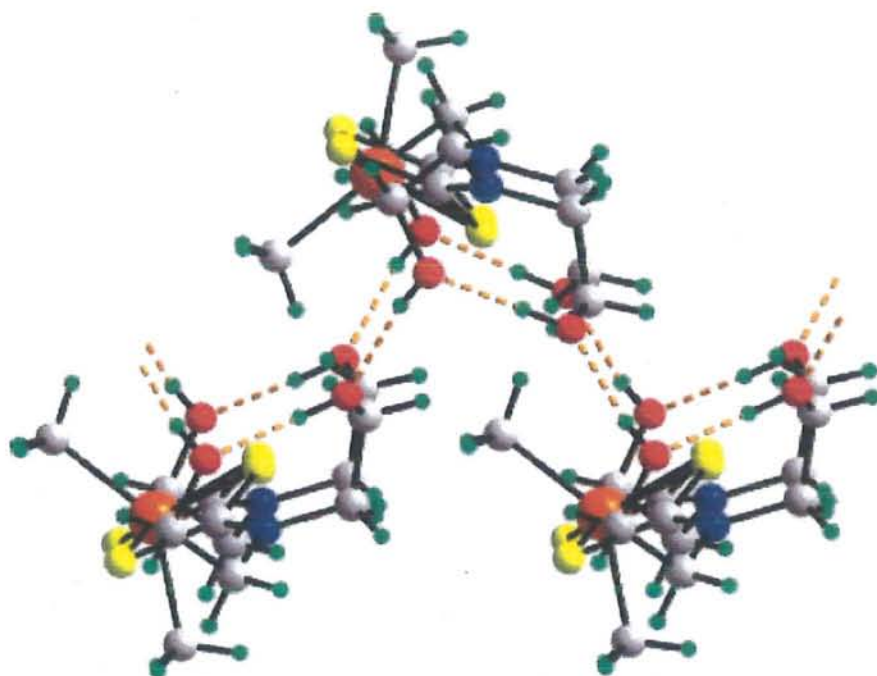


Fig. 1.15 Supramolecular zig-zag chain formation via O-H...O hydrogen (orange-dashed lines) in the structure of $\text{Me}_2\text{Sn}[\text{S}_2\text{CN}(\text{CH}_2\text{CH}_2\text{OH})_2]_2$.

The final two diorganotin structures to be discussed are dinuclear. The structure of $[\text{PhSn}(\text{S}_2\text{CNEt}_2)(\text{S})(\text{CH}_2\text{CH}_2\text{CH}_2)\text{SnPh}(\text{S}_2\text{CNEt}_2)]$ [70] has non-crystallographic two fold symmetry and a bridging organic ligand connecting the two tin atoms, Fig. 1.16 and Table 1.2. Each tin atom is chelated by an asymmetrically chelating dithiocarboxylate ligand, a sulfur atom derived from the bridging sulfide atom and two carbon atoms derived from organic substituents. Indeed, this structure can be readily related to the $\text{R}_2\text{Sn}(\text{S}_2\text{CNR}')\text{X}$ structures just described in that X is now a sulfur atom and one of the tin-bound R groups is one end of a bridging organic ligand. The pattern of Sn–S bond distances is consistent with this notion, with the longer distance occupying a position approximately *trans*- to the bridging sulfur atom. The coordination geometries are distinct, however. Based on a comparison of the values of τ , Table 1.2, the geometries for the tin atoms in the dinuclear compound are decidedly more trigonal bipyramidal. The dinuclear and centrosymmetric structure of $(t\text{-Bu})_2\text{Sn}(\text{S}_2\text{CN}(\text{H})\text{CH}_2\text{CH}_2\text{N}(\text{H})\text{CS}_2)_2\text{Sn}(t\text{-Bu})_2$, isolated as a tetrahydrofuran di-solvate [72], is shown in Fig. 1.17; see Table 1.2 for geometric parameters. This structure features two tin atoms bridged by a pair of bi-functional dithiocarboxylate ligands. The coordination geometry comprises one asymmetrically coordinating dithiocarboxylate ligand, a monodentate ligand [Sn---S is 3.607(3) Å] and two organic substituents. The coordination geometry is almost identical to that observed for motif III of the $\text{R}_2\text{Sn}(\text{S}_2\text{CNR}')_2$ structures, represented by $(t\text{-Bu})_2\text{Sn}(\text{S}_2\text{CNMe}_2)_2$ Fig. 1.12.

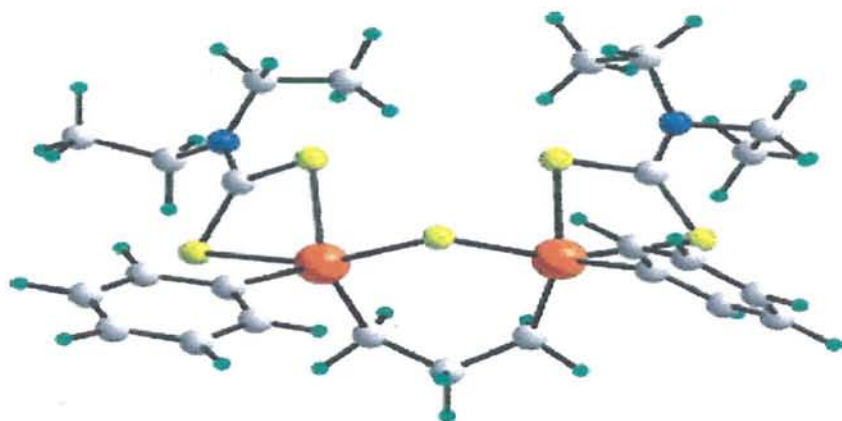


Fig. 1.16 Molecular structure of dinuclear $\text{PhSn}(\text{S}_2\text{CNEt}_2)(\text{S})(\text{CH}_2\text{CH}_2\text{CH}_2)\text{SnPh}(\text{S}_2\text{CNEt}_2)$.

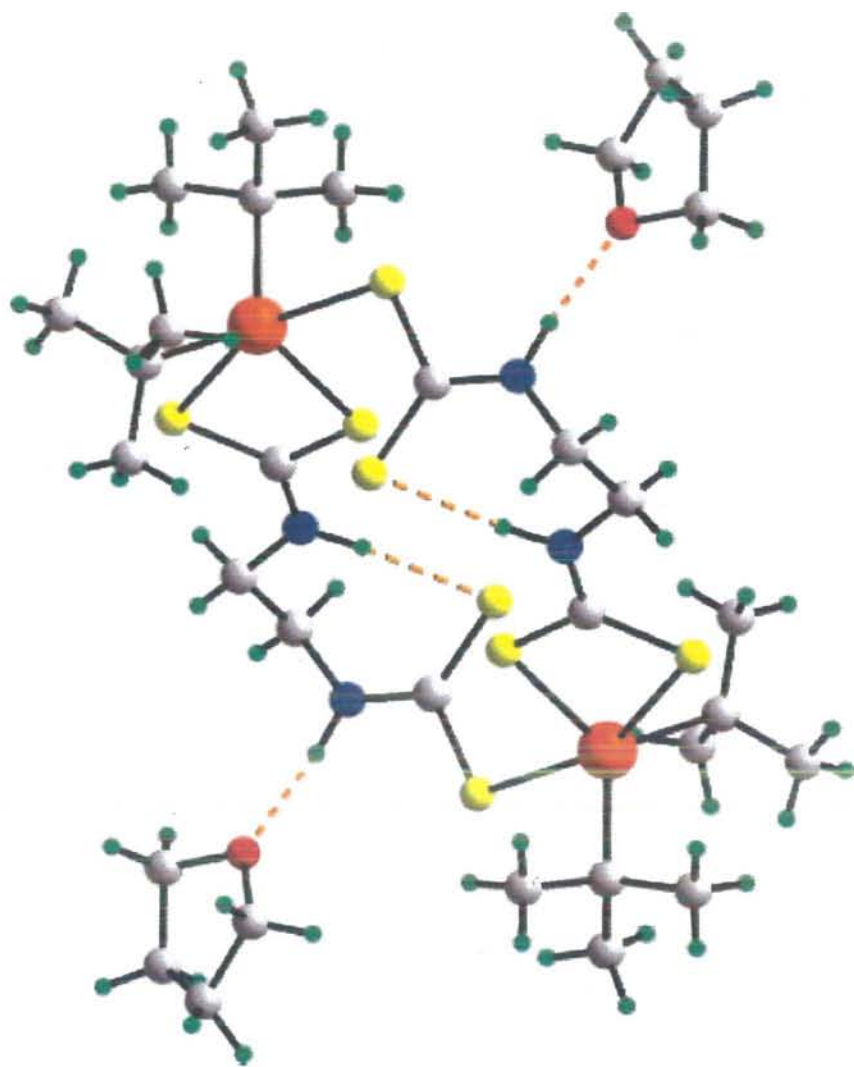


Fig. 1.17 Molecular structure of centrosymmetric $(t\text{-Bu})_2\text{Sn}[\text{S}_2\text{CN}(\text{H})\text{CH}_2\text{CH}_2\text{N}(\text{H})\text{CS}_2]_2$, featuring a bi-functional dithiocarbamate ligand. Orange dashed bonds represent $\text{N-H}\cdots\text{O}$ and $\text{N-H}\cdots\text{S}$ hydrogen bonds.

Table 1.3: Selected geometric parameters (Å, deg) for $R_2Sn(S_2CNR'_2)_2$

Compound	Sn-S _{chelate}	C-Sn-C	Reference
<i>Motif I</i>			
$Me_2Sn(S_2CNMe_2)_2$	2.4975(13), 2.9538(7); 2.5152(9), 3.0606(9)	136.449(9)	[72]
$Me_2Sn(S_2CNEt_2)_2^a$	2.4877(10), 2.9376(9); 2.515(1), 3.0544(11)	135.7(2)	[73]
$Me_2Sn(S_2CNEt_2)_2^{b,c,d}$	2.5209(8), 2.9390(9); 2.5307(8), 3.0121(9) 2.5288(9), 2.9546(11)	136.9(1) 142.0(1)	[74,75]
$Me_2Sn(S_2CNEt_2)_2^e$	2.517(3), 2.961(3); 2.528(2), 2.916(3)	142.62(5)	[75]
$Me_2Sn[S_2CN(CH_2CH_2OH)_2]_2^f$	2.5126(7), 3.0427(7)	139.3(1)	[78]
$Me_2Sn[S_2CN(Me)c-Hex]_2^f$	2.5169(7), 2.9785(6)	137.0(2)	[77]
$Me_2Sn(S_2Cpyrrole)_2$	2.510(2), 3.009(2); 2.532(2), 3.024(2)	135.9(2)	[78]
$Me_2Sn(S_2CNR^1)_2^g$	2.521(2), 2.918(2); 2.541(2), 2.908(2)	131.2(3)	[79]
$Me_2Sn(S_2CNR^2)_2^{c,h}$	2.504(1), 2.892(2); 2.533(2), 3.040(2) 2.520(2), 2.919(2); 2.536(1), 2.917(2)	134.0(2) 138.5(2)	[80]
$Me_2Sn(S_2CNR^3)_2^i$	2.5240(4), 2.9715(4); 2.5190(4), 2.9779(4)	135.64(7)	[81]
$[H_2C=(H)C]_2Sn(S_2CNEt_2)_2$	2.495(5), 2.871(5); 2.515(4), 3.078(5)	135.7(8)	[82]
$[H_2C=(H)C]_2Sn[S_2CN(Et)Cy]_2$	2.513(5), 3.071(4); 2.523(4), 2.826(5)	133.4(4)	[82]
$[H_2C=(H)C]_2Sn(S_2CNCy_2)_2$	2.514(4), 2.914(3); 2.536(3), 2.914(4)	139.5(4)	[82]
$(n-Bu)_2Sn(S_2CNEt_2)_2^c$	2.5089(16), 2.9084(17); 2.5251(15), 3.0478(18)	132.7(2)	[83]

	2.5386(16), 2.9037(15);	140.8(2)	
	2.5494(14); 2.9517(16)		
$(n\text{-Bu})_2\text{Sn}[\text{S}_2\text{CN}(\text{nPr})_2]_2$	2.5255(12), 3.0210(13);	132.6(2)	[84]
	2.5287(14), 2.9375(11)		
$(n\text{-Bu})_2\text{Sn}[\text{S}_2\text{CN}(\text{iPr})_2]_2^j$	2.5296(17), 2.9443(18)	131.4(4)	[85]
$(n\text{-Bu})_2\text{Sn}(\text{S}_2\text{CNR}^4)_2^k$	2.5338(6), 2.9697(11);	139.4(1)	[86]
	2.5323(9), 2.9834(10)		
$(n\text{-Bu})_2\text{Sn}(\text{S}_2\text{CNR}^1)_2^{g,l}$	2.477(4), 2.965(5)	147.2(5)	[87]
$(n\text{-Bu})_2\text{Sn}(\text{S}_2\text{CNR}^5)_2^{l,m}$	2.526(3), 3.001(4)	139.7(2)	[88]
$(n\text{-Bu})_2\text{Sn}(\text{S}_2\text{CNR}^2)_2^h$	2.5362(14), 2.9189(15);	135.4(1)	[89]
	2.5347(14), 2.9942(16)		
$(t\text{-Bu})_2\text{Sn}(\text{S}_2\text{CNEt}_2)_2^l$	2.5537(15), 2.9539(17)	146.16(7)	[90]
$(\text{c-Hex})_2\text{Sn}(\text{S}_2\text{CNMe}_2)_2^l$	2.568(2), 2.914(2)	150.2(3)	[91]
$(\text{c-Hex})_2\text{Sn}[\text{S}_2\text{CN}(\text{Et})(\text{c-Hex})]_2$	2.5290(14), 2.9466(15);	138.0(2)	[92]
	2.5394(15), 2.9604(15)		
$(\text{PhCH}_2)_2\text{Sn}(\text{S}_2\text{CNMe}_2)_2$	2.526(2), 2.897(2);	135.2(3)	[93]
	2.531(2), 3.046(2)		
$(\text{PhCH}_2)_2\text{Sn}(\text{S}_2\text{CNEt}_2)_2$	2.5309(9), 2.8940(11);	145.1(2)	[94]
	2.5396(9), 2.9109(10)		
$(\text{PhCH}_2)_2\text{Sn}(\text{S}_2\text{CNBen}_2)_2$	2.520(2), 2.942(2);	136.6(2)	[95]
	2.521(2), 3.004(2)		
$(\text{PhCH}_2)_2\text{Sn}(\text{S}_2\text{CNR}^4)_2^l$	2.521(1), 2.909(1)	143.5(2)	[96]
$(\text{PhCH}_2)_2\text{Sn}(\text{S}_2\text{CNR}^1)_2^g$	2.540(8), 2.954(8);	141.5(6)	[97]
	2.552(8), 2.966(8)		
$(\text{PhCH}_2)_2\text{Sn}(\text{S}_2\text{CNR}^5)_2^m$	2.532(2), 2.890(3);	139.1(4)	[98]
	2.539(2), 2.890(3)		
$(o\text{-FC}_6\text{H}_4\text{CH}_2)_2\text{Sn}(\text{S}_2\text{CNR}^4)_2^l$	2.504(2), 2.897(2)	140.1(2)	[99]
$(o\text{-ClC}_6\text{H}_4\text{CH}_2)_2\text{Sn}(\text{S}_2\text{CNR}^6)_2^n$	2.5676(13), 2.8675(11);	150.6(2)	[100]
	2.5401(13), 2.8049(12)		
$(m\text{-ClC}_6\text{H}_4\text{CH}_2)_2\text{Sn}(\text{S}_2\text{CNR}^7)_2^o$	2.520(3), 2.840(2);	147.7(2)	[101]
	2.555(2), 2.893(2)		
$(p\text{-FC}_6\text{H}_4\text{CH}_2)_2\text{Sn}(\text{S}_2\text{CNMe}_2)_2$	2.526(2), 2.953(2);	129.2(2)	[64]
	2.519(3), 3.002(2)		

$(p\text{-ClC}_6\text{H}_4\text{CH}_2)_2\text{Sn}(\text{S}_2\text{CNMe}_2)_2^{\text{a}}$	2.526(2), 2.933(3)	136.8(1)	[99]
$(p\text{-ClC}_6\text{H}_4\text{CH}_2)_2\text{Sn}(\text{S}_2\text{CNR}^6)_2^{\text{n}}$	2.534(2), 2.968(2); 2.550(2), 2.858(3)	146.9(2)	[102]
$(p\text{-ClC}_6\text{H}_4\text{CH}_2)_2\text{Sn}(\text{S}_2\text{CNR}^6)_2^{\text{l,m}}$	2.5249(14), 2.9920(16)	139.9(2)	[103]
$(p\text{-NCC}_6\text{H}_4\text{CH}_2)_2\text{Sn}(\text{S}_2\text{CNEt}_2)_2$	2.524(3), 2.885(3); 2.537(2), 2.879(2)	147.7(3)	[66]
<i>Motif II</i>			
$\text{Ph}_2\text{Sn}(\text{S}_2\text{CNEt}_2)_2^{\text{b}}$	2.558(3); 2.777(3); 2.607(3), 2.632(3)	101.7(3)	[104]
$\text{Ph}_2\text{Sn}(\text{S}_2\text{CNEt}_2)_2^{\text{lp}}$	2.556(2), 2.659(2)	101.1(3)	[24]
$\text{Ph}_2\text{Sn}[\text{S}_2\text{CN}(\text{c-Hex})_2]_2$	2.567(2), 2.692(2); 2.576(2), 2.678(2)	103.1(3)	[105]
$\text{Ph}_2\text{Sn}[\text{S}_2\text{CN}(\text{CH}_2\text{CH}_2\text{OH})_2]_2$	2.5395(9), 2.8271(9); 2.6063(9), 2.6235(11)	104.9(1)	[106]
$\text{Ph}_2\text{Sn}[\text{S}_2\text{CN}(\text{Me})\text{CH}_2\text{CH}_2\text{OH}]_2$	2.5497(14), 2.7474(16); 2.6145(15), 2.6411(17)	102.7(2)	[107]
$\text{Ph}_2\text{Sn}(\text{S}_2\text{CNR}^4)_2^{\text{k,q}}$	2.574(1), 2.950(1); 2.586(2), 2.685(2)	107.6(2)	[110]
<i>Motif III</i>			
$(t\text{-Bu})_2\text{Sn}(\text{S}_2\text{CNMe}_2)_2$	2.4892(14), 2.7952(9); 2.5727(12), 3.5319(11)	119.1(1)	[109]
<i>Motif IV</i>			
$\text{R}^1_2\text{Sn}(\text{S}_2\text{CNMe}_2)_2^{\text{r}}$	2.570(4), 2.847(4); 2.599(4), 2.914(5)	154.4(4)	[110]

^aOrthorhombic form. ^bMonoclinic form. ^cTwo independent molecules in the asymmetric unit. ^dThe second molecule has crystallographic two-fold symmetry. ^eTriclinic form. ^fMolecule has crystallographic mirror symmetry. ^g NR^1 = piperidine. ^h NR^2 = 4-methylpiperidine. ⁱ NR^3 = 4-benzylpiperidine. ^jThe tin atom is located on a crystallographic site of symmetry *mm*2. ^k NR^4 = pyrrolidine. ^lMolecule has crystallographic two-fold symmetry. ^m NR^5 = morpholine. ⁿ NR^6 = 4-methylpiperazine. ^o NR^7 = 4-ethylpiperazine and compound crystallizes as a piperidine hemi-solvate. ^pTetragonal form. ^qCompound crystallizes as a toluene solvate. ^r R^1 = $\text{CH}_2\text{CH}_2\text{C}(\text{O})\text{OMe}$.

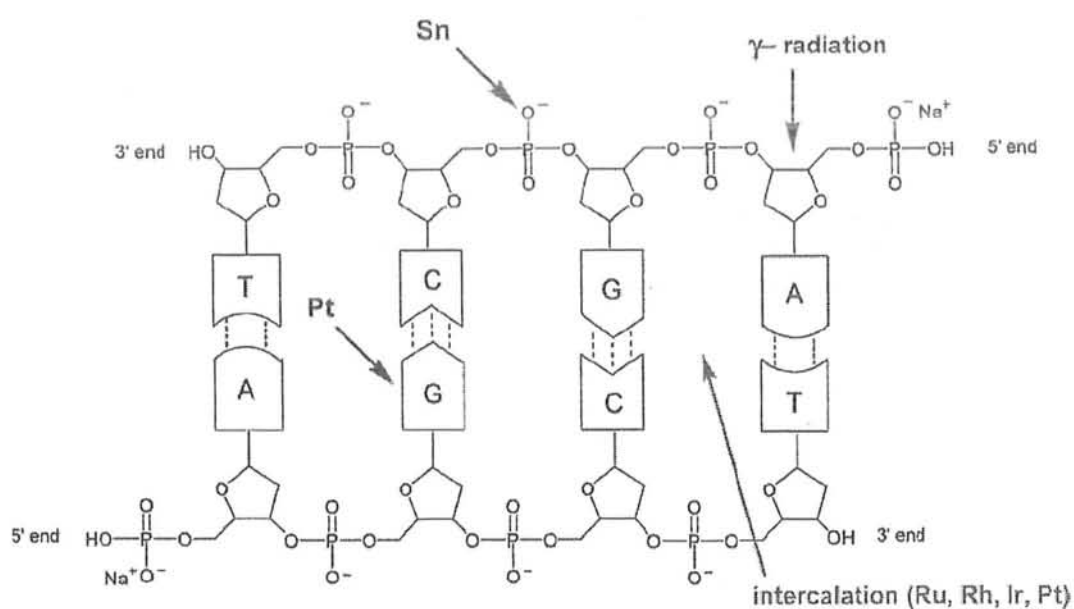
1.6 Biological activities of organotin(IV) dithiocarboxylates

The biological activities of organotin(IV) dithiocarboxylates can be briefly reviewed under the following main headings.

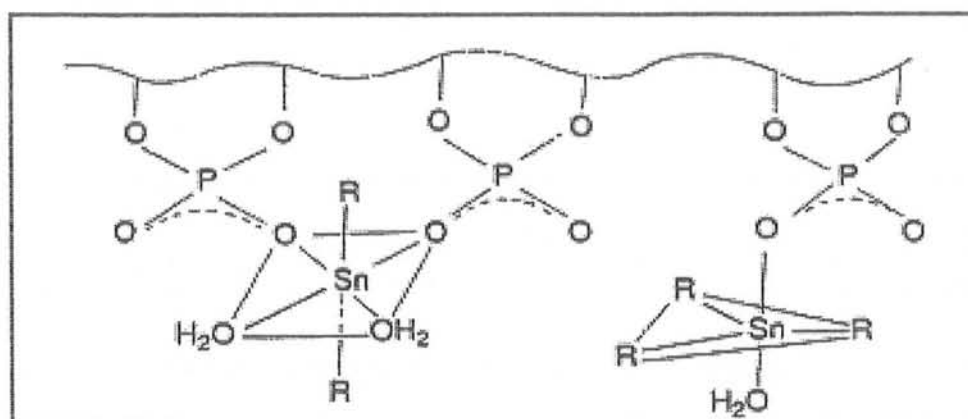
- (i) Anti-tumor activity
- (ii) Antifungal and antibacterial activities
- (iii) Insecticidal activity

1.6.1 Anti-tumor activity

Cancer is a leading cause of premature deaths in the world. It can be cured by arresting DNA replication. There are several ways to induce irreparable DNA damage, which may cause the arrest of its replication and create condition for apoptosis (scheme 1.1). Ionizing radiation causes indirect damage to the DNA via reactive oxygen species, whereas chemotherapy uses chemical substances that directly interact with DNA. Research has proven that the most effective and widely used coordination compounds as anticancer are the DNA nitrogen base binding cisplatin, oxalyplatin, nedaplatin and carboplatin, all of which are metallocomplexes of platinum(II). In spite of its high activity, the application of cisplatin and similar compounds has significant disadvantages that include: (i) poor water solubility, (ii) severe side effects that are typical of heavy metals toxicity, and (iii) the development of drug tolerance by the tumor. The last two are the major driving force behind current research in the field of novel anticancer agent development. Among these organotins received utmost attention on account of their potential apoptotic inducing character. Moreover, organotin(IV) complexes exhibit other attractive properties such as increased water solubility, lower general toxicity than platinum drugs [116], better body clearance, fewer side effects, and no emetogenesis. Most importantly, organotin complexes do not develop the tumor drug tolerance that is well established for cisplatin and its analogues. Recent first attempts in developing the quantitative structure/activity and the structure/property relationships for organotin compounds have been reviewed [117]. The interaction of organotins with the DNA is mainly of two types: (i) electrostatic interaction, in which organotins interact with the anionic phosphate of DNA backbone (Scheme 1.2), (ii) intercalation, in which organotins insert themselves into the stack base pairs of DNA.



Scheme 1.1 Mode of interaction of metal complexes with DNA.



Scheme 1.2: Interaction of tri- and diorganotins with phosphate anion of DNA.

Building upon earlier work [118], a series of phenyltin(IV) dithiocarboxylates were evaluated for their cytotoxicity against L1210 mouse leukaemia cell lines [24]. It was found that the series of compounds $\text{Ph}_{4-n}\text{Sn}(\text{S}_2\text{CNET}_2)_n$, for $n = 1-3$, gave a 50% growth inhibition ratings of 0.3 μM compared with 0.6 and 1.2 μM for the drugs cisplatin and carboplatin, respectively. Interestingly, the introduction of chloride, as in $\text{PhSn}(\text{S}_2\text{CNET}_2)_2\text{Cl}$ and $\text{Ph}_2\text{Sn}(\text{S}_2\text{CNET}_2)\text{Cl}$, resulted in less toxicity, with ratings of 0.4 and 0.08 μM , respectively, but these were still more cytotoxic than the platinum-containing drugs. In a more extensive study, a series of 10 organotin dithiocarboxylates were evaluated against a larger panel of human cancer cell lines [66]. Here, the opposite conclusion was found in those compounds of the general formula $(\text{ArCH}_2)_2\text{Sn}(\text{S}_2\text{CNR}'_2)\text{Cl}$ were more cytotoxic than their counterparts without chloride substituents, i.e. $\text{ArCH}_2)_2\text{Sn}(\text{S}_2\text{CNR}'_2)_2$. The authors of this study suggested that this observation might be related to the ease of hydrolysis of the former [66]. The most cytotoxic compound of the series was $(4\text{-NC-C}_6\text{H}_4\text{CH}_2)_2\text{Sn}[\text{S}_2\text{CN}(\text{CH}_2\text{CH}_2)_2\text{NCH}_3]\text{Cl}$, with ratings against breast- (MCF-7 and EVSA-T), colon- (WiDr), ovarian- (IGROV) and non-small-cell lung-cancer (M226) cell lines of 8, 14, 34, 11 and 16 ng ml^{-1} , at least an order of magnitude more cytotoxic than exhibited by cisplatin. The organic drug doxorubicin was the other standard, with cytotoxicity ratings intermediate between the organotin compounds and cisplatin [66].

1.6.2 Antifungal and antibacterial activities

The potential anti-fungal activity of tin dithiocarboxylates has attracted attention in terms of targeting fungi implicated in wood preservation, plant pathogens and in immuno-compromised patients [46,86,119–124]. A series of organotin dithiocarboxylates analogous to those studied in a cytotoxicity trial described above [24], were also screened for activity against *Candida albicans*, *Candida tropicalis* and resistant *Candida albicans* [121]. This study showed that, while all organotin dithiocarboxylates studied were fungicidal, it was the triphenyltin dithiocarboxylates, $\text{Ph}_3\text{Sn}(\text{S}_2\text{CNET}_2)$, and its pyrrolidine derivative that had the lowest minimal inhibitory concentrations [122]. Indeed, in terms of tin-bound substituents, the general trend of potency was $\text{Ph}_3 > n\text{-Bu}_2 > \text{Cl}_2 > \text{Ph}_2 > \text{Ph} \sim \text{Cy}_3$. A correlation was found between increasing fungicidal activity and decreasing biosynthesis of ergosterol. Finally, the importance of the presence of tin was illustrated in that all organotin compounds investigated had activities greater than those exhibited by the uncoordinated

dithiocarboxylate ligands administered on their own [122], in keeping with earlier observations [119–121]. This observation does not necessarily hold true when considering anti-bacterial activity, where the opposite trend has sometimes been reported.[46,123,124] For the series of compounds $R_2Sn[S_2CN(CH_2CH_2)_2C(H)CH_3]Cl$, where the dithiocarboxylate ligand is derived from 4-methylpiperidine, the $R = Ph$ derivative displayed the greatest anti-fungal activity but it was the $R = n\text{-Bu}$ species that probably exhibited the better antibacterial activity [46]. A series of compounds of the general formula $(SCH_2CH_2S)Sn(S_2CNR'_2)Cl$ have been evaluated against a range of bacteria [124]. While not effective against *E. coli*, some promising activity was found against a range of Gram-positive and Gram-negative bacteria. As with all the trials, usually the commercially available drugs were more active, but investigations continue in order to develop more potent derivatives so to overcome the current and projected problems of organisms developing drug-resistance.

1.6.3 Insecticidal activity

The insecticidal activity of a series of $R_3Sn(S_2CNR'_2)$ compounds, for $R = Ph$ and Cy , against the second larval instar of the *Anopheles stepensi* Liston and *Aedes aegypti* (L.) mosquitoes has been reported by the group of Eng *et al* [125]. It is of some interest that these derivatives were effective larvicides. No clear cut differentiation in activity between the $R = Ph$ and Cy derivatives was delineated [125].

1.7 Organotin(IV) dithiocarboxylates as synthetic precursors for Tin-Sulfides

Beside biological activities tin dithiocarboxylates are also exploited as precursors for Tin-Sulfides. Metal dithiocarboxylates have proved extremely useful for the synthesis of metal sulfide nanoparticles, thin films, etc [126]. Tin dithiocarboxylates are no exception and their utility in this regard was reviewed in 1994 [127]. At that time, it was known that the $Sn(II)$ species, $Sn(S_2CNEt_2)_2$, was a useful precursor for the preparation of SnS . Similarly, SnS could be prepared by thermal decomposition of $Sn(IV)$ species, $Sn(S_2CNEt_2)_2X_2$ (where $X = \text{halide}$), via X_2SnS intermediates. Less certain was the decomposition pathway of the binary $Sn(IV)$ species, $Sn(S_2CNEt_2)_4$. Degradation was thought to occur through $Sn(II)$, i.e. $Sn(S_2CNEt_2)_2$, and thiuram, intermediates. Later work [129] showed that the final product was SnS_2 , obtained via dinuclear $[(Et_2NCS_2)_2SnS]_2$, implying that each pair of dithiocarboxylate ligands in

the precursor $\text{Sn}(\text{S}_2\text{CNet}_2)_4$ species lost $[\text{Et}_2\text{NC}(\text{S})]_2\text{S}$ via initial elimination of thiuram, as indicated in earlier studies. Further work indicated that, at higher temperatures, $\text{Sn}(\text{S}_2\text{CNet}_2)_4$ lost two molar equivalents of thiuram to eventually give SnO_2 [128]. The same research group showed that by chemical vapour deposition of unsymmetrical dithiocarboxylate ligands, i.e. where the dithiocarboxylate-bound R' groups are inequivalent, as in $\text{R}_3\text{Sn}[\text{S}_2\text{CN}(n\text{-Bu})\text{Me}]$ for $\text{R} = \text{Me}$ and $n\text{-Bu}$, both SnS and Sn_2S_3 films could be formed on a glass substrate under ambient conditions with a minimal amount of H_2S present [129]. Mixtures of SnS and Sn_2S_3 are also obtained from the thermal decomposition of $\text{Ph}_2\text{Sn}[\text{S}_2\text{CN}(\text{CH}_2)_4]_2$, characterized as the toluene solvate, and $\text{Ph}_3\text{Sn}[\text{S}_2\text{CN}(\text{CH}_2)_4]$, where the dithiocarboxylate is derived from pyrrolidine [108].

REFERENCES

- [1] I. Omae, *Organotin Chemistry*, J. Organomet. Chem. Lib., 21, Elsevier, Amsterdam, (1989).
- [2] R. W. Weissin, in 'Organometallic Compounds', Compounds of Germanium, Tin and Lead, ed., M. Dub, Springer-Verlag, Berlin, 2, (1966).
- [3] R. C. Poller, '*The Chemistry of Organotin Compounds*', Logos Press Ltd., London, (1970).
- [4] R. K. Harris, J. D. Kennedy, W. McFarlan, in 'NMR and the Periodic Table', ed., R. K. Harris and B. E. Mann, Academic Press, New York, Chapt. 10, (1978).
- [5] J. Silver, *Phy. Organomet. Chem.*, 2 (Solid State Organomet. Chem.), (1999) 279.
- [6] E. Frankland, *J. Chem. Soc.*, 2, (1849) 262.
- [7] V. G. K. Das, S. W. Ng, M. Gielen, '*Chemistry and Technology of Silicon and Tin*', Oxford University Press, Oxford, (1992).
- [8] P. J. Smith, in '*Chemistry of Tin*', 2nd Edn., Blackie Academic & Professional, London, (1998).
- [9] A. G. Davies, '*Organotin Chemistry*', VCH: Weinheim, (1997).
- [10] S. W. Ng, *Z. Kristallogr. – New Cryst. Struct.* 212 (1997) 285; b) H. D. Yin, C. H. Wang, C. L. Ma, H. X. Fang, G. F. Liu, *Chin. J. Appl. Chem.* 20 (2003) 841.
- [11] A. W. Addison, T. N. Rao, J. Reedijk, J. van Rijn, G. C. Verschoor, *J. Chem. Soc., Dalton Trans.* (1984) 1349.
- [12] F. Li, H. D. Yin, D. Q. Wang, *Acta Crystallogr.* E61 (2005) m2464.
- [13] K. M. Lo, S. Selvaratnam, S. W. Ng, C. Wei, V. G. Kumar Das, *J. Organomet. Chem.* 430 (1992) 149.
- [14] M. F. Mahon, K. C. Molloy, P. C. Waterfield, *Organometallics* 12 (1993) 769.
- [15] H. D. Yin, C. L. Ma, Y. Wang, H. X. Fang, J. X. Shao, *Acta Chim. Sinica* 60 (2002) 897.
- [16] H. D. Yin, C. H. Wang, Q. J. Xing, *Chin. J. Struct. Chem.* 23 (2004) 490.
- [17] H. D. Yin, C. H. Wang, *Appl. Organomet. Chem.* 18 (2004) 145.
- [18] L. Tian, Z. Shang, Q. Yu. D. Li, G. Yang, *Appl. Organomet. Chem.* 18 (2004) 253.

- [19] G. M. Sheldrick, W. S. Sheldrick, *J. Chem. Soc. A* (1970) 490.
- [20] G. M. Sheldrick, W. S. Sheldrick, R. F. Dalton, K. Jones, *J. Chem. Soc. A* (1970) 493.
- [21] X. Song, C. Cahill, G. Eng, *Main GroupMet. Chem.* 25 (2002) 13.
- [22] X. Song, R. Pike, G. Eng, *Anal. Sci.: X-Ray Struct. Anal. Online* 22 (2006) x137.
- [23] H. D. Yin, C. H. Wang, C. L. Ma, *Chem. React. (in Chinese)*, 25 (2003) 196.
- [24] J. M. Hook, B. M. Linahan, R. L. Taylor, E. R. T. Tiekink, L. van Gorkom, L. K. Webster, *Main GroupMetal Chem.* 17 (1994) 293.
- [25] D. Zhu, R. Zhang, C. L. Ma, H. D. Yin, *Indian J. Chem. Sect. A* 41 (2002) 1634.
- [26] H. D. Yin, C. H. Wang, C. L. Ma, H. X. Fang, *J. Jilin Univ. Sci. Ed. (in chinese)*, 41 (2003) 361.
- [27] A. T. Kana, T. G. Hibbert, M. F. Mahon, K. C. Molloy, I. P. Parkin, L. S. Price, *Polyhedron* 20 (2001) 2989.
- [28] N. Awang, I. Baba, M. S. M. Yusof, B. M. Yamin, *Acta Crystallogr.* E59 (2003) m414.
- [29] H. D. Yin, G. F. He, C. H. Wang, C. L. Ma, *Chin. J. Inorg. Chem.* 19 (2003) 1019.
- [30] M. Sanuddin, Y. Farina, B. M. Yamin, *Acta Crystallogr.* E60 (2004) m1662.
- [31] N. Awang, I. Baba, M. S. M. Yusof, B. M. Yamin, *Acta Crystallogr.* E59 (2003) m594.
- [32] H. D. Yin, C. H. Wang, C. L. Ma, *Chem. React. (in Chinese)*, 6 (2003) 282; (b) E. M. Holt, F. A. K. Nasser, A. Wilson Jr, J. J. Zuckerman, *Organometallics* 4 (1985) 2073.
- [33] S. Chandra, B. D. James, R. J. Magee, W. C. Patalinghug, B. W. Skelton, A. H. White, *J. Organomet. Chem.* 346 (1988) 7.
- [34] H. D. Yin, S. C. Xue, C. H. Wang, *Chin. J. Inorg. Chem.* 21 (2005) 531.
- [35] V. G. Kumar Das, C. Wei, E. Sinn, *J. Organomet. Chem.* 290 (1985) 291.
- [36] H. D. Yin, C. L. Ma, R. Zhang, *ACH-Models Chem.* 136 (1999) 7.
- [37] D. Zhu, R. Zhang, H. D. Yin, C. L. Ma, *Orient. J. Chem.* 17 (2001) 351.
- [38] H. D. Yin, C. H. Wang, C. L. Ma, *Chin. J. Inorg. Chem.* 19 (2003) 1227.
- [39] H. Yin, C. Wang, M. Hong, D. Wang, *J. Organomet. Chem.* 689 (2004) 1277.
- [40] H. D. Yin, C. H. Wang, Q. J. Xing, *Chin. J. Struct. Chem.* 23 (2004) 1127.
- [41] H. D. Yin, C. H. Wang, C. L. Ma, *Chin. J. Org. Chem.* 24 (2004) 34.

- [42] H. D. Yin, S. C. Xue, *Appl. Organomet. Chem.* 18 (2004) 496.
- [43] K. Furue, T. Kimura, N. Yasuoka, N. Kasai, M. Kakudo, *Bull. Chem. Soc. Jpn* 43 (1970) 1661.
- [44] a) E. R. T. Tiekink, V. J. Hall, M. A. Buntine, *Z. Kristallogr.* 214 (1999) 124; b) M. A. Buntine, V. J. Hall, F. J. Kosovel, E. R. T. Tiekink, *J. Phys. Chem. A* 102 (1998) 2472.
- [45] A. H. Othman, H. K. Fun, B. M. Yamin, *Acta Crystallogr. C* 53 (1997) 1228.
- [46] S. Shahzadi, S. Ali, M. H. Bhatti, M. Fettouhi, M. Athar, *J. Organomet. Chem.* 691 (2006) 1797.
- [47] S. Ali, S. U. Ahmad, S. Shahzadi, Sadiq-ur-Rehman, M. Parvez, M. Mazhar, *Appl. Organomet. Chem.* 19 (2005) 201.
- [48] Zia-ur-Rahman, S. Ali, N. Muhammad, A. Meetsma, *Acta Crystallogr. E* 62 (2006) m3560.
- [49] C. Wei, V. G. Kumar Das, E. Sinn, *Inorg. Chim. Acta* 100 (1985) 245.
- [50] Zia-ur-Rahman, S. Ali, N. Muhammed, A. Meetsma, *Acta Crystallogr. E* 63 (2007) m89.
- [51] F. Li, H. D. Yin, J. Zhai, D. Q. Wang, *Acta Crystallogr. E* 62 (2006) m300.
- [52] D. Dakternieks, H. Zhu, D. Masi, C. Mealli, *Inorg. Chem.* 31 (1992) 3601.
- [53] H. D. Yin, S. C. Xue, C. H. Wang, *Pol. J. Chem.* 80 (2006) 873.
- [54] T. S. Basu Baul, E. R. T. Tiekink, *Main Group Met. Chem.* 16 (1993) 201.
- [55] S. Ali, S. U. Ahmad, Sadiq-ur-Rehman, S. Shahzadi, M. Parvez, M. Mazhar, *Appl. Organomet. Chem.* 19 (2005) 200.
- [56] V. J. Hall, E. R. T. Tiekink, *Main Group Met. Chem.* 18 (1995) 217.
- [57] L. J. Tian, W. T. Mao, Y. X. Sun, X. C. Liu, *Acta Crystallogr. E* 62 (2006) m1675.
- [58] L. J. Tian, W. T. Mao, G. X. Tan, Y. X. Sun, *Acta Crystallogr. E* 62 (2006) m2448.
- [59] H. D. Yin, C. L. Ma, Y. Wang, *Indian J. Chem. Sect. A* 41 (2002) 342.
- [60] H. D. Yin, C. H. Wang, C. L. Ma, Y. Wang, *Chin. J. Inorg. Chem.* 19 (2003) 617.
- [61] H. D. Yin, C. H. Wang, C. L. Ma, Y. Wang, R. F. Zhang, *Chin. J. Org. Chem.* 22 (2002) 797.
- [62] H. D. Yin, C. H. Wang, C. L. Ma, Y. Wang, *Chin. J. Chem.* 20 (2002) 913.
- [63] S. C. Xue, H. D. Yin, Q. Wang, D. Wang, *Heteroat. Chem.* 16 (2005) 271.

- [64] H. D. Yin, S. C. Xue, *Appl. Organomet. Chem.* 19 (2005) 193.
- [65] J. Y. Li, T. D. Li, *Acta Crystallogr.* E63 (2007) m708.
- [66] H. D. Yin, S. C. Xue, *Appl. Organomet. Chem.* 20 (2006) 283.
- [67] H. D. Yin, Y. Wang, C. H. Wang, *Chin. J. Inorg. Chem.* 23 (2004) 926.
- [68] H. D. Yin, M. Hong, *Chin. J. Inorg. Chem.* 20 (2004) 297.
- [69] O. S. Jung, J. H. Jeong, Y. S. Sohn, *Organometallics* 10 (1991) 2217.
- [70] D. Dakternieks, K. Jurkschat, D. Schollmeyer, Wu. Hong, *J. Organomet. Chem.* 492 (1995) 145.
- [71] O. S. Jung, Y. S. Sohn, J. A. Ibers, *Inorg. Chem.* 25 (1986) 2273.
- [72] T. Kimura, N. Yasuoka, N. Kasai, M. Kakudo, *Bull. Chem. Soc. Jpn* 45 (1972) 1649.
- [73] T. P. Lockhart, W. F. Manders, E. O. Schlemper, J. J. Zuckerman, *J. Am. Chem. Soc.* 108 (1986) 4074.
- [74] A. K. Mohamed, N. Auner, M. Bolte, *Acta Crystallogr.* E59 (2003) m190.
- [75] J. S. Morris, E. O. Schlemper, *J. Cryst. Mol. Struct.* 9 (1979) 13.
- [76] A. A. Y. Farina, A. H. Othman, I. Baba, K. Sivakumar, H. K. Fun, S. W. Ng, *Acta Crystallogr.* C56 (2000) e84.
- [77] N. Awang, I. Baba, M. S. M. Yusof, B. M. Yamin, *Acta Crystallogr.* E59 (2003) m348.
- [78] N. Seth, V. D. Gupta, H. Noth, M. Thomann, *Chem. Ber.* 125 (1992) 1523.
- [79] J. Sharma, Y. Singh, R. Bohra, A. K. Rai, *Polyhedron* 15 (1996) 1097.
- [80] S. Shahzadi, S. Ali, M. Fettouhi, *Acta Crystallogr.* E62 (2006) m1178.
- [81] Zia-ur-Rahman, S. Ali, N. Muhammed, A. Meetsma, *Acta Crystallogr.* E63 (2007) m431.
- [82] V. J. Hall, E. R. T. Tiepink, *Main GroupMet. Chem.* 21 (1998) 245.
- [83] V. Vrabel, J. Lokaj, E. Kello, J. Garaj, A. C. Batsanov, Yu. T. Struchkov, *Acta Crystallogr.* C48 (1992) 633.
- [84] V. Vrabel, J. Lokaj, V. Rattay, A. C. Batsanov, Yu. T. Struchkov, *Acta Crystallogr.* C48 (1992) 627.
- [85] Y. Farina, I. Baba, A. H. Othman, S. W. Ng, *Main Group Met. Chem.* 23 (2000) 795.
- [86] D. C. Menezes, F. T. Vieira, G. M. de Lima, A. O. Porto, M. E. Cortés, J. D. Ardisson, T. E. Albrecht-Schmitt, *Eur. J. Med. Chem.* 40 (2005) 1277.

- [87] J. Lokaj, E. Kello, V. Kettmann, V. Vrabel, V. Rattay, *Collect. Czech. Chem. Commun.* 51 (1986) 2521.
- [88] V. Vrabel, E. Kello, *Acta Crystallogr. C* 49 (1993) 873.
- [89] Zia-ur-Rehman, S. Shahzadi, S. Ali, A. Badshah, G. X. Jin, *J. Iran. Chem. Soc.* 3 (2006) 157.
- [90] D. Dakternieks, H. Zhu, D. Masi, C. Mealli, *Inorg. Chem.* 31 (1992) 3601.
- [91] O. S. Jung, M. J. Kim, J. H. Jeong, Y. S. Sohn, *Bull. Korean Chem. Soc.* 10 (1989) 343.
- [92] V. J. Hall, E. R. T. Tiekink, *Z. Kristallogr. New Cryst. Struct.* 213 (1998) 535.
- [93] H. D. Yin, C. H. Wang, C. L. Ma, *Chin. J. Struct. Chem.* 23 (2004) 316.
- [94] H. D. Yin, C. H. Wang, Y. Wang, C. L. Ma, *Chin. J. Chem.* 21 (2003) 356.
- [95] H. D. Yin, S. C. Xue, *Appl. Organomet. Chem.* 18 (2004) 415.
- [96] H. D. Yin, C. H. Wang, C. L. Ma, D. Z. Zhu, *Chin. J. Inorg. Chem.* 18 (2002) 819.
- [97] H. D. Yin, C. L. Ma, R. Zhang, L. Zhang, J. Dou, *ACH-Models Chem.* 137 (2000) 103.
- [98] H. D. Yin, C. H. Wang, Y. Wang, R. F. Zhang, C. L. Ma, *Chin. J. Inorg. Chem.* 18 (2002) 201.
- [99] H. D. Yin, C. H. Wang, M. Hong, *Chin. J. Inorg. Chem.* 20 (2004) 571.
- [100] H. D. Yin, S. C. Xue, *Appl. Organomet. Chem.* 19 (2005) 194.
- [101] H. D. Yin, C. H. Wang, *Appl. Organomet. Chem.* 18 (2004) 409.
- [102] H. D. Yin, S. C. Xue, *Appl. Organomet. Chem.* 19 (2005) 187.
- [103] H. D. Yin, Y. Wang, C. H. Wang, *Chin. J. Inorg. Chem.* 23 (2004) 926.
- [104] P. F. Lindley, P. Carr, *J. Cryst. Mol. Struct.* 4 (1974) 173; b) N. W. Alcock, J. Culver, S. M. Roe, *J. Chem. Soc. Dalton Trans.* (1992) 1477.
- [105] V. J. Hall, E. R. T. Tiekink, *Main Group Met. Chem.* 18 (1995) 611.
- [106] Y. Farina, A. H. Othman, I. A. Razak, H. K. Fun, S. W. Ng, I. Baba, *Acta Crystallogr. E* 57 (2001) m46.
- [107] Y. Farina, I. Baba, A. H. Othman, I. A. Razak, H. K. Fun, S. W. Ng, *Acta Crystallogr. E* 57 (2001) m41.
- [108] D. C. Menezes, G. M. de Lima, A. O. Porto, C. L. Donnici, J. D. Ardisson, A. C. Doriguetto, J. Ellena, *Polyhedron* 23 (2004) 2103.
- [109] K. Kim, J. A. Ibers, O. S. Jung, Y. S. Sohn, *Acta Crystallogr. C* 43 (1987) 2317.

- [110] S. W. Ng, C. Wei, V. G. K. Das, G. B. Jameson, R. J. Butcher, J. Organomet. Chem. 365 (1989) 75.
- [111] E. R. T. Tiekink, Main GroupMet. Chem. 15 (1992) 161.
- [112] (a) M.A. Buntine, V.J. Hall, F.J. Kosovel, E.R.T. Tiekink, J. Phys. Chem. A 102 (1998) 2472; (b) E. R. T. Tiekink, V. J. Hall, M. A. Buntine, Z. Kristallogr. 214 (1999) 124; (c) M. A. Buntine, F. J. Kosovel, E. R. T. Tiekink, Phosphorus., Sulfur, Silicon Related Elements 261 (1999) 150; (d) E. R. T. Tiekink, V. J. Hall, M. A. Buntine, J. Hook, Z. Kristallogr. 215 (2000) 23; (e) M. A. Buntine, F. J. Kosovel, E. R. T. Tiekink, Cryst. Eng. Comm. 5 (2003) 331.
- [115] (a) N. W. Alcock, Adv. Inorg. Chem. Radiochem. 15 (1972) 1; (b) N. W. Alcock, Bonding and Structure: Structural Principles in Inorganic and Organic Chemistry. Ellis Horwood: New York, (1990).
- [116] A. Bondi, J. Phys. Chem. 68 (1964) 441.
- [117] R. E. Benson, C. A. Ellis, C. E. Lewis, E. R.T. Tiekink, Cryst. Eng. Comm 9 (2007) 930.
- [118] (a) F. J. Lascourreges, P. Caumette, X .F. O. Donard, Appl.Organomet. Chem. 14 (2000) 98; (b) J. P. Smith, In Toxicological Data On Organotin Compounds; Publication #538, International Tin Research Institute: UK, (1978); (c) F. Browning, Toxicity of Industrial Metals, 2nd ed.; Butterworths: London, (1969); (d) H. Ishiwata, T. Inone, K. Yoshira, Bull Environ. Contam. Toxicol. 37 (1986) 638; (e) U. Schaeppi, A. I. Heyman, W. R. Fleischman, H. Rosenkrantz, V. Ilievski, R. Phelan, A. D. Cooney, D. R. Davis, Toxicol. Appl. Pharmacol. 25 (1973) 230; (f) B. D. Milne, Biochemical Elements 3 (1984) , 309.
- [119] X. Song, A. Zapata, G. Eng, J. Organomet. Chem. 691 (2006) 1756.
- [118] M. Carrara, L. Cima, S. Zampiron, C. Preti, V. Cherchi, L. Sindellari, Anticancer Res. 9 (1989) 775.
- [119] S. Chandra, B. D. James, B. J. Macauley, R. J. Magee, J. Chem. Tech. Biotech. 39 (1987) 65.
- [120] J. Kizlink, V. Rattay, M. Kosik, Surf. Coat. Int. 76 (1993) 468.
- [121] P. K. Gogoi, D. P. Phukan, D. K. Das, Asian J. Chem. 11 (1999) 1291.
- [122] D. C. Menezes, F. T. Vieira, G. M. de Lima, J. L. Wardell, M. E. Cortés, M. P. Ferreira, M. A. Soares, A. Vilas Boas, Appl. Organomet. Chem. 22 (2008) 221.
- [123] S. Shahzadi, S. Ali, M. Fettouhi, J. Chem. Crystallogr. 38 (2008) 273.

- [124] H. P. S. Chauhan, N. M. Shaik, *J. Inorg. Biochem.* 99 (2005) 538.
- [125] G. Eng, X. Song, Q. Duong, D. Strickman, J. Glass, L. May, *Appl. Organomet. Chem.* 17 (2003) 218.
- [126] (a) D. Fan, M. Afzaal, M. A. Malik, C. Q. Nguyen, P. O' Brien, P. J. Thomas, *Coord. Chem. Rev.* 251 (2007) 1878; (b) M. S. Vickers, J. Cookson, P. D. Beer, P. T. Bishop, B. Thiebaut, *J. Mat. Chem.* 16 (2006) 209; (c) Y. W. Koh, C. S. Lai, A. Y. Du, E. R. T. Tiekink, K. P. Loh, *Chem. Mater.* 15 (2003) 4544.
- [127] J. O. Hill, S. Chirawongaram, *J. Therm. Anal.* 41 (1994) 511.
- [128] G. Barone, T. Chaplin, T. G. Hibbert, A. T. Kana, M. F. Mahon, K. C. Molloy, I. D. Worsley, I. P. Parkin, L. S. Price, *J. Chem. Soc., Dalton Trans.* (2002) 1085.
- [129] A. T. Kana, T. G. Hibbert, M. F. Mahon, K. C. Molloy, I. P. Parkin, L. S. Price, *Polyhedron* 20 (2001) 2989.

EXPERIMENTAL

2.1 Chemicals

Organotin chlorides were purchased from Aldrich, Fluka & Alfa-Aesar (Johnson Matthey) Chemicals. The organic solvents (toluene, chloroform, diethyl ether, acetone etc.) used were of Merck, Germany and dried *in situ* using standard procedures [1, 2]. All the other chemicals were of analytical grade and used without further purification.

The following chemicals for ligand synthesis were purchased and used without further purification.

1-(4-Nitrophenyl)piperazine (98%)	Aldrich
1-(2-Methoxyphenyl)piperazine (98%)	Aldrich
1-(4-Methoxyphenyl)piperazine (98%)	Aldrich
1-(Diphenylmethyl)piperazine (98%)	Fluka
4-Benzylpiperidine (99%)	Aldrich
Carbon disulfide ($\geq 99\%$)	Aldrich

2.2 Instrumentation

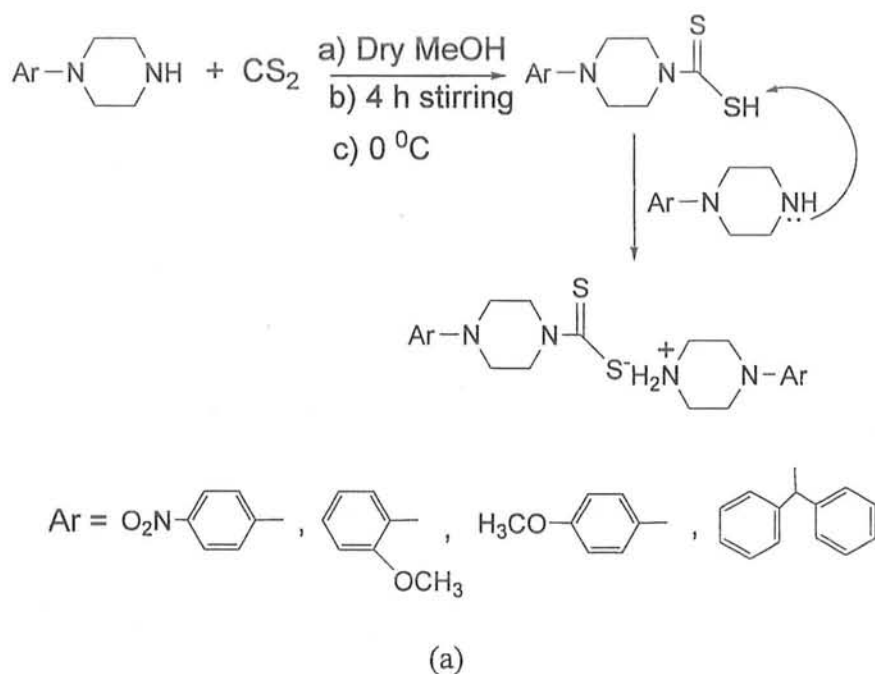
Melting points were determined in a capillary tube using a Gallenkamp (UK) electrothermal melting point apparatus. Microanalysis was done using a Leco CHNS 932 apparatus. Raman spectra ($\pm \text{cm}^{-1}$) were measured with an InVia Renishaw spectrometer, using argon-ion (514.5 nm) and near-infrared diode (785 nm) lasers. WiRE 2.0 software was used for the data acquisition and spectra manipulations. IR spectra in the range $4000\text{--}400 \text{ cm}^{-1}$ were obtained on Bio-Rad FT-IR spectrophotometer with samples investigated as KBr discs or thin film on NaCl cell. ^1H and ^{13}C -NMR were recorded on Hg-300 MHz FT-NMR spectrometer, using CDCl_3 as an internal reference for [$\delta \text{ } ^1\text{H} (\text{CDCl}_3) = 7.25$ and $\delta \text{ } ^{13}\text{C} (\text{CDCl}_3) = 77.0$ ppm]. ^{119}Sn NMR spectra were obtained with Me_4Sn as an external reference [$\Xi (^{119}\text{Sn}) = 37.290665$] [3]. Chemical shifts (δ) are given in ppm and coupling constants (J) are given in Hz. The multiplicities of signals in ^1H NMR are given with chemical

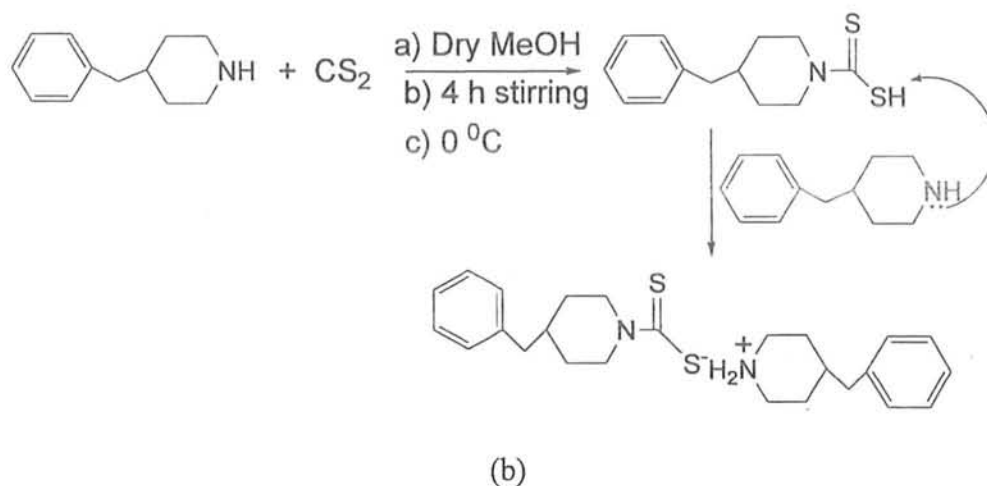
shifts; (s = singlet, d = doublet, t = triplet, q = quartet, m = multiplet). Electron impact (70 eV) mass spectra were recorded on a Kratos MS25RFA.

The m/z values were evaluated assuming that H = 1, C = 12, N = 14, O = 16, Cl = 35 and Sn = 120. X-ray single crystal analyses were collected on a Bruker SMART APEX CCD diffractometer using graphite-monochromated Mo- K_α radiation ($\lambda = 0.71073 \text{ \AA}$). Data collection used ϕ - and ω -scans, and a multi-scan absorption correction was applied. The structures were solved by direct methods using either program DIRDIF or SIR2004. Final refinement on F^2 carried out by full-matrix least squares techniques using SHELXL-97.

2.3 General procedure for the synthesis of ligand salts

Dropwise addition of CS_2 in methanol (50 mL) to substituted piperazine/piperidine in methanol (50 mL), in 1:1 molar ratio, followed by stirring for 4 h at 273 K gave corresponding ligand salt as shown in scheme 2.1a & b. The product thus obtained was filtered off, washed with diethyl ether and vacuum dried.

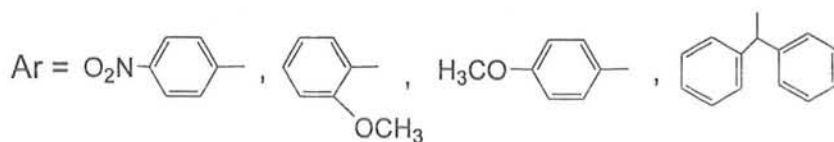
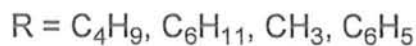
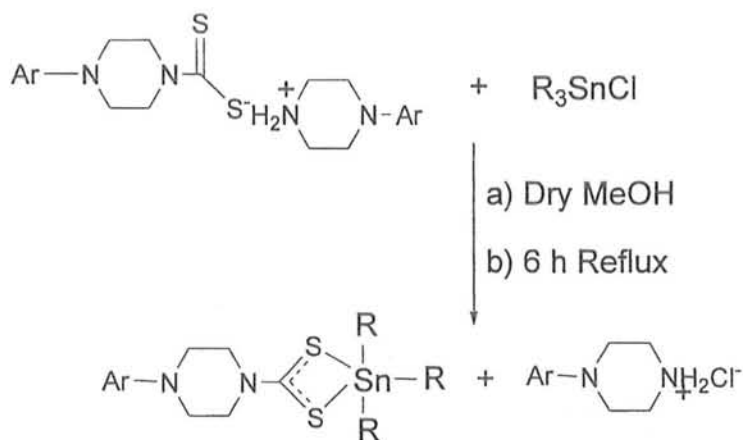




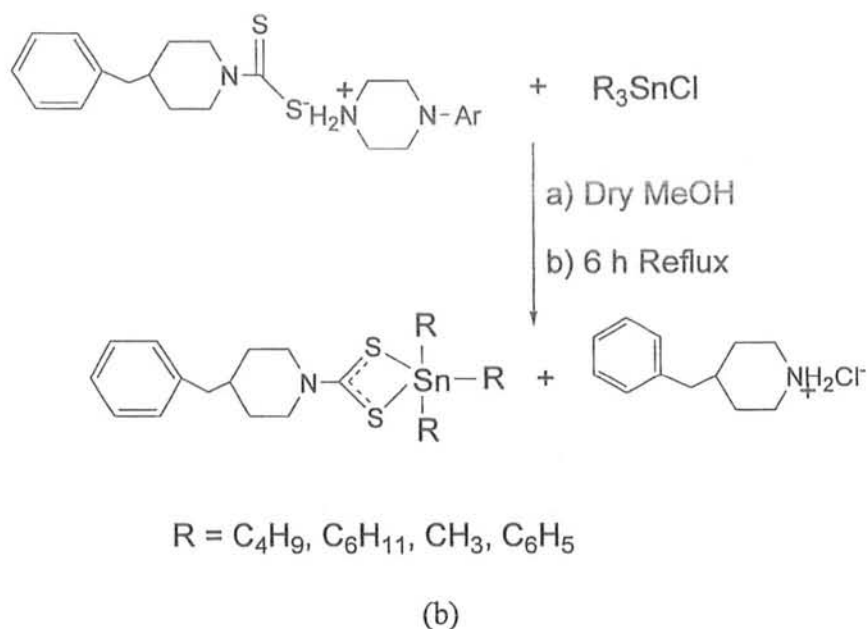
Scheme 2.1: Synthesis of ligand-salts.

2.4 General procedure for the synthesis of triorganotin(IV) dithiocarboxylates

Different triorganotin(IV) dithiocarboxylates have been prepared by 1:1 mole-ratio reactions of the ligand salts with triorganotin(IV) chlorides in dry methanol as shown in scheme 2.2a & b. The salt was removed by filtration. The filtrate was rotary evaporated and the product thus obtained, in each case, was recrystallized from chloroform-ethanol mixture (3:1).



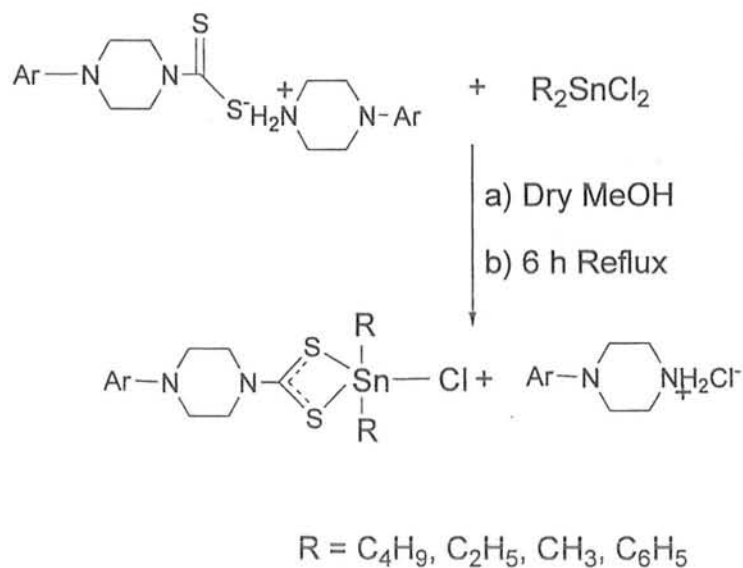
(a)

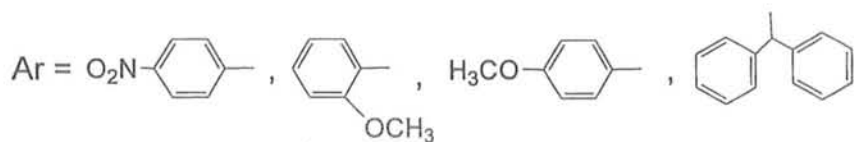


Scheme 2.2: Synthesis of triorganotin(IV) dithiocarboxylates.

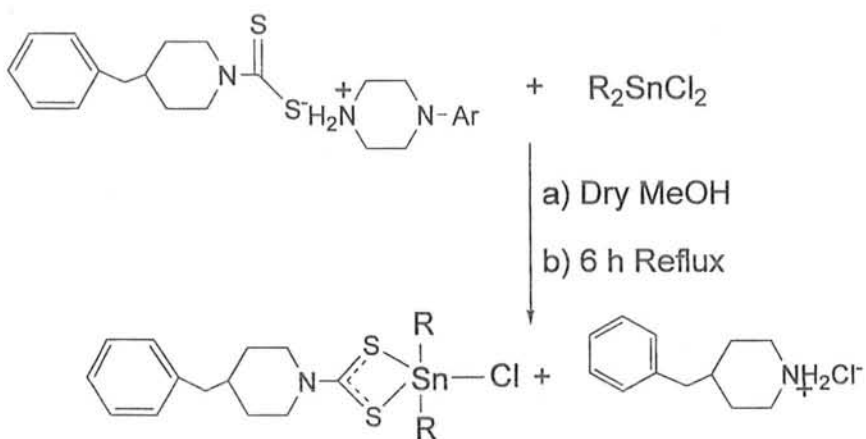
2.5 General procedure for the synthesis of chlorodiorganotin(IV) dithiocarboxylates

To a solution of ligand salt in dry methanol (50 ml) was added equimolar amount of diethyltin(IV) chloride, dissolved in dry methanol (50 ml), dropwise and the mixture was refluxed for 6 h with vigorous stirring. The substituted piperazinium/piperidinium chloride was removed on filtration. The filtrate was rotary evaporated to get the desired product (scheme 2.3a & b) and was recrystallized from chloroform-ethanol mixture (4:1).





(a)

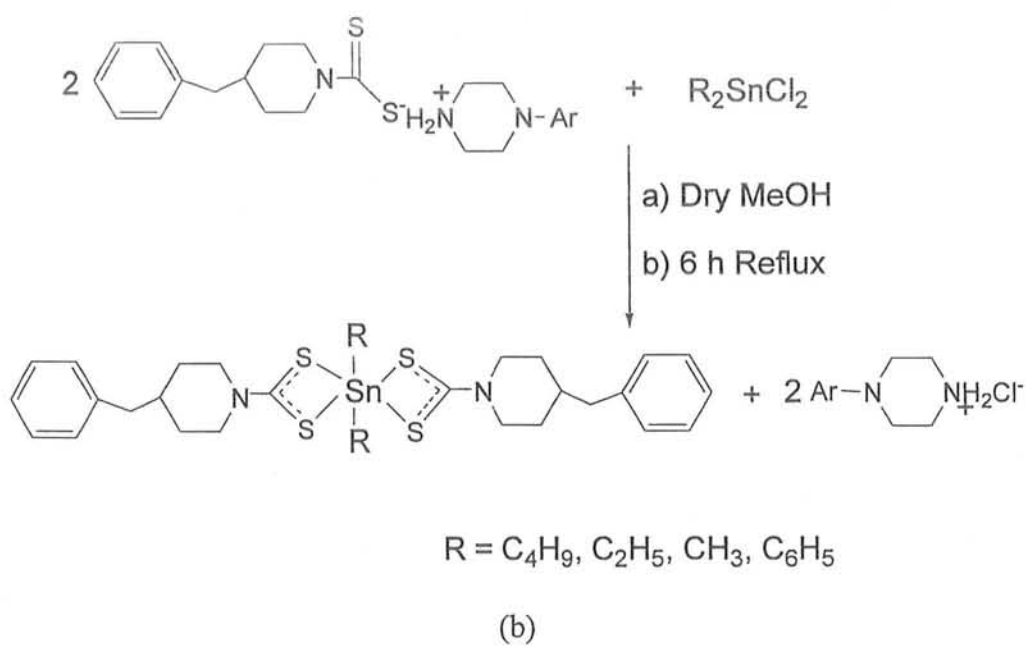
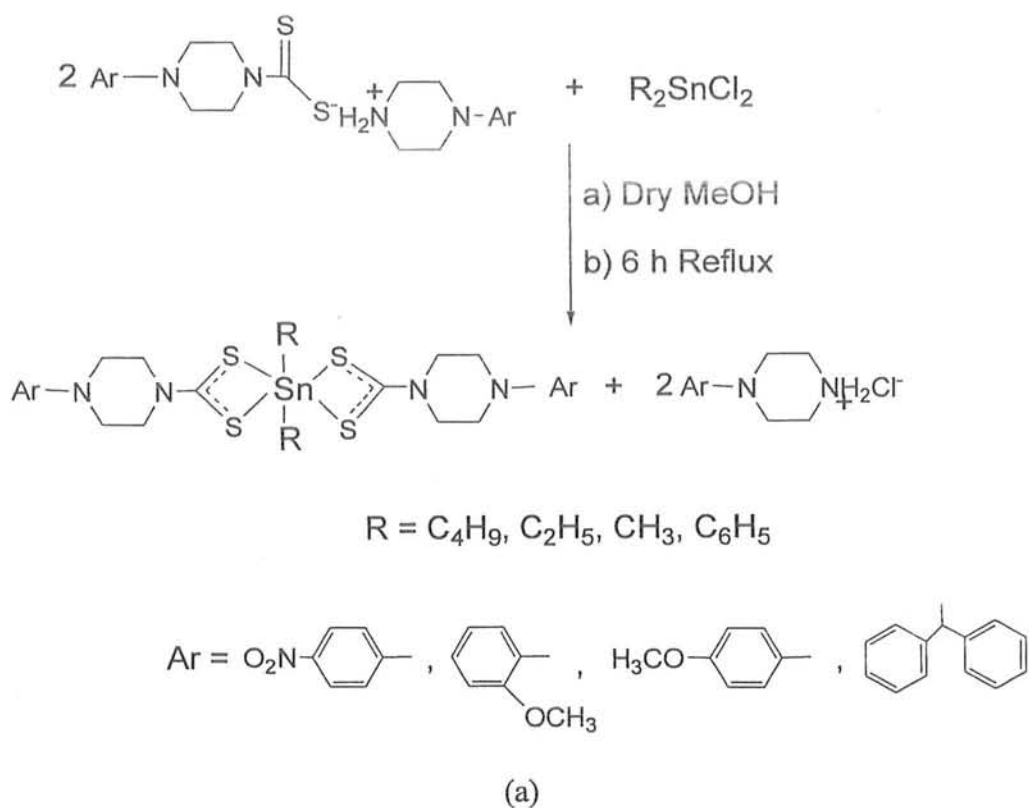


(b)

Scheme 2.3: Synthesis of chlorodiorganotin(IV) dithiocarboxylates.

2.6 General procedure for the synthesis of diorganotin(IV) dithiocarboxylates

Diorganotin(IV) dithiocarboxylates were synthesised by adopting procedure 2.4, using 1:2 mole-ratio of diorganotin(IV) dichloride and ligand salt as shown in scheme 2.4a & b. The product was recrystallized from chloroform-ethanol (4:1) mixture.



Scheme 2.4: Synthesis of diorganotin(IV) dithiocarboxylates.

4-(4-nitrophenyl)piperazinium 4-(4-nitrophenyl)piperazine-1-carbodithioate (L-salt)

(Yield: 83 %). M.p. 180-182 °C. Elemental Analysis, % Calculated (Found) for $C_{21}H_{26}N_6O_4S_2$: C, 51.42 (51.37); H, 5.30 (5.33); N, 17.14 (17.12); S, 13.06 (13.01). Raman (cm^{-1}): 664 ν (C-S), 1210 ν (C=S), 1507 ν (C-N). IR (cm^{-1}): 1030 ν (C-S), 1478 ν (C-N). EI-MS, m/z (%): $[C_{10}H_{14}N_3O_2]^+$ 208 (4.7), $[C_{10}H_{13}N_3O_2]^+$ 207 (38.7), $[C_8H_9N_2O_2]^+$ 165 (100), $[C_8H_9N_2O]^+$ 149 (4), $[C_8H_9N]^+$ 119 (19.8), $[C_6H_5]^+$ 76 (24.4).

4-(2-methoxyphenyl)piperazinium 4-(2-methoxyphenyl)piperazine-1-carbodithioate (L^a-salt)

(Yield: 85 %). M. p. 161-163 °C. Elemental Analysis, % Calculated (Found) for $C_{23}H_{32}N_4O_2S_2$: C, 60.00 (59.72); H, 6.95 (6.91); N, 12.17 (12.11); S, 13.91 (13.67). Raman (cm^{-1}): 569 ν (C-S), 1215 ν (C=S), 1466 ν (C-N). IR (cm^{-1}): 1020 ν (C-S), 1482 ν (C-N). EI-MS, m/z (%): $[C_{11}H_{17}N_2O]^+$ 192 (100), $[C_9H_{12}NO]^+$ 150 (82.4), $[C_8H_9NO]^+$ 135 (26), $[C_7H_6NO]^+$ 120 (21), $[C_6H_4O]^+$ 92 (4.4), $[C_6H_4]^+$ 76 (75).

4-(4-methoxyphenyl)piperazinium 4-(4-methoxyphenyl)piperazine-1-carbodithioate (L^b-salt)

(Yield: 85 %). M. p. 187-189 °C. Elemental Analysis, % Calculated (Found) for $C_{23}H_{32}N_4O_2S_2$: C, 60.00 (59.71); H, 6.95 (6.91); N, 12.17 (12.12); S, 13.91 (13.67). Raman (cm^{-1}): 638 ν (C-S), 1185 ν (C=S), 1466 ν (C-N). IR (cm^{-1}): 1033 ν (C-S), 1481 ν (C-N). EI-MS, m/z (%): $[C_{11}H_{17}N_2O]^+$ 192 (100), $[C_9H_{12}NO]^+$ 150 (82.4), $[C_8H_9NO]^+$ 135 (26), $[C_7H_6NO]^+$ 120 (21), $[C_6H_4O]^+$ 92 (4.4), $[C_6H_4]^+$ 76 (75).

4-Benzhydrylpiperazinium 4-Benzhydrylpiperazine-1-carbodithioate (L^c-salt)

(Yield: 80 %). M. p. 191-193 °C. Elemental Analysis, % Calculated (Found) for $C_{35}H_{40}N_4S_2$: C, 72.41 (72.11); H, 6.89 (6.69); N, 9.65 (9.45); S, 11.03 (10.87). Raman (cm^{-1}): 650 ν (C-S), 1045 ν (C=S), 1460 ν (C-N). IR (cm^{-1}): 1035 ν (C-S), 1470 ν (C-N). EI-MS, m/z (%): $[C_{18}H_{19}N_2S_2]^+$ 327 (6.5), $[C_{17}H_{21}N_2]^+$ 252 (4.5), $[C_{13}H_{11}]^+$ 167 (25).

4-Benzylpiperidinium 4-Benzylpiperidine-1-carbodithioate (L^d-salt)

(Yield: 77 %). M. p. 132-134 °C. Elemental Analysis, % Calculated (Found) for $C_{25}H_{34}N_2S_2$: C, 70.42 (70.02); H, 7.98 (7.67); N, 6.57 (6.61); S, 15.03 (14.71). Raman (cm^{-1}): 644 ν (C-S), 1075 ν (C=S), 1480 ν (C-N). IR (cm^{-1}): 1017 ν (C-S), 1480 ν (C-N). EI-MS, m/z (%): $[C_{13}H_{17}NS_2]^+$ 251 (2.3), $[C_{12}H_{17}N]^+$ 175 (100), $[C_6H_{12}N]^+$ 98 (3), $[C_5H_{10}N]^+$ 84 (58), $[C_6H_5]^+$ 77 (7).

Tributyltin(IV) 4-(4-nitrophenyl)piperazine-1-carbodithioate (1)

(Yield: 70%). M.p. 130-131 °C. Elemental Analysis, % Calculated (Found), for $C_{23}H_{39}N_3O_2S_2Sn$: C, 48.16 (47.96); H, 6.80 (6.93); N, 7.33 (7.42); S, 11.17 (10.98). Raman (cm^{-1}): 651 $\nu(C-S)$, 1202 $\nu(C=S)$, 1507 $\nu(C-N)$, 515 $\nu(Sn-C)$, 362 $\nu(Sn-S)$. IR (cm^{-1}): 980, 1007 $\nu(C-S)$, 1488 $\nu(C-N)$, 514 $\nu(Sn-C)$. EI-MS, m/z (%): $[C_{23}H_{39}N_3OS_2Sn]^+$ 557 (25), $[C_{19}H_{30}N_3O_2S_2Sn]^+$ 516 (80), $[C_{19}H_{30}N_3OS_2Sn]^+$ 500 (27), $[C_{19}H_{30}N_2OS_2Sn]^+$ 486 (20), $[C_{11}H_{12}N_3O_2S_2Sn]^+$ 402 (33), $[C_{11}H_{12}N_3OS_2Sn]^+$ 386 (2), $[C_{12}H_{27}Sn]^+$ 291 (11), $[C_8H_{18}Sn]^+$ 234 (5), $[C_4H_9Sn]^+$ 177 (37), $[Sn]^+$ 120 (9).

Tricyclohexyltin(IV) 4-(4-nitrophenyl)piperazine-1-carbodithioate (2)

(Yield: 70%). M.p. 228-231 °C. Elemental Analysis, % Calculated (Found), for $C_{29}H_{45}N_3O_2S_2Sn$: C, 53.46 (53.31); H, 6.91 (6.94); N, 6.45 (6.49); S, 9.83 (9.75). Raman (cm^{-1}): 656 $\nu(C-S)$, 1200 $\nu(C=S)$, 1507 $\nu(C-N)$, 510 $\nu(Sn-C)$, 364 $\nu(Sn-S)$. IR (cm^{-1}): 988, 1009 $\nu(C-S)$, 1497 $\nu(C-N)$, 510 $\nu(Sn-C)$. EI-MS, m/z (%): $[C_{29}H_{45}N_2S_2Sn]^+$ 605 (3), $[C_{23}H_{34}N_3O_2S_2Sn]^+$ 568 (45), $[C_{23}H_{34}N_2OS_2Sn]^+$ 538 (7), $[C_{17}H_{30}N_2S_2Sn]^+$ 446 (5), $[C_{15}H_{26}NS_2Sn]^+$ 404 (4), $[C_{18}H_{33}Sn]^+$ 369 (5), $[C_{13}H_{22}S_2Sn]^+$ 362 (17), $[C_9H_{15}N S_2Sn]^+$ 321 (63), $[C_{12}H_{22}Sn]^+$ 286 (3), $[C_6H_{11}Sn]^+$ 203 (9), $[Sn]^+$ 120 (10).

Trimethyltin(IV) 4-(4-nitrophenyl)piperazine-1-carbodithioate (3)

(Yield: 65%). M.p. 112-113 °C. Elemental Analysis, % Calculated (Found), for $C_{14}H_{21}N_3O_2S_2Sn$: C, 37.58 (37.45); H, 4.69 (4.73); N, 9.39 (9.45); S, 14.32 (14.22). Raman (cm^{-1}): 655 $\nu(C-S)$, 1202 $\nu(C=S)$, 1507 $\nu(C-N)$, 505 $\nu(Sn-C)$, 367 $\nu(Sn-S)$. IR (cm^{-1}): 971, 1001 $\nu(C-S)$, 1457 $\nu(C-N)$, 507 $\nu(Sn-C)$. EI-MS, m/z (%): $[C_{13}H_{18}N_3O_2S_2 Sn]^+$ 432 (45), $[C_{13}H_{18}N_2OS_2 Sn]^+$ 402 (23), $[C_{12}H_{18}N_2S_2 Sn]^+$ 374 (2), $[C_3H_6S_2Sn]^+$ 226 (10), $[C_2H_3S_2Sn]^+$ 211(5), $[CS_2Sn]^+$ 196 (2), $[C_3H_9Sn]^+$ 165 (55), $[C_2H_6Sn]^+$ 150 (20), $[CH_3Sn]^+$ 135 (40).

Triphenyltin(IV) 4-(4-nitrophenyl)piperazine-1-carbodithioate (4)

(Yield: 80.3%). M.p. 223-226 °C. Elemental Analysis, % Calculated (Found), for $C_{29}H_{27}N_3O_2S_2Sn$: C, 48.167 (48.121); H, 6.806 (6.811); N, 7.329 (7.34); S, 11.169 (11.145). Raman (cm^{-1}): 652 $\nu(C-S)$, 1212 $\nu(C=S)$, 1507 $\nu(C-N)$, 263 $\nu(Sn-C)$, 384 $\nu(Sn-S)$. IR (cm^{-1}): 1018 $\nu(C-S)$, 1478 $\nu(C-N)$. EI-MS, m/z (%): $[C_{23}H_{22}N_3O_2S_2Sn]^+$ 556 (36), $[C_{17}H_{17}N_3O_2S_2Sn]^+$ 479 (4), $[C_{11}H_{12}N_3O_2S_2Sn]^+$ 402 (3), $[C_{11}H_{12}N_2S_2Sn]^+$

356 (3), $[\text{C}_{18}\text{H}_{15}\text{Sn}]^+$ 351 (97), $[\text{C}_{12}\text{H}_{10}\text{Sn}]^+$ 274 (7), $[\text{C}_6\text{H}_5\text{Sn}]^+$ 197 (44), $[\text{Sn}]^+$ 120 (20).

Chlorodibutyltin(IV) 4-(4-nitrophenyl)piperazine-1-carbodithioate (5)

(Yield: 77%). M.p. 115-117 °C. Elemental Analysis, % Calculated (Found), for $\text{C}_{19}\text{H}_{30}\text{N}_3\text{O}_2\text{S}_2\text{SnCl}$: C, 41.37 (41.36); H, 5.444 (5.41); N, 7.62 (7.43); S, 11.61 (11.53). Raman (cm^{-1}): 614 $\nu(\text{C-S})$, 1202 $\nu(\text{C=S})$, 1507 $\nu(\text{C-N})$, 517 $\nu(\text{Sn-C})$, 346 $\nu(\text{Sn-S})$, 263 $\nu(\text{Sn-Cl})$. IR (cm^{-1}): 1013 $\nu(\text{C-S})$, 1487 $\nu(\text{C-N})$, 502 $\nu(\text{Sn-C})$. EI-MS, m/z (%): $[\text{C}_{15}\text{H}_{21}\text{N}_3\text{O}_2\text{S}_2\text{SnCl}]^+$ 494 (2), $[\text{C}_4\text{H}_9\text{S}_2\text{SnCl}]^+$ 276 (6), $[\text{C}_4\text{H}_9\text{S}_2\text{Sn}]^+$ 241 (21), $[\text{S}_2\text{SnCl}]^+$ 219 (30), $[\text{S}_2\text{Sn}]^+$ 184 (9), $[\text{C}_4\text{H}_9\text{Sn}]^+$ 177 (6), $[\text{SnCl}]^+$ 155 (43).

Dibutyltin(IV) bis[4-(4-nitrophenyl)piperazine-1-carbodithioate] (6)

(Yield: 69%). M.p. 94-95 °C. Elemental Analysis, % Calculated (Found), for $\text{C}_{30}\text{H}_{42}\text{N}_6\text{O}_4\text{S}_4\text{Sn}$, Elemental Analysis, % Calculated (Found): C, 45.11 (44.86); H, 5.26 (5.38); N, 10.52 (10.43); S, 16.04 (15.83). Raman (cm^{-1}): 648 $\nu(\text{C-S})$, 1205 $\nu(\text{C=S})$, 1509 $\nu(\text{C-N})$, 515 $\nu(\text{Sn-C})$, 363 $\nu(\text{Sn-S})$. IR (cm^{-1}): 1017 $\nu(\text{C-S})$, 1488 $\nu(\text{C-N})$, 502 $\nu(\text{Sn-C})$. EI-MS, m/z (%): $[\text{C}_{16}\text{H}_{23}\text{N}_3\text{O}_2\text{S}_2\text{Sn}]^+$ 473 (50), $[\text{C}_{14}\text{H}_{18}\text{N}_3\text{O}_2\text{S}_2\text{Sn}]^+$ 444 (10), $[\text{C}_{13}\text{H}_{16}\text{N}_3\text{O}_2\text{S}_2\text{Sn}]^+$ 430 (6), $[\text{C}_{12}\text{H}_{15}\text{N}_3\text{O}_2\text{S}_2\text{Sn}]^+$ 417 (5), $[\text{C}_{12}\text{H}_{15}\text{N}_2\text{O}_2\text{S}_2\text{Sn}]^+$ 387 (2), $[\text{C}_9\text{H}_{18}\text{S}_2\text{Sn}]^+$ 310 (2), $[\text{C}_6\text{H}_{11}\text{S}_2\text{Sn}]^+$ 267 (20).

Chlorodiethyltin(IV) 4-(4-nitrophenyl)piperazine-1-carbodithioate (7)

(Yield: 72%). M.p. 156-157 °C. Elemental Analysis, % Calculated (Found), for $\text{C}_{15}\text{H}_{22}\text{N}_3\text{O}_2\text{S}_2\text{SnCl}$: C, 36.36 (36.29); H, 4.44 (5.47); N 8.48 (8.41); S 12.92 (12.84). Raman (cm^{-1}): 615 $\nu(\text{C-S})$, 1202 $\nu(\text{C=S})$, 1511 $\nu(\text{C-N})$, 517 $\nu(\text{Sn-C})$, 346 $\nu(\text{Sn-S})$, 268 $\nu(\text{Sn-Cl})$. IR (cm^{-1}): 1007 $\nu(\text{C-S})$, 1490 $\nu(\text{C-N})$, 503 $\nu(\text{Sn-C})$. EI-MS, m/z (%): $[\text{C}_{13}\text{H}_{17}\text{N}_3\text{O}_2\text{S}_2\text{SnCl}]^+$ 466 (2), $[\text{C}_2\text{H}_5\text{S}_2\text{SnCl}]^+$ 248 (9), $[\text{S}_2\text{SnCl}]^+$ 219 (47), $[\text{C}_2\text{H}_5\text{S}_2\text{Sn}]^+$ 213 (21), $[\text{S}_2\text{Sn}]^+$ 184 (11), $[\text{SnCl}]^+$ 155 (51), $[\text{C}_2\text{H}_5\text{Sn}]^+$ 149 (6), $[\text{Sn}]^+$ 120 (10).

Diethyltin(IV) bis[4-(4-nitrophenyl)piperazine-1-carbodithioate] (8)

(Yield: 70%). M.p. 140-142 °C. Elemental Analysis, % Calculated (Found), for $\text{C}_{26}\text{H}_{34}\text{N}_6\text{O}_4\text{S}_4\text{Sn}$: C, 42.05 (43.89); H, 4.58 (4.53); N 11.32 (11.27); S 17.25 (17.19). Raman (cm^{-1}): 615 $\nu(\text{C-S})$, 1202 $\nu(\text{C=S})$, 1511 $\nu(\text{C-N})$, 517 $\nu(\text{Sn-C})$, 356 $\nu(\text{Sn-S})$. IR (cm^{-1}): 1007 $\nu(\text{C-S})$, 1478 $\nu(\text{C-N})$, 508 $\nu(\text{Sn-C})$. EI-MS, m/z (%): $[\text{C}_{22}\text{H}_{39}\text{N}_4\text{S}_4\text{Sn}]^+$ 597 (1), $[\text{C}_{11}\text{H}_{12}\text{N}_2\text{S}_4\text{Sn}]^+$ 420 (1), $[\text{C}_{12}\text{H}_{15}\text{N}_2\text{OS}_2\text{Sn}]^+$ 387 (39), $[\text{C}_{11}\text{H}_{15}\text{N}_2$

$\text{S}_2\text{Sn}]^+ 359$ (3), $[\text{C}_5\text{H}_{10} \text{S}_2 \text{Sn}]^+ 254$ (1.5), $[\text{C}_2\text{H}_3\text{S}_2\text{Sn}]^+ 211$ (19), $[\text{C}_2\text{H}_5\text{SSn}]^+ 184$ (5).

Chlorodimethyltin(IV) 4-(4-nitrophenyl)piperazine-1-carbodithioate (9)

(Yield: 82%). M.p. 276-280 °C. Elemental Analysis, % Calculated (Found), for $\text{C}_{13}\text{H}_{18}\text{N}_3\text{O}_2\text{S}_2\text{SnCl}$: C, 33.40 (33.32); H, 3.85 (3.81); N, 8.99 (8.87); S, 13.70 (13.63). Raman (cm^{-1}): 615 $\nu(\text{C-S})$, 1198 $\nu(\text{C=S})$, 1508 $\nu(\text{C-N})$, 508 $\nu(\text{Sn-C})$, 364 $\nu(\text{Sn-S})$, 267 $\nu(\text{Sn-Cl})$. IR (cm^{-1}): 1003 $\nu(\text{C-S})$, 1490 $\nu(\text{C-N})$, 507 $\nu(\text{Sn-C})$. EI-MS, m/z (%): $[\text{C}_{12}\text{H}_{15}\text{N}_3\text{O}_2\text{S}_2\text{SnCl}]^+ 452$ (3), $[\text{C}_{11}\text{H}_{12}\text{N}_3\text{O}_2\text{S}_2\text{SnCl}]^+ 437$ (1), $[\text{C}_{10}\text{H}_{12}\text{N}_3\text{O}_2\text{Sn}]^+ 326$ (1), $[\text{C}_2\text{H}_6\text{S}_2\text{SnCl}]^+ 249$ (10), $[\text{S}_2\text{SnCl}]^+ 219$ (7), $[\text{CH}_6\text{SSnCl}]^+ 205$ (45), $[\text{C}_2\text{H}_6\text{SnCl}]^+ 185$ (15), $[\text{CH}_3\text{SnCl}]^+ 170$ (2), $[\text{SnCl}]^+ 155$ (15), $[\text{CH}_3\text{Sn}]^+ 135$ (6), $[\text{Sn}]^+ 120$ (1.5).

Dimethyltin(IV) bis[4-(4-nitrophenyl)piperazine-1-carbodithioate] (10)

(Yield: 79%). M.p. 208-210 °C. Elemental Analysis, % Calculated (Found), for $\text{C}_{24}\text{H}_{30}\text{N}_6\text{O}_4\text{S}_4\text{Sn}$: C, 40.34 (40.29); H 4.20 (4.25); N 11.76 (7.68); S, 17.93 (17.87). Raman (cm^{-1}): 628 $\nu(\text{C-S})$, 1198 $\nu(\text{C=S})$, 1510 $\nu(\text{C-N})$, 506 $\nu(\text{Sn-C})$, 362 $\nu(\text{Sn-S})$. IR (cm^{-1}): 1005 $\nu(\text{C-S})$, 1490 $\nu(\text{C-N})$, 507 $\nu(\text{Sn-C})$. EI-MS, m/z (%): $[\text{C}_{13}\text{H}_{18}\text{N}_2 \text{S}_4\text{Sn}]^+ 450$ (3), $[\text{C}_{12}\text{H}_{15}\text{N}_3\text{O}_2\text{SSn}]^+ 417$ (10), $[\text{C}_{13}\text{H}_{18}\text{N}_2\text{OS}_2\text{Sn}]^+ 402$ (6), $[\text{C}_{13}\text{H}_{18}\text{N} \text{S}_2\text{Sn}]^+ 372$ (6), $[\text{C}_3\text{H}_6\text{S}_2\text{Sn}]^+ 226$ (2), $[\text{C}_2\text{H}_6\text{Sn}]^+ 150$ (30), $[\text{Sn}]^+ 120$ (10).

Chlorodiphenyltin(IV) 4-(4-nitrophenyl)piperazine-1-carbodithioate (11)

(Yield: 78%). M.p. 245-246 °C. Elemental Analysis, % Calculated (Found), for $\text{C}_{23}\text{H}_{22}\text{N}_3\text{O}_2\text{S}_2\text{SnCl}$: C, 46.70 (46.65); H, 3.72 (3.75); N, 7.11 (7.15); S, 10.83 (10.78). Raman (cm^{-1}): 653 $\nu(\text{C-S})$, 1196 $\nu(\text{C=S})$, 1485 $\nu(\text{C-N})$, 269 $\nu(\text{Sn-C})$, 365 $\nu(\text{Sn-S})$, 264 $\nu(\text{Sn-Cl})$. IR (cm^{-1}): 1013 $\nu(\text{C-S})$, 1488 $\nu(\text{C-N})$. EI-MS, m/z (%): $[\text{C}_{22}\text{H}_{22}\text{N}_2\text{S}_2\text{SnCl}]^+ 533$ (3), $[\text{C}_{22}\text{H}_{22}\text{N}_2\text{SSnCl}]^+ 501$ (2), $[\text{C}_{16}\text{H}_{17}\text{N}_2\text{SSn}]^+ 389$ (2), $[\text{C}_{10}\text{H}_{12}\text{N}_2\text{S}_2\text{Sn}]^+ 344$ (30), $[\text{C}_{12}\text{H}_{10}\text{SnCl}]^+ 309$ (75), $[\text{C}_6\text{H}_5\text{SnCl}]^+ 232$ (35), $[\text{C}_6\text{H}_5\text{Sn}]^+ 197$ (18), $[\text{SnCl}]^+ 155$ (62), $[\text{Sn}]^+ 120$ (12).

Diphenyltin(IV) bis[4-(4-nitrophenyl)piperazine-1-carbodithioate] (12)

(Yield: 73%). M.p. 224-226 °C. Elemental Analysis, % Calculated (Found), for $\text{C}_{34}\text{H}_{34}\text{N}_6\text{O}_4\text{S}_4\text{Sn}$: C, 48.69 (48.57); H, 4.06 (3.75); N, 10.02 (9.55); S, 15.27 (15.18). Raman (cm^{-1}): 653 $\nu(\text{C-S})$, 1196 $\nu(\text{C=S})$, 1305 $\nu(\text{C-N})$, 269 $\nu(\text{Sn-C})$, 365 $\nu(\text{Sn-S})$.

IR (cm^{-1}): 1013 $\nu(\text{C-S})$, 1488 $\nu(\text{C-N})$. EI-MS, m/z (%): $[\text{C}_{34}\text{H}_{34}\text{N}_6\text{O}_4\text{S}_4\text{Sn}]^+ 838$ (0.4), $[\text{C}_{22}\text{H}_{26}\text{N}_4\text{OS}_4\text{Sn}]^+ 610$ (1.7), $[\text{C}_{16}\text{H}_{21}\text{N}_4\text{OS}_4\text{Sn}]^+ 533$ (12), $[\text{C}_{16}\text{H}_{21}\text{N}_4\text{OS}_3\text{Sn}]^+ 501$ (8), $[\text{C}_{12}\text{H}_{13}\text{N}_2\text{OS}_3\text{Sn}]^+ 417$ (3), $[\text{C}_6\text{H}_5\text{Sn}]^+ 197$ (39), $[\text{Sn}]^+ 120$ (19).

Tributyltin(IV) 4-(2-methoxyphenyl)piperazine-1-carbodithioate (13)

(Yield: 75%). M.p. liquid. Elemental Analysis, % Calculated (Found), for $\text{C}_{24}\text{H}_{42}\text{N}_2\text{OS}_2\text{Sn}$: C, 51.61 (51.46); H, 7.52 (7.56); N, 5.01 (5.03); S, 11.46 (11.21). Raman (cm^{-1}): 627 $\nu(\text{C-S})$, 1157 $\nu(\text{C=S})$, 1457 $\nu(\text{C-N})$, 540 $\nu(\text{Sn-C})$, 362 $\nu(\text{Sn-S})$. IR (cm^{-1}): 977 $\nu(\text{C-S})$, 1460 $\nu(\text{C-N})$, 520 $\nu(\text{Sn-C})$. EI-MS, m/z (%): $[\text{C}_{24}\text{H}_{42}\text{N}_2\text{OS}_2\text{Sn}]^+ 558$ (9), $[\text{C}_{20}\text{H}_{33}\text{N}_2\text{OS}_2\text{Sn}]^+ 501$ (32), $[\text{C}_{12}\text{H}_{15}\text{N}_2\text{OS}_2\text{Sn}]^+ 387$ (5), $[\text{C}_{13}\text{H}_{27}\text{S}_2\text{Sn}]^+ 367$ (5), $[\text{C}_9\text{H}_{18}\text{S}_2\text{Sn}]^+ 310$ (8), $[\text{C}_{12}\text{H}_{27}\text{Sn}]^+ 291$ (43), $[\text{C}_6\text{H}_{11}\text{S}_2\text{Sn}]^+ 267$ (100), $[\text{C}_8\text{H}_{18}\text{Sn}]^+ 234$ (35), $[\text{C}_4\text{H}_9\text{Sn}]^+ 177$ (100), $[\text{Sn}]^+ 120$ (58).

Tricyclohexyltin(IV) 4-(2-methoxyphenyl)piperazine-1-carbodithioate (14)

(Yield: 69%). M.p. 129-130 °C. Elemental Analysis, % Calculated (Found), for $\text{C}_{30}\text{H}_{48}\text{N}_2\text{OS}_2\text{Sn}$: C, 56.60 (56.43); H, 7.54 (7.61); N, 4.40 (4.54); S, 10.06 (9.76). Raman (cm^{-1}): 598 $\nu(\text{C-S})$, 1163 $\nu(\text{C=S})$, 1439 $\nu(\text{C-N})$, 639 $\nu(\text{Sn-C})$, 387 $\nu(\text{Sn-S})$. IR (cm^{-1}): 990 $\nu(\text{C-S})$, 1461 $\nu(\text{C-N})$, 550 $\nu(\text{Sn-C})$. EI-MS, m/z (%): $[\text{C}_{29}\text{H}_{45}\text{N}_2\text{S}_2\text{Sn}]^+ 605$ (5), $[\text{C}_{24}\text{H}_{37}\text{N}_2\text{OS}_2\text{Sn}]^+ 533$ (53), $[\text{C}_{17}\text{H}_{30}\text{N}_2\text{S}_2\text{Sn}]^+ 446$ (4), $[\text{C}_{12}\text{H}_{15}\text{N}_2\text{OS}_2\text{Sn}]^+ 387$ (14), $[\text{C}_{11}\text{H}_{19}\text{N}_2\text{S}_2\text{Sn}]^+ 363$ (68), $[\text{C}_9\text{H}_{15}\text{NS}_2\text{Sn}]^+ 321$ (100), $[\text{C}_{12}\text{H}_{22}\text{Sn}]^+ 286$ (4), $[\text{C}_6\text{H}_{11}\text{Sn}]^+ 203$ (87).

Trimethyltin(IV) 4-(2-methoxyphenyl)piperazine-1-carbodithioate (15)

(Yield: 63%). M.p. 123-126 °C. Elemental Analysis, % Calculated (Found), for $\text{C}_{15}\text{H}_{24}\text{N}_2\text{OS}_2\text{Sn}$: C, 41.66 (41.48); H, 5.55 (5.58); N, 6.48 (6.51); S, 14.81 (14.73). Raman (cm^{-1}): 554 $\nu(\text{C-S})$, 1160 $\nu(\text{C=S})$, 1433 $\nu(\text{C-N})$, 514 $\nu(\text{Sn-C})$, 386 $\nu(\text{Sn-S})$. IR (cm^{-1}): 990 $\nu(\text{C-S})$, 1463 $\nu(\text{C-N})$, 507 $\nu(\text{Sn-C})$. EI-MS, m/z (%): $[\text{C}_3\text{H}_6\text{S}_2\text{Sn}]^+ 226$ (2), $[\text{C}_3\text{H}_9\text{Sn}]^+ 165$ (25), $[\text{C}_2\text{H}_6\text{Sn}]^+ 150$ (100), $[\text{C}_3\text{H}_3\text{Sn}]^+ 135$ (40).

Triphenyltin(IV) 4-(2-methoxyphenyl)piperazine-1-carbodithioate (16)

(Yield: 80%). M.p. 156-158 °C. Elemental Analysis, % Calculated (Found), for $\text{C}_{30}\text{H}_{30}\text{N}_2\text{OS}_2\text{Sn}$: C, 58.25 (58.17); H, 4.85 (4.88); N, 4.53 (4.58); S, 10.35 (10.26). Raman (cm^{-1}): 617 $\nu(\text{C-S})$, 1157 $\nu(\text{C=S})$, 1480 $\nu(\text{C-N})$, 267 $\nu(\text{Sn-C})$, 390 $\nu(\text{Sn-S})$. IR (cm^{-1}): 1007 $\nu(\text{C-S})$, 1461 $\nu(\text{C-N})$. EI-MS, m/z (%): $[\text{C}_{24}\text{H}_{25}\text{N}_2\text{OS}_2\text{Sn}]^+ 541$ (9), $[\text{C}_{12}\text{H}_{15}\text{N}_2\text{OS}_2\text{Sn}]^+ 387$ (3), $[\text{C}_{18}\text{H}_{15}\text{Sn}]^+ 351$ (10), $[\text{C}_6\text{H}_5\text{Sn}]^+ 197$ (22).

Chlorodibutyltin(IV) 4-(2-methoxyphenyl)piperazine-1-carbodithioate (17)

(Yield: 81%). M.p. 185-186 °C. Elemental Analysis, % Calculated (Found), for $\text{C}_{20}\text{H}_{33}\text{N}_2\text{OS}_2\text{SnCl}$: C, 44.77 (44.71); H, 6.15 (6.19); N, 5.22 (5.24); S, 11.94 (11.87).

Raman (cm^{-1}): 626 $\nu(\text{C-S})$, 1168 $\nu(\text{C=S})$, 1457 $\nu(\text{C-N})$, 513 $\nu(\text{Sn-C})$, 361 $\nu(\text{Sn-S})$, 259 $\nu(\text{Sn-Cl})$. IR (cm^{-1}): 970 $\nu(\text{C-S})$, 1461 $\nu(\text{C-N})$, 509 $\nu(\text{Sn-C})$. EI-MS, m/z (%): $[\text{C}_{20}\text{H}_{33}\text{N}_2\text{OS}_2\text{Sn}]^+$ 501 (4.5), $[\text{C}_{16}\text{H}_{24}\text{N}_2\text{OS}_2\text{SnCl}]^+$ 479 (10), $[\text{C}_{12}\text{H}_{15}\text{N}_2\text{OS}_2\text{SnCl}]^+$ 422 (10), $[\text{C}_{12}\text{H}_{15}\text{N}_2\text{OS}_2\text{Sn}]^+$ 387 (5), $[\text{C}_9\text{H}_{18}\text{S}_2\text{SnCl}]^+$ 345 (2), $[\text{C}_9\text{H}_{18}\text{S}_2\text{Sn}]^+$ 310 (2), $[\text{C}_8\text{H}_{18}\text{SnCl}]^+$ 269 (2), $[\text{C}_5\text{H}_9\text{S}_2\text{Sn}]^+$ 253 (8.6), $[\text{C}_4\text{H}_9\text{SnCl}]^+$ 212 (71), $[\text{C}_4\text{H}_9\text{Sn}]^+$ 177 (7), $[\text{SnCl}]^+$ 155 (53).

Dibutyltin(IV) bis[4-(2-methoxyphenyl)piperazine-1-carbodithioate] (18)

(Yield: 82%). M.p. 115-117 °C. Elemental Analysis, % Calculated (Found), for $\text{C}_{32}\text{H}_{48}\text{N}_4\text{O}_2\text{S}_4\text{Sn}$: C, 50 (49.67); H, 6.25 (6.29); N, 7.29 (7.32); S, 16.66 (16.57). Raman (cm^{-1}): 628 $\nu(\text{C-S})$, 1153 $\nu(\text{C=S})$, 1439 $\nu(\text{C-N})$, 513 $\nu(\text{Sn-C})$, 360 $\nu(\text{Sn-S})$. IR (cm^{-1}): 980 $\nu(\text{C-S})$, 1463 $\nu(\text{C-N})$, 509 $\nu(\text{Sn-C})$. EI-MS, m/z (%): $[\text{C}_{25}\text{H}_{41}\text{N}_4\text{OS}_4\text{Sn}]^+$ 661 (4), $[\text{C}_{17}\text{H}_{23}\text{N}_4\text{OS}_4\text{Sn}]^+$ 547 (3), $[\text{C}_{20}\text{H}_{33}\text{N}_2\text{O S}_2\text{Sn}]^+$ 501 (6), $[\text{C}_{12}\text{H}_{15}\text{N}_2\text{OS}_2\text{Sn}]^+$ 387 (4), $[\text{C}_4\text{H}_9\text{Sn}]^+$ 177 (12), $[\text{Sn}]^+$ 120 (20).

Chlorodiethyltin(IV) 4-(2-methoxyphenyl)piperazine-1-carbodithioate (19)

(Yield: 79%). M.p. 90-92 °C. Elemental Analysis, % Calculated (Found), for $\text{C}_{16}\text{H}_{25}\text{N}_2\text{OS}_2\text{SnCl}$: C, 40 (39.42); H, 5.21 (5.22); N, 5.83 (5.85); S, 13.33 (13.27). Raman (cm^{-1}): 626 $\nu(\text{C-S})$, 1182 $\nu(\text{C=S})$, 1456 $\nu(\text{C-N})$, 468 $\nu(\text{Sn-C})$, 396 $\nu(\text{Sn-S})$, 267 $\nu(\text{Sn-Cl})$. IR (cm^{-1}): 990 $\nu(\text{C-S})$, 1461 $\nu(\text{C-N})$, 499 $\nu(\text{Sn-C})$. EI-MS, m/z (%): $[\text{C}_{14}\text{H}_{20}\text{N}_2\text{OS}_2\text{SnCl}]^+$ 451 (18.3), $[\text{C}_{12}\text{H}_{15}\text{N}_2\text{OS}_2\text{SnCl}]^+$ 422 (7.4), $[\text{C}_{12}\text{H}_{15}\text{N}_2\text{OS}_2\text{Sn}]^+$ 387 (4), $[\text{S}_2\text{SnC}_2\text{H}_5\text{Cl}]^+$ 248 (19), $[\text{S}_2\text{SnCl}]^+$ 219 (88), $[\text{S}_2\text{Sn C}_2\text{H}_5]^+$ 213 (29.5), $[\text{S}_2\text{Sn}]^+$ 184 (16.2), $[\text{SnCl}]^+$ 155 (67.6).

Diethyltin(IV) bis[4-(2-methoxyphenyl)piperazine-1-carbodithioate] (20)

(Yield: 76%). M.p. 185-186 °C. Elemental Analysis, % Calculated (Found), for $\text{C}_{28}\text{H}_{40}\text{N}_4\text{O}_2\text{S}_4\text{Sn}$: C, 47.19 (47.14); H, 5.61 (5.64); N, 7.86 (7.89); S, 17.97 (17.93). Raman (cm^{-1}): 624 $\nu(\text{C-S})$, 1180 $\nu(\text{C=S})$, 1457 $\nu(\text{C-N})$, 486 $\nu(\text{Sn-C})$, 385 $\nu(\text{Sn-S})$. IR (cm^{-1}): 970 $\nu(\text{C-S})$, 1461 $\nu(\text{C-N})$, 509 $\nu(\text{Sn-C})$. EI-MS, m/z (%): $[\text{C}_{26}\text{H}_{35}\text{N}_4\text{O}_2\text{S}_4\text{Sn}]^+$ 683 (0.7), $[\text{C}_{24}\text{H}_{30}\text{N}_4\text{O}_2\text{S}_4\text{Sn}]^+$ 654 (3), $[\text{C}_{16}\text{H}_{25}\text{N}_2\text{OS}_2\text{Sn}]^+$ 445 (10), $[\text{C}_{12}\text{H}_{15}\text{N}_2\text{OS}_2\text{Sn}]^+$ 387 (12), $[\text{C}_7\text{H}_{13}\text{N}_2\text{S}_2\text{Sn}]^+$ 309 (6), $[\text{C}_2\text{H}_5\text{Sn}]^+$ 149 (18).

Chlorodimethyltin(IV) 4-(2-methoxyphenyl)piperazine-1-carbodithioate (21)

(Yield: 78%). M.p. 136-138 °C. Elemental Analysis, % Calculated (Found), for $\text{C}_{14}\text{H}_{21}\text{N}_2\text{OS}_2\text{SnCl}$: C, 37.16 (37.11); H, 4.64 (4.66); N, 6.19 (6.21); S, 14.15 (14.1). Raman (cm^{-1}): 623 $\nu(\text{C-S})$, 1167 $\nu(\text{C=S})$, 1462 $\nu(\text{C-N})$, 499 $\nu(\text{Sn-C})$, 394 $\nu(\text{Sn-S})$, 285 $\nu(\text{Sn-Cl})$. IR (cm^{-1}): 974 $\nu(\text{C-S})$, 1461 $\nu(\text{C-N})$, 501 $\nu(\text{Sn-C})$. EI-MS, m/z (%): $[\text{C}_{13}\text{H}_{18}\text{N}_2\text{OS}_2\text{SnCl}]^+$ 437 (1.3), $[\text{C}_{12}\text{H}_{15}\text{N}_2\text{OS}_2\text{SnCl}]^+$ 422 (< 0.5), $[\text{C}_{11}\text{H}_{15}\text{N}_2\text{OSn}]^+$

311 (< 0.5), $[\text{C}_2\text{H}_6\text{S}_2\text{SnCl}]^+$ 249 (22.7), $[\text{S}_2\text{SnCl}]^+$ 219 (5.1), $[\text{H}_3\text{SSn CH}_3\text{Cl}]^+$ 205 (100), $[\text{C}_2\text{H}_6\text{SnCl}]^+$ 185 (34), $[\text{CH}_3\text{SnCl}]^+$ 170 (5.8), $[\text{SnCl}]^+$ 155 (34.3), $[\text{CH}_3\text{Sn}]^+$ 135 (10), $[\text{Sn}]^+$ 120 (8).

Dimethyltin(IV) bis[4-(2-methoxyphenyl)piperazine-1-carbodithioate] (22)

(Yield: 79%). M.p. 191-194 °C. Elemental Analysis, % Calculated (Found), for $\text{C}_{26}\text{H}_{36}\text{N}_4\text{O}_2\text{S}_4\text{Sn}$: C, 45.61 (45.55); H, 5.26 (5.29); N, 8.18 (8.21); S, 18.71 (18.66). Raman (cm^{-1}): 626 $\nu(\text{C-S})$, 1169 $\nu(\text{C=S})$, 1458 $\nu(\text{C-N})$, 512 $\nu(\text{Sn-C})$, 361 $\nu(\text{Sn-S})$. IR (cm^{-1}): 969 $\nu(\text{C-S})$, 1461 $\nu(\text{C-N})$, 514 $\nu(\text{Sn-C})$. EI-MS, m/z (%): $[\text{C}_{24}\text{H}_{34}\text{N}_4\text{O}_2\text{S}_4\text{Sn}]^+$ 658 (100), $[\text{C}_{14}\text{H}_{21}\text{N}_2\text{OS}_2\text{Sn}]^+$ 417 (1), $[\text{C}_{13}\text{H}_{18}\text{N}_2\text{OS}_2\text{Sn}]^+$ 402 (2), $[\text{C}_3\text{H}_6\text{S}_2\text{Sn}]^+$ 226 (1), $[\text{C}_2\text{H}_3\text{S}_2\text{Sn}]^+$ 211 (4), $[\text{S}_2\text{Sn}]^+$ 184 (38), $[\text{C S}_2\text{Sn}]^+$ 196 (2), $[\text{C}_2\text{H}_6\text{Sn}]^+$ 150 (76), $[\text{CH}_3\text{Sn}]^+$ 135 (11), $[\text{Sn}]^+$ 120 (8).

Chlorodiphenyltin(IV) 4-(2-methoxyphenyl)piperazine-1-carbodithioate (23)

(Yield: 73%). M.p. 186-189 °C. Elemental Analysis, % Calculated (Found), for $\text{C}_{24}\text{H}_{25}\text{N}_2\text{OS}_2\text{SnCl}$: C, 50 (49.3); H, 4.34 (4.37); N, 4.86 (4.88); S, 11.11 (11.07). Raman (cm^{-1}): 616 $\nu(\text{C-S})$, 1162 $\nu(\text{C=S})$, 1455 $\nu(\text{C-N})$, 271 $\nu(\text{Sn-C})$, 395 $\nu(\text{Sn-S})$, 234 $\nu(\text{Sn-Cl})$. IR (cm^{-1}): 977 $\nu(\text{C-S})$, 1461 $\nu(\text{C-N})$. EI-MS, m/z (%): $[\text{C}_{12}\text{H}_{15}\text{N}_2\text{OS}_2\text{Sn}]^+$ 387 (3), $[\text{C}_{12}\text{H}_{10}\text{SnCl}]^+$ 309 (24), $[\text{C}_{10}\text{H}_{12}\text{N}_2\text{S}_2\text{Sn}]^+$ 344 (13.5), $[\text{C}_9\text{H}_{12}\text{N}_2\text{Sn}]^+$ 268 (14), $[\text{C}_6\text{H}_5\text{SnCl}]^+$ 232 (11), $[\text{SnCl}]^+$ 155 (17), $[\text{Sn}]^+$ 120 (9).

Diphenyltin(IV) bis[4-(2-methoxyphenyl)piperazine-1-carbodithioate] (24)

(Yield: 72%). M.p. 168-171 °C. Elemental Analysis, % Calculated (Found), for $\text{C}_{36}\text{H}_{40}\text{N}_4\text{O}_2\text{S}_4\text{Sn}$: C, 53.46 (53.39); H, 4.95 (4.99); N, 6.93 (6.96); S, 15.84 (15.78). Raman (cm^{-1}): 627 $\nu(\text{C-S})$, 1167 $\nu(\text{C=S})$, 1457 $\nu(\text{C-N})$, 271 $\nu(\text{Sn-C})$, 393 $\nu(\text{Sn-S})$. IR (cm^{-1}): 995 $\nu(\text{C-S})$, 1461 $\nu(\text{C-N})$. EI-MS, m/z (%): $[\text{C}_{16}\text{H}_{21}\text{N}_4\text{OS}_4\text{Sn}]^+$ 533 (2), $[\text{C}_{16}\text{H}_{17}\text{N}_2\text{S}_2\text{Sn}]^+$ 421 (5), $[\text{C}_{12}\text{H}_{15}\text{N}_2\text{O S}_2\text{Sn}]^+$ 387 (3), $[\text{C}_{10}\text{H}_{12}\text{N}_2\text{S}_2\text{Sn}]^+$ 344 (17), $[\text{C}_9\text{H}_{12}\text{N}_2\text{Sn}]^+$ 268 (2), $[\text{C}_6\text{H}_5\text{Sn}]^+$ 197 (10).

Tributyltin(IV) 4-(4-methoxyphenyl)piperazine-1-carbodithioate (25)

(Yield: 70%). M.p. 170-171 °C. Elemental Analysis, % Calculated (Found), for $\text{C}_{24}\text{H}_{42}\text{N}_2\text{OS}_2\text{Sn}$: C, 51.61 (51.59), H, 7.52 (7.53), N, 5.01 (5.00), S, 11.47 (11.43). Raman (cm^{-1}): 598 $\nu(\text{C-S})$, 1146 $\nu(\text{C=S})$, 1445 $\nu(\text{C-N})$, 471 $\nu(\text{Sn-C})$, 391 $\nu(\text{Sn-S})$. IR (cm^{-1}): 997 $\nu(\text{C-S})$, 1430 $\nu(\text{C-N})$, 540 $\nu(\text{Sn-C})$. EI-MS, m/z (%): $[\text{S}_2\text{Sn}(\text{C}_4\text{H}_9)_3]^+$ 355 (1), $[\text{SSnH}(\text{C}_4\text{H}_9)_2]^+$ 267 (30), $[\text{Sn}(\text{C}_4\text{H}_9)_3]^+$ 291 (38), $[\text{Sn}(\text{C}_4\text{H}_9)_2]^+$ 234 (2), $[\text{Sn}(\text{C}_4\text{H}_9)]^+$ 177 (45), $[\text{Sn}]^+$ 120 (13).

Tricyclohexyltin(IV) 4-(4-methoxyphenyl)piperazine-1-carbodithioate (26)

(Yield: 73%). M.p. 144-145 °C. Elemental Analysis, % Calculated (Found), for $C_{30}H_{48}N_2OS_2Sn$: C, 56.60 (56.58), H, 7.547 (7.52), N, 4.40 (4.37), S, 10.06 (10.03). Raman (cm^{-1}): 563 $\nu(C-S)$, 1166 $\nu(C=S)$, 1473 $\nu(C-N)$, 484 $\nu(Sn-C)$, 380 $\nu(Sn-S)$. IR (cm^{-1}): 1015 $\nu(C-S)$, 1440 $\nu(C-N)$, 530 $\nu(Sn-C)$. EI-MS, m/z (%): $[C_{11}H_{12}N_2S_2Sn(C_6H_{11})_3]^+$ 605 (2.3), $[C_{12}H_{15}N_2OS_2Sn(C_6H_{11})_2]^+$ 553 (64.6), $[C_{12}H_{15}N_2OS_2Sn]^+$ 387 (26), $[Sn(C_6H_{11})_3]^+$ 369 (2.2), $[C_5H_8N_2S_2Sn(C_3H_5)]^+$ 321 (82), $[Sn(C_6H_{11})_2]^+$ 286 (4), $[Sn(C_6H_{11})]^+$ 203 (100), $[Sn]^+$ 120 (15.4).

Trimethyltin(IV) 4-(4-methoxyphenyl)piperazine-1-carbodithioate (27)

(Yield: 68%). M.p. 162-164 °C. Elemental Analysis, % Calculated (Found), for $C_{15}H_{24}N_2OS_2Sn$: C, 41.66 (41.64), H, 5.55 (5.56), N, 6.48 (6.47), S, 14.81 (14.77). Raman (cm^{-1}): 545 $\nu(C-S)$, 1146 $\nu(C=S)$, 1473 $\nu(C-N)$, 507 $\nu(Sn-C)$, 380 $\nu(Sn-S)$. IR (cm^{-1}): 1015 $\nu(C-S)$, 1440 $\nu(C-N)$, 530 $\nu(Sn-C)$. EI-MS, m/z (%): $[S_2Sn(CH_3)_3]^+$ 229 (2), $[SSnH(CH_3)_2]^+$ 183 (61), $[Sn(CH_3)_3]^+$ 165 (44), $[Sn(CH_3)_2]^+$ 150 (3), $[Sn(CH_3)]^+$ 135 (40), $[Sn]^+$ 120 (20).

Triphenyltin(IV) 4-(4-methoxyphenyl)piperazine-1-carbodithioate (28)

(Yield: 78%). M.p. 136-139 °C. Elemental Analysis, % Calculated (Found), for $C_{30}H_{30}N_2OS_2Sn$: C, 58.25 (58.22), H, 4.85 (4.83), N, 4.53 (4.50), S, 10.35 (10.33). Raman (cm^{-1}): 615 $\nu(C-S)$, 1043 $\nu(C=S)$, 1480 $\nu(C-N)$, 269 $\nu(Sn-C)$, 374 $\nu(Sn-S)$. IR (cm^{-1}): 1005 $\nu(C-S)$, 1450 $\nu(C-N)$. EI-MS, m/z (%): $[C_{12}H_{15}N_2OS_2Sn(C_6H_5)_2]^+$ 541 (3), $[C_{12}H_{15}N_2OS_2Sn]^+$ 387 (4), $[Sn(C_6H_5)_3]^+$ 351 (11), $[Sn(C_6H_5)]^+$ 197 (22), $[Sn]^+$ 120 (9.6).

Chlorodibutyltin(IV) 4-(4-methoxyphenyl)piperazine-1-carbodithioate (29)

(Yield: 71%). Sticky material. Elemental Analysis, % Calculated (Found), for $C_{20}H_{33}N_2OS_2SnCl$: C, 44.77 (44.73), H, 6.15 (6.17), N, 5.22 (5.20), S, 11.94 (11.90). Raman (cm^{-1}): 593 $\nu(C-S)$, 1038 $\nu(C=S)$, 1443 $\nu(C-N)$, 437 $\nu(Sn-C)$, 388 $\nu(Sn-S)$, 274 $\nu(Sn-Cl)$. IR (cm^{-1}): 995 $\nu(C-S)$, 1430 $\nu(C-N)$. EI-MS, m/z (%): $[C_{12}H_{15}N_2OS_2Sn(C_4H_9)_2]^+$ 501 (0.7), $[C_{12}H_{15}N_2OS_2Sn(C_4H_9)Cl]^+$ 479 (1), $[C_{12}H_{15}N_2OS_2SnCl]^+$ 422 (2.3), $[C_{12}H_{15}N_2OS_2Sn]^+$ 387 (1), $[Sn(C_4H_9)_2Cl]^+$ 269 (5.7), $[Sn(C_4H_9)Cl]^+$ 212 (12.5).

Dibutyltin(IV) bis[4-(4-methoxyphenyl)piperazine-1-carbodithioate] (30)

(Yield: 75%). M.p. 141-142 °C. Elemental Analysis, % Calculated (Found), for $C_{32}H_{48}N_4O_2S_4Sn$: C, 50.00 (49.96), H, 6.25 (6.23), N, 7.29 (7.27), S, 16.66 (16.64). Raman (cm^{-1}): 586 $\nu(C-S)$, 1083 $\nu(C=S)$, 1457 $\nu(C-N)$, 445 $\nu(Sn-C)$, 376 $\nu(Sn-S)$. IR (cm^{-1}): 999 $\nu(C-S)$, 1433 $\nu(C-N)$. EI-MS, m/z (%): $[C_{24}H_{30}N_4O_2S_4Sn]^+$ 654 (0.1),

$[\text{C}_{12}\text{H}_{15}\text{N}_2\text{OS}_2\text{Sn}(\text{C}_4\text{H}_9)_2]^+$ 501 (7), $[\text{C}_{11}\text{H}_{12}\text{N}_2\text{S}_2\text{Sn}(\text{C}_4\text{H}_9)_2]^+$ 470 (6), $[\text{C}_{12}\text{H}_{15}\text{N}_2\text{OS}_2\text{Sn}]^+$ 387 (3), $[\text{Sn}(\text{C}_4\text{H}_9)_2]^+$ 234 (18), $[\text{SnC}_4\text{H}_9]^+$ 177 (13).

Chlorodiethyltin(IV) 4-(4-methoxyphenyl)piperazine-1-carbodithioate (31)

(Yield: 81%). M.p. 84-86 °C. Elemental Analysis, % Calculated (Found), for $\text{C}_{16}\text{H}_{25}\text{N}_2\text{OS}_2\text{SnCl}$: C, 40.00 (39.99), H, 5.21 (5.23), N, 5.83 (5.80), S, 13.33 (13.31). Raman (cm^{-1}): 560 $\nu(\text{C-S})$, 1093 $\nu(\text{C=S})$, 1457 $\nu(\text{C-N})$, 487 $\nu(\text{Sn-C})$, 383 $\nu(\text{Sn-S})$, 257 $\nu(\text{Sn-Cl})$. IR (cm^{-1}): 988 $\nu(\text{C-S})$, 1447 $\nu(\text{C-N})$. EI-MS, m/z (%): $[\text{C}_{12}\text{H}_{15}\text{N}_2\text{OS}_2\text{Sn}(\text{C}_2\text{H}_5)_2]^+$ 445 (2), $[\text{C}_{12}\text{H}_{15}\text{N}_2\text{OS}_2\text{SnCl}]^+$ 422 (2), $[\text{C}_{12}\text{H}_{15}\text{N}_2\text{OS}_2\text{Sn}]^+$ 387 (2), $[\text{S}_2\text{SnCl}]^+$ 219 (22), $[\text{Sn}(\text{C}_2\text{H}_5)_2\text{Cl}]^+$ 213 (20), $[\text{Sn}(\text{C}_2\text{H}_5)\text{Cl}]^+$ 184 (6), $[\text{SnCl}]^+$ 155 (29), $[\text{Sn}(\text{C}_2\text{H}_5)]^+$ 149 (17).

Diethyltin(IV) bis[4-(4-methoxyphenyl)piperazine-1-carbodithioate] (32)

(Yield: 80%). M.p. 138-142 °C. Elemental Analysis, % Calculated (Found), for $\text{C}_{28}\text{H}_{40}\text{N}_4\text{O}_2\text{S}_4\text{Sn}$: C, 47.19 (47.16), H, 5.62 (5.61), N, 7.86 (7.84), S, 17.97 (17.95). Raman (cm^{-1}): 557 $\nu(\text{C-S})$, 1096 $\nu(\text{C=S})$, 1453 $\nu(\text{C-N})$, 497 $\nu(\text{Sn-C})$, 397 $\nu(\text{Sn-S})$. IR (cm^{-1}): 978 $\nu(\text{C-S})$, 1445 $\nu(\text{C-N})$. EI-MS, m/z (%): $[\text{C}_{12}\text{H}_{15}\text{N}_2\text{OS}_2\text{Sn}(\text{CS}_2)(\text{C}_2\text{H}_5)]^+$ 492 (0.7), $[\text{C}_{12}\text{H}_{15}\text{N}_2\text{OS}_2\text{SnS}_2]^+$ 451 (2), $[\text{C}_{12}\text{H}_{15}\text{N}_2\text{OS}_2\text{Sn}(\text{C}_2\text{H}_5)_2]^+$ 445 (1), $[\text{C}_{12}\text{H}_{15}\text{N}_2\text{OS}_2\text{Sn}]^+$ 387 (1).

Chlorodimethyltin(IV) 4-(4-methoxyphenyl)piperazine-1-carbodithioate (33)

(Yield: 82%). M.p. 166-168 °C. Elemental Analysis, % Calculated (Found), for $\text{C}_{14}\text{H}_{21}\text{N}_2\text{OS}_2\text{SnCl}$: C, 37.17 (37.13), H, 4.64 (4.62), N, 6.19 (6.17), S, 14.16 (14.13). Raman (cm^{-1}): 594 $\nu(\text{C-S})$, 1044 $\nu(\text{C=S})$, 1462 $\nu(\text{C-N})$, 530 $\nu(\text{Sn-C})$, 381 $\nu(\text{Sn-S})$, 257 $\nu(\text{Sn-Cl})$. IR (cm^{-1}): 977 $\nu(\text{C-S})$, 1475 $\nu(\text{C-N})$. EI-MS, m/z (%): $[\text{C}_{12}\text{H}_{15}\text{N}_2\text{OS}_2\text{Sn}]^+$ 387 (2), $[\text{S}_2\text{Sn}(\text{CH}_3)_2\text{Cl}]^+$ 249 (26), $[\text{H}_3\text{SSn}(\text{CH}_3)\text{Cl}]^+$ 205 (78), $[\text{Sn}(\text{CH}_3)_2\text{Cl}]^+$ 185 (100), $[\text{SnCl}]^+$ 155 (59), $[\text{Sn}]^+$ 120 (22).

Dimethyltin(IV) bis[4-(4-methoxyphenyl)piperazine-1-carbodithioate] (34)

(Yield: 72%). M.p. 174-176 °C. Elemental Analysis, % Calculated (Found), for $\text{C}_{26}\text{H}_{36}\text{N}_4\text{O}_2\text{S}_4\text{Sn}$: C, 45.61 (45.59), H, 5.26 (5.27), N, 8.19 (8.16), S, 18.71 (18.67). Raman (cm^{-1}): 598 $\nu(\text{C-S})$, 1040 $\nu(\text{C=S})$, 1463 $\nu(\text{C-N})$, 507 $\nu(\text{Sn-C})$, 390 $\nu(\text{Sn-S})$. IR (cm^{-1}): 989 $\nu(\text{C-S})$, 1469 $\nu(\text{C-N})$. EI-MS, m/z (%): $[\text{C}_{24}\text{H}_{30}\text{N}_4\text{O}_2\text{S}_4\text{SnCH}_3]^+$ 669 (0.3), $[\text{C}_{12}\text{H}_{15}\text{N}_2\text{OS}_2\text{SnCH}_3]^+$ 402 (2), $[\text{C}_{12}\text{H}_{15}\text{N}_2\text{OS}_2\text{Sn}]^+$ 387 (3), $[\text{SnCH}_3]^+$ 135 (30).

Chlorodiphenyltin(IV) 4-(4-methoxyphenyl)piperazine-1-carbodithioate (35)

(Yield: 77%). M.p. 164-166 °C. Elemental Analysis, % Calculated (Found), for $\text{C}_{24}\text{H}_{25}\text{N}_2\text{OS}_2\text{SnCl}$: C, 50.00 (49.99), H, 4.34 (4.35), N, 4.86 (4.82), S, 11.11 (11.07). Raman (cm^{-1}): 562 $\nu(\text{C-S})$, 1065 $\nu(\text{C=S})$, 1475 $\nu(\text{C-N})$, 298 $\nu(\text{Sn-C})$, 397 $\nu(\text{Sn-S})$, 241

$\nu(\text{Sn-Cl})$. IR (cm^{-1}): 993 $\nu(\text{C-S})$, 1465 $\nu(\text{C-N})$. EI-MS, m/z (%): $[\text{CS}_2\text{Sn}(\text{C}_6\text{H}_5)_2\text{Cl}]^+$ 385 (3), $[\text{Sn}(\text{C}_6\text{H}_5)_2\text{Cl}]^+$ 309 (23), $[\text{Sn}(\text{C}_6\text{H}_5)\text{Cl}]^+$ 232 (13).

Diphenyltin(IV) bis[4-(4-methoxyphenyl)piperazine-1-carbodithioate] (36)

(Yield: 72%). M.p. 173-177 °C. Elemental Analysis, % Calculated (Found), for $\text{C}_{36}\text{H}_{40}\text{N}_4\text{O}_2\text{S}_4\text{Sn}$: C, 53.46 (53.43), H, 4.95 (4.93), N, 6.93 (6.92), S, 15.84 (15.81). Raman (cm^{-1}): 596 $\nu(\text{C-S})$, 1042 $\nu(\text{C=S})$, 1455 $\nu(\text{C-N})$, 291 $\nu(\text{Sn-C})$, 394 $\nu(\text{Sn-S})$. IR (cm^{-1}): 1001 $\nu(\text{C-S})$, 1461 $\nu(\text{C-N})$. EI-MS, m/z (%): $[\text{C}_{24}\text{H}_{30}\text{N}_4\text{O}_2\text{S}_4\text{Sn}(\text{C}_6\text{H}_5)]^+$ 731 (2), $[\text{C}_{12}\text{H}_{15}\text{N}_2\text{OS}_2\text{Sn}(\text{C}_6\text{H}_5)]^+$ 464 (5), $[\text{C}_{12}\text{H}_{15}\text{N}_2\text{OS}_2\text{Sn}]^+$ 387 (2), $[\text{Sn}(\text{C}_6\text{H}_5)]^+$ 197 (6).

Tributyltin(IV) 4-benzhydrylpiperazine-1-carbodithioate (37)

(Yield: 69%). M.p. 77-79 °C. Elemental Analysis, % Calculated (Found), for $\text{C}_{30}\text{H}_{46}\text{N}_2\text{S}_2\text{Sn}$: C, 58.25 (58.23), H, 7.44 (7.43), N, 4.53 (4.50), S, 10.35 (10.31). Raman (cm^{-1}): 644 $\nu(\text{C-S})$, 1026 $\nu(\text{C=S})$, 1462 $\nu(\text{C-N})$, 590 $\nu(\text{Sn-C})$, 371 $\nu(\text{Sn-S})$. IR (cm^{-1}): 955 $\nu(\text{C-S})$, 1450 $\nu(\text{C-N})$. EI-MS, m/z (%): $[\text{CS}_2\text{Sn}(\text{C}_4\text{H}_9)_3]^+$ 367 (1), $[\text{CS}_2\text{Sn}(\text{C}_4\text{H}_9)_2]^+$ 310 (3), $[\text{Sn}(\text{C}_4\text{H}_9)_3]^+$ 291 (4), $[\text{CS}_2\text{SnC}_4\text{H}_9]^+$ 253 (56), $[\text{Sn}(\text{C}_4\text{H}_9)_2]^+$ 234 (3), $[\text{CS}_2\text{Sn}]^+$ 196 (60), $[\text{SnC}_4\text{H}_9]^+$ 177 (3), $[\text{Sn}]^+$ 120 (10).

Tricyclohexyltin(IV) 4-benzhydrylpiperazine-1-carbodithioate (38)

(Yield: 65%). M.p. 164-166 °C. Elemental Analysis, % Calculated (Found), for $\text{C}_{36}\text{H}_{52}\text{N}_2\text{S}_2\text{Sn}$: C, 62.06 (62.01), H, 7.47 (7.45), N, 4.02 (4.01), S, 9.19 (9.17). Raman (cm^{-1}): 635 $\nu(\text{C-S})$, 1024 $\nu(\text{C=S})$, 1437 $\nu(\text{C-N})$, 646 $\nu(\text{Sn-C})$, 376 $\nu(\text{Sn-S})$. IR (cm^{-1}): 960 $\nu(\text{C-S})$, 1460 $\nu(\text{C-N})$. EI-MS, m/z (%): $[\text{C}_{18}\text{H}_{19}\text{N}_2\text{S}_2\text{Sn}(\text{C}_6\text{H}_{11})_2]^+$ 613 (24), $[\text{C}_{18}\text{H}_{19}\text{N}_2\text{S}_2\text{Sn}]^+$ 447 (6), $[\text{Sn}(\text{C}_6\text{H}_{11})_3]^+$ 369 (40), $[\text{C}_5\text{H}_8\text{N}_2\text{S}_2\text{Sn}(\text{C}_3\text{H}_5)]^+$ 321 (58), $[\text{SnC}_6\text{H}_{11}]^+$ 203 (75), $[\text{Sn}]^+$ 120 (8).

Trimethyltin(IV) 4-benzhydrylpiperazine-1-carbodithioate (39)

(Yield: 69%). M.p. 197-201 °C. Elemental Analysis, % Calculated (Found), for $\text{C}_{21}\text{H}_{28}\text{N}_2\text{S}_2\text{Sn}$: C, 51.22 (51.19), H, 5.69 (5.67), N, 5.69 (5.67), S, 13.01 (12.98). Raman (cm^{-1}): 547 $\nu(\text{C-S})$, 1031 $\nu(\text{C=S})$, 1466 $\nu(\text{C-N})$, 506 $\nu(\text{Sn-C})$, 375 $\nu(\text{Sn-S})$. IR (cm^{-1}): 965 $\nu(\text{C-S})$, 1451 $\nu(\text{C-N})$. EI-MS, m/z (%): $[\text{SSn}(\text{CH}_3)_3]^+$ 197 (25), $[\text{Sn}(\text{CH}_3)_3]^+$ 165 (100), $[\text{Sn}(\text{CH}_3)_2]^+$ 150 (20), $[\text{Sn}]^+$ 120 (3).

Triphenyltin(IV) 4-benzhydrylpiperazine-1-carbodithioate (40)

(Yield: 75%). M.p. 140-142 °C. Elemental Analysis, % Calculated (Found), for $\text{C}_{36}\text{H}_{34}\text{N}_2\text{S}_2\text{Sn}$: C, 63.71 (63.69), H, 5.01 (5.00), N, 4.13 (4.11), S, 9.44 (9.41). Raman (cm^{-1}): 652 $\nu(\text{C-S})$, 1022 $\nu(\text{C=S})$, 1480 $\nu(\text{C-N})$, 268 $\nu(\text{Sn-C})$, 392 $\nu(\text{Sn-S})$. IR (cm^{-1}):

955, 985 $\nu(\text{C-S})$, 1469 $\nu(\text{C-N})$. EI-MS, m/z (%): $[\text{C}_{18}\text{H}_{19}\text{N}_2\text{S}_2\text{Sn}(\text{C}_6\text{H}_5)_2]^+$ 601 (25), $[\text{C}_{18}\text{H}_{19}\text{N}_2\text{S}_2\text{Sn}]^+$ 447 (3), $[\text{Sn}(\text{C}_6\text{H}_5)_3]^+$ 351 (89), $[\text{SnC}_6\text{H}_5]^+$ 197 (48), $[\text{Sn}]^+$ 120 (10).

Chlorodibutyltin(IV) 4-benzhydrylpiperazine-1-carbodithioate (41)

(Yield: 85%). M.p. 211-216 °C. Elemental Analysis, % Calculated (Found), for $\text{C}_{26}\text{H}_{37}\text{N}_2\text{S}_2\text{SnCl}$: C, 52.35 (52.30), H, 6.21 (6.18), N, 4.69 (4.66), S, 10.74 (10.70). Raman (cm^{-1}): 617 $\nu(\text{C-S})$, 1029 $\nu(\text{C=S})$, 1443 $\nu(\text{C-N})$, 588 $\nu(\text{Sn-C})$, 382 $\nu(\text{Sn-S})$, 272 $\nu(\text{Sn-Cl})$. IR (cm^{-1}): 935 $\nu(\text{C-S})$, 1469 $\nu(\text{C-N})$. EI-MS, m/z (%): $[\text{C}_{18}\text{H}_{19}\text{N}_2\text{S}_2\text{Sn}(\text{C}_4\text{H}_9)\text{Cl}]^+$ 539 (2), $[\text{C}_{18}\text{H}_{19}\text{N}_2\text{S}_2\text{Sn}]^+$ 447 (1), $[\text{S}_2\text{Sn}(\text{C}_4\text{H}_9)_2\text{Cl}]^+$ 333 (3), $[\text{Sn}(\text{C}_4\text{H}_9)_2\text{Cl}]^+$ 269 (7), $[\text{Sn}(\text{C}_4\text{H}_9)\text{Cl}]^+$ 212 (9), $[\text{SnCl}]^+$ 155 (8).

Dibutyltin(IV) bis[4-benzhydrylpiperazine-1-carbodithioate] (42)

(Yield: 85%). M.p. 207-209 °C. Elemental Analysis, % Calculated (Found), for $\text{C}_{44}\text{H}_{56}\text{N}_4\text{S}_4\text{Sn}$: C, 59.46 (59.44), H, 6.30 (6.29), N, 6.30 (6.27), S, 14.41 (14.38). Raman (cm^{-1}): 617 $\nu(\text{C-S})$, 1025 $\nu(\text{C=S})$, 1443 $\nu(\text{C-N})$, 587 $\nu(\text{Sn-C})$, 384 $\nu(\text{Sn-S})$. IR (cm^{-1}): 937 $\nu(\text{C-S})$, 1469 $\nu(\text{C-N})$. EI-MS, m/z (%): $[\text{C}_{36}\text{H}_{38}\text{N}_4\text{S}_4\text{SnC}_4\text{H}_9]^+$ 831 (5), $[\text{C}_{18}\text{H}_{19}\text{N}_2\text{S}_2\text{Sn}(\text{CS}_2)\text{C}_4\text{H}_9]^+$ 580 (10), $[\text{C}_{18}\text{H}_{19}\text{N}_2\text{S}_2\text{Sn}]^+$ 447 (4), $[\text{Sn}(\text{C}_4\text{H}_9)_2]^+$ 234 (7), $[\text{SnCS}_2]^+$ 197 (13).

Chlorodiethyltin(IV) 4-benzhydrylpiperazine-1-carbodithioate (43)

(Yield: 81%). M.p. 133-134 °C. Elemental Analysis, % Calculated (Found), for $\text{C}_{22}\text{H}_{29}\text{N}_2\text{S}_2\text{SnCl}$: 48.88 (48.84), H, 5.37 (5.38), N, 5.18 (5.16), S, 11.85 (11.81). Raman (cm^{-1}): 592 $\nu(\text{C-S})$, 1024 $\nu(\text{C=S})$, 1484 $\nu(\text{C-N})$, 490 $\nu(\text{Sn-C})$, 387 $\nu(\text{Sn-S})$, 259 $\nu(\text{Sn-Cl})$. IR (cm^{-1}): 945 $\nu(\text{C-S})$, 1470 $\nu(\text{C-N})$. EI-MS, m/z (%): $[\text{C}_{18}\text{H}_{19}\text{N}_2\text{S}_2\text{Sn}(\text{C}_2\text{H}_5)\text{Cl}]^+$ 511 (22), $[\text{S}_2\text{Sn}(\text{C}_2\text{H}_5)\text{Cl}]^+$ 248 (6), $[\text{S}_2\text{Sn}(\text{C}_2\text{H}_5)]^+$ 213 (13), $[\text{S}_2\text{SnCl}]^+$ 219 (30), $[\text{SnCl}]^+$ 155 (24), $[\text{S}_2\text{Sn}]^+$ 184 (6).

Diethyltin(IV) bis[4-benzhydrylpiperazine-1-carbodithioate] (44)

(Yield: 71%). M.p. 153-154 °C. Elemental Analysis, % Calculated (Found), for $\text{C}_{40}\text{H}_{48}\text{N}_4\text{S}_4\text{Sn}$: C, 57.69 (57.66), H, 5.77 (5.73), N, 6.73 (6.71), S, 15.38 (15.36). Raman (cm^{-1}): 621 $\nu(\text{C-S})$, 1031 $\nu(\text{C=S})$, 1464 $\nu(\text{C-N})$, 492 $\nu(\text{Sn-C})$, 385 $\nu(\text{Sn-S})$. IR (cm^{-1}): 955 $\nu(\text{C-S})$, 1460 $\nu(\text{C-N})$. EI-MS, m/z (%): $[\text{C}_{36}\text{H}_{38}\text{N}_4\text{S}_4\text{SnC}_2\text{H}_5]^+$ 803 (6), $[\text{C}_{18}\text{H}_{19}\text{N}_2\text{S}_2\text{Sn}(\text{CS}_2)\text{C}_2\text{H}_5]^+$ 552 (8), $[\text{S}_2\text{Sn}]^+$ 184 (9).

Chlorodimethyltin(IV) 4-benzhydrylpiperazine-1-carbodithioate (45)

(Yield: 81%). M.p. 166-167 °C. Elemental Analysis, % Calculated (Found), for $\text{C}_{20}\text{H}_{25}\text{N}_2\text{S}_2\text{SnCl}$: C, 46.87 (46.85), H, 4.88 (4.86), N, 5.47 (5.44), S, 12.50 (12.48). Raman (cm^{-1}): 561 $\nu(\text{C-S})$, 1026 $\nu(\text{C=S})$, 1462 $\nu(\text{C-N})$, 518 $\nu(\text{Sn-C})$, 389 $\nu(\text{Sn-S})$, 261 $\nu(\text{Sn-Cl})$. IR (cm^{-1}): 995 $\nu(\text{C-S})$, 1460 $\nu(\text{C-N})$. EI-MS, m/z (%): $[\text{C}_{18}\text{H}_{19}\text{N}_2$

$\text{S}_2\text{Sn}(\text{CH}_3)\text{Cl}]^+$ 497 (7), $[\text{C}_5\text{H}_8\text{N}_2\text{S}_2\text{Sn}(\text{CH}_3)_2\text{Cl}]^+$ 345 (10), $[\text{S}_2\text{Sn}(\text{CH}_3)_2\text{Cl}]^+$ 249 (17), $[\text{H}_3\text{SSn}(\text{CH}_3)\text{Cl}]^+$ 205 (38), $[\text{Sn}(\text{CH}_3)_2\text{Cl}]^+$ 185 (25), $[\text{SnCl}]^+$ 155 (16).

Dimethyltin(IV) bis[4-benzhydrylpiperazine-1-carbodithioate] (46)

(Yield: 74%). M.p. 216-218 °C. Elemental Analysis, % Calculated (Found), for $\text{C}_{38}\text{H}_{44}\text{N}_4\text{S}_4\text{Sn}$: C, 56.71 (56.69), H, 5.47 (5.46), N, 6.96 (6.93), S, 15.92 (15.90). Raman (cm^{-1}): 558 $\nu(\text{C-S})$, 1026 $\nu(\text{C=S})$, 1475 $\nu(\text{C-N})$, 509 $\nu(\text{Sn-C})$, 376 $\nu(\text{Sn-S})$. IR (cm^{-1}): 991 $\nu(\text{C-S})$, 1461 $\nu(\text{C-N})$. EI-MS, m/z (%): $[\text{C}_{18}\text{H}_{19}\text{N}_2\text{S}_2\text{Sn}(\text{CH}_3)_2]^+$ 477 (4), $[\text{C}_{18}\text{H}_{19}\text{N}_2\text{Sn}(\text{CH}_3)_2]^+$ 413 (3), $[\text{S}_2\text{Sn}]^+$ 184 (6), $[\text{SSn CH}_3]^+$ 167 (80).

Chlorodiphenyltin(IV) 4-benzhydrylpiperazine-1-carbodithioate (47)

(Yield: 76%). M.p. 188-191 °C. Elemental Analysis, % Calculated (Found), for $\text{C}_{30}\text{H}_{29}\text{N}_2\text{S}_2\text{SnCl}$: C, 56.60 (56.58), H, 4.56 (4.57), N, 4.40 (4.38), S, 10.06 (10.02). Raman (cm^{-1}): 651 $\nu(\text{C-S})$, 1018 $\nu(\text{C=S})$, 1477 $\nu(\text{C-N})$, 274 $\nu(\text{Sn-C})$, 382 $\nu(\text{Sn-S})$, 268 $\nu(\text{Sn-Cl})$. IR (cm^{-1}): 971 $\nu(\text{C-S})$, 1465 $\nu(\text{C-N})$. EI-MS, m/z (%): $[\text{C}_{18}\text{H}_{19}\text{N}_2\text{S}_2\text{Sn}(\text{C}_6\text{H}_5)_2]^+$, $[\text{Sn}(\text{C}_6\text{H}_5)_2\text{Cl}]^+$ 309 (93), $[\text{Sn}(\text{C}_6\text{H}_5)_2]^+$ 274 (3), $[\text{Sn}(\text{C}_6\text{H}_5)\text{Cl}]^+$ 232 (13), $[\text{SnC}_6\text{H}_5]^+$ 197 (18), $[\text{SnCl}]^+$ 155 (17), $[\text{Sn}]^+$ 120 (4).

Diphenyltin(IV) bis[4-benzhydrylpiperazine-1-carbodithioate] (48)

(Yield: 72%). M.p. 179-181 °C. Elemental Analysis, % Calculated (Found), for $\text{C}_{48}\text{H}_{48}\text{N}_4\text{S}_4\text{Sn}$: C, 62.07 (62.03), H, 5.17 (5.16), N, 6.03 (6.01), S, 13.79 (13.76). Raman (cm^{-1}): 653 $\nu(\text{C-S})$, 1020 $\nu(\text{C=S})$, 1477 $\nu(\text{C-N})$, 271 $\nu(\text{Sn-C})$, 380 $\nu(\text{Sn-S})$. IR (cm^{-1}): 977 $\nu(\text{C-S})$, 1465 $\nu(\text{C-N})$. EI-MS, m/z (%): $[\text{C}_{36}\text{H}_{38}\text{N}_4\text{S}_4\text{SnC}_6\text{H}_5]^+$ 851 (2), $[\text{C}_{18}\text{H}_{19}\text{N}_2\text{S}_2\text{SnC}_6\text{H}_5]^+$ 524 (5), $[\text{C}_6\text{H}_9\text{N}_2\text{S}_2\text{SnC}_4\text{H}_3]^+$ 344 (9), $[\text{SnC}_6\text{H}_5]^+$ 197 (4).

Tributyltin(IV) 4-benzylpiperidine-1-carbodithioate (49)

(Yield: 74%). Sticky material. Elemental Analysis, % Calculated (Found), for $\text{C}_{25}\text{H}_{43}\text{NS}_2\text{Sn}$: C, 55.45 (55.44), H, 7.85 (7.83), N, 2.59 (2.56), S, 11.83 (11.81). Raman (cm^{-1}): 587 $\nu(\text{C-S})$, 1030 $\nu(\text{C=S})$, 1440 $\nu(\text{C-N})$, 504 $\nu(\text{Sn-C})$, 380 $\nu(\text{Sn-S})$. IR (cm^{-1}): 965 $\nu(\text{C-S})$, 1460 $\nu(\text{C-N})$. EI-MS, m/z (%): $[\text{C}_{13}\text{H}_{16}\text{NS}_2\text{Sn}(\text{C}_4\text{H}_9)_2]^+$ 484 (75), $[\text{C}_{13}\text{H}_{16}\text{NS}_2\text{Sn}]^+$ 370 (40), $[\text{Sn}(\text{C}_4\text{H}_9)_3]^+$ 291 (13), $[\text{SnC}_4\text{H}_9]^+$ 177 (46), $[\text{Sn}]^+$ 120 (13).

Tricyclohexyltin(IV) 4-benzylpiperidine-1-carbodithioate (50)

(Yield: 70%). M.p. 122-124 °C. Elemental Analysis, % Calculated (Found), for $\text{C}_{31}\text{H}_{49}\text{NS}_2\text{Sn}$: C, 60.09 (60.07), H, 7.91 (7.90), N, 2.26 (2.23), S, 10.34 (10.30). Raman (cm^{-1}): 547 $\nu(\text{C-S})$, 1077 $\nu(\text{C=S})$, 1472 $\nu(\text{C-N})$, 645 $\nu(\text{Sn-C})$, 370 $\nu(\text{Sn-S})$. IR (cm^{-1}): 963 $\nu(\text{C-S})$, 1460 $\nu(\text{C-N})$. EI-MS, m/z (%): $[\text{C}_{13}\text{H}_{16}\text{NS}_2\text{Sn}(\text{C}_6\text{H}_{11})_2]^+$ 536 (70), $[\text{C}_{13}\text{H}_{16}\text{NS}_2\text{Sn}]^+$ 370 (42), $[\text{Sn}(\text{C}_6\text{H}_{11})_2]^+$ 286 (3), $[\text{SnC}_6\text{H}_{11}]^+$ 203 (78), $[\text{Sn}]^+$ 120 (13).

Trimethyltin(IV) 4-benzylpiperidine-1-carbodithioate (51)

(Yield: 71%). M.p. 133-134 °C. Elemental Analysis, % Calculated (Found), for $C_{16}H_{25}NS_2Sn$: C, 46.26 (46.23), H, 6.02 (6.01), N, 3.37 (3.35), S, 15.42 (15.39). Raman (cm^{-1}): 618 $\nu(C-S)$, 1030 $\nu(C=S)$, 1474 $\nu(C-N)$, 521 $\nu(Sn-C)$, 361 $\nu(Sn-S)$. IR (cm^{-1}): 970 $\nu(C-S)$, 1445 $\nu(C-N)$. EI-MS, m/z (%): $[C_{13}H_{16}NS_2Sn(CH_3)_2]^+$ 400 (14), $[C_{13}H_{16}NS_2Sn]^+$ 370 (5), $[Sn(CH_3)_3]^+$ 165 (13), $[SnCH_3]^+$ 135 (23), $[Sn]^+$ 120 (5).

Triphenyltin(IV) 4-benzylpiperidine-1-carbodithioate (52)

(Yield: 79%). M.p. 138-139 °C. Elemental Analysis, % Calculated (Found), for $C_{31}H_{31}NS_2Sn$: C, 61.89 (61.88), H, 5.16 (5.17), N, 2.33 (2.31), S, 10.65 (10.62). Raman (cm^{-1}): 617 $\nu(C-S)$, 1019 $\nu(C=S)$, 1488 $\nu(C-N)$, 264 $\nu(Sn-C)$, 370 $\nu(Sn-S)$. IR (cm^{-1}): 988 $\nu(C-S)$, 1470 $\nu(C-N)$. EI-MS, m/z (%): $[C_{13}H_{16}NS_2Sn(C_6H_5)_2]^+$ 523 (23), $[Sn(C_6H_5)_3]^+$ 351 (32), $[SnC_6H_5]^+$ 197 (40), $[Sn]^+$ 120 (28).

Chlorodibutyltin(IV) 4-benzylpiperidine-1-carbodithioate (53)

(Yield: 77%). Sticky material. Elemental Analysis, % Calculated (Found), for $C_{21}H_{34}NS_2SnCl$: C, 48.55 (48.53), H, 6.55 (6.54), N, 2.69 (2.67), S, 12.33 (12.30). Raman (cm^{-1}): 619 $\nu(C-S)$, 1031 $\nu(C=S)$, 1445 $\nu(C-N)$, 581 $\nu(Sn-C)$, 345 $\nu(Sn-S)$, 255 $\nu(Sn-Cl)$. IR (cm^{-1}): 968 $\nu(C-S)$, 1455 $\nu(C-N)$. EI-MS, m/z (%): $[C_{13}H_{16}NS_2Sn(C_4H_9)Cl]^+$ 462 (6), $[C_{13}H_{16}NS_2Sn]^+$ 370 (6), $[Sn(C_4H_9)_2Cl]^+$ 269 (5), $[Sn(C_4H_9)Cl]^+$ 212 (11), $[SnCl]^+$ 155 (15), $[Sn]^+$ 120 (3).

Dibutyltin(IV) bis[4-benzylpiperidine-1-carbodithioate] (54)

(Yield: 76%). M.p. 141-142 °C. Elemental Analysis, % Calculated (Found), for $C_{34}H_{50}N_2S_4Sn$: C, 55.58 (55.56), H, 6.81 (6.80), N, 3.81 (3.78), S, 17.44 (17.41). Raman (cm^{-1}): 587 $\nu(C-S)$, 1028 $\nu(C=S)$, 1473 $\nu(C-N)$, 503 $\nu(Sn-C)$, 334 $\nu(Sn-S)$. IR (cm^{-1}): 969 $\nu(C-S)$, 1465 $\nu(C-N)$. EI-MS, m/z (%): $[(C_{13}H_{16}NS_2)_2Sn(C_4H_9)]^+$ 677 (3), $[C_{13}H_{16}NS_2Sn(C_4H_9)_2]^+$ 484, $[C_{13}H_{16}NS_2SnC_4H_9]^+$ 427 (21), $[C_{13}H_{16}NS_2Sn]^+$ 370 (19), $[SnC_4H_9]^+$ 177 (55).

Chlorodiethyltin(IV) 4-benzylpiperidine-1-carbodithioate (55)

(Yield: 79%). 125-126 °C. Elemental Analysis, % Calculated (Found), for $C_{17}H_{26}NS_2SnCl$: 44.06 (44.03), H, 5.61 (5.59), N, 3.02 (3.00), S, 13.82 (13.79). Raman (cm^{-1}): 620 $\nu(C-S)$, 1031 $\nu(C=S)$, 1446 $\nu(C-N)$, 476 $\nu(Sn-C)$, 370 $\nu(Sn-S)$, 271 $\nu(Sn-Cl)$. IR (cm^{-1}): 963 $\nu(C-S)$, 1459 $\nu(C-N)$. EI-MS, m/z (%): $[C_{13}H_{16}NS_2Sn(C_2H_5)Cl]^+$ 434 (4), $[C_{13}H_{16}NS_2SnCl]^+$ 405 (7), $[C_{13}H_{16}NS_2Sn]^+$ 370 (16), $[S_2Sn(C_2H_5)Cl]^+$ 248 (11), $[S_2SnCl]^+$ 219 (55), $[S_2Sn]^+$ 184 (2), $[SnCl]^+$ 155 (63), $[Sn]^+$ 120 (11).

Diethyltin(IV) bis[4-benzylpiperidine-1-carbodithioate] (56)

(Yield: 74%). Sticky material. Elemental Analysis, % Calculated (Found), for $C_{30}H_{42}N_2S_4Sn$: 53.09 (52.99), H, 6.19 (6.11), N, 4.13 (4.10), S, 18.88 (18.85). Raman (cm^{-1}): 619 $\nu(C-S)$, 1028 $\nu(C=S)$, 1455 $\nu(C-N)$, 493 $\nu(Sn-C)$, 372 $\nu(Sn-S)$. IR (cm^{-1}): 961 $\nu(C-S)$, 1459 $\nu(C-N)$. EI-MS, m/z (%): $[(C_{13}H_{16}NS_2)_2Sn(C_2H_5)]^+$ 649 (4), $[C_{13}H_{16}NS_2Sn(C_2H_5)_2]^+$ 428 (20), $[C_{13}H_{16}NS_2Sn]^+$ 370 (13), $[Sn(C_2H_5)_2]^+$ 178 (34), $[Sn]^+$ 120 (3).

Chlorodimethyltin(IV) 4-benzylpiperidine-1-carbodithioate (57)

(Yield: 77%). 161-163 °C. Elemental Analysis, % Calculated (Found), for $C_{15}H_{22}NS_2SnCl$: C, 41.38 (41.35), H, 5.06 (5.04), N, 3.22 (3.19), S, 14.71 (14.69). Raman (cm^{-1}): 621 $\nu(C-S)$, 1024 $\nu(C=S)$, 1500 $\nu(C-N)$, 514 $\nu(Sn-C)$, 368 $\nu(Sn-S)$, 249 $\nu(Sn-Cl)$. IR (cm^{-1}): 961 $\nu(C-S)$, 1459 $\nu(C-N)$. EI-MS, m/z (%): $[C_{13}H_{16}NS_2Sn(CH_3)Cl]^+$ 420 (60), $[C_{13}H_{16}NS_2Sn]^+$ 370 (30), $[S_2Sn(CH_3)_2Cl]^+$ 249 (25), $[H_3S Sn(CH_3)Cl]^+$ 205 (97), $[Sn(CH_3)_2Cl]^+$ 185 (41), $[SnCl]^+$ 155 (48).

Dimethyltin(IV) bis[4-benzylpiperidine-1-carbodithioate] (58)

(Yield: 80%). 180-184 °C. Elemental Analysis, % Calculated (Found), for $C_{28}H_{38}N_2S_4Sn$: C, 51.69 (51.67), H, 5.84 (5.82), N, 4.31 (4.28), S, 19.69 (19.66). Raman (cm^{-1}): 622 $\nu(C-S)$, 1030 $\nu(C=S)$, 1474 $\nu(C-N)$, 511 $\nu(Sn-C)$, 364 $\nu(Sn-S)$. IR (cm^{-1}): 971 $\nu(C-S)$, 1451 $\nu(C-N)$. EI-MS, m/z (%): $[(C_{13}H_{16}NS_2)_2Sn]^+$ 620 (13), $[C_{13}H_{16}NS_2Sn]^+$ 370 (66), $[C_{13}H_{16}NS_2Sn(CH_3)_2]^+$ 400 (52).

Chlorodiphenyltin(IV) 4-benzylpiperidine-1-carbodithioate (59)

(Yield: 75%). 168-169 °C. Elemental Analysis, % Calculated (Found), for $C_{25}H_{26}N_2S_2SnCl$: C, 55.66 (55.65), H, 4.65 (4.66), N, 2.50 (2.48), S, 11.45 (11.42). Raman (cm^{-1}): 619 $\nu(C-S)$, 1018 $\nu(C=S)$, 1476 $\nu(C-N)$, 270 $\nu(Sn-C)$, 369 $\nu(Sn-S)$, 264 $\nu(Sn-Cl)$. IR (cm^{-1}): 995 $\nu(C-S)$, 1473 $\nu(C-N)$. EI-MS, m/z (%): $[C_{13}H_{16}NS_2Sn(C_6H_5)_2]^+$ 524 (2), $[C_{13}H_{16}NS_2Sn(C_6H_5)Cl]^+$ 482 (14), $[C_{13}H_{16}NS_2SnCl]^+$ 405 (4), $[C_{13}H_{16}NS_2Sn]^+$ 370 (9), $[Sn(C_6H_5)_2Cl]^+$ 309 (84), $[Sn(C_6H_5)Cl]^+$ 232 (23), $[SnC_6H_5]^+$ 197 (26), $[SnCl]^+$ 155 (13), $[Sn]^+$ 120 (14).

Diphenyltin(IV) bis[4-benzylpiperidine-1-carbodithioate] (60)

(Yield: 76%). 90-92 °C. Elemental Analysis, % Calculated (Found), for $C_{38}H_{42}N_2S_4Sn$: C, 58.91 (58.89), H, 5.42 (5.41), N, 3.62 (3.60), S, 16.54 (16.51). Raman (cm^{-1}): 616 $\nu(C-S)$, 1019 $\nu(C=S)$, 1478 $\nu(C-N)$, 270 $\nu(Sn-C)$, 371 $\nu(Sn-S)$. IR (cm^{-1}): 991 $\nu(C-S)$, 1469 $\nu(C-N)$. EI-MS, m/z (%): $[(C_{13}H_{16}NS_2)_2SnC_6H_5]^+$ 697 (8), $[C_{13}H_{16}NS_2Sn(C_6H_5)_2]^+$ 524 (1), $[Sn(C_6H_5)_2]^+$ 274 (11), $[SnC_6H_5]^+$ 197 (31).

2.7 Biological studies

2.7.1 DNA binding studies

DNA was extracted from chicken blood by Falcon method [4]. The purity of DNA was spectroscopically determined from the ratio of absorbance at 260 and 280 nm ($A_{260}/A_{280} = 1.85$). The concentration of the stock solution of DNA (2.3 mM in nucleotide phosphate, NP) was determined by monitoring the absorbance at 260 nm using the molar extinction coefficient (ϵ) of $6600 \text{ M}^{-1}\text{cm}^{-1}$. Tetra-n-butyl ammonium perchlorate (TBAP) purchased from Fluka (99% purity) was further purified by recrystallization, using methanol as a solvent.

2.7.2 Antibacterial activity

Almost all of the synthesized compounds were screened for antibacterial activity against different bacterial strains including, *Escherichia coli*, *Salmonella typhi*, *Pseudomonas aeruginosa*, *Staphylococcus aureus* and *Streptococcus*, using the agar well diffusion method [5]. Streptomycin was used as standard drug and the wells (6 mm in diameter) were dug in the media with the help of a sterile metallic borer. Two to eight hours old bacterial inoculums containing approximately 10^4 – 10^6 colony forming units (CFU)/mL were spread on the surface of a nutrient agar with the help of a sterile cotton swab. The recommended concentration of the test sample (2 mg/mL in DMSO) was introduced into the respective wells. Other wells supplemented with DMSO and reference antibacterial drug served as negative and positive controls, respectively. The plates were incubated immediately at 37°C for 20 h. The activity was determined by measuring the diameter of the inhibition zone (in mm), showing complete inhibition. Growth inhibition was calculated with reference to the positive control. The results of the antibacterial activity so obtained are collected in Tables 3.22-3.24.

2.7.3 Antifungal activity

The synthesized complexes were also tested for antifungal activity against six different human, animal and plant pathogens namely: *Aspergillus niger*, *Aspergillus flavus*, *Helminthosporium solani*, *Alternaria solani* and *Fusarium sp.* by using tube diffusion test [6]. Clomitrazone were used as standard antifungal agents for comparison test.

Stock solutions of pure compounds (200 µg/mL) were prepared in sterile DMSO. Sabouraud dextrose agar was prepared by mixing Sabouraud (32.5 g), glucose agar (4%) and agar-agar (4 g) in 500 mL of distilled water followed by dissolution at 90-95 °C on a water bath. The media (4 mL) was dispensed into screw-capped tubes and autoclaved at 121 °C for 15 min. Test compounds (66.6 µL) was added from the stock solution to non-solidified Sabouraud agar media (50 °C). The tubes were then solidified at room temperature and inoculated with 4 mm diameter portion of inoculums derived from a 7 days old respective fungal culture. For non-mycelial growth, an agar surface streak was employed. The tubes were incubated at 27-29 °C for 7-10 days and growth in the compound containing media was determined by measuring the linear growth (in mm) and growth inhibition with reference to the respective control. The results of the antifungal activity obtained are listed in Tables 3.25-3.27.

References

- [1] W. L. F. Armarego and D. D. Perrin , in “Purification of Laboratory Chemicals”, 4th Edn., Pergoman,Oxord ,1997.
- [2] W. L. F. Armarego and C. L. L. Chai, in “Purification of Laboratory Chemicals”, 5th Edn., Butterworth-Heinemann, London, New York, 2003.
- [3] (a) B. Wrackmeyer, Annu. Rep. NMR Spectrosc. 16 (1985) 73; (b) B. Wrackmeyer, Annu. Rep. NMR Spectrosc. 203 (1999) 38.
- [4] J. Sambrook, E. F. Fritsch, T. Maniatis, Molecular cloning:a laboratory manual 2nd Ed. cod. Spring harbour laboratory press New York. 1989.
- [5] A. Rahman, M. I. Choudhary and W. J. Thomsen, in ‘Bioassay Techniques for Drug Development’, Harward Academic Press, Amsterdam, (2001) pp.14-20.
- [6] S. S. Shaukat, N. A. Khan and F. Ahmad, Pak. J. Bot., 12 (1980) 97.

Results and discussion

3.1 Synthesis of organotin(IV) dithiocarboxylates

Substituted piperazinium/piperidinium salts of dithiocarboxylate ligands were synthesized by the methods described in section 2.3 with all the necessary conditions. The yields are given in the range of 75-85%. All the synthesized ligand salts are crystalline solid, having sharp melting points.

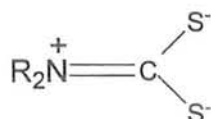
Tri-, chlorordi- and diorganotin(IV) dithiocarboxylates (**1-60**) were synthesized following schemes 2.2-2.4. All the newly synthesized compounds are crystalline solids with only exception of some of tributyl- (**13** and **49**), chlorodibutyl- (**53**) and diethyl(IV) (**56**) derivatives which are semi solids or liquids. They are air stable and soluble in common organic solvents. These compounds have been characterized by various analytical techniques such as elemental analysis, Raman spectroscopy, IR spectroscopy, multinuclear NMR (^1H , ^{13}C and ^{119}Sn), mass spectrometry and X-ray single crystal analysis in order to ascertain their structures. DNA binding parameters were evaluated as well, for representative complexes.

3.2 Raman spectra

The assignment of Raman bands for all complexes has been made by comparison with the Raman spectra of their related precursors. The explicit feature in the spectra of all the complexes was the appearance of a new absorption band in the range of 334-397 cm^{-1} , which was absent from the spectra of the free ligands, can be assigned to the Sn-S stretching mode of vibration. Very sharp Sn-C peak was observed in the range 468-646 cm^{-1} in all complexes except for phenyltin(IV) derivatives where a weak vibration mode in the range 263-298 cm^{-1} was found for Sn-C stretching vibration mode [1]. In addition, Raman spectra of chlorodiorganotin(IV) derivatives display peaks associated with $\nu(\text{Sn-Cl})$ in the range 234-285 cm^{-1} . In the investigated complexes, C-S and C=S illustrate Raman peaks in the region consistent with early report [2].

3.3 Infrared spectra

Of particular interest in the IR spectra are the C-N, C-S stretching frequencies. Both can be used to determine the denticity of 1,1-dithioate moiety. The presence of single band in the region of 900-1000 cm^{-1} due to $\nu(\text{C-S})$ is an indication of bidentate character whereas the presence of two bands with separation value $> 20 \text{ cm}^{-1}$ suggests that ligand bonding is monodentate [3]. In our present study, a single C-S vibration mode was observed in all complexes (except for compounds 1-3) which is an indication of bidentate coordination of 1,1-dithioate moiety and is consistent with the crystal structures. The stretching vibration peaks of the C-N, in the studied complexes, lie between the range of C-N single bond (1250-1360 cm^{-1}) and C=N double bond (1640-1690 cm^{-1}) which is an indication of partial double bond character in C-N bond [4] as shown in scheme 3.1. Sn-C bond gave absorption peaks in expected region.



Scheme 3.1

3.4 $^1\text{H-NMR}$ spectra

The $^1\text{H-NMR}$ spectra of the investigated compounds were recorded in DMSO and CDCl_3 and their data is collected in Tables 3.1-3.6. The assignment of the proton resonances were made by their peaks multiplicity, intensity pattern and comparison of the integration values of the protons with the expected composition. In the spectra of all complexes, the disappearance of duplicate peaks pattern due to aromatic substituted piperazinium/piperidinium ion and appearance of proton signals for the organic groups attached to Sn confirmed the formation of complexes.

In the spectra of organotin(IV) derivatives of ligands 1-4, the protons of piperazine moiety of the ligand showed two multiplets (~ 4.15 and ~ 3.62) in the aliphatic region. The aromatic part of the ligand gave two doublets due to two non-equivalent set of protons in complexes of ligand 1 while these protons appeared as a multiplet in complexes of ligands 2-4. For ligand 5, the piperidine protons demonstrate three triplets (1.78-1.85, 1.27-1.39 and 3.04-3.08 ppm) in the aliphatic region as demanded by the structure. The protons of the benzyl part resonate in two regions; a doublet (~ 5.07 ppm) due to CH_2 protons and a multiplet (7.12-7.33 ppm) due to phenyl moiety.

The methyl protons of trimethyl-, chlorodimethyl- and dimethyl(IV) derivatives appeared as sharp singlets in the range of 0.61-1.56, 1.36-1.50 and 1.03-1.53 ppm respectively, most of them with well-defined satellites. $^2J [^{119}\text{Sn}, ^1\text{H}]$ coupling constants (Tables 3.13-3.17) and the C-Sn-C angles calculated from the satellites demonstrate that trimethyltin(IV) derivatives are tetrahedral in solution. In the chlorodimethyltin(IV) complexes Sn atom is five coordinate while for the later class two type of geometries are feasible in solution; a trigonal bipyramidal and an octahedral. The $\alpha\text{-CH}_2$ protons of chlorodiethyl- and diethyltin(IV) compounds resonate as a quartet in the range 1.36-2.11 ppm while a triplet was observed for $\beta\text{-CH}_3$ protons in the range 1.43-1.87 ppm with $^3J(^1\text{H}, ^1\text{H}) = 6.0\text{-}7.8$ Hz. The protons of tri-n-butyl-, tricyclohexyl-, triphenyl-, chlorodibutyl- and dibutyltin(IV) complexes exhibit a complex pattern and were assigned according to literature [5-7]. Despite the complex pattern of ^1H -NMR spectra of tri-, chlorodi- and n-dibutyltin(IV) derivatives, a clear triplet due to terminal methyl group appeared in the range of 0.83-0.96 ppm with $^3J(^1\text{H}, ^1\text{H}) = 6\text{-}9$ Hz. Difficulty in obtaining the $^2J [^{119}\text{Sn}, ^1\text{H}]$ coupling in these complexes is due to complex nature of the proton resonances of organic groups attached to the Sn, render almost no information about the geometry around Sn atom. However, in case of triphenyltin derivatives, the proton spectrum is informative regarding the geometry around the Sn. The signals for protons of the phenyl groups attached to the Sn were distinguished into two sets. The *ortho* protons were observed at down field (~ 7.76 ppm) and those for *meta* and *para* protons at upfield (~ 7.39 ppm). In addition, the difference in chemical shift resonance between *ortho* and *meta* and *para* (~ 0.37 ppm) is an indication of anisobidentate bonding of 1,1-dithiolate moiety in solution. All these observations are in agreement with the previously reported literature for triphenyltin dithiocarboxylates [8].

Table 3.1: ^1H -NMR data^{a,b} of ligands-salt

^1H	L	L ^a	L ^b	L ^c	L ^d
2, 2', 2a, 2' a	3.50-3.47, 3.27-3.24 (m)	3.63-3.60 3.12-3.09 (m)	2.91-2.89, 2.48-2.46 (m)	2.62, 2.46 (bs)	3.04-2.96 2.60-2.58 (m)
3, 3', 3a, 3' a	4.42-4.39, 3.69-3.65 (m)	4.64-4.63, 3.39-3.38 (m)	4.43-4.40, 3.18-3.17 (m)	4.40, 3.32 (bs)	2.82-2.67, 2.60-2.58 (m)
4	-	-	-	4.28 (s)	1.84-1.64, 1.35-1.27 (m)
5	-	-	-	-	5.77, 3.79 (d)
OCH ₃	-	3.90, 3.86 (s)	3.66, 3.65 (s)	-	-
Ar-H	8.1, 8.0, 7.1, 6.9 (d)	7.07-6.84 (m)	6.92-6.77 (m)	7.48-7.17 (m)	7.34-7.14 (m)
NH ₂	8.9 (s)	8.5 (s)	8.4 (s)	8.1 (s)	8.3

^aNumbering in accordance with Figs. 3.22.

^bMultiplicity is given as s = singlet, d = doublet, m = multiplet, bs = broad signal.

Table 3.2: ^1H -NMR data^{a,b} of organotin(IV) derivatives of 4-(4-nitrophenyl)piperazine-1-carbodithioate

^1H	(1) n-Bu ₃ SnL	(2) Cy ₃ SnL	(3) Me ₃ SnL	(4) Ph ₃ SnL	(5) n-Bu ₂ SnCIL	(6) n-Bu ₂ SnL ₂	(7) Et ₂ SnCIL	(8) Et ₂ SnL ₂	(9) Me ₂ SnCIL	(10) Me ₂ SnL ₂	(11) Ph ₂ SnCIL	(12) Ph ₂ SnL ₂
2,2	3.60-3.56	3.60-3.56	3.58-3.51	3.62-3.60	3.64-3.57	3.67-3.37	3.65-3.55	3.65-3.55	3.71-3.35	3.71-3.35	3.72-3.69	3.72-3.69
	(m)	(m)	(m)	(m)	(m)	(m)	(m)	(m)	(m)	(m)	(m)	(m)
3,3	4.37-4.34	4.39-4.35	4.35-4.30	4.15-4.13	4.29-4.19	4.20-4.17	4.20-4.17	4.20-4.17	4.14-4.02	4.14-4.02	4.12-4.06	4.13-4.06
	(m)	(m)	(m)	(m)	(m)	(m)	(m)	(m)	(m)	(m)	(m)	(m)
Ar-H	6.76	6.79	6.94	6.89	6.77	6.82	6.81	6.81	6.96	6.96	6.92	6.91
	(d, 9.6)	(d, 9.6)	(d, 9.6)	(d, 9.6)	(d, 9.3)	(d, 9.6)	(d, 9)	(d, 9)	(d, 9.3)	(d, 9.3)	(d, 9.3)	(d, 9.6)
	8.12	8.12	8.12	8.07	8.08	8.15	8.12	8.12	8.09	8.09	8.06	8.06
	(d, 9.6)	(d, 9.6)	(d, 9.6)	(d, 9.6)	(d, 9.3)	(d, 9.6)	(d, 9)	(d, 9)	(d, 9.3)	(d, 9.3)	(d, 9.3)	(d, 9.3)
α	1.41-1.22	2.05-1.24	1.61 (s)	-	2.08-1.65	2.01-1.16	1.84	1.84	1.50	1.29	-	-
	(m)	(m)			(m)	(m)	(q, 6)	(q, 9)	[75]	[90]		
β	1.41-1.22	2.05-1.24	-	7.66	2.08-1.65	2.01-1.16	1.47	1.47	-	-	7.94 (bs)	7.94 (bs)
	(m)	(m)		(bs),	(m)	(m)	(t, 6)	(t, 9)				
γ	1.67-1.57	2.05-1.24	-	7.38 (bs)	1.46-1.35	1.49-1.36	-	-	-	-	7.46 (bs)	7.46 (bs)
	(m)	(m)			(m)	(m)						
δ	0.89	2.05-1.24	-	7.38 (bs)	0.92	0.94	-	-	-	-	7.46 (bs)	7.46 (bs)
	(t, 7.2)	(m)			(t, 7.2)	(t, 9)						

^aChemical shift (δ) in ppm. ² $J(^{119}\text{Sn}, ^1\text{H})$, ³ $J(^1\text{H}, ^1\text{H})$ in Hz are listed in square brackets and parenthesis, respectively. Multiplicity is given as s = singlet, d = doublet, m = multiplet, bs = broad signal. ^bNumbering in accordance with Figs. 3.22 and 3.23.

Table 3.3: ^1H -NMR data^{a,b} of organotin(IV) derivatives of 4-(2-methoxyphenyl)piperazine-1-carbodithioate

^1H	(13) n-Bu ₃ SnL ^a	(14) Cy ₃ SnL ^a	(15) Me ₃ SnL ^a	(16) Ph ₃ SnL ^a	(17) n-Bu ₂ SnCIL ^a	(18) n-Bu ₂ SnL ₂ ^a	(19) Et ₂ SnCIL ^a	(20) Et ₂ SnL ₂ ^a	(21) Me ₂ SnCIL ^a	(22) Me ₂ SnL ₂ ^a	(23) Ph ₂ SnCIL ^a	(24) Ph ₂ SnL ₂ ^a
2,2'	3.14-3.12 (m)	3.17-3.14 (m)	3.18-3.15 (m)	3.19-3.16 (m)	3.22-3.19 (m)	3.22-3.19 (m)	3.22-3.19 (m)	3.18-3.15 (m)	3.22-3.19 (m)	3.21-3.16 (m)	3.16-3.13 (m)	3.16-3.13 (m)
3,3'	4.36-4.32 (m)	4.42-4.39 (m)	4.3-4.28 (m)	4.33-4.30 (m)	4.20-4.17 (m)	4.20-4.17 (m)	4.21-4.17 (m)	4.33-4.30 (m)	4.17-4.14 (m)	4.17-4.14 (m)	4.14-4.10 (m)	4.14-4.10 (m)
Ar-H	7.01-6.84 (m)	7.08-6.89 (m)	7.09-6.90 (m)	7.12-6.91 (m)	7.12-6.89 (m)	7.12-6.87 (m)	7.12-6.91 (m)	7.09-6.90 (m)	7.12-6.89 (m)	7.12-6.89 (m)	7.01-6.85 (m)	7.01-6.85 (m)
OCH ₃	3.85 (s)	3.90 (s)	3.90 (s)	3.91 (s)	3.91 (s)	3.91 (s)	3.91 (s)	3.91 (s)	3.90 (s)	3.74 (s)	3.84 (s)	3.84 (s)
α	1.67-1.19 (m)	2.05-1.28 (m)	1.58 [81]	-	1.90-1.34 (m)	1.90-1.34 (m)	2.11 (q)	2.11 (q)	1.45 (s), [78]	1.19 (s), [98]	-	-
β	1.67-1.19 (m)	2.05-1.28 (m)	-	7.89-7.66 (m), [52]	1.90-1.34 (m)	1.90-1.34 (m)	1.87 (t)	1.63 (t)	-	-	8.03 (bs)	8.03 (bs)
γ	1.67-1.19 (m)	2.05-1.28 (m)	-	7.48-7.39 (m)	1.90-1.34 (m)	1.90-1.34 (m)	-	-	-	-	7.44 (bs)	7.44 (bs)
δ	0.94 (t), (6)	2.05-1.28 (m)	-	7.48-7.39 (m)	0.96 (t), (6)	0.96 (t), (6)	-	-	-	-	7.44 (bs)	7.44 (bs)

^aChemical shift (δ) in ppm. ² $J(^{119}\text{Sn}, ^1\text{H})$, ³ $J(^1\text{H}, ^1\text{H})$ in Hz are listed in square brackets and parenthesis, respectively. Multiplicity is given as s = singlet, d = doublet, m = multiplet, bs = broad signal. ^bNumbering in accordance with Figs. 3.22 and 3.23.

Table 3.4: ^1H -NMR data of organotin(IV) derivatives of 4-(4-methoxyphenyl)piperazine-1-carbodithioate

^1H	(25) $\text{n-Bu}_3\text{SnL}^b$	(26) Cy_3SnL^b	(27) Me_3SnL^b	(28) Ph_3SnL^b	(29) $\text{n-Bu}_2\text{SnCIL}^b$	(30) $\text{n-Bu}_2\text{SnL}_2^b$	(31) $\text{Et}_2\text{SnCIL}^b$	(32) $\text{Et}_2\text{SnL}_2^b$	(33) $\text{Me}_2\text{SnCIL}^b$	(34) $\text{Me}_2\text{SnL}_2^b$	(35) $\text{Ph}_2\text{SnCIL}^b$	(36) $\text{Ph}_2\text{SnL}_2^b$
2,2	3.20-3.14 (m)	3.15-3.12 (m)	3.19 (bs)	3.16-3.13 (m)	3.19-3.16 (m)	3.16-3.13 (m)	3.20-3.16 (m)	3.19-3.16 (m)	3.16-3.13 (m)	3.17 (bs)	3.19-3.16 (m)	3.19-3.16 (m)
3,3'	4.35-4.31 (m)	4.36-4.33 (m)	3.19 (bs)	4.26-4.42 (m)	4.14-4.11 (m)	4.28-4.25 (m)	4.15-4.12 (m)	4.15 (bs)	4.21 (bs)	3.17 (bs)	4.13-4.10 (m)	4.13-4.10 (m)
Ar-H	6.92-6.80 (m)	6.91-6.83 (m)	6.90-6.81 (m)	6.93-6.84 (m)	6.90-6.81 (m)	6.92-6.83 (m)	6.92-6.82 (m)	6.91-6.82 (m)	6.91-6.82 (m)	6.91-6.79 (m)	6.91-6.86 (m)	6.91-6.86 (m)
OCH_3	3.66 (s)	3.76 (s)	3.76 (s)	3.78 (s)	3.76 (s)	3.77 (s)	3.76 (s)	3.77 (s)	3.76 (s)	3.66 (s)	3.77 (s)	3.77 (s)
α	1.63-1.08 (m)	2.02-1.25 (m)	0.65 s [58,56]	-	1.98-1.31 (m)	2.12-1.38 (m)	1.84 (q)	1.85 (q),(7.8)	1.46 (s) [79]	1.03 (s) [112,110]	-	-
β	1.63-1.08 (m)	2.02-1.25 (m)	-	7.86-7.63 (m)	1.98-1.31 (m)	2.12-1.38 (m)	1.48 (t),(7.5)	1.49 (t),(7.8)	-	-	8.08-8.05 (m)	8.08-8.05 (m) [93,84]
γ	1.63-1.08 (m)	2.02-1.25 (m)	-	7.47-7.37 (m)	1.98-1.31 (m)	2.12-1.38 (m)	-	-	-	-	7.53-7.36 (m)	7.53-7.36 (m)
δ	0.83 (t),(7.5)	2.02-1.25 (m)	-	7.47-7.37 (m)	0.94 (t),(7.5)	0.94 (t),(6.9)	-	-	-	-	7.53-7.36 (m)	7.53-7.36 (m)

^aChemical shift (δ) in ppm. ² $J(^{119}\text{Sn}, ^1\text{H})$, ³ $J(^1\text{H}, ^1\text{H})$ in Hz are listed in square brackets and parenthesis, respectively. Multiplicity is given as s = singlet, d = doublet, m = multiplet, bs = broad signal. ^bNumbering in accordance with Figs. 3.22 and 3.23.

Table 3.5: ^1H -NMR data of organotin(IV) derivatives of 4-benzhydrylpiperazine-1-carbodithioate

^1H	(37) n-Bu ₃ SnL ^c	(38) Cy ₃ SnL ^c	(39) Me ₃ SnL ^c	(40) Ph ₃ SnL ^c	(41) n-Bu ₂ SnCIL ^c	(42) n-Bu ₂ SnL ^c ₂	(43) Et ₂ SnCIL ^c	(44) Et ₂ SnL ^c ₂	(45) Me ₂ SnCIL ^c	(46) Me ₂ SnL ^c ₂	(47) Ph ₂ SnCIL ^c	(48) Ph ₂ SnL ^c ₂
2,2'	2.65 (bs)	2.48-2.45 (m)	2.47 (bs)	2.57 (bs)	3.22 (bs)	3.22 (bs)	2.63 (bs)	2.63 (bs)	2.54-2.51 (m)	2.49-2.46 (m)	2.66 (b)	2.52-2.50 (m)
3,3'	3.15 (bs)	4.20-4.17 (m)	2.95 (bs)	3.07 (bs)	3.97 (bs)	3.97 (bs)	3.15-3.12 (m)	3.15-3.12 (m)	3.96-3.93 (m)	4.10-4.05 (m)	3.16 (b)	3.95-3.94 (m)
Ar-H	7.40-7.15 (m)	7.42-7.17 (m)	7.41-7.12 (m)	7.37-7.18 (m)	7.41-7.16 (m)	7.41-7.16 (m)	7.40-7.14 (m)	7.40-7.14 (m)	7.42-7.18 (m)	7.42-7.17 (m)	7.37-7.15 (m)	7.43-7.19 (m)
4	4.23 (s)	4.26 (s)	4.23 (s)	4.27 (s)	4.29 (s)	4.29 (s)	4.29 (s)	4.29 (s)	4.29 (s)	4.26 (s)	4.30 (s)	4.27 (s)
α	1.62-1.26 (m)	2.00-1.28 (m)	0.61 (s) [62,55]	-	1.85-1.35 (m)	1.85-1.35 (m)	1.81 (q),(7.5)	1.81 (q),(7.5)	1.28 (s) [75,73]	1.48 (s) [85]	-	-
β	1.62-1.26 (m)	2.00-1.28 (m)	-	7.70-7.66 (m)	1.85-1.35 (m)	1.85-1.35 (m)	1.46 (t),(7.5)	1.46 (t),(7.5)	-	-	8.04-8.02 (m) [74]	8.08-8.05 (m) [94,85]
γ	1.62-1.26 (m)	2.00-1.28 (m)	-	7.44-7.36 (m)	1.85-1.35 (m)	1.85-1.35 (m)	-	-	-	-	7.70-7.30 (m)	7.54-7.39 (m)
δ	0.89 (t),(7)	2.00-1.28 (m)	-	7.44-7.36 (m)	0.94 (t),(7.5)	0.94 (t),(7.5)	-	-	-	-	7.70-7.30 (m)	7.54-7.39 (m)

^aChemical shift (δ) in ppm. ² $J(^{119}\text{Sn}, ^1\text{H})$, ³ $J(^1\text{H}, ^1\text{H})$ in Hz are listed in square brackets and parenthesis, respectively. Multiplicity is given as s = singlet, d = doublet, m = multiplet, bs = broad signal. ^bNumbering in accordance with Figs. 3.22 and 3.23.

Table 3.6: ^1H -NMR data of organotin(IV) derivatives of 4-benzylpiperidine-1-carbodithioate

^1H	(49) $n\text{-Bu}_3\text{SnL}^{\text{d}}$	(50) $\text{Cy}_3\text{SnL}^{\text{d}}$	(51) $\text{Me}_3\text{SnL}^{\text{d}}$	(52) $\text{Ph}_3\text{SnL}^{\text{d}}$	(53) $n\text{-Bu}_2\text{SnCIL}^{\text{d}}$	(54) $n\text{-Bu}_2\text{SnL}_2^{\text{d}}$	(55) $\text{Et}_2\text{SnCIL}^{\text{d}}$	(56) $\text{Et}_2\text{SnL}_2^{\text{d}}$	(57) $\text{Me}_2\text{SnCIL}^{\text{d}}$	(58) $\text{Me}_2\text{SnL}_2^{\text{d}}$	(59) $\text{Ph}_2\text{SnCIL}^{\text{d}}$	(60) $\text{Ph}_2\text{SnL}_2^{\text{d}}$
2,2	3.08-3.04 (m)	3.07-2.99 (m)	3.07-3.03 (m)	3.29-3.21 (m)	3.11-3.03 (m)	3.42-3.37 (m)	3.11-3.02 (m)	3.11-3.02 (m)	3.10-3.02 (m)	3.04-2.95 (m)	3.13-3.06 (m)	3.14-3.06 (m)
3,3'	1.85-1.78 (m)	-	1.82-1.75 (m)	1.91-1.79 (m)	-	-	-	-	1.82-1.78 (m)	1.83-1.80 (m)	1.82-1.78 (m)	1.82-1.78 (m)
4	1.38-1.28 (m)	1.34-1.29 (m)	1.39-1.27 (m)	1.37-1.33 (m)	1.37-1.27 (m)	1.40-1.30 (m)	1.32-1.19 (m)	1.38-1.19 (m)	1.39-1.36 (m)	1.39-1.28 (m)	1.44-1.32 (m)	1.44-1.32 (m)
5	5.19 (d),(12.9)	5.19 (d),(13.2)	5.07 (d),(12.6)	4.89 (d),(12.3)	4.72 (d),(12.9)	4.89 (d),(12.3)	4.72 (d),(13.2)	4.74 (d),(13.2)	4.66 (d),(13.2)	5.02 (d),(12.9)	4.66 (d),(12.6)	4.66 (d),(12.6)
Ar-H	7.33-7.12 (m)	7.30-7.11 (m)	7.34-7.14 (m)	7.32-7.17 (m)	7.31-7.09 (m)	7.28-7.09 (m)	7.30-7.08 (m)	7.28-7.08 (m)	7.30-7.10 (m)	7.30-7.11 (m)	7.30-7.11 (m)	7.30-7.11 (m)
α	1.65-1.20 (m)	1.96-1.24 (m)	1.56 (s)	-	1.99-1.31 (m)	1.85-1.33 (m)	1.81 (q),(7.5)	1.81 (q),(7.5)	1.36 (s)	1.53 (s)	-	-
β	1.65-1.20 (m)	1.96-1.24 (m)	-	7.71 (bs)	1.99-1.31 (m)	1.85-1.33 (m)	1.46 (t),(7.5)	1.43 (t),(7.5)	-	-	8.05 (bs)	8.08-8.05 (m),[93,83]
γ	1.65-1.20 (m)	1.96-1.24 (m)	-	7.42-7.41 (m)	1.99-1.31 (m)	1.85-1.33 (m)	-	-	-	-	7.50 (bs)	7.54-7.41 (m)
δ	0.93 (t),(7.3)	1.96-1.24 (m)	-	7.42-7.41 (m)	0.93 (t),(6.9)	0.93 (t),(7.2)	-	-	-	-	7.50 (bs)	7.54-7.41 (m)

^aChemical shift (δ) in ppm. ² $J(^{119}\text{Sn}, ^1\text{H})$, ³ $J(^1\text{H}, ^1\text{H})$ in Hz are listed in square brackets and parenthesis, respectively. Multiplicity is given as s = singlet, d = doublet, m = multiplet, bs = broad signal. ^bNumbering in accordance with Figs. 3.22 and 3.23.

3.5 ^{13}C -NMR spectra

^{13}C -NMR of the ligands and complexes were recorded in DMSO and CDCl_3 and their data are collected in Tables 3.7-3.12. The ^{13}C -NMR spectral for the R groups attached to Sn, where R = n-Bu, Cy, Et, Me and Ph were assigned by comparison with related analogues as model compounds, combined with the $^nJ[^{119}\text{Sn}, ^{13}\text{C}]$ coupling constant [5, 7, 9-12]. The ^{13}C chemical shifts observed for complexes **1-60** were similar to those for the parent ligand salts but with two main changes, (i) a duplicate peaks pattern vanished due to detachment of aromatic substituted piperazinium/piperidinium cation and (ii) a small shift in the position of C(1) confirmed the coordination of anionic ligands with Sn via CSS moiety. The magnitude for $^nJ[^{119}\text{Sn}, ^{13}\text{C}]$ coupling were also observed and are given in Tables 3.13-3.17. The coupling constants, $^nJ[^{119}\text{Sn}, ^{13}\text{C}]$ are important parameters for structure characterization of organotin(IV) compounds. For triorganotin compounds the magnitudes of $^1J[^{119}\text{Sn}, ^{13}\text{C}]$ coupling suggest the typical tetrahedral geometry around Sn atom in solution except for $\text{Ph}_3\text{Sn(IV)}$ derivatives which express trigonal-bipyramidal geometry. Although, no coupling was observed, however, the geometry confirmation for $\text{Ph}_3\text{Sn(IV)}$ derivatives were made from the value of *ipso*-carbon. According to literature, the value around 138 ppm [13] is a confirmation of tetrahedral environment around Sn while the value near 142 ppm [14] corresponds to five-coordinate Sn atom in solution. The chlorodiethyl-, chlorodimethyl- and chlorodiphenyltin(IV) derivatives revealed trigonal-bipyramidal geometry as shown by the $^1J[^{119}\text{Sn}, ^{13}\text{C}]$ values and their corresponding CSnC angles, calculated from 1J values using Lockhart's equation, $^1J[^{119}\text{Sn}, ^{13}\text{C}] = 11.40 \theta - 875$, [15]. Dibutyl-, diethyl-, dimethyltin(IV) derivatives, the coordination number of Sn atom reduced from six (solid state) to five in solution but in some cases, they retained their octahedral geometry even in solution. In our present investigation the ^{13}C -NMR data of diphenyltin(IV) dithiocarboxylates suggest that these complexes exhibit a skew-trapezoidal geometry in which the two ligands are anisobidentatically coordinated to the central Sn atom.

3.6 ^{119}Sn -NMR spectra

In the complexes, the mono or bidentate bonding of the ligand to the organotin moiety and hence the coordination geometry around Sn, were further confirmed by ^{119}Sn -NMR spectroscopy and data is collected in Tables 3.8-3.12. It has been reported that δ

(^{119}Sn) values (in ppm) for organotin(IV) dithiocarboxylate with four-coordinate Sn vary from +120 to -145 ppm, ^{119}Sn signal in the range of -150 to -250 ppm correspond to five-coordinate Sn while six coordinate Sn atom gave ^{119}Sn signal in the range -300 to -500 ppm [16]. With this in mind, the ^{119}Sn -NMR spectra were recorded in DMSO solution, using Me_4Sn as an external reference. The ^{119}Sn chemical shift values obtained for triorganotin(IV) complexes lie in the range expected for tetrahedral geometry with exception of $\text{Ph}_3\text{Sn(IV)}$ derivatives which gave ^{119}Sn response in the region correspond to five-coordinated Sn atom. Chlorodiorganotin(IV) compounds exhibit trigonal-bipyramidal geometry as demonstrated by the ^{119}Sn -NMR spectra of these complexes. Most of the diorganotin(IV) derivatives change their coordination number from six to five, however, all diphenyltin(IV) compounds and some dimethyltin(IV) complexes express ^{119}Sn peak in the range reported for octahedral geometry. All these observations from the ^{119}Sn -NMR spectroscopy are consistent with the information gathered from the ^1H and ^{13}C -NMR spectra.

Table 3.7: ^{13}C -NMR data^a of ligands-salt

^{13}C	L	L ^a	L ^b	L ^c	L ^d
1	213.5	209.6	210.1	209.6	208.8
2, 2', 2a, 2'a	43.1, 40.9	48.3, 44.7	48.2, 44.3	49.6, 44.8	51.2, 44.7
3, 3', 3a, 3'a	49.0, 46.3	50.8, 50.7	50.9, 50.4	52.4, 50.8	38.2, 36.5
4	-	-	-	69.8	32.4, 29.7
5	-	-	-	-	42.9, 42.8
OCH ₃		55.5, 55.4	55.2, 54.8	-	-
		152.3, 152.1,	152.3, 152.1,		
Ar-C	154.9, 54.7,	140.6, 140.2,	140.5, 140.2,	142.5, 142.0,	140.1, 139.4,
	138.4, 37.1,	123.8, 123.4	123.9, 123.4	128.9, 128.8,	129.1, 129.0,
	131.3, 126.3,	121.1, 121.0,	121.1, 121.0,	128.1, 127.9,	128.4, 128.3,
	114.0, 112.6	118.4, 118.3,	118.4, 118.3,	127.6, 127.4	126.3, 126.0
		111.4, 111.3	112.4, 112.1		

^aNumber in accordance with Fig. 3.22.

Table 3.8: ^{13}C -NMR data^{a,b} of organotin(IV) derivatives of 4-(4-nitrophenyl)piperazine-1-carbodithioate

^{13}C	(1) n-Bu ₃ SnL	(2) Cy ₃ SnL	(3) Me ₃ SnL	(4) Ph ₃ SnL	(5) n-Bu ₂ SnCIL	(6) n-Bu ₂ SnL ₂	(7) Et ₂ SnCIL	(8) Et ₂ SnL ₂	(9) Me ₂ SnCIL	(10) Me ₂ SnL ₂	(11) Ph ₂ SnCIL	(12) Ph ₂ SnL ₂
1	199.9	200.1	197.5	195.9	198.5	198.8	197	198.6	199	198.3	199.6	197.5
2,2'	50.6	50.7	49.3	51.4	50.7	50.6	50.7	50.7	50.8	50.6	51.8	51.8
3,3'	46.1	46.1	46.2	45.5	46	46.1	46	46	45.5	45.4	45.1	45.1
Ar-C	154.1,139, 126.3,112.6	154,138.9, 126.2,112.5	154.9,138.3 126.4,112.6	154.4,137.5, 126.4, 112.6	154,138.9, 126.2,112.6	153.7,139.6, 126.2,112.8	153.7,139, 126.2,112.6	153.7,139, 126.2,112.6	154.4,137.6, 126.5,112.7	154.4,137. 6,126.5,11 2.7	154.2,137.7, 126.5,112.8	154.2,137.7 126.4,112.8
α	17.8 [346, 331]	35 [330,315]	19.5	143.1	26.5	26.5	23.0	21.6 [530]	15.6 [515]	17.9	135.7	135.7
β	29.1 [21]	32.3 [17]	-	136.9	29.6	29.6	13.0	10.5	-	-	131.3	131.3
γ	27.3 [68]	29.5 [68.6]	-	129.3	28	28	-	-	-	-	130.7	130.1
δ	13.9	27.2	-	129.8	13.9	13.9	-	-	-	-	129.5	129.5
^{119}Sn	39.6	-17.5	25.5	-195	-185.4	-183	-216	-176.8	-170.5	-247.6	-240.5	-333

^aChemical shifts (δ) in ppm. $^nJ[^{119}\text{Sn}, ^{13}\text{C}]$ in Hz are listed in square brackets.

^bNumber in accordance with Figs. 3.22 and 3.23.

Table 3.9: ^{13}C -NMR data^{a,b} of organotin(IV) derivatives of 4-(2-methoxyphenyl)piperazine-1-carbodithioate

^{13}C	(13) n-Bu ₃ SnL ^a	(14) Cy ₃ SnL ^a	(15) Me ₃ SnL ^a	(16) Ph ₃ SnL ^a	(17) n-Bu ₂ SnCIL ^a	(18) n-Bu ₂ SnL ^a ₂	(19) Et ₂ SnCIL ^a	(20) Et ₂ SnL ^a ₂	(21) Me ₂ SnCIL ^a	(22) Me ₂ SnL ^a ₂	(23) Ph ₂ SnCIL ^a	(24) Ph ₂ SnL ^a ₂
1	190.6	198.8	199.3	196.1	196.9	197.4	196.8	200.4	196.1	196.2	190.6	190.6
2,2'	45.9	50.3	50.1	50.1	49.9	49.9	49.9	50.2	49.8	44.0	46.1	44.3
3,3'	51.2	52	51.3	52.6	51.9	51.9	51.9	51.3	51.9	48.2	48.3	48.1
Ar-C	152.5,141.4 123.5,121.2, 118.6,111.5	152.2,140.2, 123.7,121.1, 118.5,111.3	152.2,139.9, 123.8,121.1, 118.5,111.3	152.2,139.9, 123.9,121.1, 118.6,111.3	152.2,139.5, 124.3,121.1, 118.6,111.4	152.2,139.5, 124.1,121.1, 118.6,111.4	152.2,139.5, 124.1,121.1, 118.6,111.4	152.2,140.0, 123.8,121.1, 118.5,111.3	152.2,139.4, 124.2,121.1, 118.6,111.4	152.6,140.8, 123.9,121.5, 118.8,112.6	152.4,139.9, 124.3,121.3, 118.9,111.6	152.4,139.9, 124.3,121.3, 118.9,111.6
OCH ₃	55.6	55.5	55.5	55.5	55.5	55.5	55.5	55.5	55.9	56.0	55.5	55.5
α	17.7 [331]	36.9 [340,319]	15.5	142.3	26.5	26.5 [492,472]	21.3 [531,509]	27.9 [621,594]	12.8	12.1	135.3	135
β	28.1	32.1 [16.5]	-	136.8 [47.3,45]	29.3	29.2	10.3 [153]	1.89 [49.5,45.7]	-	-	129	129
γ	27.1 [63]	29.3 [67.5]	-	128.6 [61.5,59.2]	27.9	27.1	-	-	-	-	121.5	121.3
δ	13.8	27.0 [7.5]	-	129.2 [12.8]	13.7	13.7	-	-	-	-	118.7	118.9
^{119}Sn	-13.4	-26.9	29.2	-183.1	-193.2	-193.2	-187	-186.4	-192.9	-331.2	-245.5	-319.5

^aChemical shifts (δ) in ppm. ^aJ(^{119}Sn , ^{13}C) in Hz are listed in square brackets.

^bNumber in accordance with Figs. 3.22 and 3.23.

Table 3.10: ^{13}C -NMR data^{a,b} of organotin(IV) derivatives of 4-(4-methoxyphenyl)piperazine-1-carbodithioate

^{13}C	(25) n-Bu ₃ SnL ^b	(26) Cy ₃ SnL ^b	(27) Me ₃ SnL ^b	(28) Ph ₃ SnL ^b	(29) n-Bu ₂ SnCIL ^b	(30) n-Bu ₂ SnL ^b ₂	(31) Et ₂ SnCIL ^b	(32) Et ₂ SnL ^b ₂	(33) Me ₂ SnCIL ^b	(34) Me ₂ SnL ^b ₂	(35) Ph ₂ SnCIL ^b	(36) Ph ₂ SnL ^b ₂
1	197.6	199.2	201.2	196.6	197.4	200.8	197.5	202.4	199.7	190.6	194.4	196.1
2,2'	43.5	50.7	45.1	50.7	50.6	50.7	50.6	50.6	41	50.6	50.6	50.6
3,3'	47.6	51.9	50.3	52.5	51.8	51.3	51.8	51.8	47.5	51.3	52.6	52.6
Ar-C	154.3,145.1, 118.7, 115.1	154.6,145, 119,114.7	154.7,145.4, 119.2,114.7	154.8,144.7, 119.5,114.8	154.8,144.4, 119.3,114.8	154.7,144.9, 119.1,114.8	155.4,144.4, 119.4,	155,144.8, 119.3,114.8	154.2,145, 118.7,115	154.2,144.7, 119.2,114.8	155.1,144.2, 119.5,114.9	155.1,144.2, 119.5,114.9
OCH ₃	55.8	55.8	55.8	55.8	55.8	55.8	55.7	55.7	55.8	55.7	55.8	55.8
α	24 [341,315]	35 [337,314]	-0.6 [382,366]	142.4	26.5	26.6	21.5	21.5	25	25	142.1	142.1
β	28.6 [28.4]	32.3 [17]	-	137	28	34.8	10.4	10.5	-	-	135	136
γ	27 [75]	29.5 [67]	-	128.8	27.5	28.8	-	-	-	-	130.5	130.5
δ	14.4	27.2	-	129.4	13.9	14.1	-	-	-	-	129.1	129.1
^{119}Sn	31.4	-24	-26.6	-181	-191.5	-345	-185	-217.9	-186.6	-238.7	-343	-393

^aChemical shifts (δ) in ppm. ^aJ[^{119}Sn , ^{13}C] in Hz are listed in square brackets.

^bNumber in accordance with Figs. 3.22 and 3.23.

Table 3.11: ^{13}C -NMR data^{a,b} of organotin(IV) derivatives of 4-benzhydrylpiperazine-1-carbodithioate

^{13}C	(37) n-Bu ₃ SnL ^c	(38) Cy ₃ SnL ^c	(39) Me ₃ SnL ^c	(40) Ph ₃ SnL ^c	(41) n-Bu ₂ SnCIL ^c	(42) n-Bu ₂ SnL ^c ₂	(43) Et ₂ SnCIL ^c	(44) Et ₂ SnL ^c ₂	(45) Me ₂ SnCIL ^c	(46) Me ₂ SnL ^c ₂	(47) Ph ₂ SnCIL ^c	(48) Ph ₂ SnL ^c ₂
1	198.4	199.3	190.6	196.9	196.6	198.1	196.5	202.4	195.9	199.1	196.1	198.2
2,2'	52.0	52.0	51.4	52.7	52.0	52.0	52.1	51.9	52.1	51.4	52.0	52.0
3,3'	51.6	51.6	45.3	51.4	51.2	51.2	51.2	51.2	51.1	44.4	51.2	51.2
Ar-C	141.7,129.0, 127.8,127.6	141.7,129.0, 127.8,127.6	142.2,128.8, 128.0,127.4	142.0,128.9, 127.9,127.5	141.7,129.0, 127.8,127.7	141.7,129.0, 127.8,127.7	141.7,129.0, 127.9,127.7	141.8,129.0, 127.9,127.6	141.7,129.0, 128.0,127.7	142.1,128.9, 128.0,127.5	141.7,129.0, 127.8,127.7	141.7,129.0, 127.8,127.7
4	75.8	75.8	75.8	75.7	75.7		75.6	75.6	75.6	75.8		
α	17.9 [340]	35.5 [335,318]	-0.3 [404,386]	142.6	26.5	26.6	21.4	21.4	10.3	15.1	142.1	142.1
β	29.1	32.1 [17]	-	136.4	28	34.1	10.5 [38]	10.5	-	-	136	136
γ	27.3	29.6 [68]	-	129.3	27.3	28.8	-	-	-	-	130.5	130.5
δ	13.9	27.4	-	130.5	13.8	13.9	-	-	-	-	129.1	129.1
^{119}Sn	27.6	-26.9	26.8	-185.4	-195.1	-194.9	-188.5	-188.1	-194.3	-331.1	-250	-320.9

^aChemical shifts (δ) in ppm. ⁿJ(^{119}Sn , ^{13}C) in Hz are listed in square brackets.

^bNumber in accordance with Figs. 3.22 and 3.23.

Table 3.12: ^{13}C -NMR data^{a,b} of organotin(IV) derivatives of 4-benzylpiperidine-1-carbodithioate

^{13}C	(49) $\text{n-Bu}_3\text{SnL}^{\text{d}}$	(50) $\text{Cy}_3\text{SnL}^{\text{d}}$	(51) $\text{Me}_3\text{SnL}^{\text{d}}$	(52) $\text{Ph}_3\text{SnL}^{\text{d}}$	(53) $\text{n-Bu}_2\text{SnCIL}^{\text{d}}$	(54) $\text{n-Bu}_2\text{SnL}_2^{\text{d}}$	(55) $\text{Et}_2\text{SnCIL}^{\text{d}}$	(56) $\text{Et}_2\text{SnL}_2^{\text{d}}$	(57) $\text{Me}_2\text{SnCIL}^{\text{d}}$	(58) $\text{Me}_2\text{SnL}_2^{\text{d}}$	(59) $\text{Ph}_2\text{SnCIL}^{\text{d}}$	(60) $\text{Ph}_2\text{SnL}_2^{\text{d}}$
1	197.2	198.7	201.1	193.3	195.6	190.6	195.5	191.6	194.9	195.1	196.1	194.2
2,2'	52.4	52.8	51.8	53.2	52.7	52.5	52.7	52.6	52.7	52.7	53.3	53.6
3,3'	36.5	37.7	36.5	36.6	36.4	36.7	36.4	36.6	36.9	36.9	36.2	36.7
4	42.6	42.8	42.5	41.8	42.5	42.5	42.5	42.6	42.4	42.1	42.4	42.4
5	31.9		31.8	31.6	31.9	31.9	31.9	31.9	31.8	31.6	31.9	31.9
Ar-C	139.8,129.1, 128.5,126.3	140.1,129.3, 128.5,126.3	139.7,129.1, 128.4,126.2	140.1,129.0, 128.5,125.9	139.2,129.2 126.6,126.5	139.4,129.2, 128.7,126.5	139.1,129.2, 128.7,126.6	139.3,129.2, 128.7,126.6	139.5,129.2, 128.7,126.6	139.3,129.2, 128.7,126.6	139.4,129.2, 128.7,126.6	139.4,129.2, 128.7,126.6
α	17.5	35.0 [334]	15	142.9	26.5	26.5	21.3 [534,511]	29.1	10.2 [571,545]	10.5	142.2	142.3
β	29.1	32.2 [16]	-	136.4 [46]	36.4	36.7	10.4	10.5	-	-	136.1	135.9 [64]
γ	27.8	29.5 [67]	-	128.9	28.7	29.3	-	-	-	-	130.4	130.4 [18]
δ	13.7	27.2	-	129.1 [13.5]	13.9	13.9	-	-	-	-	128.5	129.0 [87]
^{119}Sn	-129.6	82.3	-49.8	-182.2	-175	-202.1	-180.2	-84.6	-201.2	-337	-207.8	-336.6

^aChemical shifts (δ) in ppm. $^nJ(^{119}\text{Sn}, ^{13}\text{C})$ in Hz are listed in square brackets.

^bNumber in accordance with Figs. 3.22 and 3.23.

Table 3.13: (C-Sn-C) angles (°) based on NMR parameters of selected organotin(IV) derivatives of 4-(4-nitrophenyl)piperazine-1-carbodithioate

Comp. No.	Compound	$^1J(^{119}\text{Sn}, ^{13}\text{C})$	$^2J(^{119}\text{Sn}, ^1\text{H})$	Angle(°)	
		(Hz)	(Hz)	1J	2J
1	n-Bu ₃ SnL	346	-	107.1	-
2	Cy ₃ SnCl	330	-	105.7	-
8	Et ₂ SnL ₂	530	-	123.2	-
9	Me ₂ SnCIL	-	75	121.9	121.5
10	Me ₂ SnL ₂	-	90	-	135.5

Table 3.14: (C-Sn-C) angles (°) based on NMR parameters of selected organotin(IV) derivatives of 4-(2-methoxyphenyl)piperazine-1-carbodithioate

Comp. No.	Compound	$^1J(^{119}\text{Sn}, ^{13}\text{C})$	$^2J(^{119}\text{Sn}, ^1\text{H})$	Angle(°)	
		(Hz)	(Hz)	1J	2J
13	n-Bu ₃ SnL ^a	331	-	105.8	-
14	Cy ₃ SnL ^a	340	-	106.6	-
15	Me ₃ SnL ^a	-	81	-	126.5
18	n-Bu ₂ SnL ₂ ^a	492	-	119.9	-
19	Et ₂ SnCIL ^a	531	-	123.3	-
20	Et ₂ SnL ₂ ^a	621	-	131.2	-
21	Me ₂ SnCIL ^a	-	78	-	123.9
22	Me ₂ SnL ₂ ^a	-	98	-	144.9

Table 3.15: (C-Sn-C) angles (°) based on NMR parameters of selected organotin(IV) derivatives of 4-(4-methoxyphenyl)piperazine-1-carbodithioate

Comp. No.	Compound	$^1J(^{119}\text{Sn}, ^{13}\text{C})$ (Hz)	$^2J(^{119}\text{Sn}, ^1\text{H})$ (Hz)	Angle(°)	
				1J	2J
25	n-Bu ₃ SnL ^b	341	-	106.6	-
26	Cy ₃ SnL ^b	337	-	106.3	-
27	Me ₃ SnL ^b	382	58	110.2	111.4
33	Me ₂ SnCIL ^b	-	79	-	124
34	Me ₂ SnL ^b ₂	-	112	-	164.6
36	Ph ₂ SnL ^b ₂	-	93	-	138.9

Table 3.16: (C-Sn-C) angles (°) based on NMR parameters of selected organotin(IV) derivatives of 4-benzhydrylpiperazine-1-carbodithioate

Comp. No.	Compound	$^1J(^{119}\text{Sn}, ^{13}\text{C})$ (Hz)	$^2J(^{119}\text{Sn}, ^1\text{H})$ (Hz)	Angle(°)	
				1J	2J
37	n-Bu ₃ SnL ^c	340	-	106.6	-
38	Cy ₃ SnL ^c	335	-	106.1	-
39	Me ₃ SnL ^c	404	62	112.2	113.2
43	Et ₂ SnCIL ^c	532	-	123.4	-
45	Me ₂ SnCIL ^c	570	75	126.7	121.5
46	Me ₂ SnL ^c ₂	-	85	-	130.3
47	Ph ₂ SnCIL ^c	-	74	-	120.7
48	Ph ₂ SnL ^c ₂	-	94	-	140.1

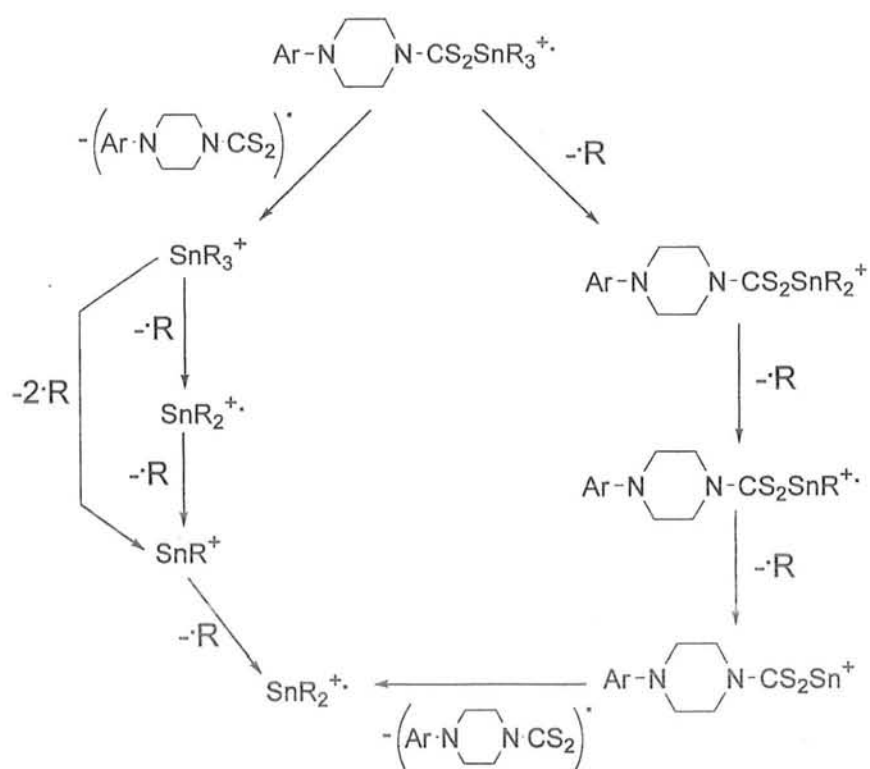
Table 3.17: (C-Sn-C) angles (°) based on NMR parameters of selected organotin(IV) derivatives of 4-benzylpiperidine-1-carbodithioate

Comp. No.	Compound	$^1J(^{119}\text{Sn}, ^{13}\text{C})$ (Hz)	$^2J(^{119}\text{Sn}, ^1\text{H})$ (Hz)	Angle(°)	
				1J	2J
50	Cy ₃ SnL ^d	334	-	106.0	-
55	Et ₂ SnCIL ^d	534	-	123.6	-
57	Me ₂ SnCIL ^d	571	-	126.8	-
60	Ph ₂ SnL ^d ₂	-	93	-	138.9

3.7 Mass spectrometry

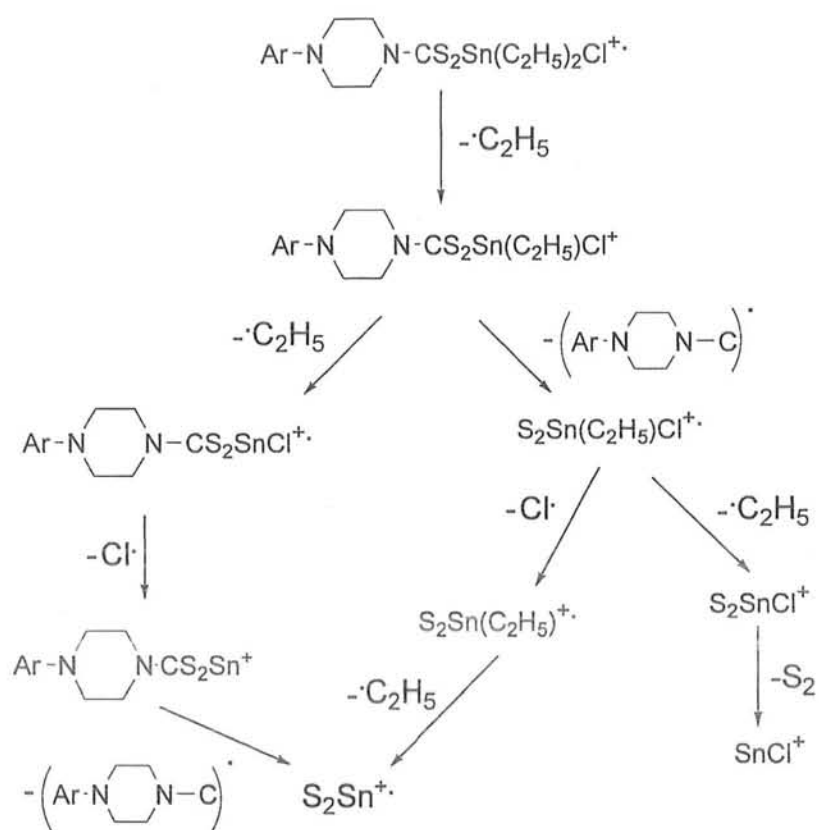
The EI spectral data obtained at 70 eV, for all the synthesized complexes have been reported along with their synthesis in the experimental section (Chapter 2). Mass-spectral data for complexes show rich ion distributions but our interest lies in those ions containing tin. These were easily qualitatively identified by inspection from the characteristic isotope peak patterns for "Sn" and "SnCl" (in case of chlorodiorganotins) species [17]. The spectra show little or no molecular ion (M^{+}) present as is generally the case for main group organometallics. In triorganotin(IV) dithiocarboxylates, the primary fragmentation occurs via the loss of ligand or tin-bonded R group, where R = Me, Cy, n-Bu and Ph. In both fragmentation routes, the daughter ion of the primary fragmentation, loss R groups in successive steps to give $[Sn]^{+}$ ion as the end product in most cases (Scheme 3.2). Fragmentation patterns are proposed for the tin-containing ions observed in R_2SnCl derivatives, where R = Me and Et, and these patterns are shown in Scheme 3.3 and Scheme 3.4, respectively. The relative intensities reported for the ions given were qualitatively estimated from the ion current for the ^{120}Sn or $^{120}Sn^{35}Cl$ peak in each species, and must be regarded as approximate. The first fragmentation appears to be loss of R^{\bullet} (R = CH_3 or C_2H_5) or the organic part of the anion, $[ArN(CH_2)_4NC^{\bullet}]$. For dimethyltin(IV) derivatives, the latter strongly predominates giving the dimethyl species $S_2Sn(CH_3)_2Cl^{+}$ which can then lose C_2H_6 , S_2 , or CS to form further (EE^{+}) ions. The last, due to loss of CS, $H_3SSn(CH_3)Cl^{+}$, is the most abundant tin-containing ion and can be written as a sulphonium species (Scheme 3.4). This type of ion may well originate from the initial ionization occurring from the CS_2Sn unit rather than $Sn(CH_3)_2Cl$ moiety [18] and be sufficiently stable to survive intact. Ions formed by loss of CH_3^{\bullet} provide approximately <3% of the current carried by tin-containing ions with only small amounts of possible tin-piperazine fragments being observed. The terminal species are $SnCl^{+}$ and Sn^{++} , the latter perhaps derived from $SnCH_3^{+}$. The mass spectrum of chlorodiethyltin(IV) derivatives significantly differ from that of chlorodimethyl tin(IV) complexes. Initial loss of ethyl from (M^{+}) is total but then, like $(CH_3)_2SnCl$ -class, loss of $ArN(CH_2)_4NC^{\bullet}$ then greatly predominates. Several " S_2Sn " species are observed including the most abundant ion, S_2SnCl^{+} and terminal (OE^{+}) S_2Sn^{++} . The other terminal ion is $SnCl^{+}$ but no Sn^{++} was evident. Ions formed by loss of the second ethyl group from $(M-C_2H_5^{+})$ are only 4.6% of the current carried by tin-containing ions and may also account for some of terminal S_2Sn^{++} . The steric effects of the larger

ethyl groups compared to smaller methyl may be sufficient to account for the ease of their loss from high energy $\text{ArN}(\text{CH}_2)_4\text{NCS}_2 \text{Sn}(\text{C}_2\text{H}_5)_2\text{Cl}^{++}$ when compared with the very similar methyl analogue. Of more interest is the loss of only part of the anion from M^{++} (chlorodimethyltin(IV) complexes) or $\text{M-C}_2\text{H}_5^+$ (chlorodiethyltin(IV) derivatives). If as proposed above, ionization occurs from the CS_2Sn region, perhaps from the $\text{C}=\text{S}$ bond itself, this could then make possible the preferential weakening of the CS_2 structure and thus facilitate loss of the organic fragment $[\text{ArN}(\text{CH}_2)_4\text{NC}]^+$, leaving the S_2Sn frame intact. Dibutyl-, chlorodiphenyl- and diphenyltin(IV) dithiocarboxylates are quite similar in their mass behaviour with triorganotin-category. However, chlorodibutyltin(IV) complexes show similarity in their fragmentation pattern with chlorodiorganotins as well as with triorganotins complexes.

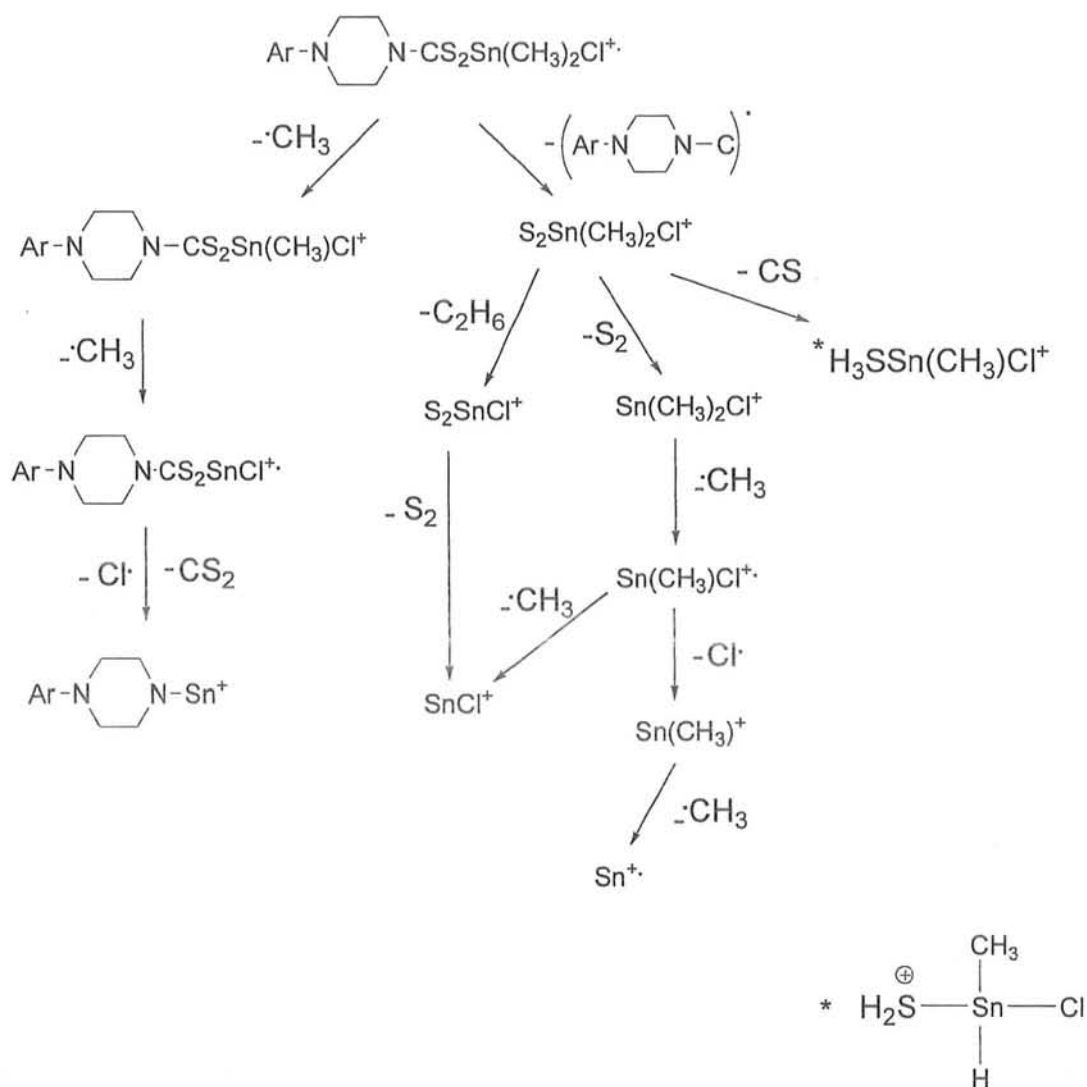


$$\text{R} = \text{C}_4\text{H}_9, \text{C}_6\text{H}_{11}, \text{CH}_3, \text{C}_6\text{H}_5$$

Scheme 3.2: Mass fragmentation pattern of triorganotin(IV) dithiocarboxylates



Scheme 3.3: Mass fragmentation pattern of chlorodiethyltin(IV) dithiocarboxylates



Scheme 3.4: Mass fragmentation pattern of chlorodimethyltin(IV) dithiocarboxylates

3.8 Evaluation of DNA binding parameters

3.8.1 Evaluation of DNA binding parameters of triorganotin(IV) dithiocarboxylates

DNA binding parameters were evaluated for three triorganotin(IV) 4-(4-nitrophenyl)piperazine-1-carbodithioate using cyclic voltammetry and electronic absorption spectroscopy.

3.8.1.1 Cyclic voltammetry of compounds 1, 2 and 4 and their DNA adduct

The cyclic voltammetric behavior of 3 mM compound 1 and the effect of addition of different concentrations of DNA on its electrochemical response in 10% aqueous dimethylsulphoxide (DMSO), containing 10^{-1} M tetra-*n*-butyl ammonium perchlorate at 100 mVs⁻¹ is depicted in Fig. 3.1. The free drug gave a single cathodic peak at -1.261 V and an anodic peak at -1.181 V upon scan reversal, in the potential range of -1.0 to -1.5 V. The appearance of these two peaks is an indication of interconversion of Sn⁺⁴ to Sn⁺² and vice versa during the whole process [19]. The peak potentials separation of 80 mV, greater than the ideal value of 60 mV for a fully reversible redox process may be due to kinetic complications. With stepwise addition of DNA, the voltammetric wave demonstrated a gradual shift in the positive direction accompanied by decrease in peak current. The positive shift in peak potentials indicates intercalative mode of binding in which the complex inserts itself into the stacked base pairs of DNA. The decay in peak current is because of decrease in free complex concentration due to the formation of drug-DNA association complex and hence lowering of the diffusion coefficient of complex-DNA adduct.

Typical CV behavior of 2 with and without DNA is shown in Fig. 3.5. The redox process of compound 2 without DNA featured reduction and oxidation at -1.193 V and -1.293 V, respectively. By the addition of 3.2×10^{-5} M DNA, the cathodic peak current dropped by 13.38% and cathodic peak potential shifted to less negative values by 22 mV. These observations unequivocally reflect the intercalation of the complex into the double helical structure of DNA resulting in the formation of slowly diffusing supramolecular complex-DNA adduct.

Compound 4 showed analogous CV behavior to 1 and 2 as illustrated in Fig. 3.9. Peaks associated with Sn^{IV/II} reduction and with Sn^{II/IV} oxidation appeared at -1.288 V and at -1.188 V, respectively. The cathodic peak, for compound 3, in the presence of 5.0×10^{-5} M DNA was observed at -1.249 V and for anodic one at -1.156 V accompanied by 19% reduction in peak current. Such peculiar voltammetric

characteristics are indicative of compound 3-DNA interaction. The voltammetric parameters are given in Table 3.18.

The diffusion coefficients of the free (D_f) and DNA bound complexes (D_b) were determined by the application of Randles-Sevcik equation [20, 21]:

$$i_p = 2.69 \times 10^5 n^{3/2} A C_o^* D^{1/2} \nu^{1/2} \quad (3.1)$$

Where i_p is the peak current (A), A is the surface area of the electrode (cm^2), C_o^* is the bulk concentration (mol cm^{-3}) of the electroactive species, D is the diffusion coefficient ($\text{cm}^2 \text{s}^{-1}$) and ν is the scan rate (V s^{-1}).

The linearity of i_p vs. $\nu^{1/2}$ plots in all cases indicated the redox processes to be diffusion controlled [22]. The lower diffusion coefficients of the DNA bound species are responsible for the decay of current signals in CV behavior of 1-3 as shown in Fig. 3.1, 3.5 and 3.9. Based upon the decay in peak current of all these complexes by the addition of varying concentration of DNA, the binding constants (Table 3.19) were calculated from the plots of $1/[\text{DNA}]$ versus $1/(1-i/i_o)$, according to the following equation [23]:

$$\frac{1}{[\text{DNA}]} = \frac{K(1-A)}{1-i/i_o} - K \quad (3.2)$$

Where, K is the association constant, i and i_o are the peak currents with and without DNA and A is the proportionality constant.

An examination of Table 3.19 reveals that the binding of these complexes with DNA are greater than the K observed for similar DNA-intercalating Cr complex, $[\text{CrCl}_2(\text{dicnq})_2]^+$, for which the binding constant has been reported as $1.20 \times 10^3 \text{ M}^{-1}$ [24].

The rationale behind this is the greater intercalating ability of aromatic 4-(4-nitrophenyl)piperazine-1-carbodithioate ligand, into the stacked base pairs domain of DNA. So an effort to further improve the binding affinity of these complexes, our current research work is concentrated on the extension of aromatic 4-(4-nitrophenyl)piperazine-1-carbodithioate system. The greater K value of 4 than 2 is due to the planar phenyl groups which can better intercalate into the double helix of DNA.

The reason for greater association constant of **1** is the additional hydrophobic interaction of the butyl groups with bases of DNA [25] Moreover, Table 3.19 reveals that the complex-DNA adduct formation is a spontaneous process and both spectroscopic and voltammetric results agree well with each other.

3.8.1.2 Electronic absorption spectra of compounds **1**, **2** and **4** and their DNA adduct

The interactions of complexes **1**, **2** and **4** with DNA were further examined by UV-Vis spectroscopy, in order to get some more clues about their mode of interaction and binding strength. The absorption spectra of **1**, **2** and **4** in the absence and presence of different concentrations of DNA are shown in Fig. 3.3, 3.7 and 3.11, respectively. The binding of complexes **1**, **2** and **4** to DNA caused a progressive blue shift of 10 (401-391), 8 (400-392) and 4 nm (398-394), respectively. These spectral characteristics are indicative of their binding to DNA. The peculiar hypochromism observed here is attributed to the intercalation of these drugs into the DNA base pairs [26]. The hypochromic effect is caused by the overlapping of the electronic states of the intercalating chromophore of the ligand with the DNA bases [27].

Based upon the variation in absorbance, the association constants of these complexes with DNA were determined according to Benesi-Hildebrand equation [28]:

$$\frac{A_0}{A-A_0} = \frac{\epsilon_G}{\epsilon_{H-G} - \epsilon_G} + \frac{\epsilon_G}{\epsilon_{H-G} - \epsilon_G} \frac{1}{K[DNA]} \quad (3.3)$$

Where K is the association constant, A_0 and A are the absorbances of the drug and its complex with DNA, respectively, and ϵ_G and ϵ_{H-G} are the absorption coefficients of the drug and the drug-DNA complex, respectively.

The association constants, shown in Table 3.19, were obtained from the intercept-to-slope ratios of $A_0/(A-A_0)$ vs. $1/[DNA]$ plots.

Table 3.18: Voltammetric parameters of compound 1, 2 and 4 in the absence and presence of DNA

Substance	$\nu/V\ s^{-1}$	[DNA]/ μM	E_{pa}/V	E_{pc}/V	$E_f^{o'}/V$	$D_f\ 10^9/cm^2\ s^{-1}$	$D_b\ 10^9/cm^2\ s^{-1}$
1	0.1	0	-1.181	-1.261	-1.221	8.05	-
1-DNA	0.1	30	-1.132	-1.225	-1.178	-	7.39
2	0.1	0	-1.193	-1.293	-1.243	15.13	-
2-DNA	0.1	32	-1.161	-1.271	-1.216	-	8.86
4	0.1	0	-1.188	-1.288	-1.238	8.62	-
4-DNA	0.1	50	-1.156	-1.249	-1.202	-	5.36

Table 3.19: The association constants and Gibbs free energies of 1-DNA, 2-DNA and 4-DNA complexes as determined by voltammetry and UV-Vis spectroscopy

Drug-DNA complex	CV		Spectroscopy	
	K/M^{-1}	$-\Delta G/kJmol^{-1}$	K/M^{-1}	$-\Delta G/kJmol^{-1}$
1-DNA	6.90×10^3	21.90	6.05×10^3	21.57
2-DNA	2.40×10^3	18.76	2.30×10^3	19.18
4-DNA	3.60×10^3	20.29	3.25×10^3	20.03

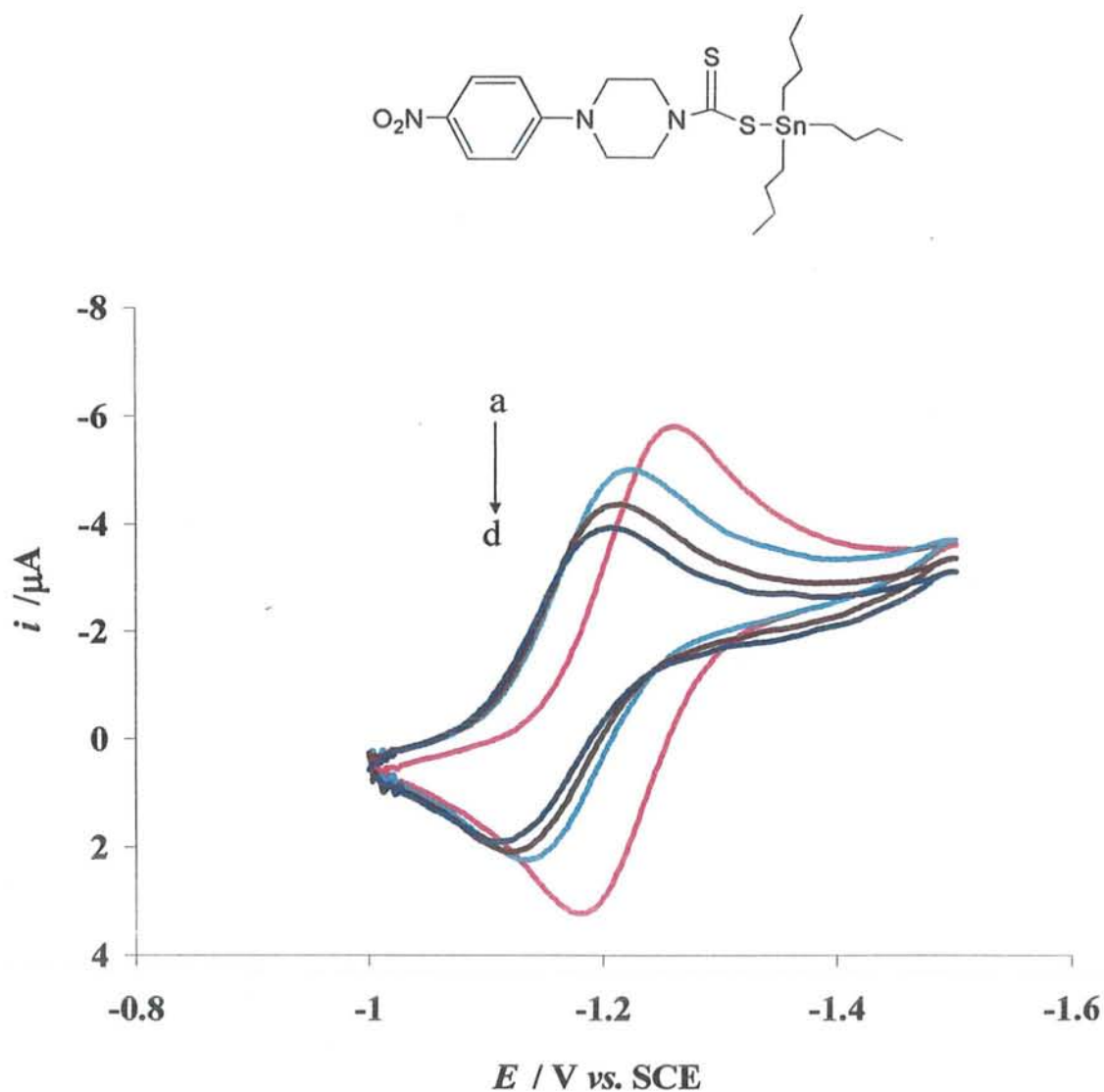


Fig. 3.1: Cyclic voltammograms of 3.00 mM of compound 1 in 10 % aqueous DMSO with 0.1 M TBAP as supporting electrolyte in the absence (a) and presence of 3.0×10^{-5} , (b) 6.5×10^{-5} (c) and 1.05×10^{-4} M DNA (d) at 25°C temperature. Glassy carbon electrode (0.071 cm^2) was used as working electrode and all potentials were reported vs. SCE at 100 mV/s scan rate.

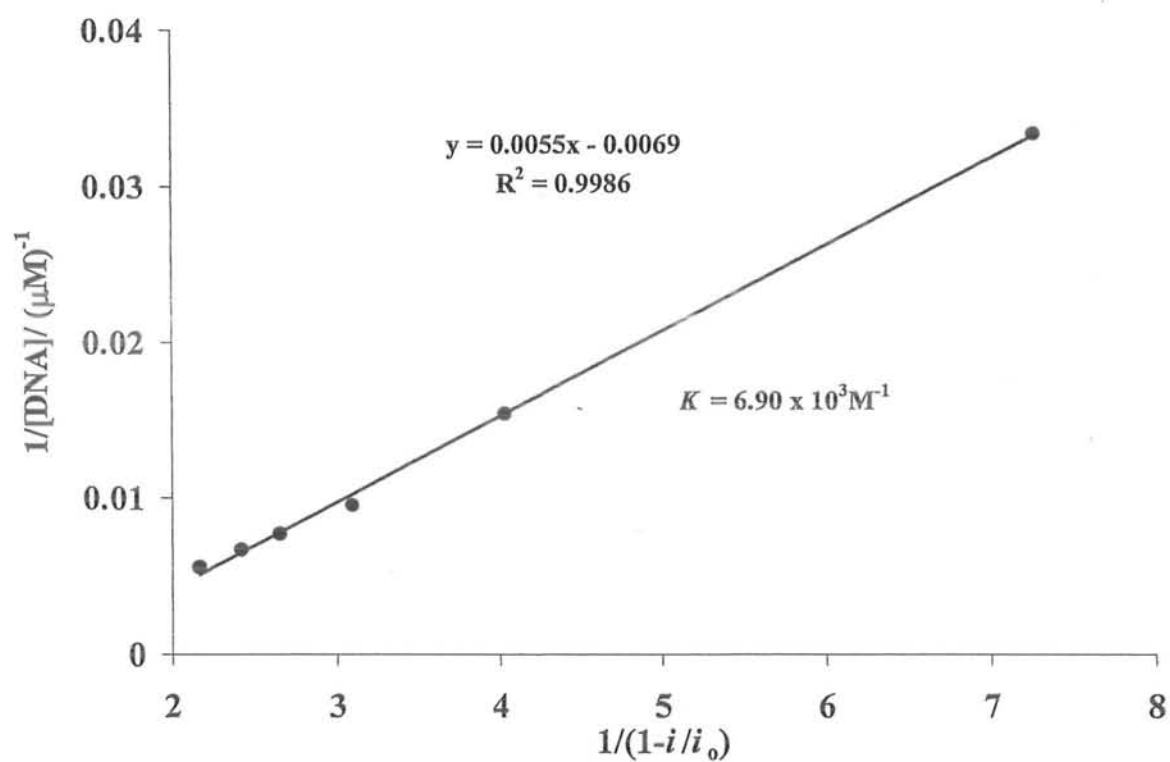
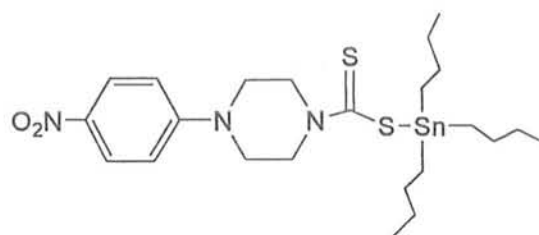


Fig. 3.2: Plot of $1/(1-i/i_0)$ vs. $1 / [\text{DNA}]$ used to calculate the binding constant of 1-DNA adduct.

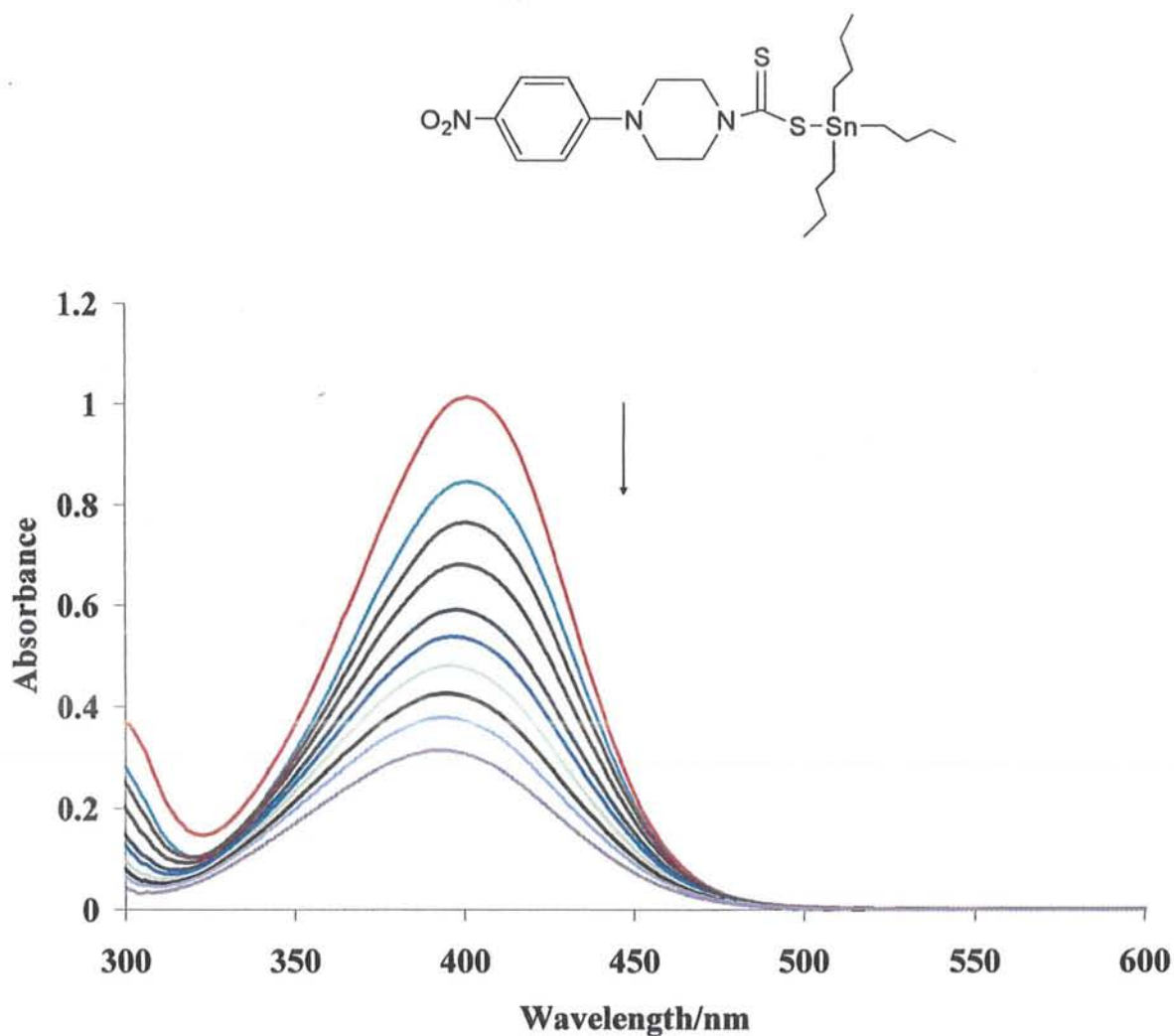


Fig. 3.3: Absorption spectra of 3mM of compound 1 in the absence (a) and presence of 2.0×10^{-5} , (b) 3.0×10^{-5} , (c) 4.5×10^{-5} , (d) 6.0×10^{-5} , (e) 7.0×10^{-5} , (f) 9.0×10^{-5} , (g) 1.0×10^{-4} , (h) 1.15×10^{-4} (i) and 1.25×10^{-4} M DNA (j). The arrow direction indicates increasing concentrations of DNA.

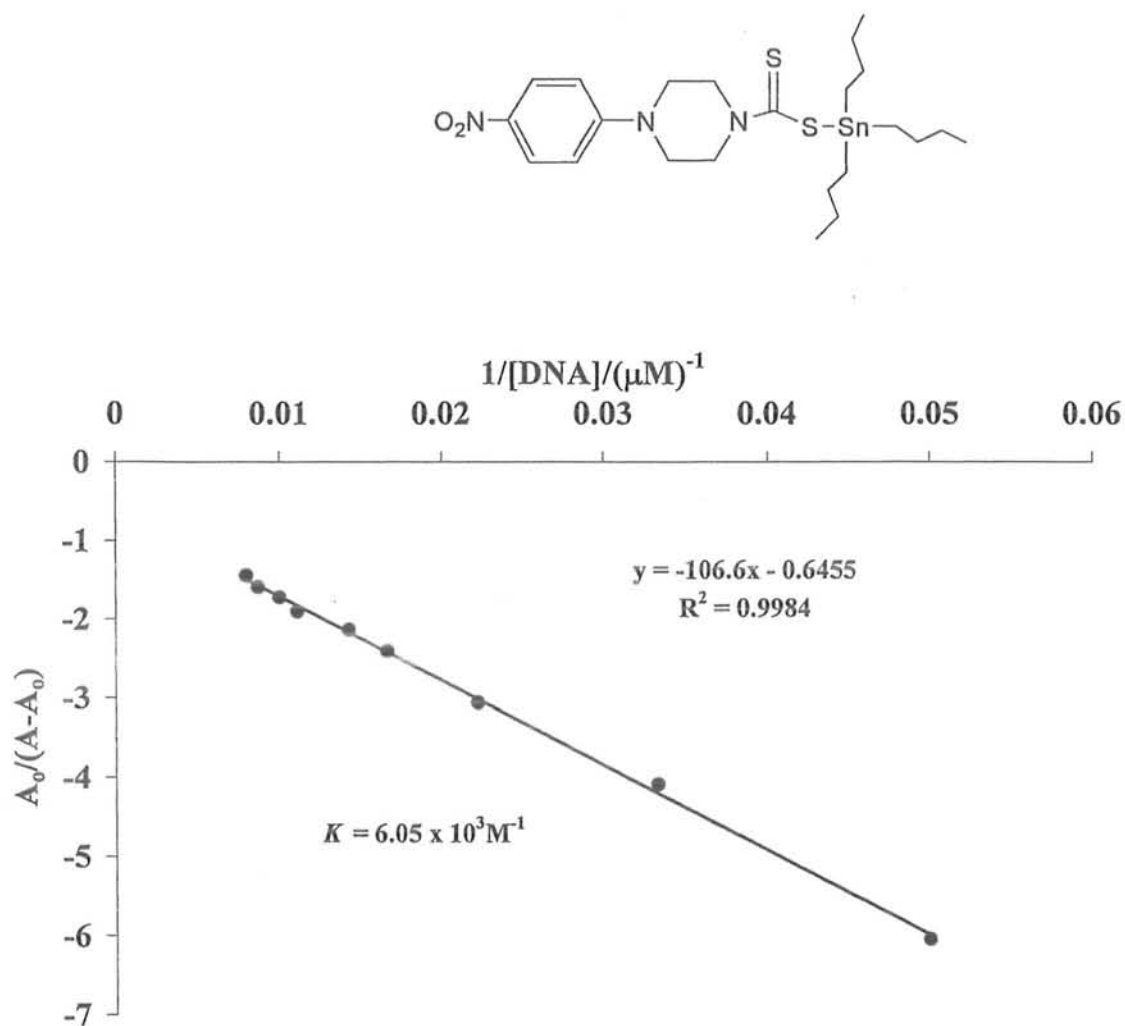


Fig. 3.4: Plot of $A_0/(A-A_0)$ vs. $1/[DNA]$ for the determination of binding constant of 1-DNA adduct.

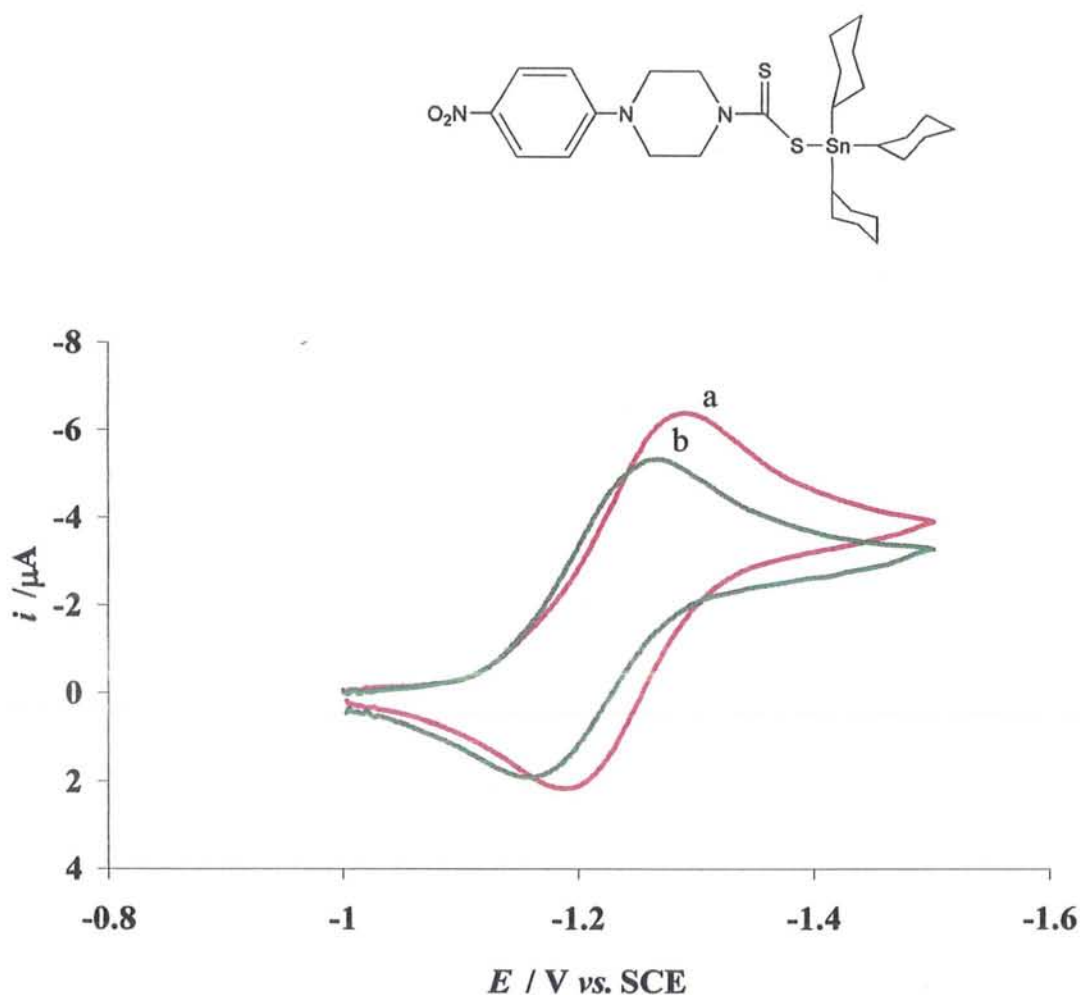


Fig. 3.5: Cyclic voltammograms of 3.00 mM of compound 2 in 10 % aqueous DMSO with 0.1 M TBAP as supporting electrolyte in the absence (a) and presence of 3.2×10^{-5} M DNA (b) at 25°C temperature. Glassy carbon electrode (0.071 cm^2) was used as working electrode and all potentials were reported vs. SCE at 100 mV/s scan rate.

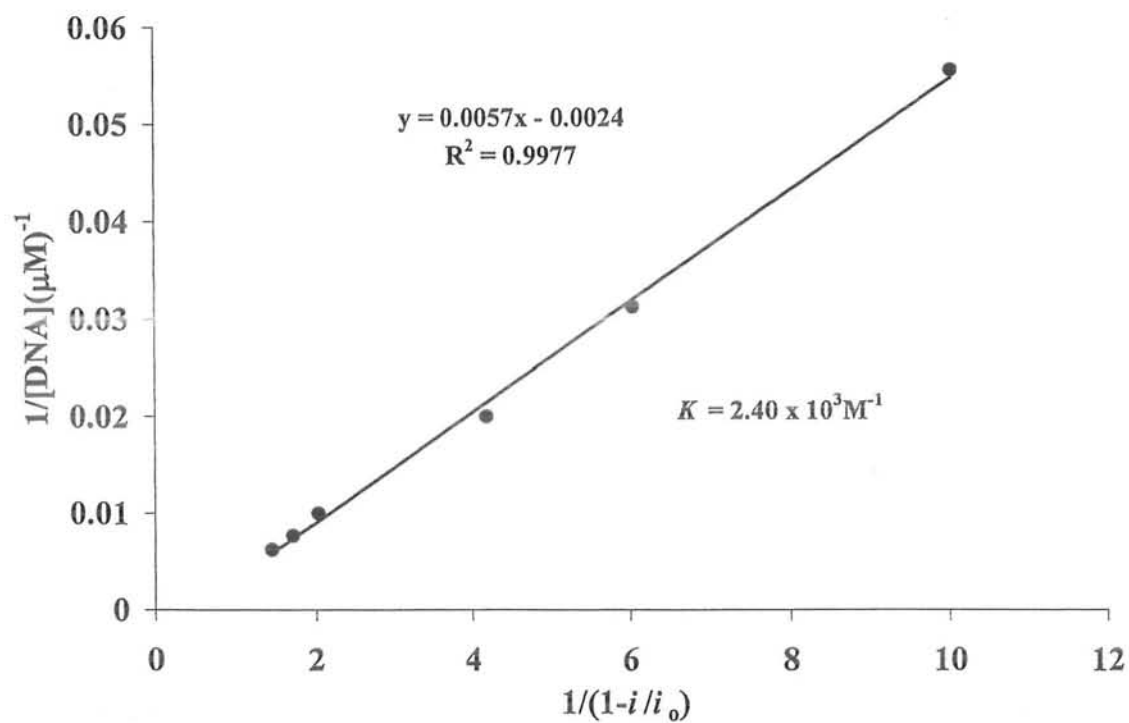
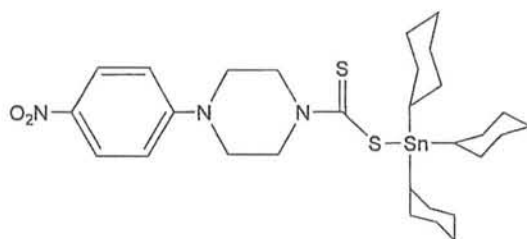


Fig. 3.6: Plot of $1/(1-i/i_0)$ vs. $1/[\text{DNA}]$ used to calculate the binding constant of 2-DNA adduct.

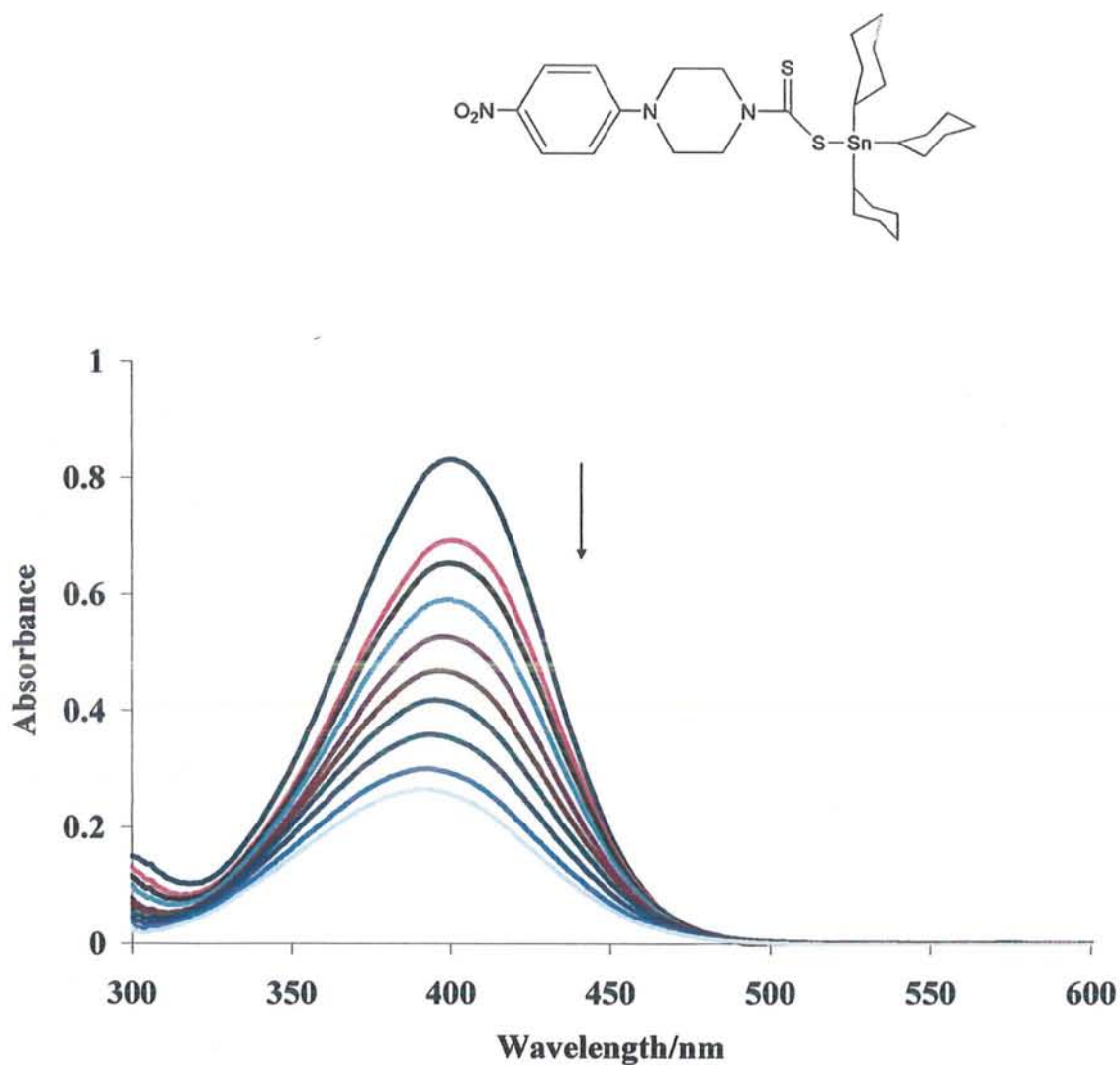


Fig. 3.7: Absorption spectra of 3mM of compound 2 in the absence (a) and presence of 2.0×10^{-5} , (b) 2.5×10^{-5} , (c) 3.5×10^{-5} , (d) 4.5×10^{-5} , (e) 5.5×10^{-5} , (f) 6.5×10^{-5} , (g) 7.5×10^{-4} , (h) 8.5×10^{-4} (i) and 9.5×10^{-4} M DNA (j). The arrow direction indicates increasing concentrations of DNA.

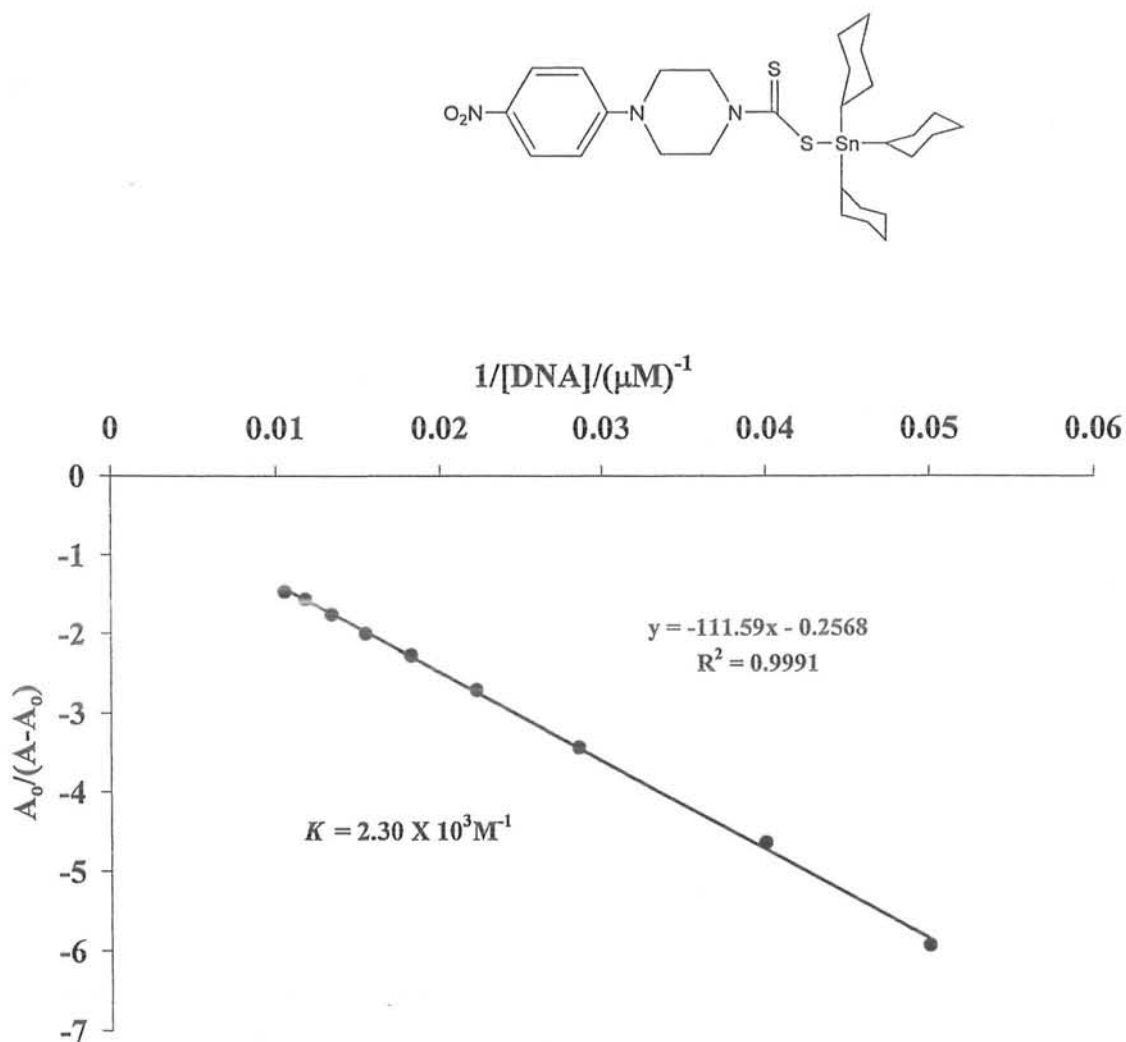


Fig. 3.8: Plot of $A_0/(A-A_0)$ vs. $1/[DNA]$ for the determination of binding constant of 2-DNA adduct.

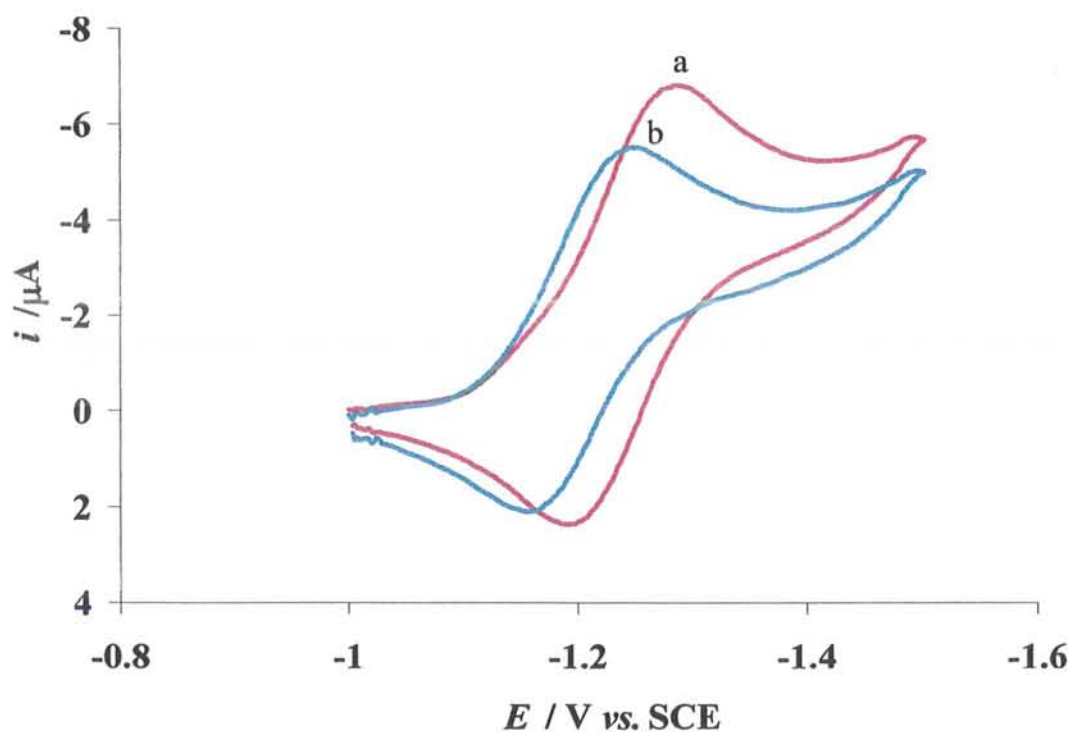
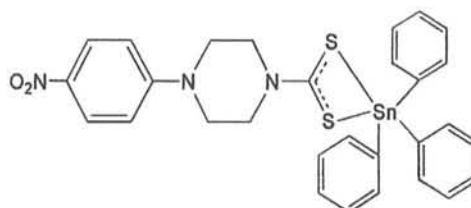


Fig. 3.9: Cyclic voltammograms of 3.00 mM of compound 4 in 10 % aqueous DMSO with 0.1 M TBAP as supporting electrolyte in the absence (a) and presence of 5.0×10^{-5} M DNA (b) at 25°C temperature. Glassy carbon electrode (0.071 cm^2) was used as working electrode and all potentials were reported vs. SCE at 100 mV/s scan rate.

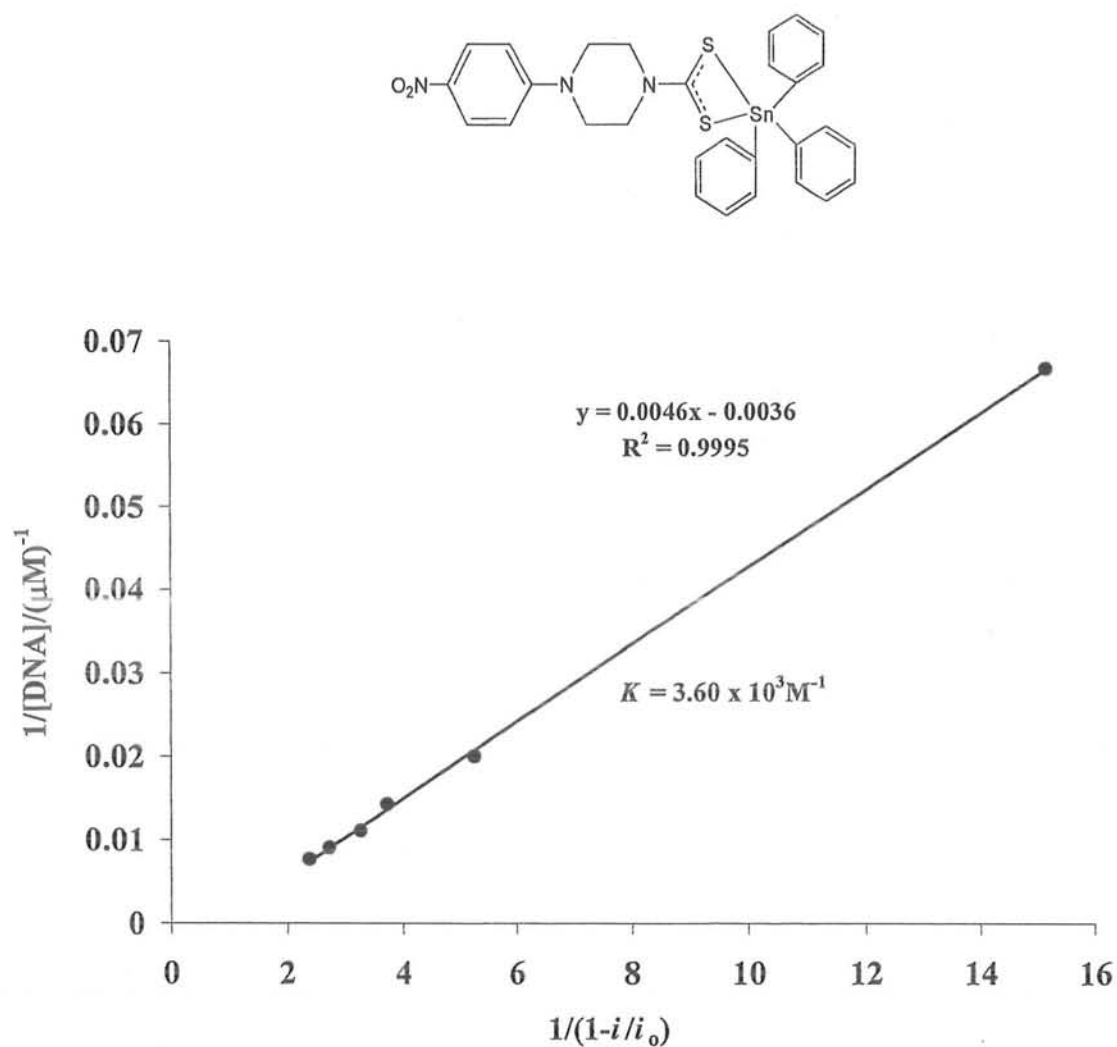


Fig. 3.10: Plot of $1/(1-i/i_0)$ vs. $1/[\text{DNA}]$ used to calculate the binding constant of 4-DNA adduct.

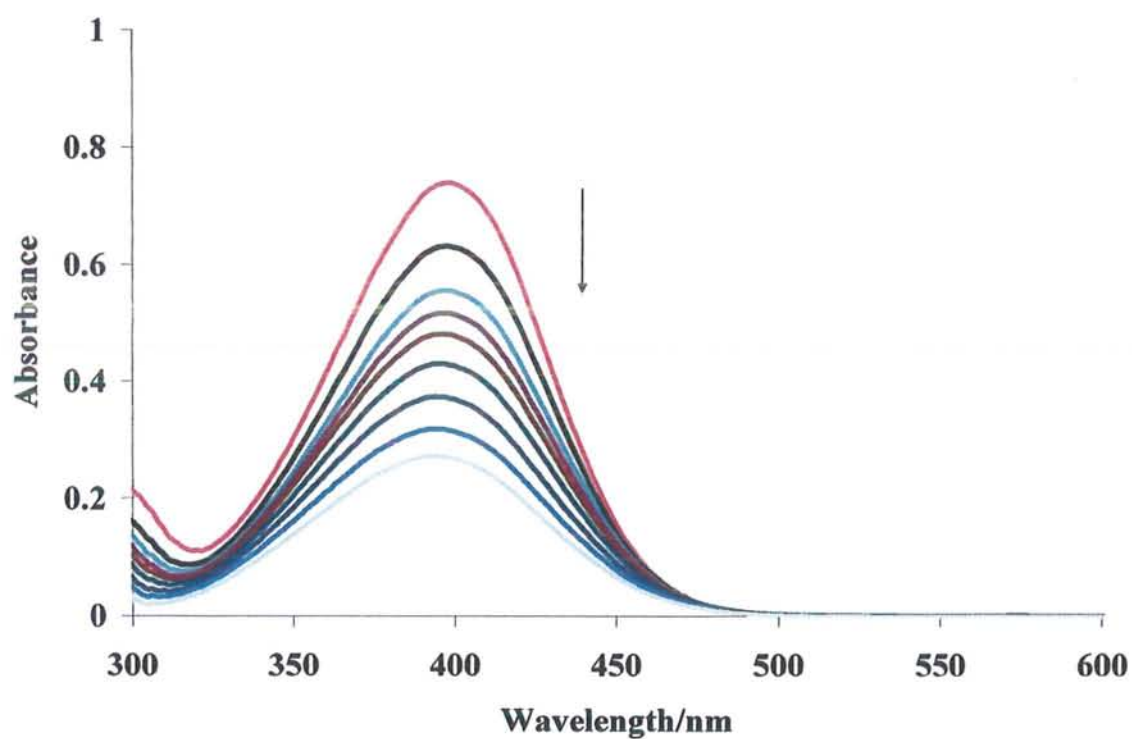
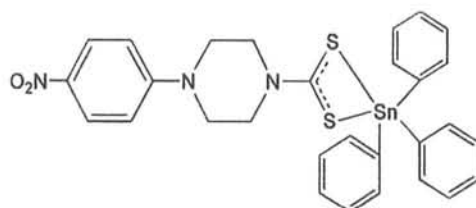


Fig. 3.11: Absorption spectra of 3mM of compound 4 in the absence (a) and presence of 2.0×10^{-5} , (b) 3.5×10^{-5} , (c) 4.5×10^{-5} , (d) 5.5×10^{-5} , (e) 6.5×10^{-5} , (f) 7.5×10^{-5} , (g) 9.5×10^{-4} (h) and 1.15×10^{-4} M DNA (i). The arrow direction indicates increasing concentrations of DNA.

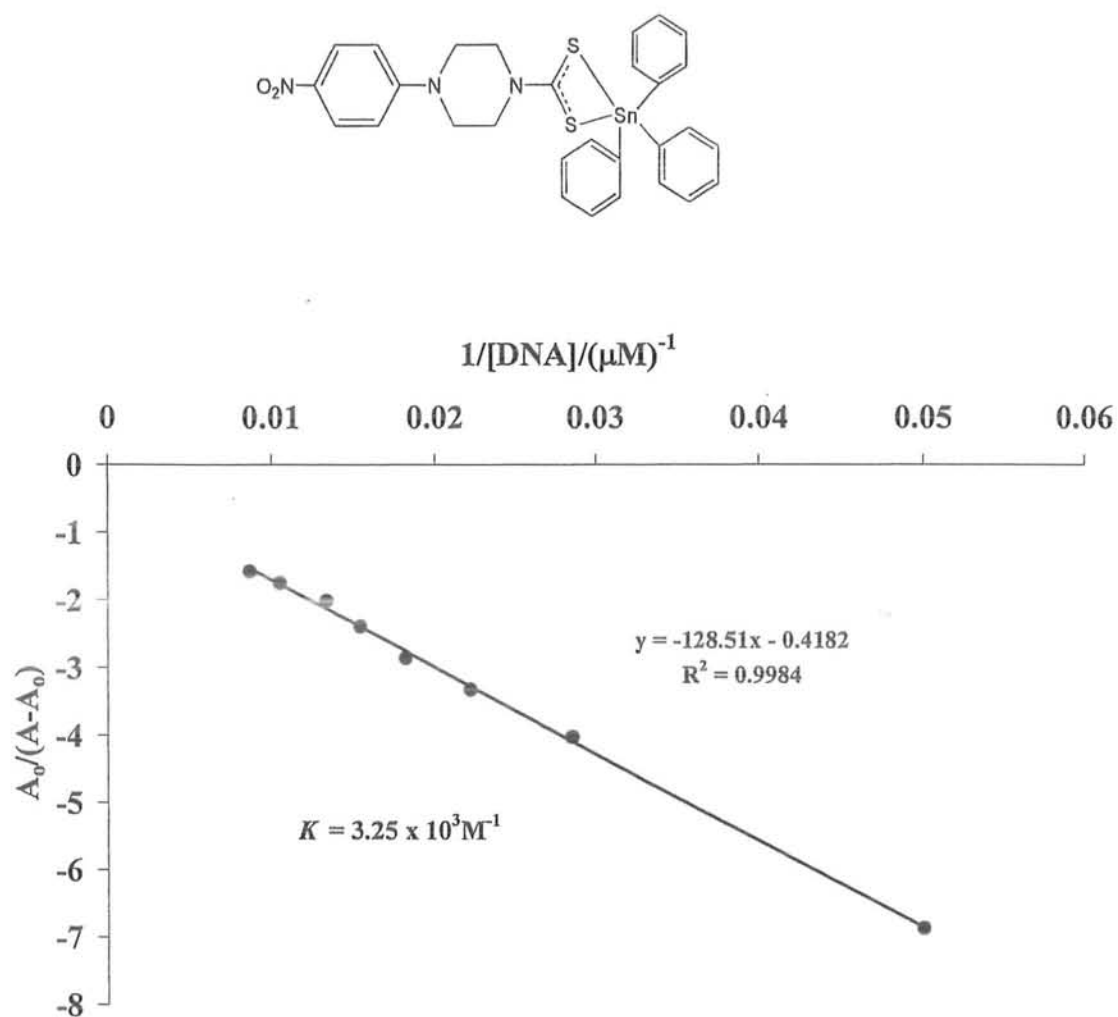


Fig. 3.12: Plot of $A_0/(A-A_0)$ vs. $1/[\text{DNA}]$ for the determination of binding constant of 4-DNA adduct.

3.8.2 Evaluation of DNA binding parameters of chlorodiorganotin(IV) and diorganotin (IV) dithiocarboxylates

DNA binding parameters were evaluated for chlorodibutylstannyl (5), chlorodiethylstannyl (7) and Diphenylstannyl (12) derivatives of 4-(4-nitrophenyl)piperazine-1-carbodithioate using cyclic voltammetry and electronic absorption spectroscopy.

3.8.2.1 Cyclic voltammetry of compounds 5, 7 and 12 and their DNA adduct

The redox behavior of complexes 5, 7 and 12 on clean glassy carbon electrode was investigated in the absence and presence of DNA, using 10 % aqueous DMSO at 25 °C. The CV of all the complexes (with and without DNA) showed a pair of redox waves with electrochemical parameters tabulated in Table 3.20. Typical CV behavior of 5, in the absence and presence of DNA is shown in Fig. 3.13. The voltammogram of the free complex 5 shows cathodic peak at $E_{pc} = -1.308$ V, due to the reduction of 5. On scanning in the positive direction, an oxidation peak is observed at $E_{pa} = -1.174$ V. This peak is presumably due to the oxidation of the reduction product of 5. The difference of anodic and cathodic peak potential of about 134 mV and the ratio of their currents $I_{pc}/I_{pa} > 1$ designate the electrochemical process to be quasi-reversible. In the presence of 60 μ M DNA, the cathodic peak current (I_{pc}) dropped by 21.5 % in comparison of free complex and is pointing towards the interaction of 5 with DNA. The negative shift (107 mV) in potential is ascribed to electrostatic interaction of 5 with the anionic phosphate of DNA [29]. Such an interaction of 5 with DNA can be explained by the probable labile nature of dithiocarboxylate ligand due to the steric repulsion of bulky butyl groups.

The CV of 3 mM 7 at 100 mVs⁻¹ scan rate (Fig. 3.14) shows reduction at $E_{pc} = -1.191$ V and oxidation of the reduced product at $E_{pa} = -1.083$ V. In the presence of 60 μ M DNA, the cathodic peak is displaced in the positive direction accompanied with the decrease in peak current. The same trend was also observed for 12. Such peculiar CV characteristics are suggestive of intercalation of 5 and 12 in to the DNA double strand [30]. The electrochemical parameters (as obtained from CV) of complexes 5, 7 and 12, in the absence and presence of 60 μ M DNA are listed in Table 3.21. The electron-donating groups disfavor reduction by shifting the formal potential (E°) in the more negative direction while the electron-withdrawing groups facilitate reduction by shifting the E° to less negative values. The results reveal that the formal potential

varies in the sequence: **5** > **12** > **7**, symptomatic of easy reduction of **7** due to the lower electron donating ability of ethyl than butyl and phenyl groups. The shift of formal potentials of complexes **7** and **12** to less negative values by the addition of DNA can be attributed to their intercalation into the stacked base pairs domain of DNA. Whereas the cathodic shift of E° (in case of **5**) signify electrostatic interaction of **5** with negatively charged oxygen of phosphate backbone of DNA.

The diffusion coefficients of the free and DNA-bound forms of these complexes were determined by the application of Randle-Sevcik expression (equation 3.1).

The linearity of I vs $\nu^{1/2}$ plots (Fig. 3.15,3.16) demonstrates, that the main mass transport of these complexes (in the absence and presence of DNA) to the electrode surface is diffusion controlled. The values of the diffusion coefficient (D_f) listed in Table 3.21 vary in the order: **12** > **5** > **7**, indicating greater D_f of **12**, due to the absence of chloro group which can interact strongly with the solvent, thus causing lowering of the diffusion coefficient in case of **5** and **7**. The higher D_f value of **7** as compared to **5** may be due to more hydrophobic butyl than ethyl groups. The variation of molecular weights in the same order in which the D_f varies disprove the idea that a heavy molecule diffuses slowly to the electrode surface. The results reveal that the nature of the groups attached to the central metal ion play a dominant role as well in deciding the order in which D_f values change. The D_b values of the DNA bound complexes, summarized in Table 3.21, are an order of magnitude smaller than the D_f values of the free complexes. The reason could be the slow mobility of the heavy complex-DNA adducts.

The values of standard rate constant (k_s) of the electron transfer reaction of these complexes at the electrode surface were obtained from Nicholson equation [31]:

$$\psi = \frac{k_s}{\left[\pi D_o \frac{nf\nu}{RT} \right]^{1/2}} \quad (3.4)$$

Where ψ is a dimensionless parameter (depending upon peak separation, ΔE_p) and all other parameters have their usual significance.

An examination of Table 3.21 reflects that the k_s values of DNA bound complexes are lower as compared to the free complexes. The magnitude of k_s with an order of 10^{-4} corresponds to the quasi-reversible nature of the redox processes with slow electron

transfer kinetics. The sequence ($12 > 7 > 5$) of the k_s values without DNA, is pinpointing of the fact, that the fast diffusing **12** with no chloro group is more favorable for electron transfer than complexes **5** and **7**. The slow electron transfer of **5** than **7** may be due to its greater molecular weight. For getting further evidences about the nature of the electrochemical processes of the free and DNA bound complexes **5**, **7** and **12**, the charge transfer coefficients (α) were determined by the application of Kocchi formula [32]:

$$\alpha = \left[\frac{(E_{1/2} - E_p^c)}{(E_p^a - E_p^c)} \right] \quad (3.5)$$

α with values of more than 0.5 (Table 3.21) for all the complexes (with and without DNA) unambiguously symbolize the quasi-reversibility of the electrochemical processes.

The sequential drop in the peak current of the complexes by the addition of increasing concentration of DNA, ranging from 20 to 60 μM , can be used to quantify the binding constant by using the equation given below [33]:

$$\log (1/[\text{DNA}]) = \log K + \log (I_{\text{H-G}}/(I_{\text{G}}-I_{\text{H-G}})) \quad (3.6)$$

Where, K is the binding constant, I_{G} and $I_{\text{H-G}}$ are the peak currents of the free guest (G) and the complex (H-G), respectively.

The intercept of $\log (1/[\text{DNA}])$ versus $\log (I_{\text{H-G}}/(I_{\text{G}}-I_{\text{H-G}}))$ plots (Figure 3.17) yielded the binding constant K , varying in the sequence: **7**-DNA > **12**-DNA > **5**-DNA. The binding of these complexes with DNA will damage the genetic machinery resulting in the failure of the cancerous cell to replicate.

The greater K of these Sn complexes than those observed for similar DNA-intercalating Cr and Ru complexes; $[\text{CrCl}_2(\text{dicnq})_2]^+$ and $[\text{Ru}((\text{dicnq})_3)]^{+2}$, with K reported as 1.20×10^3 and $9.70 \times 10^3 \text{ M}^{-1}$ [24,34,35], suggests their potential candidature as chemotherapeutic agents. The negative values of standard Gibbs free energy ($\Delta G = -RT \ln K$) indicate the spontaneity of their binding interaction with DNA.

For the determination of binding site size the following simple binding model was used [36]:

$$C_b/C_f = K\{[\text{free base pairs}]/s\} \quad 3.7$$

Where 's' is the binding site size in terms of base pairs. Measuring the concentration of DNA in terms of [NP], the concentration of base pairs can be expressed as [DNA]/2. So equation 3.7 can be written as:

$$C_b/C_f = K \{[\text{DNA}]/2s\} \quad (3.8)$$

C_f and C_b denote the concentrations of free and DNA-bound species respectively. The C_b/C_f ratio was determined by the equation given below [37]:

$$C_b/C_f = (I - I_{\text{DNA}})/I_{\text{DNA}} \quad (3.9)$$

Where, I_{DNA} and I represent the peak current of the drug with and without DNA. Putting the values of K as calculated according to equation 3.6, the values of binding site size as listed in Table 3.21 were obtained from the slopes of C_b/C_f vs. [DNA] plots. (Fig. 3.18) The values of 's' decrease in the order: **7** > **12** > **5**. The small binding site size of **5** may be due to its electrostatic interaction with DNA. The results demonstrate that two molecules of complexes **7** and **12** cover one base pair when intercalate into DNA.

Table 3.20: CV data of compounds 5, 7 and 12.

Compound	CV data				
	E_{pa} (V)	E_{pc} (V)	ΔE_p (mV)	E^o (V)	I_{pc}/I_{pa}
5	-1.174	-1.308	134	-1.241	1.76
5-DNA	-1.274	-1.415	141	-1.344	2.10
7	-1.083	-1.191	108	-1.137	2.32
7-DNA	-0.947	-1.073	126	-1.01	1.80
12	-1.169	-1.271	102	-1.22	1.29
12-DNA	-1.096	-1.201	105	-1.148	1.37

(a) All potentials were measured versus SCE in ethanol at 0.1 Vs⁻¹.

(b) $\Delta E_p = (E_{pa} - E_{pc})$

(c) $E^o = (E_{pa} + E_{pc})/2$

Table 3.21: Summary of kinetic and binding parameters of compounds 5, 7 and 12., as obtained from electrochemical measurements.

Compound	Kinetic parameters				Binding parameters		
	$D_f \times 10^7$ (cm ² /s)	$D_b \times 10^8$ (cm ² /s)	α	$k_s \times 10^4$ (cm/s)	s (bp)	$K \times 10^{-4}$ (M ⁻¹)	ΔG (kJmol ⁻¹)
5	2.98	-	0.69	2.31	-	-	-
5-DNA	-	4.57	0.67	0.82	0.42	0.54	-21.29
7	2.61	-	0.74	3.59	-	-	-
7-DNA	-	9.28	0.69	1.51	0.5	1.24	-23.35
12	5.25	-	0.68	6.09	-	-	-
12-DNA	-	2.12	0.57	1.13	0.45	0.84	-22.39

3.8.2.2 UV-Vis spectroscopy of compounds 5, 7 and 12 and their DNA adduct

The interaction of complexes 5, 7 and 12 with DNA was also examined by UV-Vis absorption titration for getting further clues about the mode of interaction and binding strength. The effect of varying concentration of DNA (20 -80 μM) on the electronic absorption spectra of 30 μM of 5, 7 and 12 is shown in Fig. 3.19-3.21, respectively. The maximum absorption of complex 5 (Fig. 3.19) at $\lambda_{\text{max}} = 397 \text{ nm}$, exhibited blue shift of 6 nm, indicating electrostatic interaction of 5 with DNA. Fig. 3.20 shows that the peak position of 30 μM 7 is shifted bathochromically from $\lambda_{\text{max}} = 396$ to 403 nm by the addition of 80 μM DNA, accompanied with hypochromic shift from 0.796 to 0.307. These remarkable spectral characteristics suggest intercalation of 7 into the stacked base pairs domain of DNA [26,38,39]. The hypochromic effect is caused by the overlapping of the electronic states of the intercalating chromophore of the complex 7 with the DNA bases [27] and the bathochromic shift is caused by the lowering in $\pi\text{-}\pi^*$ transition energy of the complex due to its ordered stacking between the DNA base pairs after intercalation. By the addition of DNA, a slight red shift of peak at 410 nm and pronounce hypochromic effect suggestive of intercalative mode of interaction of 12 (Fig. 3.21). In a nutshell, UV-Vis results are quite consistent with the CV results. The binding constants were calculated according to equation 3.3.

The slope to intercept ratio of the plot between $A_0/(A-A_0)$ vs. $1/[\text{DNA}]$ yielded the binding constant, $K = 1.32 \times 10^3$, 7.21×10^3 and $6.22 \times 10^3 \text{ M}^{-1}$ for 5, 7 and 12, respectively. The K obtained here follows the same order as was obtained from CV data. The slight difference in the values of UV-Vis and CV binding constant may be due to the use of supporting electrolyte in CV measurements.

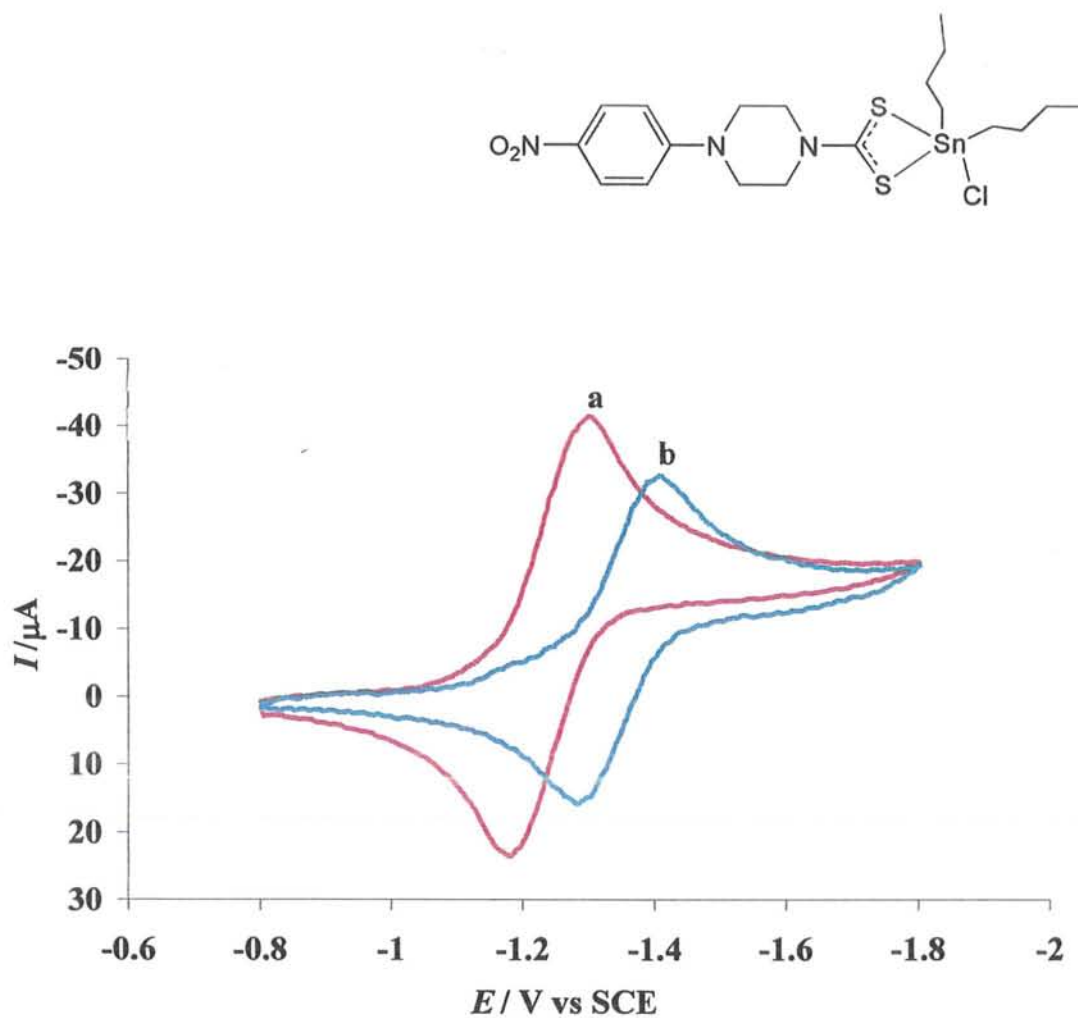


Fig. 3.13: CV behavior of 3 mM of compound 5 at clean GC electrode in the absence (a) and presence of 60 μM DNA (b) in 10 % aqueous DMSO using 0.1 M TBAFB as supporting electrolyte at 0.1 V/s scan rate.

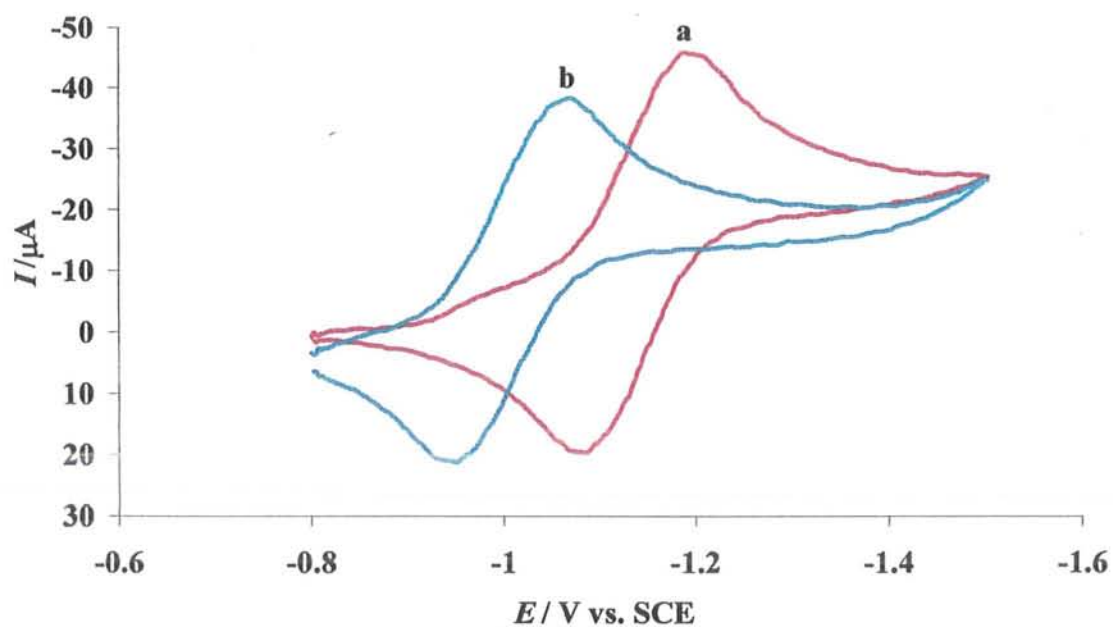
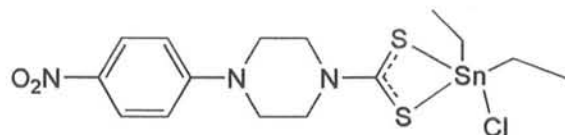


Fig. 3.14: CV behavior of 3 mM of compound 7 at clean GC electrode in the absence (a) and presence of 60 μ M DNA (b) in 10 % aqueous DMSO using 0.1 M TBAFB as supporting electrolyte at 0.1 V/s scan rate.

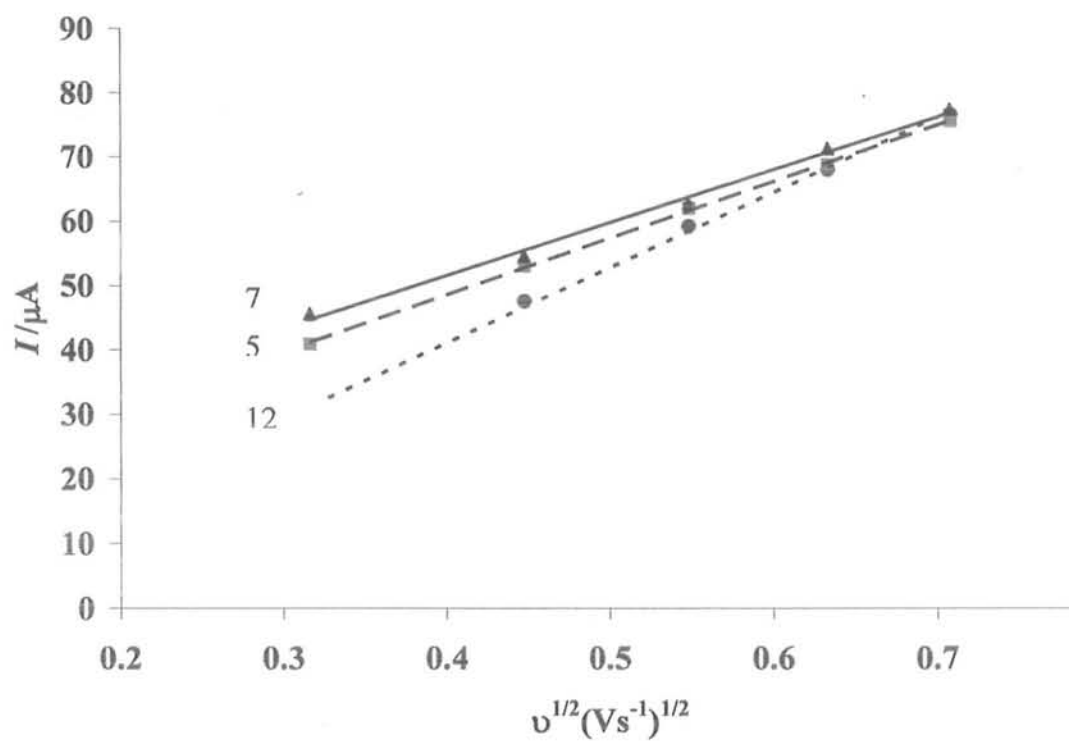


Fig. 3.15: Plots of I vs. $v^{1/2}$, for the determination of the diffusion coefficients of 3 mM of compounds 5, 7 and 12. Scan rates: 0.1, 0.2, 0.3, 0.4 and 0.5 Vs^{-1} .

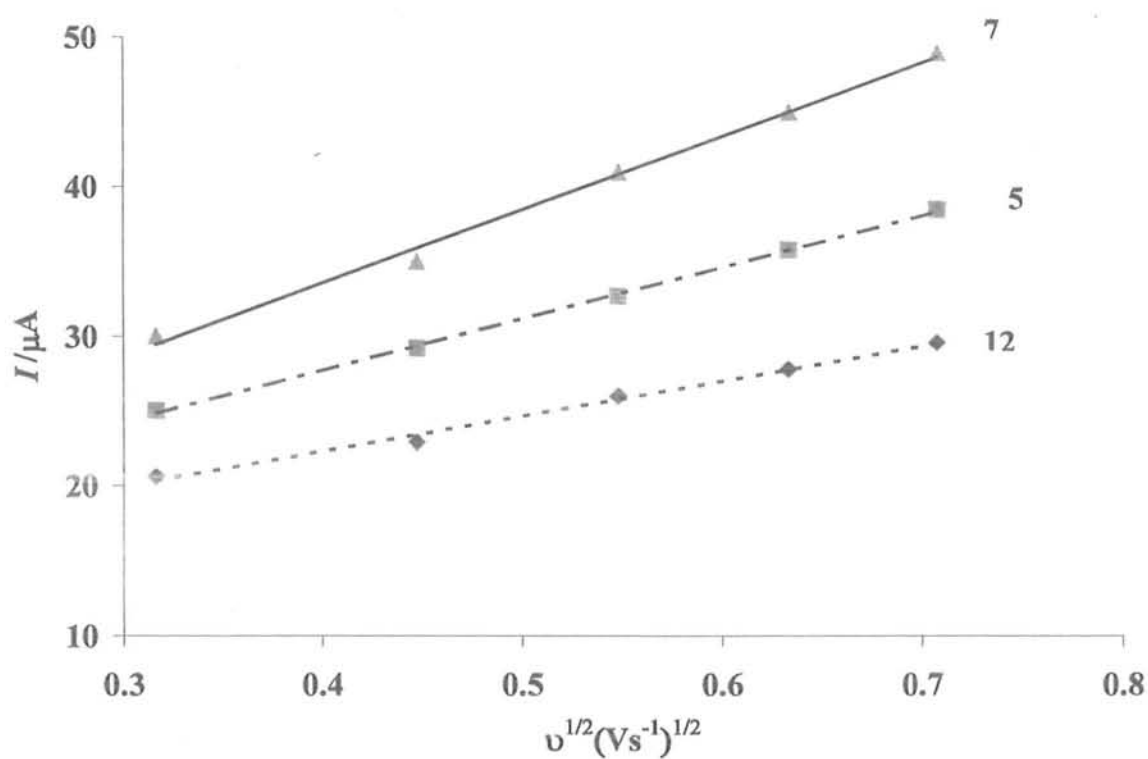


Fig. 3.16: Plots of I vs. $v^{1/2}$, for the determination of the diffusion coefficients of 3 mM of compounds 5, 7 and 12 in the presence of 60 μM DNA. Scan rates: 0.1, 0.2, 0.3, 0.4 and 0.5 Vs^{-1} .

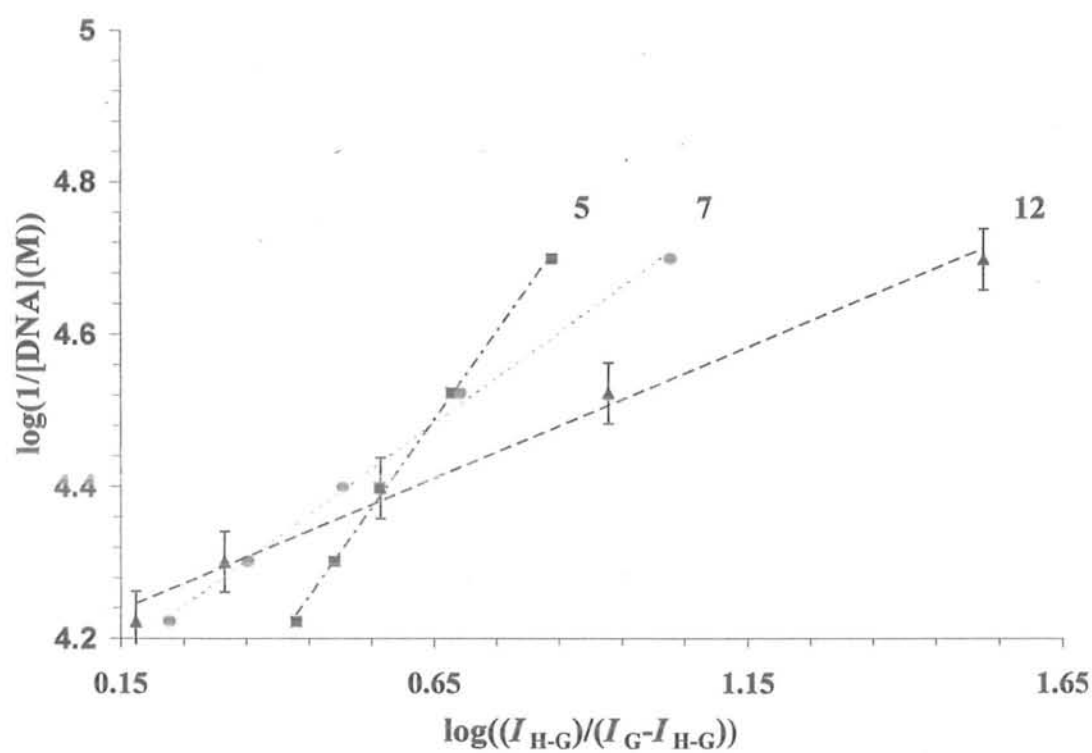


Fig. 3.17: Plots of $\log(I_{H-G}/(I_G - I_{H-G}))$ vs. $\log(1/[DNA])$ used to calculate the binding constants of complexes 5, 7 and 12 with DNA.

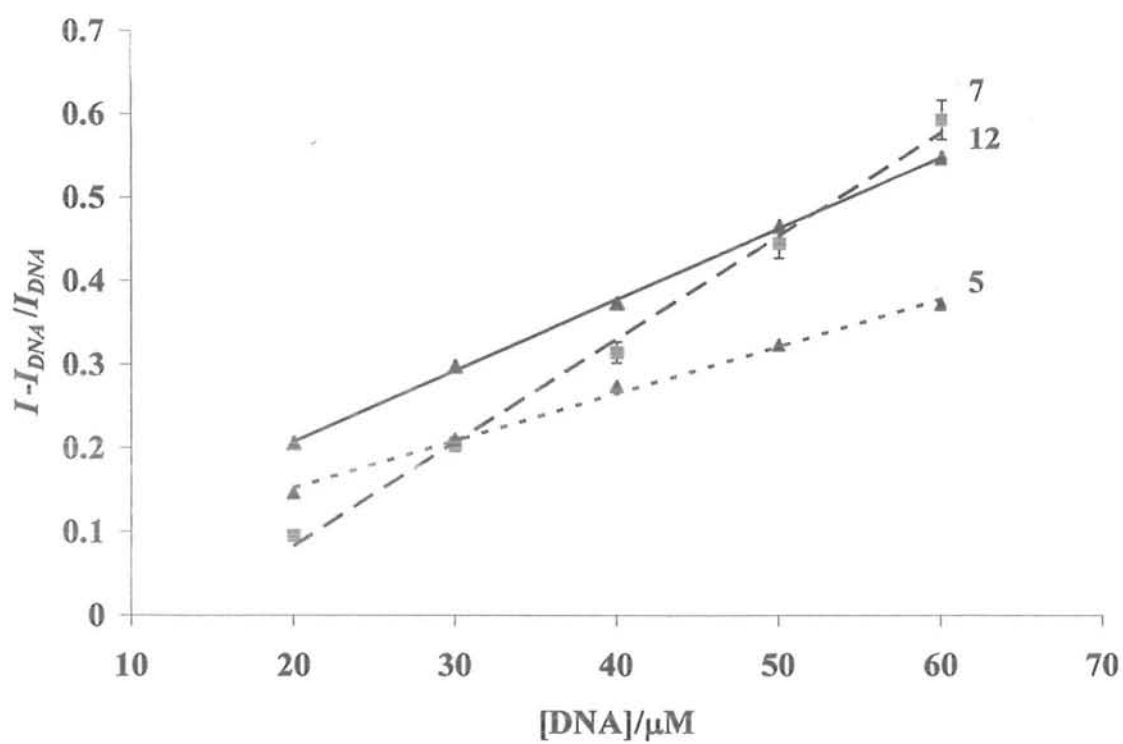


Fig. 3.18: $I - I_{\text{DNA}} / I_{\text{DNA}}$ vs [DNA] for the determination of binding site size.

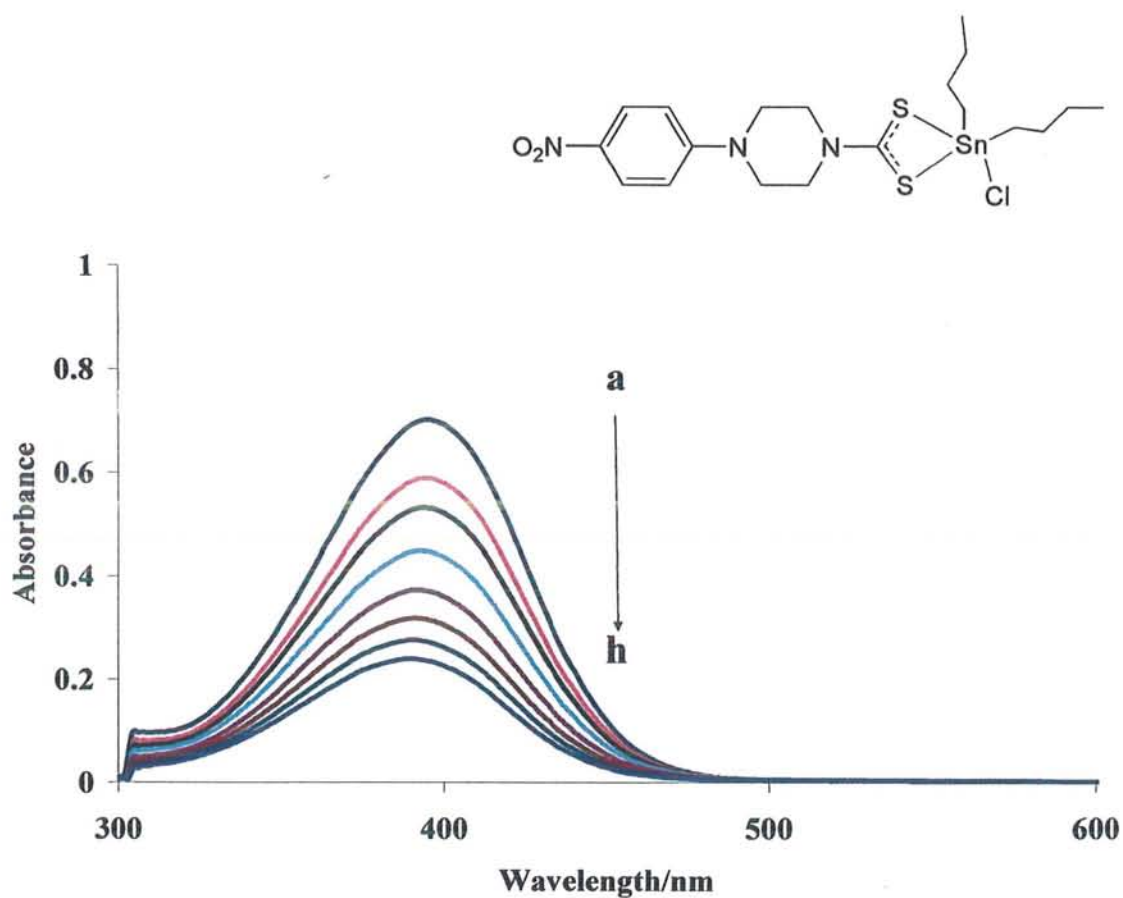


Fig. 3.19: Absorption spectra of 30 μM of compound 5 in the absence (a) and presence of 20 μM , (b) 30 μM , (c) 40 μM , (d) 50 μM , (e), 60 μM (f), 70 μM (g) and 80 μM DNA (h) in 10 % aqueous DMSO at 25 $^{\circ}\text{C}$.

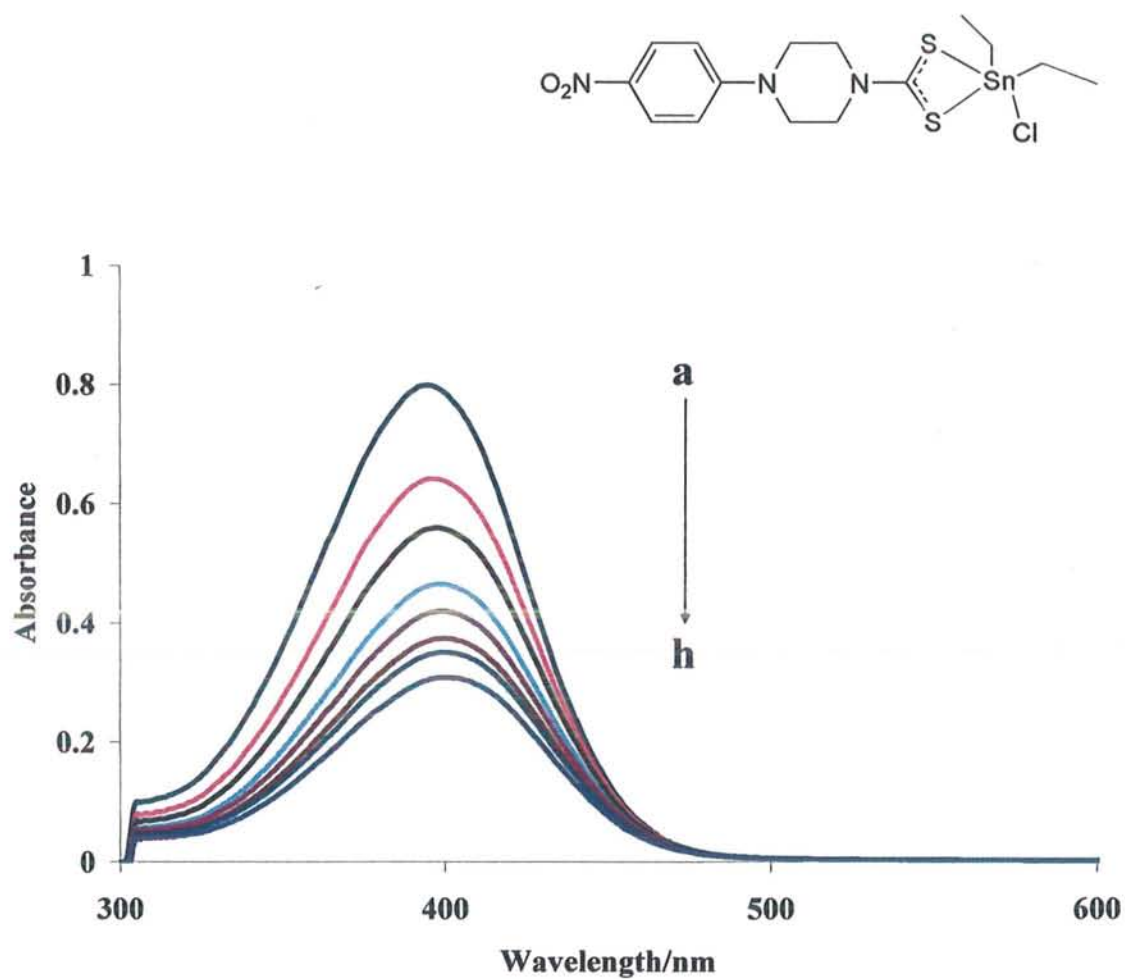
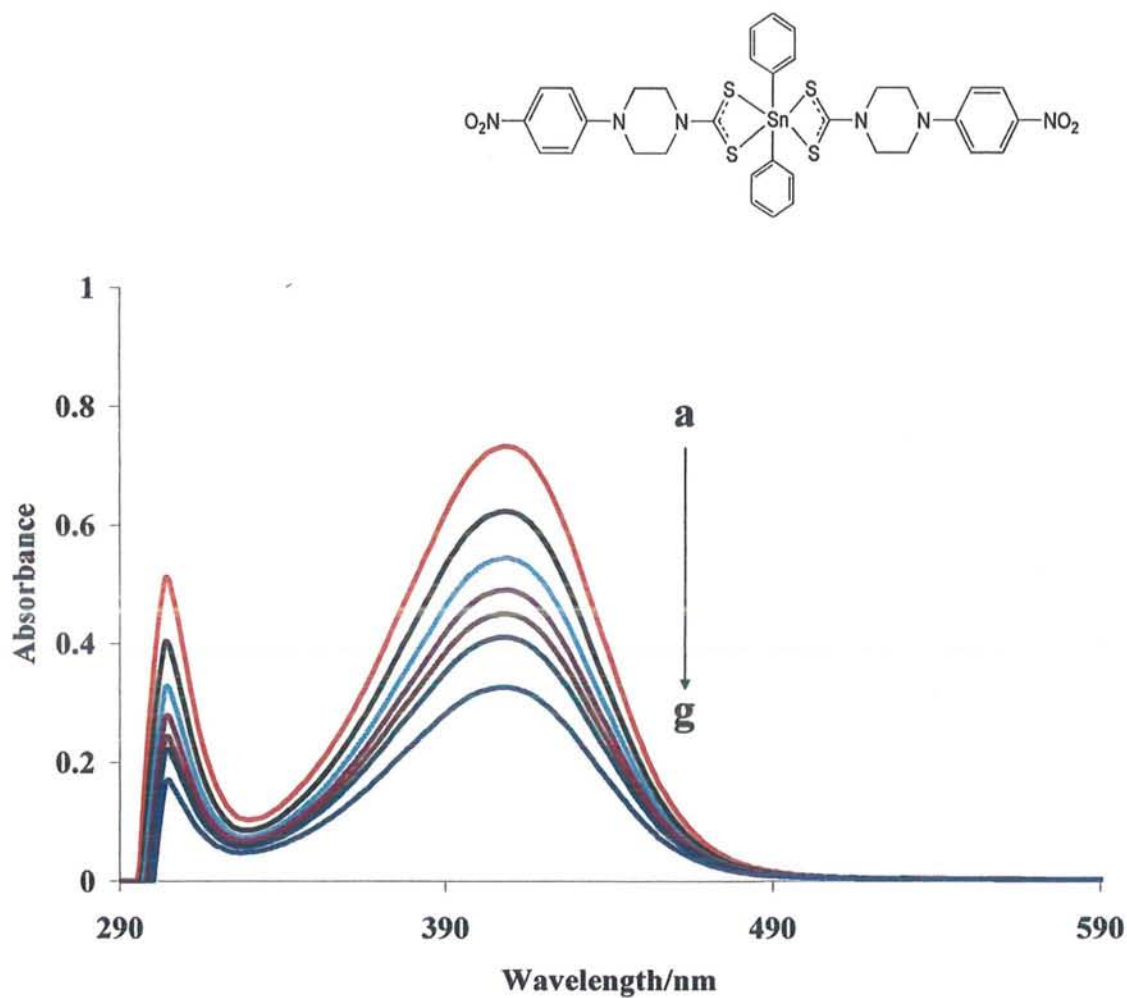


Fig. 3.20: Absorption spectra of 30 μM of compound 7 in the absence (a) and presence of 20 μM , (b) 30 μM , (c) 40 μM , (d) 50 μM , (e), 60 μM (f), 70 μM (g) and 80 μM DNA (h) in 10 % aqueous DMSO at 25 $^{\circ}\text{C}$.



3.9 Antibacterial activity

The synthesized ligands and some of the complexes were screened for antibacterial activity against five different strains of bacteria (*E. coli*, *Salmonella typhi*, *Pseudomonas aeruginosa*, *Staphylococcus aureus* and *Streptococcus*) by the agar well diffusion method [40] in DMSO. Streptomycin was used as a standard drug and the zone of inhibition was measured in millimeter. The results are shown in Tables 3.22-3.24.

The investigated complexes exhibit higher activity than the corresponding ligand-salts and in most cases a comparable activity with standard drug. Against *Salmonella typhi*, complexes **19** and **20** are as active as standard drug while the zone of inhibition of **42** is higher than that. The antibacterial action of the complexes vary from strain to strain but it can be generalize that the triorganotin(IV) complexes are more active than the diorganotin(IV) complexes, however, in some cases the results are reverse. The anionic ligand, may also play an important role in the antibacterial activity of organotin(IV) compounds.

It can be proposed that the microorganisms may have taken in the compound as food particle which arrested the proper working of either mitochondria, proteins or DNA of the bacterial cell and ultimate result is the death of microorganism.

3.10 Antifungal activity

The synthesized compounds were also screened against various fungi using the agar tube diffusion test [41]. The percent growth inhibition (%) of the synthesized ligands and the compounds are listed in Tables 3.25-3.27. Clomitrazone was as standard drug. The fungicidal data show that the organotin(IV) derivatives of 4-(2-methoxyphenyl)piperazine-1-carbodithioate are good fungicides. Following points are evident from the antifungal screening.

- i) All the complexes are more active than the ligand-salts.
- ii) The triorganotin(IV) complexes express high activity than diorganotin(IV) complexes.
- iii) Triorganotin(IV) complexes, especially Tributyl- and triphenyltin(IV) derivatives inhibit fungal growth more efficiently than the standard drug.

- iv) Chlorodiorganotin(IV) complexes are good antifungal agent than the diorganotin(IV) counterpart.
- v) Among the diorganotin(IV) derivatives, the chlorodiphenyl- and diphenyltin(IV) complexes are good fungicides than the clomitrazone, however, the activity of the rest of the diorganotin(IV) compound are comparable with the drug.

Organotin(IV) derivatives 4-benzhydrylpiperazine-1-carbodithioate and 4-benzhydrylpiperazine-1-carbodithioate ligands were found to be poor antifungal agents. In both these cases, the ligand was found to be more active in comparison to its complexes.

Table 3.22: Antibacterial activity data of organotin(IV) derivatives of 4-(2-methoxyphenyl)piperazine-1-carbodithioate.^{a,b} (continue---)

Name of Bacterium	Clinical Implication	Zone of Inhibition (mm)							Ref. Drug
		L ^a -salt	(13) n-Bu ₃ SnL ^a	(14) Cy ₃ SnL ^a	(15) Me ₃ SnL ^a	(16) Ph ₃ SnL ^a	(17) n-Bu ₂ SnCIL ^a	(18) n-Bu ₂ SnL ^a ₂	
<i>Escherichia coli</i>	Infection of wounds, urinary tract and dysentery	28	30	12	20	29	22	21	34
<i>Salmonella typhi</i>	Typhoid fever, localized infection	14	30	22	24	28	28	22	31
<i>Pseudomonas aeruginosa</i>	Infection of wounds, eyes, septicemia	0	8	0	20	6	10	14	24
<i>Staphylococcus aureus</i>	Food poisoning, scaled skin syndrome, endocarditis	0	0	0	20	0	23	23	38
<i>Streptococcus</i>	Strep throat	30	31	0	30	30	20	24	38

^a *In vitro*, agar well diffusion method, conc. 1 mg/mL of DMSO.

^b Reference drug, Streptomycin.

Table 3.22: Antibacterial activity data of organotin(IV) derivatives of 4-(2-methoxyphenyl)piperazine-1-carbodithioate.^{a,b}

Name of Bacterium	Clinical Implication	Zone of Inhibition (mm)						Ref. Drug
		(19) Et ₂ SnCIL ^a	(20) Et ₂ SnL ₂ ^a	(21) Me ₂ SnCIL ^a	(22) Me ₂ SnL ₂ ^a	(23) Ph ₂ SnCIL ^a	(24) Ph ₂ SnL ₂ ^a	
<i>Escherichia coli</i>	Infection of wounds, urinary tract and dysentery	30	27	22	21	21	24	34
<i>Salmonella typhi</i>	Typhoid fever, localized infection	31	31	24	20	19	23	31
<i>Pseudomonas aeruginosa</i>	Infection of wounds, eyes, septicemia	22	20	16	18	8	6	24
<i>Staphylococcus aureus</i>	Food poisoning, scaled skin syndrome, endocarditis	28	23	24	16	4	0	38
<i>Streptococcus</i>	Strep throat	30	28	18	18	27	28	38

^a *In vitro*, agar well diffusion method, conc. 1 mg/mL of DMSO.

^b Reference drug, Streptomycin.

Table 3.23: Antibacterial activity data of organotin(IV) derivatives of 4-benzhydrylpiperazine-1-carbodithioate.^{a,b} (continue---)

Name of Bacterium	Clinical Implication	Zone of Inhibition (mm)							Ref. Drug
		L ^c -salt	(37) n-Bu ₃ SnL ^c	(38) Cy ₃ SnL ^c	(39) Me ₃ SnL ^c	(40) Ph ₃ SnL ^c	(41) n-Bu ₂ SnCIL ^c	(42) n-Bu ₂ SnL ^c ₂	
<i>Escherichia coli</i>	Infection of wounds, urinary tract and dysentery	20	25	13	25	21	22	18	34
<i>Salmonella typhi</i>	Typhoid fever, localized infection	21	0	0	21	25	22	35	31
<i>Pseudomonas aeruginosa</i>	Infection of wounds, eyes, septicemia	0	13	0	14	0	12	0	24
<i>Staphylococcus aureus</i>	Food poisoning, scaled skin syndrome, endocarditis	0	0	0	14	0	14	13	38
<i>Streptococcus</i>	Strep throat	12	0	13	10	0	13	0	38

^a *In vitro*, agar well diffusion method, conc. 1 mg/mL of DMSO.

^b Reference drug, Streptomycin.

Table 3.23: Antibacterial activity data of organotin(IV) derivatives of 4-benzhydrylpiperazine-1-carbodithioate.^{a,b}

Name of Bacterium	Clinical Implication	Zone of Inhibition (mm)						Ref. Drug
		(43) Et ₂ SnClL ^c	(44) Et ₂ SnL ₂ ^c	(45) Me ₂ SnClL ^c	(46) Me ₂ SnL ₂ ^c	(47) Ph ₂ SnClL ^c	(48) Ph ₂ SnL ₂ ^c	
<i>Escherichia coli</i>	Infection of wounds, urinary tract and dysentery	26	19	0	0	21	20	34
<i>Salmonella typhi</i>	Typhoid fever, localized infection	32	0	17	11	20	23	31
<i>Pseudomonas aeruginosa</i>	Infection of wounds, eyes, septicemia	13	12	0	0	0	0	24
<i>Staphylococcus aureus</i>	Food poisoning, scaled skin syndrome, endocarditis	18	13	12	0	15	13	38
<i>Streptococcus</i>	Strep throat	20	20	12	13	6	0	38

^a *In vitro*, agar well diffusion method, conc. 1 mg/mL of DMSO.

^b Reference drug, Streptomycin.

Table 3.24: Antibacterial activity data of organotin(IV) derivatives of 4-benzylpiperidine-1-carbodithioate.^{a,b} (continue---)

Name of Bacterium	Clinical Implication	Zone of Inhibition (mm)							Ref. Drug
		L ^d	(49) n-Bu ₃ SnL ^d	(50) Cy ₃ SnL ^d	(51) Me ₃ SnL ^d	(52) Ph ₃ SnL ^d	(53) n-Bu ₂ SnCIL ^d	(54) n-Bu ₂ SnL ^d ₂	
<i>Escherichia coli</i>	Infection of wounds, urinary tract and dysentery	22	25	12	11	23	14	13	34
<i>Salmonella typhi</i>	Typhoid fever, localized infection	16	23	12	17	19	19	17	31
<i>Pseudomonas aeruginosa</i>	Infection of wounds, eyes, septicemia	17	16	0	13	0	10	0	24
<i>Staphylococcus aureus</i>	Food poisoning, scaled skin syndrome, endocarditis	12	0	0	0	0	15	19	38
<i>Streptococcus</i>	Strep throat	0	18	11	0	21	11	13	38

^a *In vitro*, agar well diffusion method, conc. 1 mg/mL of DMSO.

^b Reference drug, Streptomycin.

Table 3.24: Antibacterial activity data of organotin(IV) derivatives of 4-benzylpiperidine-1-carbodithioate.^{a,b}

Name of Bacterium	Clinical Implication	Zone of Inhibition (mm)						Ref. Drug
		(55) Et ₂ SnCIL ^d	(56) Et ₂ SnL ₂ ^d	(57) Me ₂ SnCIL ^d	(58) Me ₂ SnL ₂ ^d	(59) Ph ₂ SnCIL ^d	(60) Ph ₂ SnL ₂ ^d	
<i>Escherichia coli</i>	Infection of wounds, urinary tract and dysentery	19	17	18	0	10	9	34
<i>Salmonella typhi</i>	Typhoid fever, localized infection	23	20	21	13	11	7	31
<i>Pseudomonas aeruginosa</i>	Infection of wounds, eyes, septicemia	14	16	14	0	8	10	24
<i>Staphylococcus aureus</i>	Food poisoning, scaled skin syndrome, endocarditis	15	11	11	10	0	0	38
<i>Streptococcus</i>	Strep throat	17	17	17	11	0	0	38

^a *In vitro*, agar well diffusion method, conc. 1 mg/mL of DMSO.

^b Reference drug, Streptomycin.

Table 3.25: Antifungal activity^a of organotin(IV) 4-(2-methoxyphenyl)piperazine-1-carbodithioate.

Sample	Tested Fungi									
	<i>Aspergillus niger</i>		<i>Aspergillus flavus</i>		<i>Helminthosporium solani</i>		<i>Alternaria solani</i>		<i>Fusarium sp.</i>	
	Linear growth	% inhibition	Linear growth	% inhibition	Linear growth	% inhibition	Linear growth	% inhibition	Linear growth	% inhibition
Control	85		86		87		90		70	
L ^a	82.0	3.5	86	0.0	12	86.2	10	55.6	17	75.7
(13)										
n-Bu ₃ SnL ^a	10.0	88.2	10	88.4	10	88.5	12	62.2	8	88.6
(14)										
Cy ₃ SnL ^a	53.0	37.6	68	20.9	71	18.4	82	7.8	54	22.9
(15)										
Me ₃ SnL ^a	20.0	76.5	20	76.7	83	5.7	83	88.9	60	14.3
(16)										
Ph ₃ SnL ^a	12.0	85.9	10	88.4	12	86.2	10	86.7	17	75.7
(17)										
n-Bu ₂ SnCIL ^a	45.0	47.1	82	4.7	87	0.0	80	11.1	35	50.0
(18)										
n-Bu ₂ SnL ^a ₂	80.0	5.9	85	1.2	85	2.3	60	33.3	54	22.9
(19)										
Et ₂ SnCIL ^a	45.0	47.1	82	4.7	87	0.0	80	11.1	35	50.0
(20)										
Et ₂ SnL ^a ₂	50	41.2	86	0.0	87	0.0	90	0.0	34	51.4
(21)										
Me ₂ SnCIL ^a	78.0	8.2	86	0.0	79	9.2	40	11.1	45	35.7
(22)										
Me ₂ SnL ^a ₂	85	0.0	86	0.0	78	10.3	51	43.3	60	14.3
(23)										
Ph ₂ SnCIL ^a	16	81.2	53	38.4	50	42.5	30	66.7	14	80.0
(24)										
Ph ₂ SnL ^a ₂	18.0	78.8	59	31.4	50	42.5	34	62.2	14	80.0
Clotrimazole	60	29.4	52	39.5	51	41.4	48	46.7	44	37.1

^a Concentration: 200 µg/mL of DMSO.

Table 3.26: Antifungal activity^a of organotin(IV) derivatives of 4-benzhydrylpiperazine-1-carbodithioate

Sample	Tested Fungi									
	<i>Aspergillus nigar</i>		<i>Aspergillus flavus</i>		<i>Helminthosporium solani</i>		<i>Alternaria solani</i>		<i>Fusarium sp.</i>	
	Linear growth	% inhibition	Linear growth	% inhibition	Linear growth	% inhibition	Linear growth	% inhibition	Linear growth	% inhibition
Control	85		86		87		90		70	
L ^c	68.0	20.0	70.0	18.6	74.0	14.9	68.0	24.4	62	11.4
(37)										
n-Bu ₃ SnL ^c	80.0	5.9	81.0	5.8	78.0	10.3	74.0	17.8	70	0
(38)										
Cy ₃ SnL ^c	78.0	8.2	78.0	9.3	74.0	14.9	80.0	11.1	70	0
(39)										
Me ₃ SnL ^c	72.0	15.3	73.0	15.1	72.0	17.2	66.0	26.7	60	14.2
(40)										
Ph ₃ SnL ^c	74.0	12.9	78.0	9.3	72.0	17.2	80.0	11.1	70	0
(41)										
n-Bu ₂ SnCIL ^c	66.0	22.4	78.0	9.3	76.0	12.6	70.0	22.2	68	2.8
(42)										
n-Bu ₂ SnL ^c ₂	78.0	8.2	78.0	9.3	73.0	16.1	74.0	17.8	68	2.8
(43)										
Et ₂ SnCIL ^c	66.0	22.4	72.0	16.3	73.0	16.1	66.0	26.7	60	14.2
(44)										
Et ₂ SnL ^c ₂	83.0	2.4	82.0	4.7	76.0	12.6	73.0	18.9	70	0
(45)										
Me ₂ SnCIL ^c	80.0	5.9	83.0	3.5	80.0	8.0	78.0	13.3	68	2.8
(46)										
Me ₂ SnL ^c ₂	80.0	5.9	78.0	9.3	68.0	21.8	64.0	28.9	61	12.8
(47)										
Ph ₂ SnCIL ^c	81.0	4.7	79.0	8.1	70.0	19.5	61.0	32.2	65	7.1
(48)										
Ph ₂ SnL ^c ₂	80.0	5.9	68.0	20.9	73.0	16.1	74.0	17.8	68	2.8
Clotrimazole	60	29.4	52	39.5	51	41.4	48	46.7	44	37.1

^a Concentration: 200 µg/mL of DMSO.

Table 3.27: Antifungal activity^a of organotin(IV) derivatives of 4-benzylpiperidine-1-carbodithioate.

Sample	Tested Fungi									
	<i>Aspergillus nigar</i>		<i>Aspergillus flavus</i>		<i>Helminthosporium solani</i>		<i>Alternaria solani</i>		<i>Fusarium sp.</i>	
	Linear growth	% inhibition	Linear growth	% inhibition	Linear growth	% inhibition	Linear growth	% inhibition	Linear growth	% inhibition
Control	85		86		87		90		70	
L ^d	48.0	43.5	63.0	26.7	76.0	12.6	74.0	17.8	56	20
(49)										
n-Bu ₃ SnL ^d	50.0	41.2	65.0	24.4	80.0	8.0	84.0	6.7	70	0
(50)										
Cy ₃ SnL ^d	78.0	8.2	73.0	15.1	80.0	8.0	76.0	15.6	70	0
(51)										
Me ₃ SnL ^d	80.0	5.9	78.0	9.3	81.0	6.9	76.0	15.6	70	0
(52)										
Ph ₃ SnL ^d	68.0	20.0	66.0	23.3	70.0	19.5	68.0	24.4	60	14.2
(53)										
n-Bu ₂ SnCIL ^d	72.0	15.3	73.0	15.1	61.0	29.9	66.0	26.7	56	20
(54)										
n-Bu ₂ SnL ₂ ^d	66.0	22.4	80.0	7.0	73.0	16.1	70.0	22.2	63	10
(55)										
Et ₂ SnCIL ^d	72.0	15.3	74.0	14.0	78.0	10.3	68.0	24.4	63	10
(56)										
Et ₂ SnL ₂ ^d	80.0	5.9	78.0	9.3	68.0	21.8	64.0	28.9	61	12.8
(57)										
Me ₂ SnCIL ^c	66.0	22.4	69.0	19.8	73.0	16.1	66.0	26.7	60	14.2
(58)										
Me ₂ SnL ₂ ^d	76.0	10.6	76.0	11.6	80.0	8.0	73.0	18.9	70	0
(59)										
Ph ₂ SnCIL ^d	60.0	29.4	66.0	23.3	72.0	17.2	80.0	11.1	45	35.7
(60)										
Ph ₂ SnL ₂ ^d	82.0	3.5	83.0	3.5	80.0	8.0	78.0	13.3	70	0
Clotrimazole	60	29.4	52	39.5	51	41.4	48	46.7	44	37.1

^a Concentration: 200 µg/mL of DMSO.

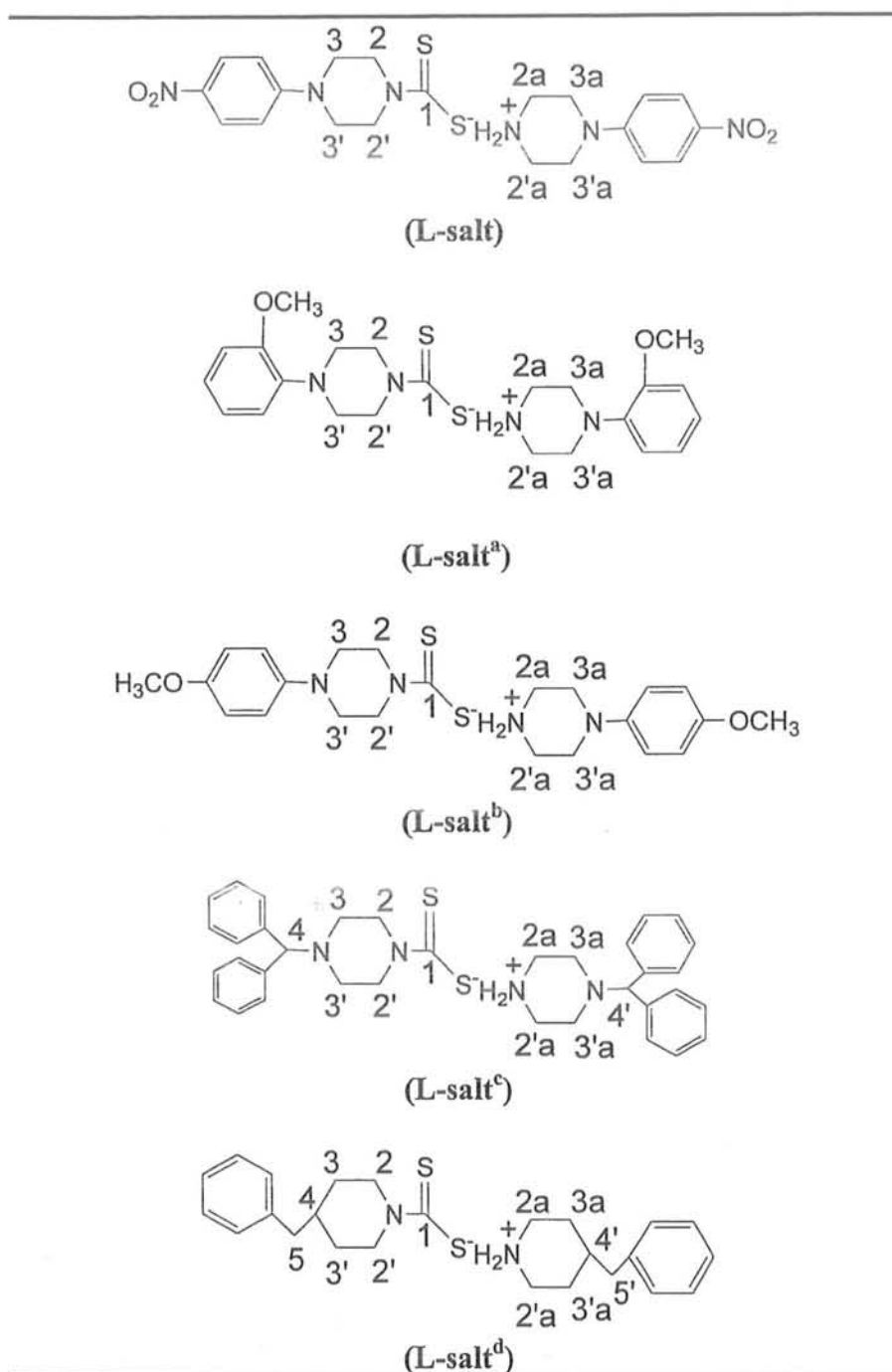


Fig. 3.22: Numbering scheme for ^1H and ^{13}C -NMR of ligands

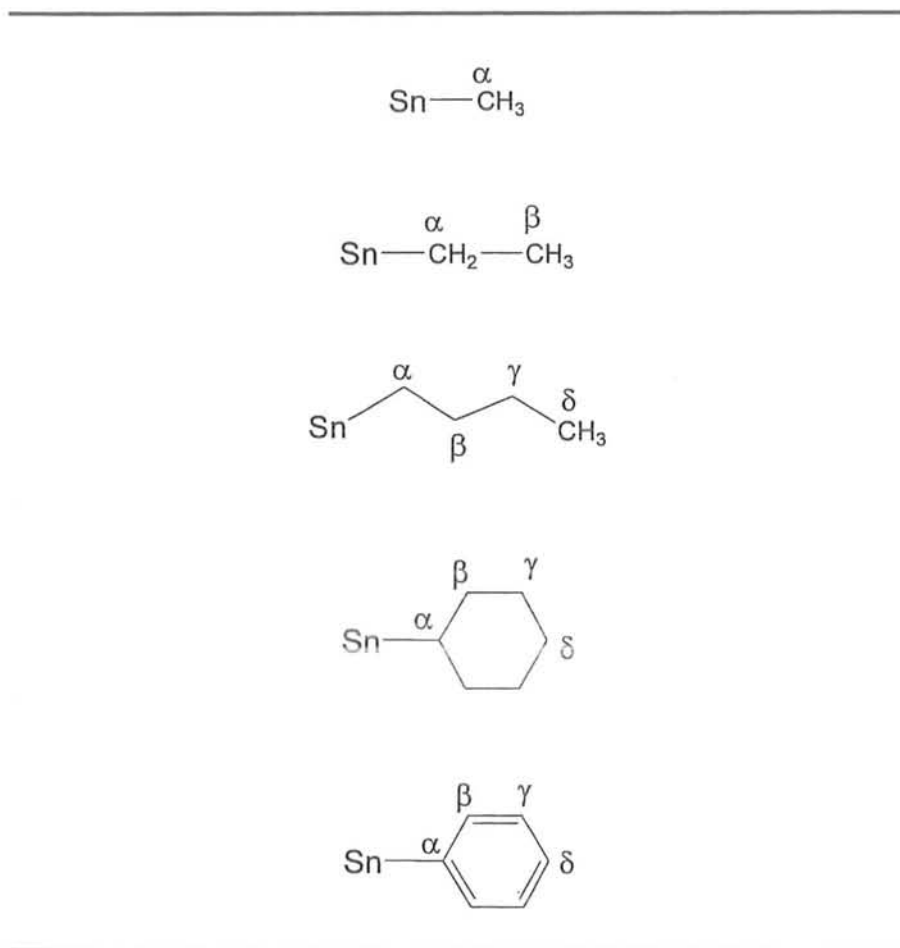


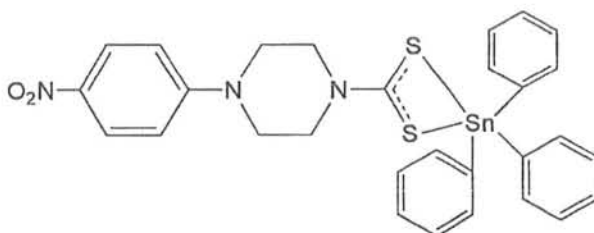
Fig. 3.23: Numbering scheme of organic moiety attached to Sn atom.

References

-
- [1] J. S. Casas, A. Castiñeiras, F. Condori, M. D. Couce, U. Russo, A. Sánchez, J. Sorodo, J. M. Varela, *Eur. J. Inorg. Chem.* (2003) 2790.
- [2] H. S. Randhawa, W. Walter, *J. Raman Spectroscopy*, 11 (1981) 138.
- [3] O. Jung, Y. S. Sohn, J. A. Ibers, *Inorg. Chem.* 25 (1986) 2273.
- [4] H. D. Yin, S. C. Xue, *Appl. Organometal. Chem.* 20 (2006) 283.
- [5] M. H. Bhatti, S. Ali, H. Masood, M. Mazhar, S. I. Qureshi, *Synth. React. Inorg. Met.-Org. Chem.* 30 (2000) 1715.
- [6] S. Ali, F. Ahmad, M. Mazhar, A. Munir, M. T. Masood, *Synth. React. Inorg. Met.-Org. Chem.* 32 (2001) 357.
- [7] I. Din, K. C. Molloy, M. Mazhar, S. Dastgir, S. Ali, M. F. Mahon, *Appl. Organomet. Chem.* 17 (2003) 781.
- [8] S. Shahzadi, S. Ali, K. Wurst, M. N. Haq, *Heteroatom Chem.* 18 (2007) 664, and refs. therein.
- [9] S. Shahzadi, M. H. Bhatti, K. Shahid, S. Ali, S. R. Tariq, M. Mazhar, K. M. Khan, *Monatsh. Chemie*, 133 (2002) 1089.
- [10] F. Ahmad, S. Ali, M. Parvez, A. Munir, M. Mazhar, T. A. Shah, *Heteroatom Chem.* 13 (2002) 638.
- [11] M. Danish, S. Ali, M. Mazhar, A. Badshah, M. I. Choudhary, H. G. Alt, G. Kehr, *Polyhedron*, 14 (1995) 3115.
- [12] K. Shahid, S. Ali, S. Shahzadi, A. Badshah, K. M. Khan, G. M. Maharvi, *Synth. React. Inorg. Met.-Org. Chem.* 33 (2003) 1221.
- [13] A. Lycka, M. Nadvornik, K. Handlir, J. Holecek, *Collect. Czech. Chem. Commun.* 49 (1984) 2903.
- [14] T. S. B. Baul, S. Dhar, S. M. Pyke, E. R. T. Tiekink, E. Rivarola, R. Butcher, F. E. Smith, *J. Organomet. Chem.* 633 (2001) 7.
- [15] T. P. Lockhart, W. F. Manders and E. M. Holts, *J. Am. Chem. Soc.*, 108 (1986) 6611.
- [16] A. Tarassoli, T. Sedaghat, B. Neumüller, M. Ghassemzadeh, *Inorg. Chim. Acta* 318 (2001) 15-22.
- [17] P.G. Harrison, in P.G. Harrison (Ed.), *Chemistry of Tin*, Blackie Academic and Professional, London, 1st Edn., (1989) p. 105.

- [18] I. Wharf, G. Cerone, Y. Luo, W. Yan, J.M. Miller, *Main Group Metal Chem.* 27 (2004) 91, and refs. therein.
- [19] D. C. Menezes, F. T. Vieira, G. M. de Lima, J. L. Wardell, M. E. Cortés, M. P. Ferreira, M. A. Soares, A. V. Boas, *Appl. Organomet. Chem.* 22 (2008) 221.
- [20] J. E. B. Randles, *Trans Faraday Soc.* 44 (1948) 327.
- [21] A. Sevcik, *Collect. Czech Chem. Commun.* 13 (1948) 349.
- [22] S. Wang, T. Penz, C. F. Yang, *Biophys. Chem.* 104 (2003) 239.
- [23] G.C. Zhao, J. J. Zhu, J. J. Zhang, H.Y. Chen, *Anal. Chim. Acta.* 394 (1999) 337.
- [24] V. G. Vaidynathan and B. U. Nair, *J. Inorg. Biochem.* 95 (2003) 334.
- [25] Q. Lie, P. Yang, H. Wang, M. Guo, *J. Inorg. Biochem.* 64 (1996) 181.
- [26] E. C. Long, J. K. Barton, *Acc. Chem. Res.* 23 (1990) 271.
- [27] R. Fukuda, S. Takenaka, M. Takagi. *J. Chem. Soc. Chem. Commun.* (1990) 1028.
- [28] M. S. Ibrahim, I. S. Shehatta, A. A. Al-Nayeli, *J. Pharm. Biomed. Anal.* 28 (2002) 217.
- [29] X. Jiang, X. Lin, *Bioelectrochemistry*, 68 (2006) 206-212.
- [30] A. Shah, A. M. Khan, R. Qureshi, F. L. Ansari, M. F. Nazar and S. S. Shah *Int. J. Mol. Sci.* 9 (2008) 1424.
- [31] E. Niranjana, R. R. Naik, B. E. K. Swamy, Y. D. Bodke, B. S. Sherigara, H. Jayadevappa, B. V. Badami, *Int. J. Electrochem. Sci.*, 3 (2008) 980.
- [32] R. J. Klinger, J. K Kochi, *J. Phy. Chem.* 85, (1981) 12.
- [33] Q. Feng, N. Q. Li, Y.Y. Jiang, *Anal. Chim. Acta* 344 (1997) 97.
- [34] J. Rusanova, S. Decurtins, E. Rosanov, H.S. Evans, S. Delahaye, A. Hauser, J. Chem. Soc. Dalton. Trans. (2002) 4318.
- [35] A. Ambroise, B. G. Maiya, *Inorg. Chem.* 39 (2000) 4264.
- [36] M. T. Carter, M. Rodriguez, A. J. Bard, *J. Am. Chem. Soc.* 111 (1989) 8901.
- [37] M. Aslanoglu, C.J. Isaac, A. Houlton, B.R. Horrocks, *Analyst.* 125 (2000) 1791.
- [38] G. J. Yang, J. J. Xu, H. Y. Chen, Z. Z. Leng, *Chinese J. Chem.* 22 (2004) 1325
- [39] L. Z. Zhang, G. Q. Tang, *J. Photochem. and Photobiol B: Biology* 74 (2004) 119.
- [40] A. Rahman, M. I. Choudhry, W. J. Thomson, *Bioassay Techniques for Drug Development*, Harvard Academic Press, Amsterdam (2001) *pp.* 14-20.
- [41] S. S. Shaukat, N. A. Khan, F. Ahmad, *Pak. J. Bot.* 12 (1980) 97.

CRYSTALLOGRAPHIC ANALYSIS

4.1 X-ray structure of Ph_3SnL (4)

The molecular structure of compound (4) is depicted in Fig. 4.1, while crystal data and selected bond lengths and bond angles are given in Tables 4.1 and 4.2, respectively. The geometry around the Sn atom is distorted trigonal-bipyramidal, the equatorial plane being defined by the two α -carbons of the phenyl groups and a sulfur atom of the dithiocarboxylate ligand. According to Addison et al., the geometry around the Sn atom can be characterized by the value of $\tau = (\beta - \alpha)/60$ [1], where β is the largest of the basal angles around the Sn atom. For compound 4 it is $\text{S1-Sn-C24} = 152.35^\circ$. The second largest of the basal angles around the Sn atom, α for compound 4 is $\text{S2-Sn-C18} = 118.29^\circ$. The angle values $\alpha = \beta = 180^\circ$ corresponds to a square-pyramidal geometry, and the value of $\alpha = 120^\circ$ correspond to perfectly trigonal-bipyramidal geometry. Thus, the τ value is equal to zero for a perfect square-pyramidal and unity for a perfect trigonal-bipyramidal [1, 2]. The calculated τ value for the complex is 0.57. The value indicates a highly distorted trigonal-bipyramidal arrangement around Sn atom with C24 from a phenyl group and the S1 from the dithiocarboxylate at the axial positions while C12 and C18 from two phenyl groups and S2 in the plane positions. The sum of the equatorial angles, [$\text{S2-Sn-C12} = 108.73(13)^\circ$, $\text{S2-Sn-C18} = 118.29$ and $\text{C12-Sn-C18} = 115.57(11)^\circ$], is 342.59° instead of the ideal 360° . Being a part of chelate, the angle S2-Sn-S1 is not 90° but only 62.27° , so the S1 cannot occupy exactly the corresponding *trans* apical position of C24 and the angle between the apical groups is 152.35° . The axial Sn-C bond length [$\text{Sn-C24} = 2.151(5) \text{ \AA}$] is very similar to equatorial ones [$\text{Sn-C18} = 2.135(5) \text{ \AA}$] and is in agreement with Sn-C values reported for $\text{Ph}_3\text{SnS}_2\text{CN}(\text{CH}_3)(\text{C}_4\text{H}_9)$ [3]. Finally, the C-

S bond lengths are characteristic of the 1,1-dithioate moiety and are intermediate between the values reported for single and double bonds [4].

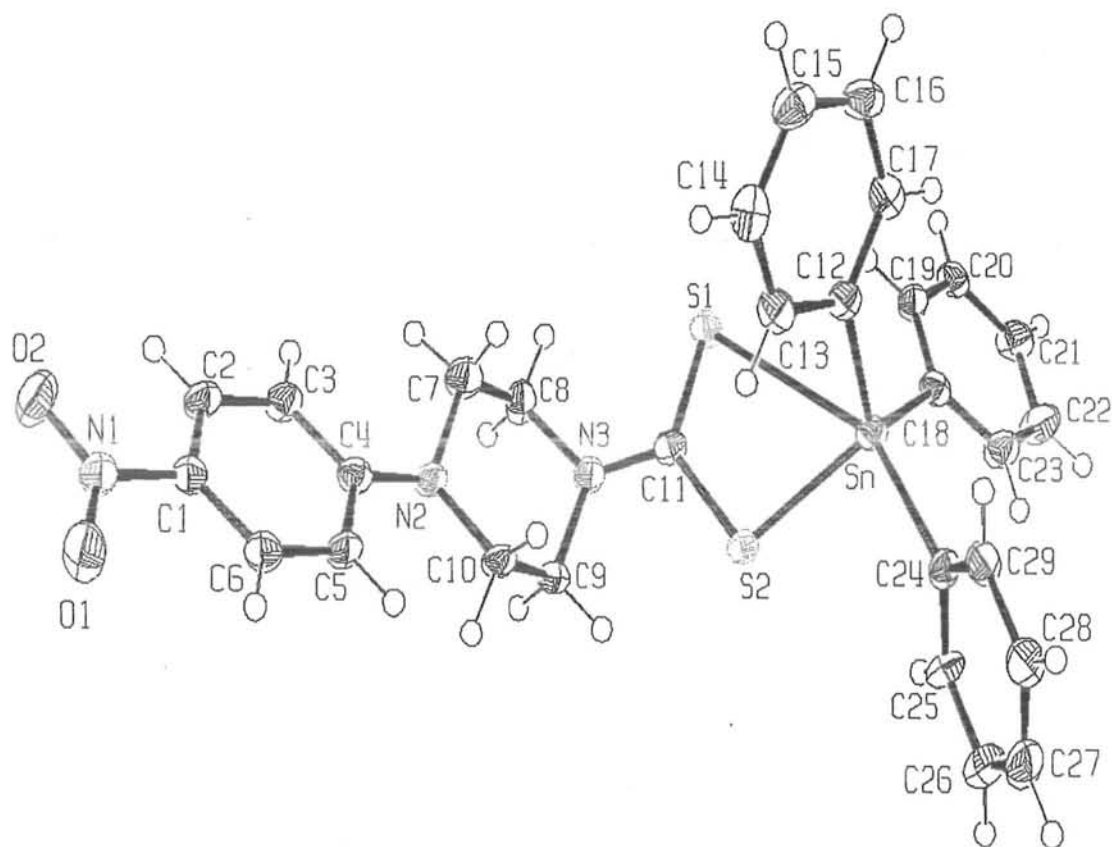


Fig 4.1: ORTEP drawing of Ph_3SnL (4) with atomic numbering scheme

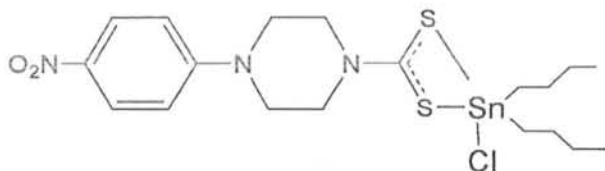
Table 4.1: Crystal data and structure refinement parameters for Ph₃SnL (4)

Empirical formula	C ₂₉ H ₂₇ N ₃ O ₂ S ₂ Sn
Formula mass	632.39
Crystal system	Triclinic
Space group, no.	<i>P</i> -1, 2
<i>a</i> (Å)	9.546(2)
<i>b</i> (Å)	10.986(2)
<i>c</i> (Å)	13.650(3)
α (°)	91.966(3)
β (°)	98.752(3)
γ (°)	107.833(3)
<i>V</i> (Å ³)	1341.9(5)
<i>Z</i> (<i>Z'</i>)	2 (1)
Crystal habit/size (mm)	Block/0.55 x 0.33 x 0.24
<i>T</i> (K)	100(1)
$\mu(\text{Mo K}\alpha^-)$ (cm ⁻¹)	11.4
Total reflections	11783
Independent reflections	6288
All	
For $F_o \geq 4.0 \sigma(F_o)$	5541
$R(F) = \sum (F_o - F_c) / \sum F_o $	0.0388
For $F_o > 4.0 \sigma(F_o)$	
$wR(F^2) = [\sum [w(F_o^2 - F_c^2)^2] / \sum [w(F_o^2)^2]]^{1/2}$	0.1195
Goodness-of-fit	1.239
θ range for data collections (°)	2.51-28.28
Data/restraints/parameters	6288/0/334

Table 4.2: Selected bond lengths (Å) and bond angles (°) for Ph₃SnL (4)

Sn-S2	2.4419(14)	Sn-C24	2.151(5)
Sn-C12	2.114(5)	S-C11	1.674(5)
Sn-C18	2.135(5)	S2 –C11	1.760(4)
Sn-S1	3.179		
S2-Sn-C12	108.73(13)	S1-Sn-C12	77.54
S2-Sn-C18	118.29(11)	S1-Sn-C18	87.53
S2-Sn-C24	90.15(12)	S1-Sn-C24	152.35
C12-Sn-C18	115.57(18)	S1-Sn-S2	62.27
C12-Sn-C24	112.44(18)	S1-Sn-C24	152.35
C18-Sn-C24	108.96(18)	S1-C11-S2	120.0(3)
Sn-C12-C13	120.3(4)	Sn-C12-C17	120.3(4)
Sn-C18-C19	123.0(3)	Sn-C18-C23	118.7(4)
Sn-C24-C25	119.6(3)	Sn-C24-C29	121.2(4)
Sn-S2-C11	99.33(15)	Sn-S1-C11	76.65

4.2 X-ray structure of n-Bu₂SnCIL (5)



A stereoview of the molecules and atomic numbering scheme are shown in Fig. 4.2, while crystal data and selected bond lengths and bond angles are given in Tables 4.3 and 4.4, respectively. The configuration about the Sn atom is five-coordinate, but distorted trigonal-bipyramidal with atoms S11, C112 and C116 occupying equatorial positions for molecule 1, and S22, C212 and C216 for molecule 2. The sums of the ligand-Sn-ligand angles in the trigonal girdle of the molecules are 359.47° and 358.70°, respectively. The Sn atoms show no large deviations from the equatorial planes, viz. 0.0935(1) and 0.1468(1) Å, respectively. The distortion is also illustrated by the τ descriptor for five-coordination: 0.46 and 0.45 [1] for ideal trigonal-pyramidal coordination τ is 1. Atoms Cl1 and Cl2 each occupy one of the axial positions of the trigonal-bipyramid. As a result of being part of the chelate ring the S11-Sn1-S12 and S21-Sn2-S22 angles are not 90° but only 69.13(2)° and 68.94 (2)°, so atoms S12 and S22 do not occupy exactly the corresponding *trans* axial positions to Cl1 and Cl2. The Cl1-Sn1-S12 angle is 155.67(2)° and Cl2-Sn2-S21 is 155.11(2)°. The Sn1-S12 and Sn2-S21 bonds are markedly elongated [2.7088(5) Å and 2.7315(5) Å], compared with the Sn1-S11 and Sn2-S22 bonds [2.4690(5) and 2.4720(7) Å]. This indicates that the dithiocarboxylate coordination is unsymmetrical.

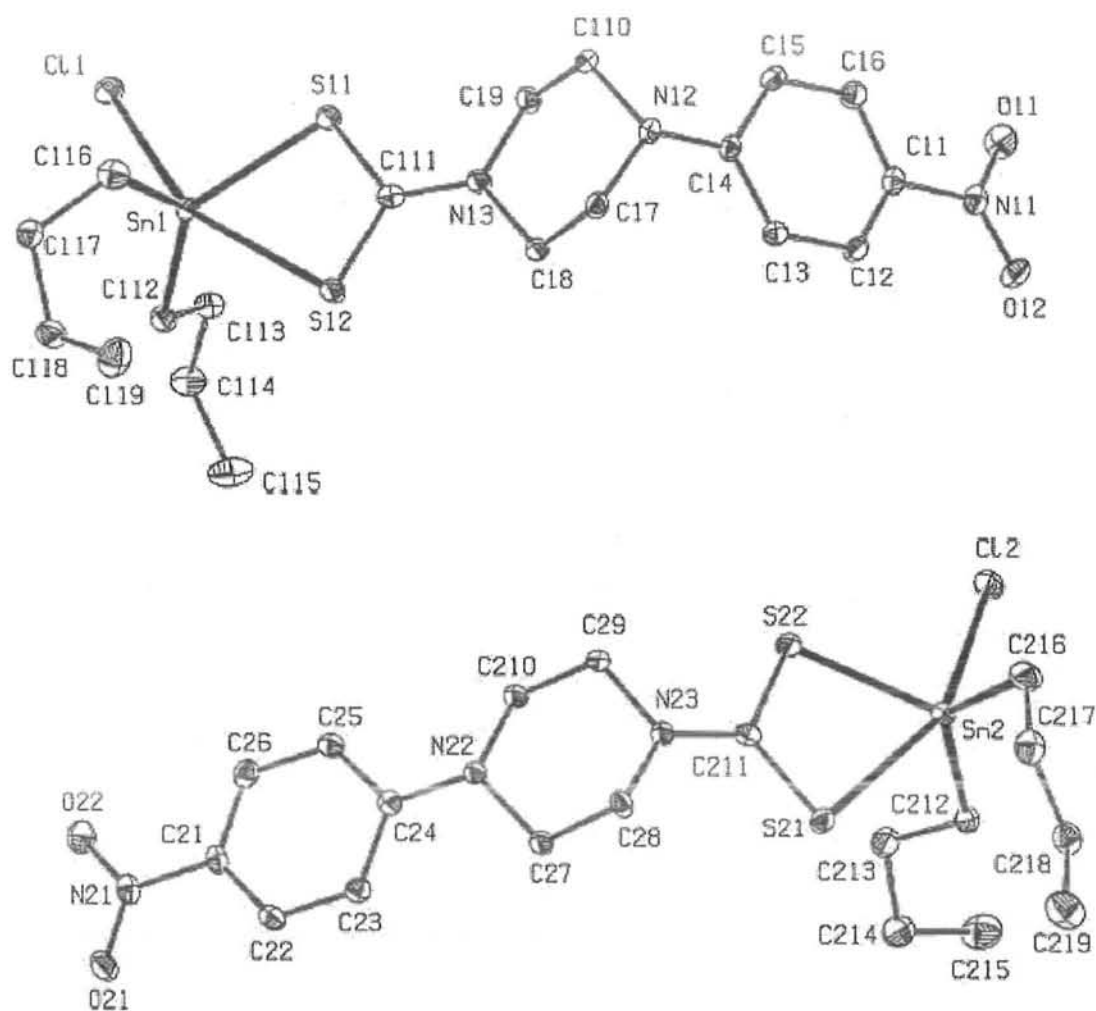


Fig. 4.2: The ORTEP drawing of molecule 1 (top) and molecule 2 (lower) of the $n\text{-Bu}_2\text{SnCIL}$ (5). Displacement ellipsoids for non-H atoms are drawn at the 50% probability level. H atoms have been omitted to improve clarity.

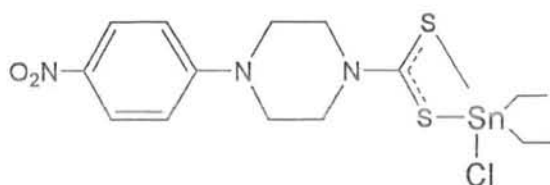
Table 4.3: Crystal data and structure refinement parameters for n-Bu₂SnCIL (5)

Empirical formula	C ₁₉ H ₃₀ N ₃ O ₂ S ₂ SnCl
Formula mass	550.76
Crystal system	Triclinic
Space group, no.	P-1, 2
<i>a</i> (Å)	9.7151(7)
<i>b</i> (Å)	14.978(1)
<i>c</i> (Å)	16.152(1)
α (°)	76.553(1)
β (°)	88.464(1)
γ (°)	87.508 (1)
<i>V</i> (Å ³)	2283.4(3)
<i>Z</i> (<i>Z'</i>)	2 (2)
Crystal habit/size (mm)	Block/0.51 x 0.21 x 0.18
<i>T</i> (K)	100(1)
$\mu(\text{Mo K}\alpha^-)$ (cm ⁻¹)	14.39
Total reflections	21022
Independent reflections	10881
All	
For $F_o \geq 4.0 \sigma(F_o)$	9782
$R(F) = \sum (F_o - F_c) / \sum F_o $	0.0255
For $F_o > 4.0 \sigma(F_o)$	
$wR(F^2) = [\sum [w(F_o^2 - F_c^2)^2] / \sum [w(F_o^2)^2]]^{1/2}$	0.0593
Goodness-of-fit	1.048
θ range for data collections (°)	2.57-28.28
Data/restraints/parameters	10881/0/745

Table 4.4: Selected bond lengths (Å) and bond angles (°) for n-Bu₂SnCIL (5)

	x = 1	x = 2		x = 1	x = 2
Snx-Clx	2.4976(5)	2.4886(6)	Snx-Sx1	2.4690(5)	2.7315(5)
Snx-Sx2	2.7088(5)	2.4720(5)	Snx-Cx12	2.135(2)	2.129(2)
Snx-Cx16	2.137(5)	2.150(3)	Sx1-Cx11	1.744(2)	1.704(2)
Sx2-Cx11	1.708(2)	1.748(2)			
Clx-Snx-Sx1	86.64(2)	155.11(2)	Clx-Snx-Sx2	155.67(2)	86.40(2)
Clx-Snx-Cx12	95.63(5)	97.45(5)	Clx-Snx-Cx16	94.16(6)	96.37(7)
Sx1-Snx-Sx2	69.13(2)	68.94(2)	Sx1-Snx-Cx12	118.58(5)	91.07(6)
Sx1-Snx-Cx16	112.77(6)	96.53(7)	Sx2-Snx-Cx12	94.20(6)	117.11(6)
Sx2-Snx-Cx16	97.16(6)	113.24(7)	Cx12-Snx-Cx16	128.12(8)	128.35(9)
Snx-Sx1-Cx11	90.35(7)	82.97(7)	Snx-Sx2-Cx11	83.38(7)	90.38(7)
Sx1-Cx11-Sx2	117.03(11)	117.61(11)	Snx-Cx12-Cx13	112.70(13)	114.58(14)
Snx-Cx16-Cx17	113.36(14)	114.72(15)			

4.3 X-Ray Structure of Et₂SnCIL (7)



The molecular structure of compound 7 is given in Fig. 4.3, while crystal data and selected bond lengths and bond angles are reported in Tables 4.5 and 4.6, respectively. As in a similar compound in the literature [5], the Sn atom is five-coordinate. The geometry of the complex 7 is approximately trigonal-bipyramidal, with atoms C12, S1 and C14 occupying the equatorial positions. The sum of the equatorial angles (359.27°) at the tin atom involving the two coordinated C atoms and one S atom [$S1-Sn-C12 = 119.25(6)^\circ$, $S1-Sn-C14 = 116.36(7)^\circ$ and $C12-Sn-C14 = 123.66(9)^\circ$] deviates by only 0.7° from 360° , so atoms C12, S1, C14 and Sn are approximately coplanar; the Sn atom is displaced by $0.111(1) \text{ \AA}$ from the least-squares plane formed by S1, C12 and C14, and is on the same side as Cl. The Cl atom occupies approximately one axial position of the trigonal-bipyramid; the angle between the Sn-Cl bond and the equatorial plane is $83.66(9)^\circ$. Conversely, because of the constraint of the chelate [the $S1-Sn-S2$ angle is only $69.59(2)^\circ$, the angle between the Sn-S2 bond and the equatorial plane is $72.10(9)^\circ$]; atom S2 cannot exactly occupy the second *trans* axial position of the trigonal-bipyramid, the angle Cl-Sn-S2 being $156.58(2)^\circ$. The S-C bond lengths [$S1-C11 = 1.752(3) \text{ \AA}$ and $S2-C11 = 1.716(2) \text{ \AA}$] appear to be characteristic of the dithiocarboxylate group and these distances are all intermediate between the values expected for single and double bonds [6].

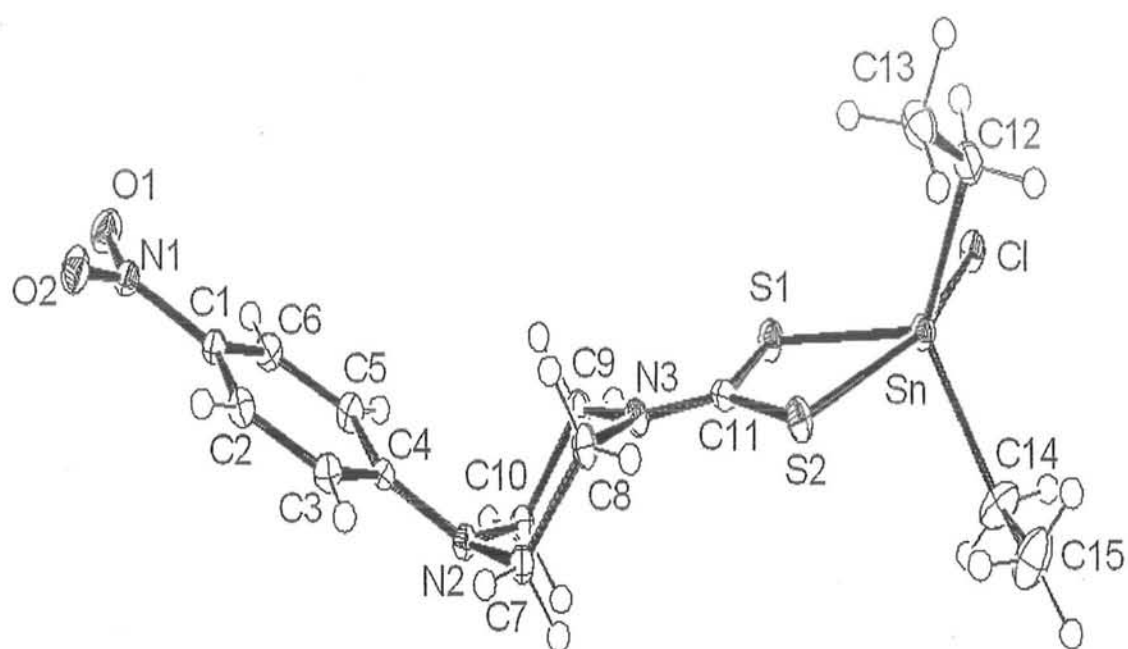


Fig 4.3: ORTEP drawing of Et₂SnCIL (7) with atomic numbering scheme

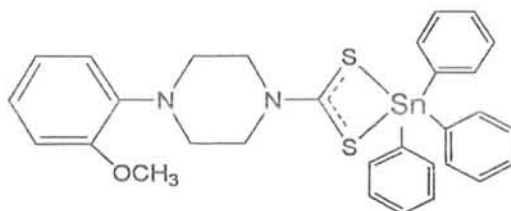
Table 4.5: Crystal data and structure refinement parameters for Et₂SnCIL (7)

Empirical formula	C ₁₅ H ₂₂ N ₃ O ₂ S ₂ SnCl
Formula mass	494.65
Crystal system	Monoclinic
Space group, no.	<i>P</i> 2 ₁ /c, 14
<i>a</i> (Å)	14.1638(9)
<i>b</i> (Å)	10.5851(7)
<i>c</i> (Å)	14.0247(9)
β (°)	115.799(1)
<i>V</i> (Å ³)	1893.1(2)
<i>Z</i> (<i>Z'</i>)	4 (1)
Crystal habit/size (mm)	Triangle block/0.49 x 0.42 x 0.35
<i>T</i> (K)	100(1)
μ(Mo Kα) (cm ⁻¹)	17.25
Total reflections	16982
Independent reflections	4661
All	
For <i>F_o</i> ≥ 4.0 σ (<i>F_o</i>)	4332
$R(F) = \sum (F_o - F_c) / \sum F_o $	0.0243
For <i>F_o</i> > 4.0 σ (<i>F_o</i>)	
$wR(F^2) = [\sum [w(F_o^2 - F_c^2)^2] / \sum [w(F_o^2)^2]]^{1/2}$	0.0618
Goodness-of-fit	1.072
θ range for data collections (°)	2.51-28.28
Data/restraints/parameters	4661/0/305

Table 4.6: Selected bond lengths (Å) and bond angles (°) for Et₂SnCIL (7)

Sn-Cl	2.5243(7)	Sn-S1	2.4758(6)
Sn-S2	2.6959(6)	Sn-C12	2.146(2)
Sn-C14	2.136(3)	S1-C11	1.752(3)
S2-C11	1.716(2)		
Cl-Sn-S1	87.03(2)	Cl-Sn-S2	156.58(2)
Cl-Sn-C12	92.99(8)	Cl-Sn-C14	98.21(8)
S1-Sn-S2	69.59(2)	S1-Sn-C12	119.25(6)
S1-Sn-C14	116.36(7)	S2-Sn-C12	97.14(8)
S2-Sn-C14	93.65(8)	C12-Sn-C14	123.66(9)
Sn-S1-C11	89.82(7)	Sn-S2-C11	83.54(8)
S1-C11-S2	117.04(12)	Sn-C12-C13	118.10(17)
Sn-C14-C15	114.2(2)		

4.4 X-Ray Structure of $\text{Ph}_3\text{SnL}^{\text{a}}$ (**16**)



The crystal data and selected interatomic parameters are collected in Tables 4.7 and 4.8, respectively. The ORTEP diagram for **16** together with an example of the atomic numbering scheme used here is depicted in Fig. 4.4. In crystal structure, Sn atom is coordinated to two sulfur atoms of the dithiocarboxylate ligand and three α -carbon atoms of the phenyl groups. The 1,1-dithioate moiety is coordinated asymmetrically to Sn, with shorter Sn-S1 [2.4747(16) Å] bond and long Sn-S2 [3.0737(17) Å] bond. The difference between the two Sn-S bonds is 0.599 Å. The shorter bond length is closed to the sum of the covalent radii of Sn and S (2.42 Å) and long Sn-S bond length is much shorter than the sum of the van der Waal's radii (4.0 Å) of two atoms. In this way, the ligand coordinated in anisobidentate manner and chelated the Sn atom by its two S atoms, giving *cis*-trigonal-bipyramidal geometry around the Sn atom. The geometry around the Sn atom can be characterized by the value of $\tau = (\beta - \alpha)/60$, where β is the largest of the basal angles around the Sn atom. The calculate τ value for compound **16** is 0.59. The value indicates highly distorted trigonal-bipyramidal geometry around Sn atom with C13 of a phenyl group and the S2 of the ligand moiety at the axial positions while C19A and C25A of the two phenyl groups and S1 at the plane positions. The sum of the equatorial angles involving the two α -carbons of the phenyl groups and a S atom, 1: 343.9°, as well shows a mark deviation from the ideal angle of 360°. The C13 atom occupies one of the apical positions of the trigonal-bipyramidal with the S1-Sn-C13 angle of 91.8(2)°. As a result 4-(2-methoxyphenyl)piperazine-1-carbodithioate being a chelating ligand with the small bite forming a four-membered ring, S1-Sn-S2 angle is not 90°, but only 63.84(5)°. Therefore, the S2 atom cannot occupy exactly the corresponding *trans* axial position to C13 and C13-Sn-S2 angle is 155.6(2)°. The S-C bond lengths [S1-C1 = 1.760(6) Å and S2-C12 = 1.693(6) Å] also show the asymmetric nature of the dithiocarboxylate group.

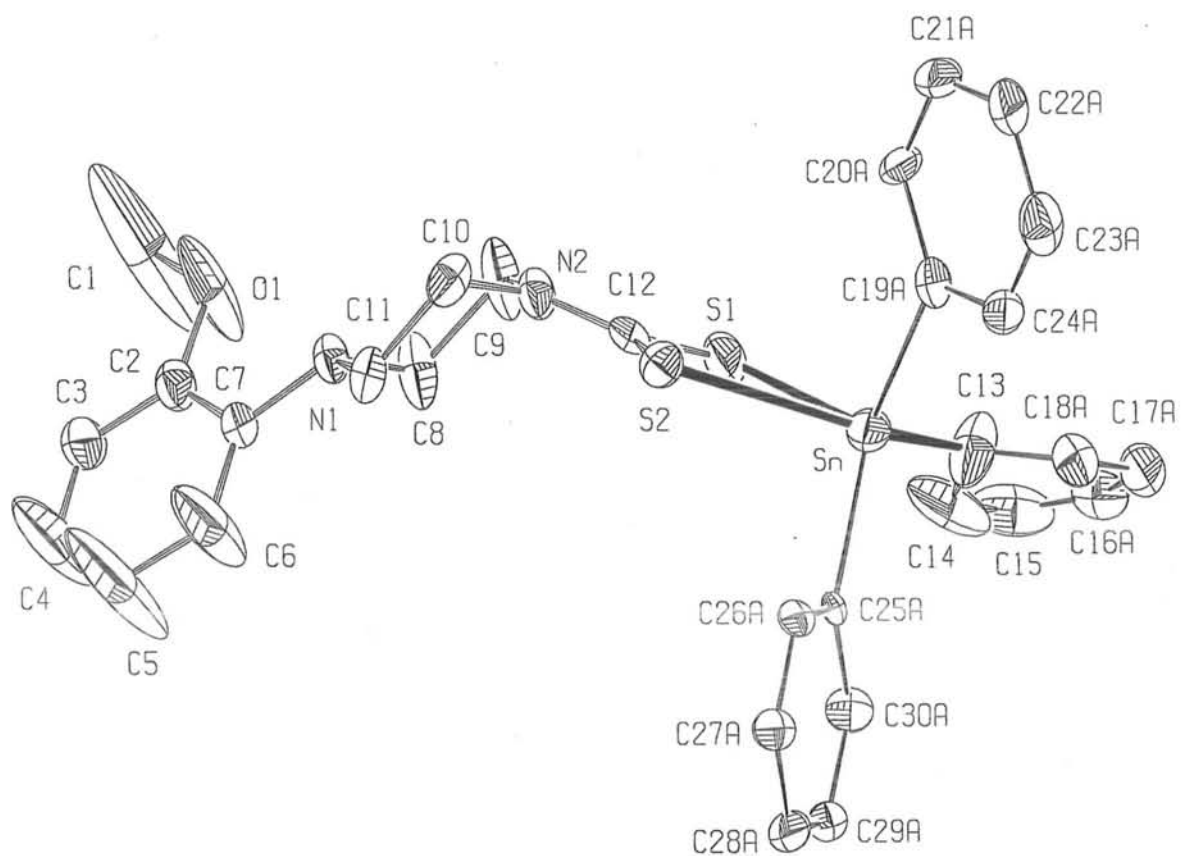


Fig 4.4: ORTEP drawing of Ph_3SnL^a (16) with atomic numbering scheme

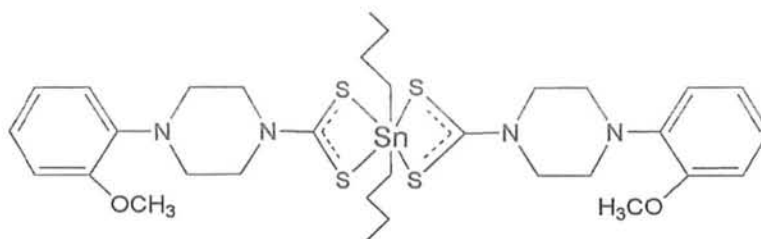
Table 4.7: Crystal data and structure refinement parameters for Ph₃SnL^a (16)

Empirical formula	C ₃₀ H ₃₀ N ₂ OS ₂ Sn
Formula mass	617.42
Crystal system	Triclinic
Space group, no.	<i>P</i> -1, 2
<i>a</i> (Å)	9.2973(8)
<i>b</i> (Å)	11.9648(10)
<i>c</i> (Å)	13.5149(11)
α (°)	88.9179(13)
β (°)	77.7142(13)
γ (°)	70.3200(13)
<i>V</i> (Å ³)	1380.9(2)
<i>Z</i> (<i>Z'</i>)	2 (1)
Crystal habit/size (mm)	Polyhedral/ 0.30 x 0.27 x 0.23
<i>T</i> (K)	100(1)
$\mu(\text{Mo K}\alpha^-)$ (cm ⁻¹)	11.02
Total reflections	10486
Independent reflections	5292
All	
For $F_o \geq 4.0 \sigma(F_o)$	4449
$R(F) = \sum (F_o - F_c) / \sum F_o $	0.0604
For $F_o > 4.0 \sigma(F_o)$	
$wR(F^2) = [\sum [w(F_o^2 - F_c^2)^2] / \sum [w(F_o^2)^2]]^{1/2}$	0.1359
Goodness-of-fit	1.047
θ range for data collections (°)	2.54-26.02
Data/restraints/parameters	5292/0/417

Table 4.8: Selected bond lengths (Å) and bond angles (°) for Ph₃SnL^a (16)

Sn-S1	2.4747(16)	Sn-S2	3.0737(17)
Sn-C13	2.164(9)	Sn-C19A	2.128(9)
Sn-C25A	2.316(8)	S1-C12	1.760(6)
S2-C12	1.693(6)		
S1-Sn-S2	63.84(5)	S1-Sn-C13	91.8(2)
S1-Sn-C19A	109.9(2)	S1-Sn-C25A	114.1(2)
S2-Sn-C13	155.6(2)	S2-Sn-C19A	85.4(3)
S2-Sn-C25A	79.51(19)	C13-Sn-C19A	103.4(4)
C13-Sn-C25A	113.8(4)	Sn-S1-C12	97.68(19)
Sn-S2-C12	79.3(2)	Sn-C13-C18A	114.5(6)
Sn-C19a-C20A	123.7(6)	Sn-C19a-C24A	116.0(7)
Sn-C25a-C26A	125.4(6)	Sn-C25a-C30A	114.6(5)

4.5 X-Ray Structure of $n\text{-Bu}_2\text{SnL}_2$ (**18**)



Relevant bond lengths and bond angles are given in Table 4.10, while Table 4.9 comprise of crystal data. A view of the molecule including numbering scheme is shown in Fig. 4.5. The dithiocarboxylate ligands are coordinated asymmetrically with shorter Sn-S2 [2.5364(9) Å] and Sn-S2_a [2.5364(9) Å] and long Sn-S1 [2.9693(10) Å] and Sn-S1_a [2.9693(10) Å] distances. The long Sn-S distances are significantly less than the sum of the van der Waal's radii (4.0 Å), and the coordination number of Sn is assigned as six. Further, the degree of asymmetry in Sn-S bond distances is same in the two dithiocarboxylate ligands. The overall geometry at Sn is, however, highly distorted from the *trans* octahedral: the C13-Sn-C13_a angle is only 143.37 (11)° which is intermediate between *cis* and *trans*, the Sn and the four S atoms of the ligands are nearly coplanar but distorted from square-planar geometry, so that the *cis* S2-Sn-S2_a angle is only 82.06(3)° and the *cis* S1-Sn-S1_a angle is 148.37(2)°. In both anisobidentate ligands each shorter Sn-S bond is associated with a longer C-S bond and vice versa; this is in consonance with the bonding asymmetry of the ligands. The bond angles subtended at the Sn atom by the methylene carbons and S2 and S2_a atoms range from 101.15(10)° to 106.31(8)° demonstrating that the Sn-C bonds are bent toward the longer Sn-S bonds. This obviously a consequence of repulsion between the bonding electron pairs around the central Sn atom. Electronic and steric arguments have also been invoked to account the distortion of the similar structures from the regular octahedral geometry. Thus, the coordination geometry about the Sn atom, in compound **18**, is best described as being distorted skew trapezoidal-biyrarnidal. The geometry and bond lengths of SnC_2S_4 core are comparable with those usually observed for most of the octahedral complexes [7, 8].

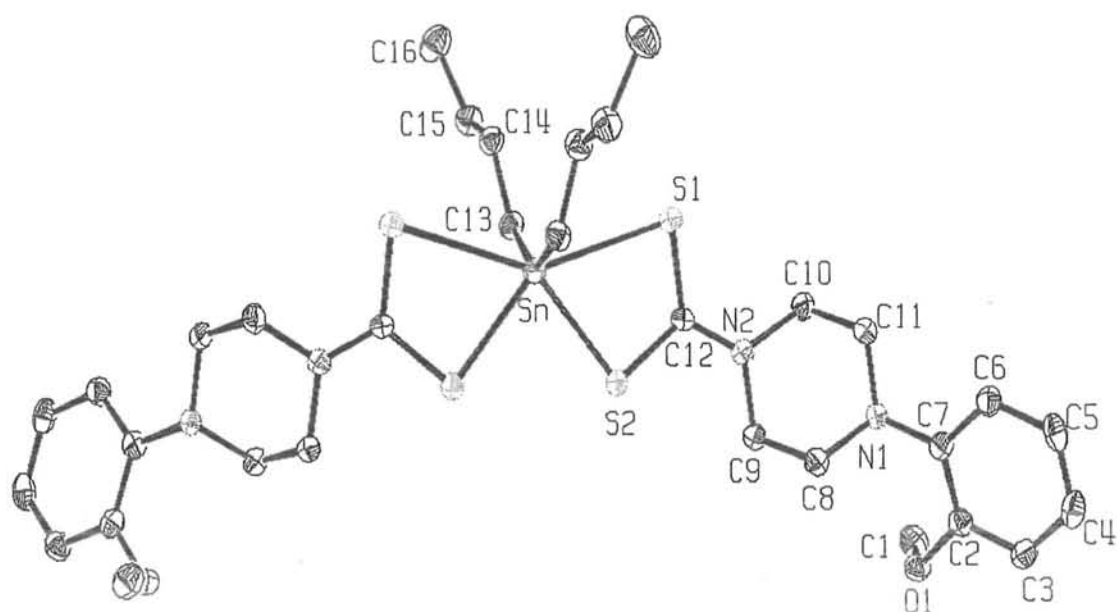


Fig 4.5: ORTEP drawing of $n\text{-Bu}_2\text{SnL}^a_2$ (18) with atomic numbering scheme

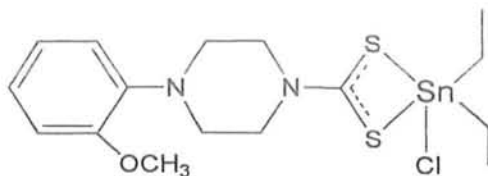
Table 4.9: Crystal data and structure refinement parameters for n-Bu₂SnL^a₂ (18)

Empirical formula	(C ₁₆ H ₂₄ N ₂ OS ₂ S) ₂ Sn
Formula mass	767.73
Crystal system	Monoclinic
Space group, no.	C2/c, 15
<i>a</i> (Å)	30.779(2)
<i>b</i> (Å)	7.0293(4)
<i>c</i> (Å)	22.3630(14)
β (°)	133.0181(8)
<i>V</i> (Å ³)	3537.5(4)
<i>Z</i> (<i>Z'</i>)	4 (0.5)
Crystal habit/size (mm)	Platelet/0.34 x 0.21 x 0.08
<i>T</i> (K)	100(1)
μ(Mo Kα ⁻) (cm ⁻¹)	9.93
Total reflections	14495
Independent reflections	4058
All	
For <i>F_o</i> ≥ 4.0 σ (<i>F_o</i>)	3426
$R(F) = \sum (F_o - F_c) / \sum F_o $	0.0333
For <i>F_o</i> > 4.0 σ (<i>F_o</i>)	
$wR(F^2) = [\sum [w(F_o^2 - F_c^2)^2] / \sum [w(F_o^2)^2]]^{1/2}$	0.0805
Goodness-of-fit	1.045
θ range for data collections (°)	2.49-27.52
Data/restraints/parameters	4058/0/197

Table 4.10: Selected bond lengths (Å) and bond angles (°) for n-Bu₂SnL^a₂ (18)

Sn-S1	2.9693(10)	Sn-S2	2.5364(9)
Sn-C13	2.146(3)	Sn-S1_a	2.9693(10)
Sn-S2_a	2.5364(9)	Sn-C13_a	2.146(3)
S1-C12	1.703(2)	S2-C12	1.738(3)
S1-Sn-S2	64.95(2)	S1-Sn-C13	83.97(10)
S1-Sn-S1_a	148.37(2)	S1-Sn-S2_a	146.57(2)
S1-Sn-C13_a	86.21(10)	S2-Sn-C13	106.31(8)
S2-Sn-S1_a	146.57(2)	S2-Sn-S2_a	82.06(3)
S2-Sn-C13_a	101.15(10)	C13-Sn-S1_a	86.21(10)
C13-Sn-S2_a	101.15(9)	C13-Sn-C13_a	143.37(11)
S1_a-Sn-S2_a	64.95(2)	S1_a-Sn-C13_a	83.97(10)
S2_a-Sn-C13_a	106.31(8)	Sn-S1-C12	80.87(12)
Sn-S2-C12	94.29(9)		

4.6 X-Ray Structure of Et₂SnClL^a (19)



The asymmetric unit of **19** contains three different molecules; The ORTEP diagram for one of these, molecule (1), together with an example of the atom numbering scheme used here is shown in Fig. 4.6, and crystal data and selected interatomic parameters are collected in Tables 4.11 and 4.12, respectively. The configuration about the tin atom is five-coordinate, with distorted trigonal-bipyramidal geometry at the central tin atom. The sums of the equatorial angles involving the two α -carbons of the ethyl groups and a S atom, (1): 360(2)°, (2): 358(2)°, (3): 359(3)°, show little deviation from the ideal angle of 360°. For each molecule, the Cl atom occupies one of the apical positions of the trigonal-bipyramid but the quasi-axial S atom again cannot occupy exactly the position *trans* to Cl. Thus, the dithiocarboxylate groups are asymmetrically coordinated as in the structure of **7**. While there appear to be differences in detail for the geometries around tin for the three different molecules in the 8 asymmetric units of **19**, the less than optimal data set and the large number of constraints used in the structure solution would indicate that more detailed discussion would be premature at this point.

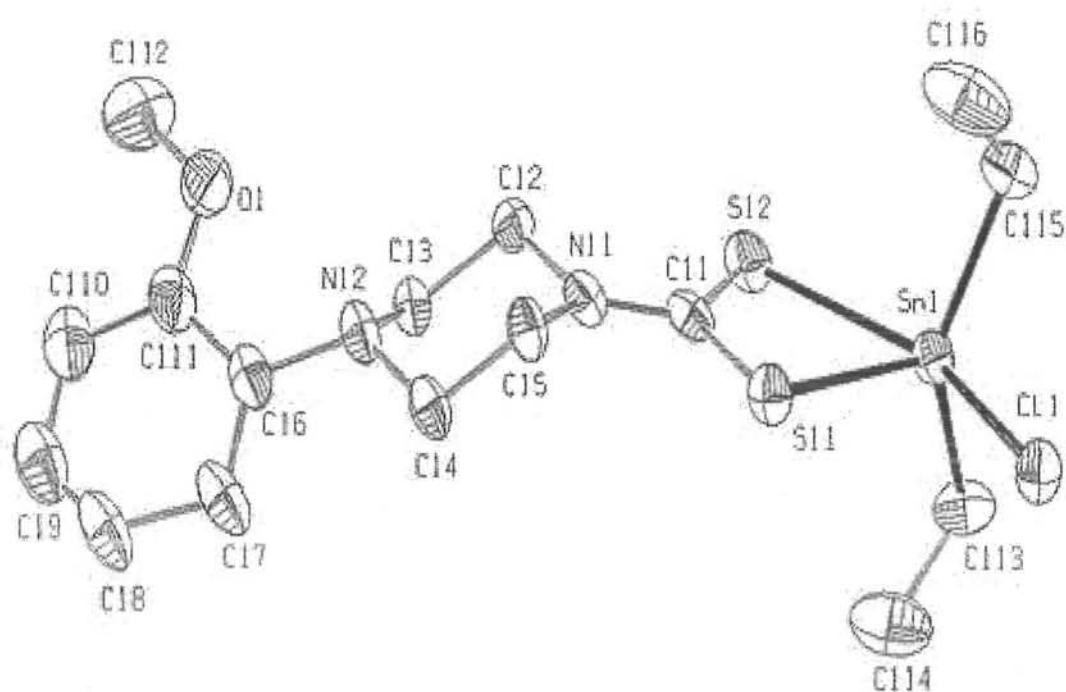


Fig 4.6: ORTEP drawing of one of the three independent molecules of $\text{Et}_2\text{SnCIL}^a(19)$ with atomic numbering scheme

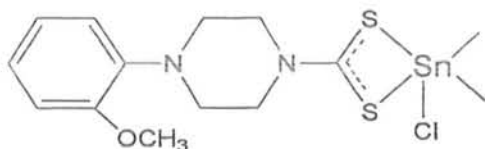
Table 4.11: Crystal data and structure refinement parameters for Et₂SnCIL^a (19)

Empirical formula	C ₁₆ H ₂₅ N ₂ OS ₂ SnCl
Formula mass	479.68
Crystal system	Monoclinic
Space group, no.	C2/c,15
<i>a</i> (Å)	58.88(6)
<i>b</i> (Å)	9.387(10)
<i>c</i> (Å)	26.08(3)
β (°)	114.026(16)
<i>V</i> (Å ³)	13166(25)
<i>Z</i> (<i>Z'</i>)	24 (3)
Crystal habit/size (mm)	Platelet/ 0.42 x 0.31 x 0.23
<i>T</i> (K)	293(1)
μ(Mo Kα) (cm ⁻¹)	14.81
Total reflections	33353
Independent reflections	
All	9430
For <i>F_o</i> ≥ 4.0 σ (<i>F_o</i>)	3964
$R(F) = \sum (F_o - F_c) / \sum F_o $	0.1122
For <i>F_o</i> > 4.0 σ (<i>F_o</i>)	
$wR(F^2) = [\sum [w(F_o^2 - F_c^2)^2] / \sum [w(F_o^2)^2]]^{1/2}$	0.3306
Goodness-of-fit	0.972
θ range for data collections (°)	2.22-23.53
Data/restraints/parameters	9430/515/631

Table 4.12: Selected bond lengths (Å) and bond angles (°) for Et₂SnCIL^a (19)

	x = 1	x = 2	x = 3
Snx-Clx	2.520(6)	2.505 (7)	2.536(9)
Snx-S1x	2.500(5)	2.779(8)	2.451(6)
Snx-S2x	2.747(6)	2.471(5)	2.710(8)
Snx-C13x	2.181(16)	2.13(2)	2.19(3)
Snx-Cx15	2.156(15)	2.20(3)	2.01(4)
Sx1-Cx1	1.722(19)	1.785(17)	1.84(2)
Sx2-Cx1	1.719(15)	1.82(2)	1.722(18)
Clx-Snx-Sx1	85.89(15)	153.74(15)	87.7(2)
ClxSnx-Sx2	154.53(12)	85.06(18)	157.7(2)
Clx-Snx-Cx13	94.2(5)	98.2(8)	94.6(9)
Clx-Snx-Cx15	95.3(6)	96.6(10)	97.6(12)
Sx1-Snx-Sx2	68.65(14)	68.70(17)	70.07(18)
Sx1-Snx-Cx13	114.9(5)	92.8(8)	116.2(8)
Sx1-Snx-Cx15	114.5(5)	89.8(10)	128.6(10)
Sx2-Snx-Cx13	95.9(5)	112.5(6)	94.9(8)
Sx2-Snx-Cx15	95.9(7)	105.1(8)	96.8(12)
Cx13-Snx-Cx15	130.2(7)	140.5(10)	114.2(13)
Snx-Sx1-Clx1	90.0(5)	85.1(7)	91.4(6)
Snx-Sx2-Clx1	82.2(6)	94.0(6)	85.7(7)
Sx1-Cx1-Sx2	119.0(1)	111.1(10)	112.9(10)

4.7 X-Ray Structure of $\text{Me}_2\text{SnClL}^a$ (**21**)



Crystal data for compound **21** is given in Table 4.13 with selected geometric parameters listed in Table 4.14. The ORTEP diagram for the molecule of **21** together with the atom numbering scheme used here is shown in Fig. 4.7. The configuration about the tin atom is five-coordinate, with a distorted trigonal-bipyramidal geometry with atoms S2, C13 and C14 occupying the equatorial positions. The sum of the equatorial angles [$356.5(3)^\circ$] at the tin atom involving the C13, C14 and S2 atoms deviates only by 3.5° from the ideal angle of 360° . The Cl atom occupies one of the apical positions of the trigonal bipyramid with the Cl-Sn-S2 angle of $85.81(3)^\circ$. As a result of 'L^a' being a chelating ligand with a small bite forming a four-membered ring, the S1-Sn-S2 angle is not 90° , but only $68.43(3)^\circ$. Therefore, the S1 atom cannot occupy exactly the corresponding *trans* axial position to Cl and the Cl-Sn-S1 angle is $154.23(3)^\circ$. Thus, the dithiocarboxylate group is asymmetrically coordinated as shown by Sn-S1(ax), 2.760 (12) Å, and Sn-S2(eq), 2.464(11) Å, bond lengths. The S-C bond lengths [S1-C1 = 1.704(3) Å and S2-C1 = 1.750(3) Å] also show the asymmetric nature of the dithiocarboxylate group.

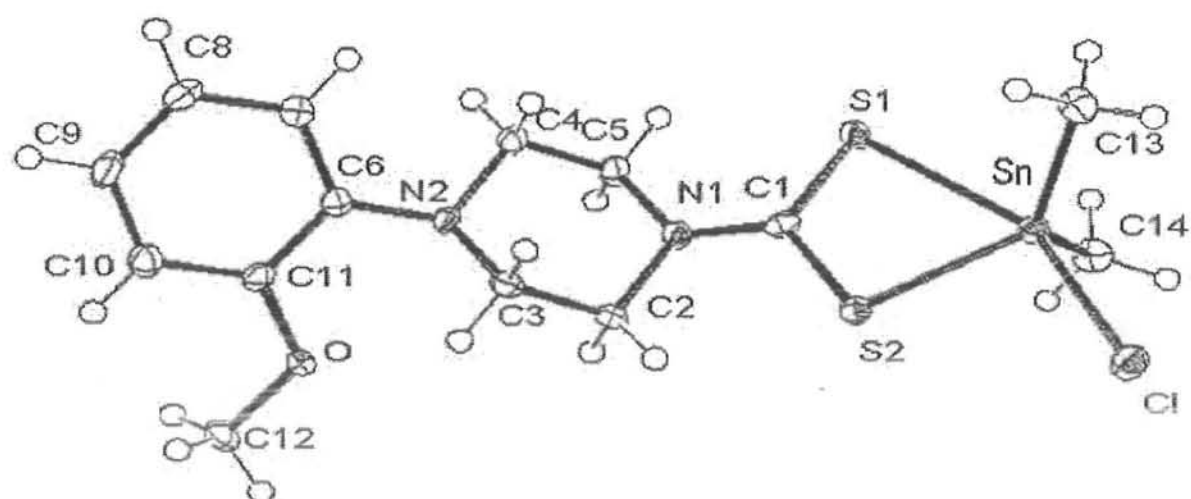


Fig 4.7: ORTEP drawing of $\text{Me}_2\text{SnCIL}^a$ (21) with atomic numbering scheme

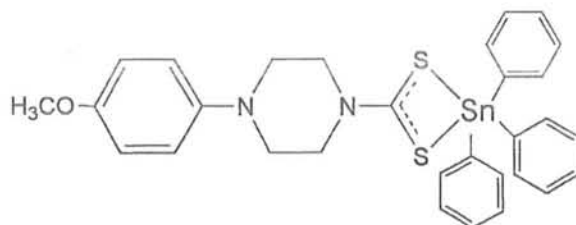
Table 4.13: Crystal data and structure refinement parameters for Me₂SnCIL^a (21)

Empirical formula	C ₁₄ H ₂₁ N ₂ OS ₂ SnCl
Formula mass	451.63
Crystal system	Orthorhombic
Space group, no.	<i>Pbcn</i> , 60
<i>a</i> (Å)	20.190(6)
<i>b</i> (Å)	6.906(2)
<i>c</i> (Å)	25.676(8)
<i>V</i> (Å ³)	3580.1(19)
<i>Z</i> (<i>Z'</i>)	8 (1)
Crystal habit/size (mm)	Needle/0.43 x 0.09 x 0.07
<i>T</i> (K)	100(1)
$\mu(\text{Mo K}\alpha)$ (cm ⁻¹)	18.07
Total reflections	24431
Independent reflections	
All	3621
For $F_o \geq 4.0 \sigma(F_o)$	2855
$R(F) = \sum (F_o - F_c) / \sum F_o $	
For $F_o > 4.0 \sigma(F_o)$	0.0332
$wR(F^2) = [\sum [w(F_o^2 - F_c^2)^2] / \sum [w(F_o^2)^2]]^{1/2}$	
	0.0692
Goodness-of-fit	0.996
θ range for data collections (°)	3.12-26.37
Data/restraints/parameters	3621/0/193

Table 4.14: Selected bond lengths (Å) and bond angles (°) for Me₂SnCIL^a (21)

Sn-Cl	2.438(11)	Sn-S1	2.7603(12)
Sn-S2	2.4645(11)	Sn-C13	2.104(3)
Sn-C14	2.107(4)	S1-C1	1.704(3)
S2-C1	1.750(3)		
Cl-Sn-S1	154.23(3)	Cl-Sn-S2	85.81(3)
Cl-Sn-C13	101.81(9)	Cl-Sn-C14	100.09(10)
S1-Sn-S2	68.43(3)	S1-Sn-C13	89.47(9)
S1-Sn-C14	92.35(10)	S2-Sn-C13	116.56(9)
S2-Sn-C14	115.99(10)	C13-Sn-C14	123.93(13)
Sn-S1-C1	82.84(11)	Sn-S2-C1	91.43(10)
S1-C1-S2	117.19(18)		

4.8 X-Ray Structure of Ph_3SnL^b (**28**)



An ORTEP view of the molecule **28** including numbering scheme is shown in Fig. 4.8. Relevant bond lengths and bond angles are illustrated in Table 4.15, while Table 4.16 comprises of crystal data. The crystal structure shows the Sn atom is coordinated to the α -carbon atoms of three phenyl groups and two sulfur of 4-(4-methoxyphenyl)piperazine-1-carbodithioate ligand. The geometry around Sn atom can be characterized by the value of $\tau = (\beta - \alpha)/60$, where β is the largest of the basal angles around the Sn atom. For compound **28**, it is $\text{S2-Sn-C19} = 154.67(8)^\circ$. The second largest of the basal angles around the Sn atom, α for **28** is $\text{S1-Sn-C25} = 129.23(9)^\circ$. So the calculate τ value for compound **28** is 0.42. The value indicates highly distorted trigonal-bipyramidal geometry around Sn atom with C19 of a phenyl group and the S2 of the ligand moiety in the axial positions while C13 and C25 of the two phenyl groups and S1 in the plane positions. The sum of the equatorial angles involving the two α -carbons of the phenyl groups and a sulfur atom, 1: 353.7° , shows a mark deviation from the ideal angle of 360° . The C19 atom occupies one of the apical positions of the trigonal-bipyramidal with the S1-Sn-C19 angle of $90.98(8)^\circ$. As a result 4-(4-methoxyphenyl)piperazine-1-carbodithioate being a chelating ligand with the small bite forming a four-membered ring, S1-Sn-S2 angle is not 90° , but only $65.84(2)^\circ$. Therefore, the S2 atom cannot occupy exactly the corresponding *trans* axial position to C19 and C19-Sn-S2 angle is $154.67(8)^\circ$. The unsymmetrical coordination mode of the ligand can also be easily visualize from the two Sn-S bond lengths, a shorter Sn-S1 [$2.4957(7) \text{ \AA}$] bond length and a long Sn-S2 [$2.9170(8) \text{ \AA}$] bond, with difference of 0.421 \AA between the two tin-sulfur bonds. The shorter bond length is closed to the sum of the covalent radii of Sn and S (2.42 \AA) and long Sn-S bond length is much shorter than the sum of the van der Waal's radii (4.0 \AA) of two atoms. The S-C bond lengths [$\text{S1-C12} = 1.758(3) \text{ \AA}$ and $\text{S2-C12} = 1.702(3) \text{ \AA}$] also show the anisobidentate nature of the ligand.

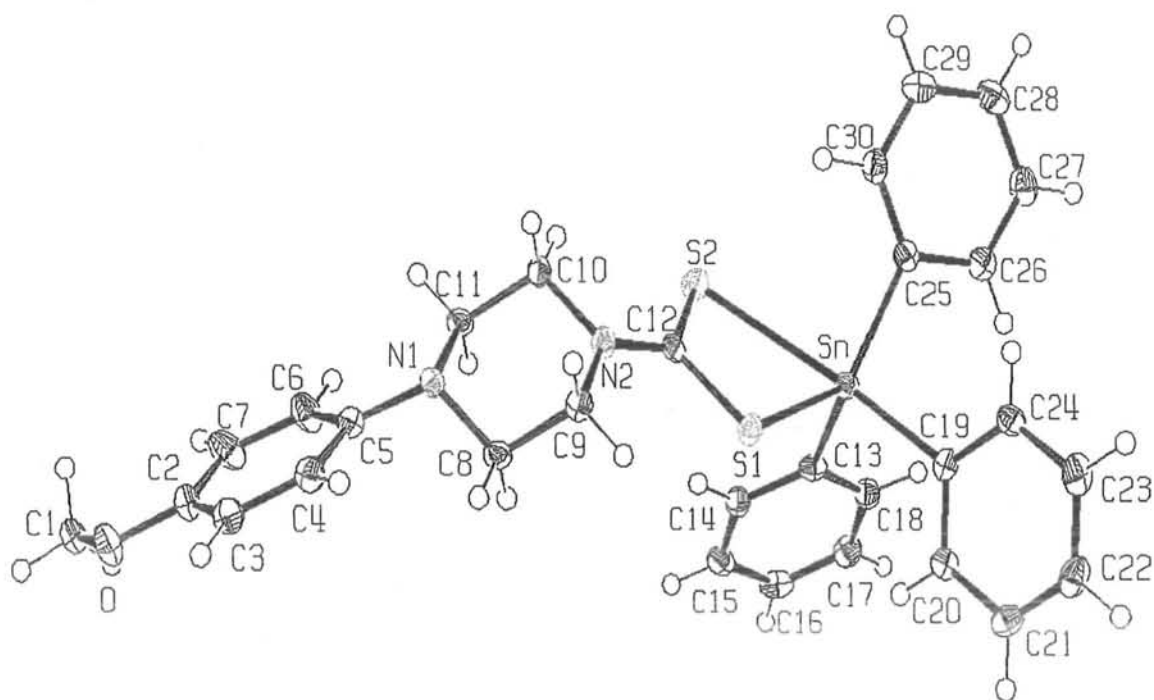


Fig 4.8: ORTEP drawing of Ph_3SnL^b (28) with atomic numbering scheme

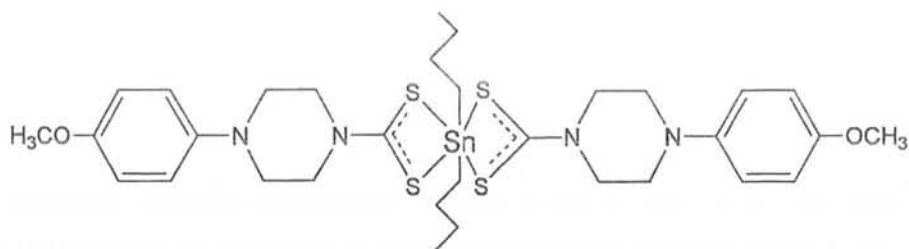
Table 4.15: Crystal data and structure refinement parameters for Ph₃SnL^b (28)

Empirical formula	C ₃₀ H ₃₀ N ₂ OS ₂ Sn
Formula mass	617.42
Crystal system	Monoclinic
Space group, no.	<i>P</i> 2 ₁ / <i>n</i> , 14
<i>a</i> (Å)	10.0253(8)
<i>b</i> (Å)	29.974(2)
<i>c</i> (Å)	10.3297(8)
β (°)	117.9951(9)
<i>V</i> (Å ³)	2740.9(4)
<i>Z</i> (<i>Z'</i>)	4 (1)
Crystal habit/size (mm)	Platelet/0.35 x 0.24 x 0.07
<i>T</i> (K)	100(1)
μ(Mo Kα) (cm ⁻¹)	11.11
Total reflections	24147
Independent reflections	6767
All	
For <i>F_o</i> ≥ 4.0 σ (<i>F_o</i>)	5418
$R(F) = \sum (F_o - F_c) / \sum F_o $	0.0365
For <i>F_o</i> > 4.0 σ (<i>F_o</i>)	
$wR(F^2) = [\sum [w(F_o^2 - F_c^2)^2] / \sum [w(F_o^2)^2]]^{1/2}$	0.0866
Goodness-of-fit	1.019
θ range for data collections (°)	2.40-28.28
Data/restraints/parameters	6767/0/326

Table 4.16: Selected bond lengths (Å) and bond angles (°) for Ph₃SnL^b (28)

Sn-S1	2.4957(7)	Sn-S2	2.9170(8)
Sn-C13	2.144(3)	Sn-C19	2.170(3)
Sn-C25	2.161(3)	S1-C12	1.758(3)
S2-C12	1.702(3)		
S1-Sn-S2	65.83(2)	S1-Sn-C13	105.49(8)
S1-Sn-C19	90.98(8)	S1-Sn-C25	129.23(9)
S2-Sn-C13	92.39(8)	S2-Sn-C19	154.67(8)
S2-Sn-C25	88.14(8)	C13-Sn-C19	104.09(12)
C13-Sn-C25	119.04(11)	C19-Sn-C25	100.07(11)
Sn-S1-C12	94.49(9)	Sn-S2-C12	81.89(10)
S1-C12-S2	117.80(17)	Sn-C13-C14	121.0(2)
Sn-C13-C18	119.9(2)	Sn-C19-C20	120.0(2)
Sn-C19-24	121.8(2)	Sn-C25-C26	116.3(2)
Sn-C25-C30	125.8(2)		

4.9 X-Ray Structure of $n\text{-Bu}_2\text{SnL}_2$ (**30**)



The structure of compound **30** is shown in Fig. 4.9. Crystal data and selected interatomic parameters are collected in Tables 4.17 and 4.18, respectively. The Sn atom in **30** is coordinated by two butyl groups and two 4-(4-methoxyphenyl) piperazine-1-carbodithioate ligands, with the latter adopting similar behaviour in coordination modes. The two dithiocarboxylate ligands are anisobidentically chelated to Sn, with one longer and one shorter Sn-S bond (av = 2.9685(6) Å and 2.5235 (6) Å, respectively). The longer Sn-S distances are significantly less than the sum of the van der Waal's radii (4.0 Å), and the coordination number of Sn is unambiguously assigned as six. The overall geometry at Sn is, however, highly distorted from the *trans* octahedral: the C-Sn-C angle is only 136.24(8)°, and the Sn and four NCS₂ sulfur atoms of the dithiocarboxylate ligands are nearly coplanar but are badly distorted from square-planar geometry (*cis* S-Sn-S angles range from 64.96(1)° to 147.60(2)°). In both anisobidentate ligands, each shorter Sn-S bond is associated with a longer C-S bond and vice versa; this is in consonance with the bonding asymmetry of the ligands. The bond angles subtended at the Sn atom by the methylene carbons and S2 and S2a atoms range from 108.09(6)° to 104.34(6)° demonstrating that the Sn-C bonds are bent toward the longer Sn-S bonds. This obviously a consequence of repulsion between the bonding electron pairs around the central Sn atom. Electronic and steric arguments have also been invoked to account the distortion of the similar structures from the regular octahedral geometry. Thus, the coordination geometry about the Sn atom in compound **30** is best described as being distorted skew trapezoidal-bipyramidal. The geometry and bond lengths of SnC₂S₄ core are comparable with those usually observed for most of the octahedral complexes [7, 8].

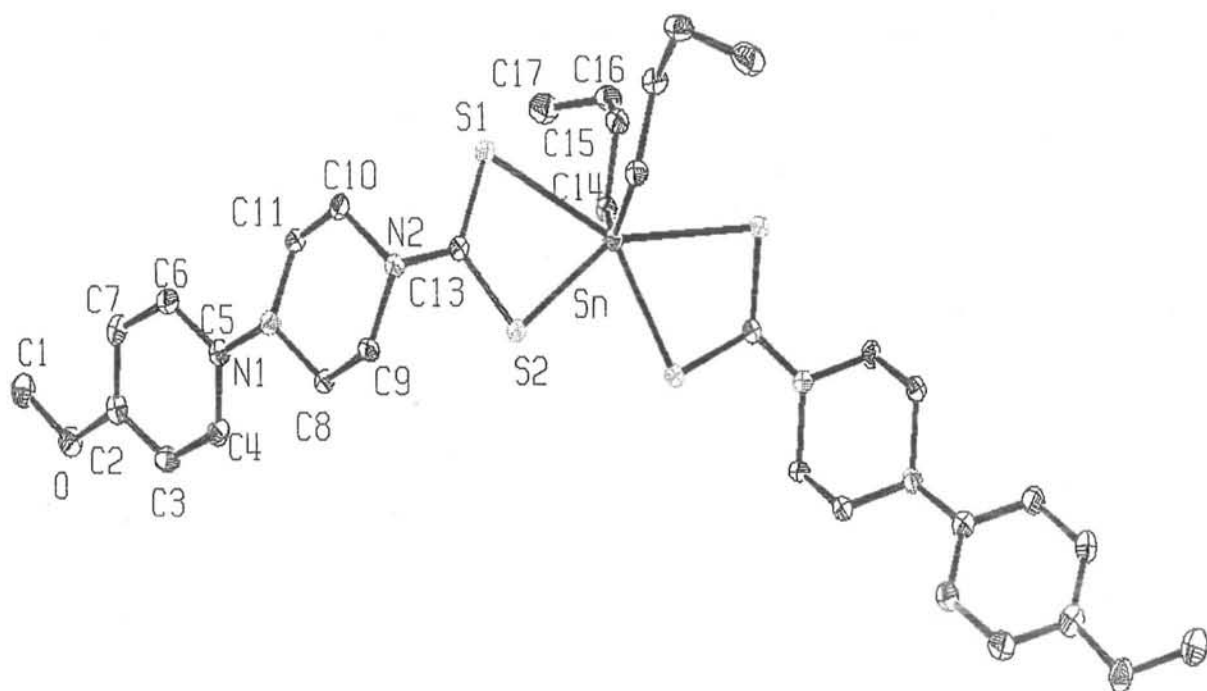


Fig 4.9: ORTEP drawing of $n\text{-Bu}_2\text{SnL}_2$ (30) with atomic numbering scheme

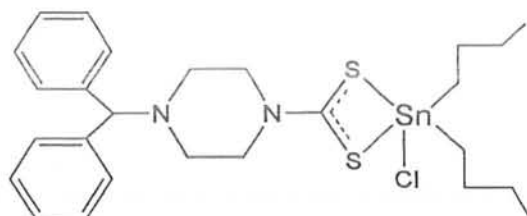
**Table 4.17: Crystal data and structure refinement parameters for n-Bu₂SnL₂^b
(30)**

Empirical formula	(C ₁₆ H ₂₄ N ₂ OS ₂) ₂ Sn
Formula mass	767.74
Crystal system	Monoclinic
Space group, no.	C2/c, 15
a (Å)	32.768(4)
b (Å)	6.9313(9)
c (Å)	18.877(2)
β (°)	124.2004(13)
V (Å ³)	3546.0(7)
Z (Z')	4 (0.5)
Crystal habit/size (mm)	block/0.51 x 0.46 x 0.37
T (K)	100(1)
μ(Mo Kα ⁻) (cm ⁻¹)	9.9
Total reflections	14351
Independent reflections	4040
All	
For $F_o \geq 4.0 \sigma(F_o)$	3727
$R(F) = \sum (F_o - F_c) / \sum F_o $	0.0267
For $F_o > 4.0 \sigma(F_o)$	
$wR(F^2) = [\sum [w(F_o^2 - F_c^2)^2] / \sum [w(F_o^2)^2]]^{1/2}$	0.0731
Goodness-of-fit	1.077
θ range for data collections (°)	2.65-27.48
Data/restraints/parameters	4040/0/197

Table 4.18: Selected bond lengths (Å) and bond angles (°) for n-Bu₂SnL^b₂ (30)

Sn-S1	2.9685(6)	Sn-S2	2.5235(6)
Sn-C14	2.136(3)	Sn-S1a	2.9685(6)
Sn-S2_a	2.5235(6)	Sn-C14a	2.136(3)
S1-C13	1.697(2)	S2-C13	1.743(2)
S1-Sn-S2	64.96(1)	S1-Sn-C14	82.36(6)
S1-Sn-S1a	147.35(2)	S1-Sn-S2a	147.60(2)
S1-Sn-C14a	85.61(6)	S2-Sn-C14	108.09(6)
S2-Sn-S1a	147.60(2)	S2-Sn-S2a	83.01(2)
S2-Sn-C14a	104.34(6)	C14-Sn-S1a	85.61(6)
C14-Sn-S2a	104.34(6)	C14-Sn-C14a	136.24(8)
S1a-Sn-S2a	64.96(1)	S1a-Sn-C14a	82.36(6)
S2a-Sn-C14a	108.09(6)	Sn-S1-C13	80.88(7)
Sn-S2-C13	94.51(7)		

4.10 X-Ray Structure of $n\text{-Bu}_2\text{SnCIL}^c$ (**41**)



The asymmetric unit of **41** contains two different molecules; The ORTEP diagram for one of these, molecule (1), together with an example of the atom numbering scheme used here is shown in Fig. 4.10, and crystal data and selected interatomic parameters are collected in Table 4.19 and 4.20, respectively. The configuration about the tin atom is five-coordinate, with distorted trigonal-bipyramidal geometry at the central Sn atom. The sums of the equatorial angles involving the two α -carbons of the butyl groups and a S atom, (x1): 359° : 357.5° , show little deviation from the ideal angle of 360° . For each molecule, the Cl atom occupies one of the apical positions of the trigonal-bipyramid with the Cl1-Sn1-S11 and Cl2-Sn2-S21 angles of $88.07(6)^\circ$ and $85.52(4)^\circ$, respectively. The quasi-axial S11 and S12 atoms cannot occupy exactly the position *trans* to Cl and Cl1-Sn1-S12 and Cl2-Sn2-S22 angles are $156.57(7)^\circ$ and $153.84(4)^\circ$. Thus, the dithiocarboxylate groups in both molecules are asymmetrically coordinated as shown by Snx-Sx2(ax) [$2.754(2) \text{ \AA}$ and $2.7849(13) \text{ \AA}$] and Sn-Sx2(eq), [$2.4705(15) \text{ \AA}$ and $2.4688(13) \text{ \AA}$] bond lengths. The S-C bond lengths [(Sx1-Cx18 = $1.740(6)$ and $1.756(4) \text{ \AA}$) and (Sx2-Cx18 = $1.716(6) \text{ \AA}$ and $1.705(4) \text{ \AA}$)] also show the asymmetric nature of the dithiocarboxylate group in each molecule.

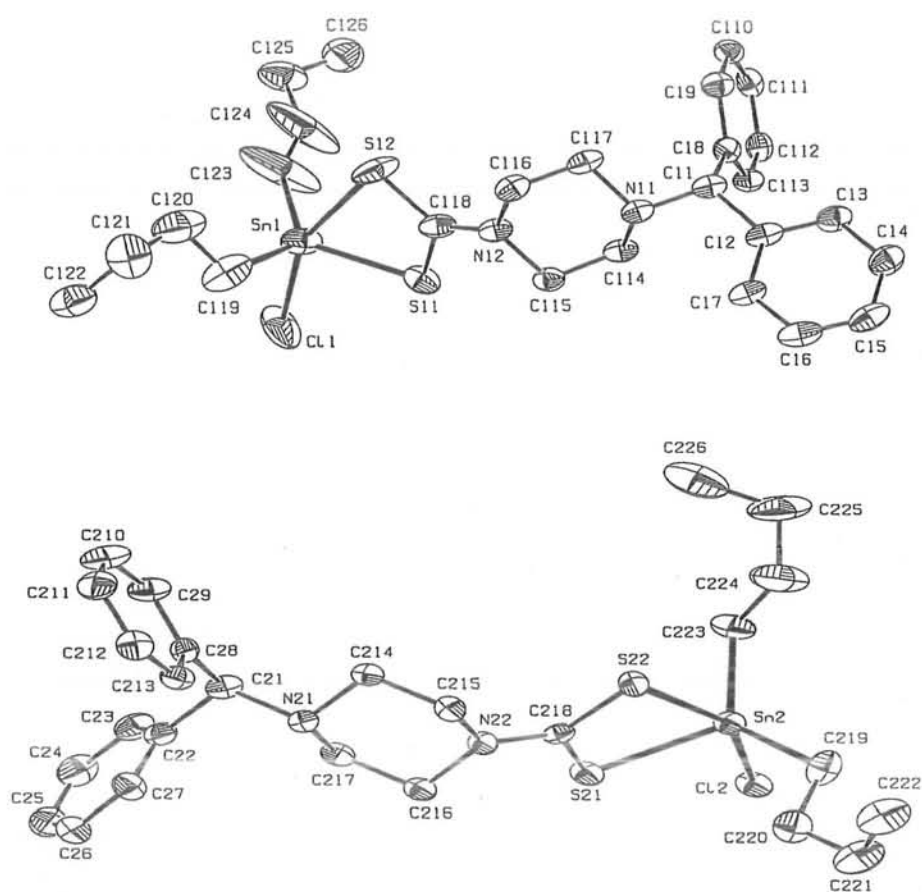


Fig 4.10: ORTEP drawing of molecule 1 (top) and molecule 2 (lower) of the n-Bu₂SnCIL^c (41) with atomic numbering scheme

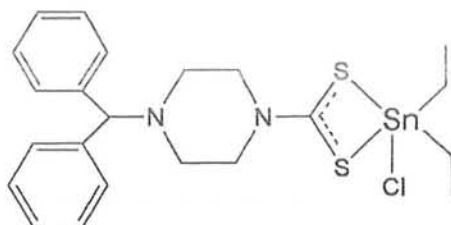
Table 4.19: Crystal data and structure refinement parameters for n-Bu₂SnClL^c (41)

Empirical formula	C ₂₆ H ₃₇ N ₂ S ₂ SnCl
Formula mass	595.89
Crystal system	Triclinic
Space group, no.	<i>P</i> -1, 2
<i>a</i> (Å)	9.9510(10)
<i>b</i> (Å)	13.3727(14)
<i>c</i> (Å)	21.113(2)
α (°)	100.6968(14)
β (°)	91.2796(14)
γ (°)	92.3442(14)
<i>V</i> (Å ³)	2757.1(5)
<i>Z</i> (<i>Z'</i>)	4 (2)
Crystal habit/size (mm)	block/0.49 x 0.23 x 0.14
<i>T</i> (K)	100(1)
μ(Mo Kα) (cm ⁻¹)	11.92
Total reflections	20874
Independent reflections	10225
All	
For <i>F_o</i> ≥ 4.0 σ (<i>F_o</i>)	7585
$R(F) = \sum (F_o - F_c) / \sum F_o $	0.0528
For <i>F_o</i> > 4.0 σ (<i>F_o</i>)	
$wR(F^2) = [\sum [w(F_o^2 - F_c^2)^2] / \sum [w(F_o^2)^2]]^{1/2}$	0.1302
Goodness-of-fit	1.034
θ range for data collections (°)	2.51-25.68
Data/restraints/parameters	10225/0/581

Table 4.20: Selected bond lengths (Å) and bond angles (°) for n-Bu₂SnCIL^c (41)

	x = 1	x =2		x = 1	x =2
Snx-Clx	2.446(2)	2.4721(13)	Snx-Sx1	2.4705(15)	2.4688(13)
Snx-Sx2	2.754(2)	2.7849(13)	Snx-Cx19	2.208(8)	2.137(6)
Snx-Cx23	2.125(11)	2.145(6)	Sx1-Cx18	1.740(6)	1.756(4)
Sx2-Cx18	1.716(6)	1.705(4)			
Clx-Snx-Sx1	88.07(6)	85.52(4)	Clx-Snx-Sx2	156.57(7)	153.84(4)
Clx-Snx-Cx19	95.4(2)	99.27(16)	Clx-Snx-Cx23	96.2(4)	99.55(14)
Sx1-Snx-Sx2	68.55(5)	68.31(4)	Sx1-Snx-Cx19	115.3(2)	116.18(17)
Sx1-Snx-Cx23	119.7(4)	114.57(16)	Sx2-Snx-Cx19	93.4(2)	92.43(16)
Sx2-Snx-Cx23	96.8(3)	91.83(14)	Cx19-Snx-Cx23	124.0(5)	126.8(2)
Snx-Sx1-Cx18	90.9(2)	91.58(14)	Snx-Sx2-Cx18	82.3(2)	82.45(14)
Sx1-Cx18-Sx2	117.3(3)	117.7(2)	Snx-Cx19-Cx20	115.9(6)	113.3(4)
Snx-Cx23-Cx24	138.5(11)	115.8(4)			

4.11 X-Ray Structure of Et₂SnCIL^c (43)



For compound **43**, pertinent crystallographic parameters, selected bond lengths and bond angles are given in Tables 4.21 and 4.22, respectively. An ORTEP view of the **43** together with atomic numbering scheme is presented in Fig. 4.11. The Sn atom is five-coordinate, being chelated by an asymmetrically coordinating 4-benzhydrylpiperazine-1-carbodithioate ligand, a chloride and two ethyl substituents. The Sn-S2 [2.784(4) Å] bond distance approximately *trans*- to the chloride is longer than the other Sn-S1 [2.457(4) Å] bond distance. The coordination geometry is almost intermediate between square-pyramidal and trigonal bipyramidal with having a small bias towards the former, at least based on the τ value (0.24), and is consistent with value (0.29) for (MeO(O=)CCH₂CH₂)₂Sn (S₂CNMe₂)Cl [9]. The Cl atom occupies one of the apical positions of the highly distorted trigonal-bipyramid with the Cl-Sn-S1 angle of 85.43(12)°. The quasi-axial S2 atom again cannot occupy exactly the position *trans* to Cl and Cl-Sn-S2 is 153.29(12)°. Thus, 4-benzhydrylpiperazine-1-carbodithioate ligand chelates the Sn atom via its two sulfur atoms in anisobidentate fashion, forming a four-membered ring with S1-Sn-S2 bond angle of 67.87(12)°. The S-C bond lengths [S1-C18 = 1.724(15) Å and S2-C18 = 1.707(17) Å] also demonstrate the asymmetric nature of the ligand.

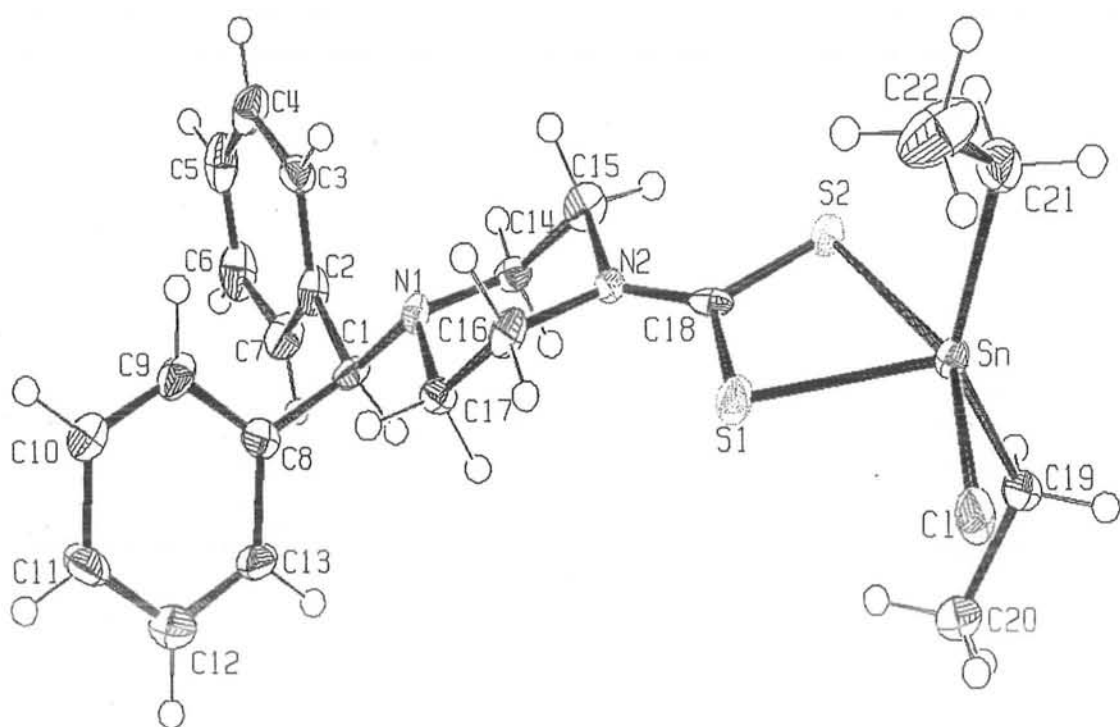


Fig 4.11: ORTEP drawing of $\text{Et}_2\text{SnCIL}^c$ (43) with atomic numbering scheme

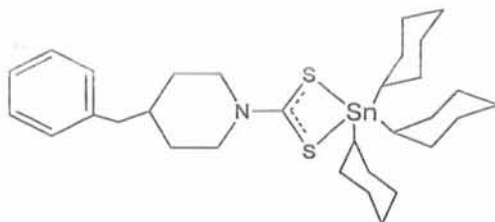
Table 4.21: Crystal data and structure refinement parameters for Et₂SnCIL^c (43)

Empirical formula	C ₂₂ H ₂₉ N ₂ S ₂ SnCl
Formula mass	539.77
Crystal system	Monoclinic
Space group, no.	<i>C2/c</i> , 15
<i>a</i> (Å)	29.612(15)
<i>b</i> (Å)	9.609(5)
<i>c</i> (Å)	18.082(10)
β (°)	117.844(10)
<i>V</i> (Å ³)	4549(4)
<i>Z</i> (<i>Z'</i>)	8 (1)
Crystal habit/size (mm)	block/0.32 x 0.28 x 0.16
<i>T</i> (K)	100(1)
μ(Mo Kα [−]) (cm ^{−1})	14.35
Total reflections	3682
Independent reflections	3682
All	
For <i>F</i> _o ≥ 4.0 σ (<i>F</i> _o)	2448
$R(F) = \sum (F_o - F_c) / \sum F_o $	0.0716
For <i>F</i> _o > 4.0 σ (<i>F</i> _o)	
$wR(F^2) = [\sum [w(F_o^2 - F_c^2)^2] / \sum [w(F_o^2)^2]]^{1/2}$	0.2084
Goodness-of-fit	1.138
θ range for data collections (°)	2.77-25.03
Data/restraints/parameters	3682/0/256

Table 4.22: Selected bond lengths (Å) and bond angles (°) for Et₂SnCIL^c (43)

Sn-Cl	2.462(4)	Sn-S1	2.457(4)
Sn-S2	2.784(4)	Sn-C19	2.120(14)
Sn-C21	2.113(15)	S1-C18	1.724(15)
S2-C18	1.707(17)		
Cl-Sn-S1	85.43(12)	Cl-Sn-S2	153.29(12)
Cl-Sn-C19	97.1(4)	Cl-Sn-C21	97.6(4)
S1-Sn-S2	67.87(12)	S1-Sn-C19	108.9(4)
S1-Sn-C21	110.5(4)	S2-Sn-C19	91.1(4)
S2-Sn-C21	92.6(4)	C19-Sn-C21	138.9(6)
Sn-S1-C18	92.3(5)	Sn-S2-C18	82.0(5)
S1-C18-S2	117.8(8)		

4.12 X-Ray Structure of $\text{Cy}_3\text{SnL}^{\text{d}}$ (**50**)



An ORTEP view of the compound **50** together with atomic numbering scheme is depicted in Fig. 4.12. Pertinent crystallographic parameters, relevant bond lengths and bond angles are given in Tables 4.23 and 4.24. The Sn atom is five-coordinate, being chelated by asymmetrically coordinating 4-benzylpiperidine-1-carbodithioate ligand and three cyclohexyl substituents. The Sn-S1 [3.160 Å] bond distance approximately *trans*- to the C26 is longer than the other Sn-S2 [2.4756(9) Å] bond distance. The geometry around Sn is almost a midway between square-pyramidal and trigonal bipyramidal as evident from the τ value (0.67). The C26 atom occupies one of the apical positions of the highly distorted trigonal-bipyramid with the C26-Sn-S2 angle of 95.36(8)°. The quasi-axial S1 atom cannot occupy exactly the position *trans* to C26 and C26-Sn-S2 angle is 157.39°. Thus, ligand chelates the Sn atom via its two sulfur atoms in anisobidentate fashion, forming a four-membered ring with S1-Sn-S2 bond angle of 62.80°. The S-C bond lengths [S1-C13 = 1.691(3) Å and S2-C13 = 1.768(3) Å] also demonstrate the asymmetric nature of the ligand.

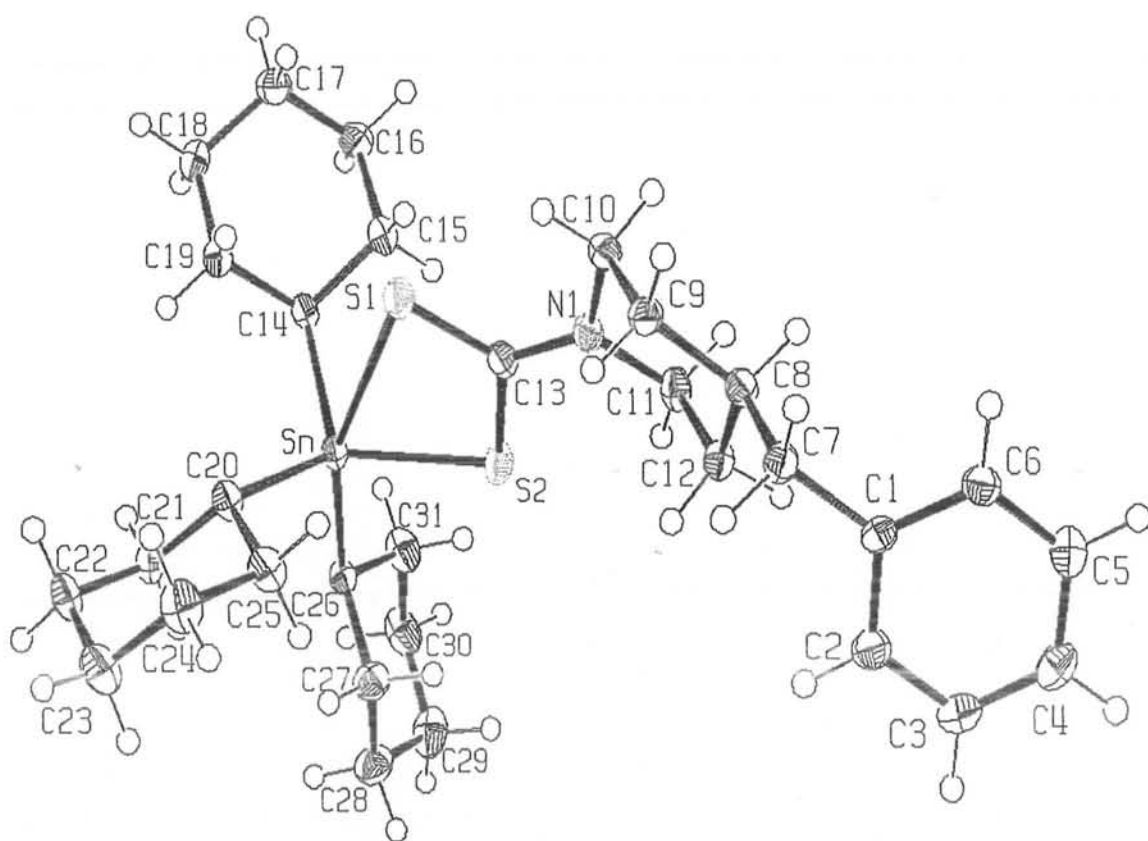


Fig 4.12: ORTEP drawing of Cy_3SnL^d (50) with atomic numbering scheme

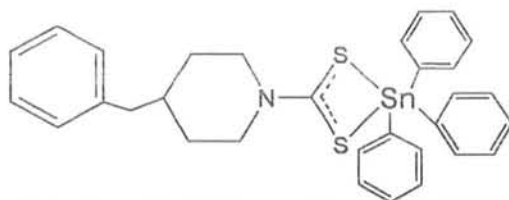
Table 4.23: Crystal data and structure refinement parameters for Cy₃SnL^d (50)

Empirical formula	C ₃₁ H ₄₉ NS ₂ Sn
Formula mass	618.6
Crystal system	Triclinic
Space group, no.	<i>P</i> -1, 2
<i>a</i> (Å)	10.5063(10)
<i>b</i> (Å)	10.6281(10)
<i>c</i> (Å)	15.0438(15)
α (°)	109.3918(12)
β (°)	103.1745(12)
γ (°)	92.5424(13)
<i>V</i> (Å ³)	1529.6(3)
<i>Z</i> (<i>Z'</i>)	2(1)
Crystal habit/size (mm)	Cut fragment/0.44 x 0.37 x 0.17
<i>T</i> (K)	100(1)
μ (Mo K α) (cm ⁻¹)	9.92
Total reflections	13801
Independent reflections	7234
All	
For $F_o \geq 4.0 \sigma(F_o)$	6477
$R(F) = \sum (F_o - F_c) / \sum F_o $	0.0401
For $F_o > 4.0 \sigma(F_o)$	
$wR(F^2) = [\sum [w(F_o^2 - F_c^2)^2] / \sum [w(F_o^2)^2]]^{1/2}$	0.1180
Goodness-of-fit	1.037
θ range for data collections (°)	2.68-28.28
Data/restraints/parameters	7234/0/316

Table 4.24: Selected bond lengths (Å) and bond angles (°) for Cy₃SnL^d (50)

Sn-S2	2.4756(9)	Sn-C14	2.170(3)
Sn-C20	2.181(3)	Sn-C26	2.184(3)
S1-C13	1.691(3)	S2 –C13	1.768(3)
Sn-S1	3.160		
S2-Sn-C14	112.09(8)	S1-Sn-C14	86.33
S2-Sn-C20	116.84(8)	S1-Sn-C20	80.78
S2-Sn-C26	95.35(8)	S1-Sn-C26	157.39
C14-Sn-C20	115.11(12)	S1-Sn-S2	62.80
C14-Sn-C26	108.77(11)	Sn-S2-C13	98.97(1)
C20-Sn-C26	106.30(12)	Sn-S1-C13	78.00
Sn-C14-C15	114.36(19)	Sn-C14-C19	109.9(2)
Sn-C20-C21	109.4(2)	Sn-C20-C25	113.4(2)
Sn-C26-C27	112.2(2)	Sn-C26-C31	112.4(2)

4.13 X-Ray Structure of $\text{Ph}_3\text{SnL}^{\text{d}}$ (**52**)



The molecular structure of compound (**52**) is depicted in Fig. 4.13, while crystal data and selected bond lengths and bond angles are given in Tables 4.25 and 4.26, respectively. The geometry around the Sn atom is distorted trigonal-bipyramidal, the equatorial plane being defined by the two carbons of the phenyl groups and a sulfur atom of the 4-benzylpiperidine-1-carbodithioate ligand. According to Addison et al., the geometry around the Sn atom can be characterized by the value of $\tau = (\beta - \alpha)/60$ [1], where β is the largest of the basal angles around the Sn atom. For compound **52** it is $\text{S2-Sn1-C26} = 158.88^\circ$. The second largest of the basal angles around the Sn atom, α for compound **52** is $\text{S1-Sn1-C20} = 119.21(9)^\circ$. The calculated τ value for the **52** is 0.66. The value indicates a highly distorted trigonal-bipyramidal arrangement around Sn1 atom with C26 from a phenyl group and the S2 from the dithiocarboxylate at the axial positions while C14 and C24 from two phenyl groups and S1 in the plane positions. The sum of the equatorial angles is 350° instead of the ideal 360° . Being a part of chelate, the angle S2-Sn1-S1 is not 90° but only 65.70° , so the S2 cannot occupy exactly the corresponding *trans* apical position of C26 and the angle between the apical groups is 158.88° . Finally, the C-S bond lengths are characteristic of the 1,1-dithioate moiety and are intermediate between the values expected for single and double bonds [4].

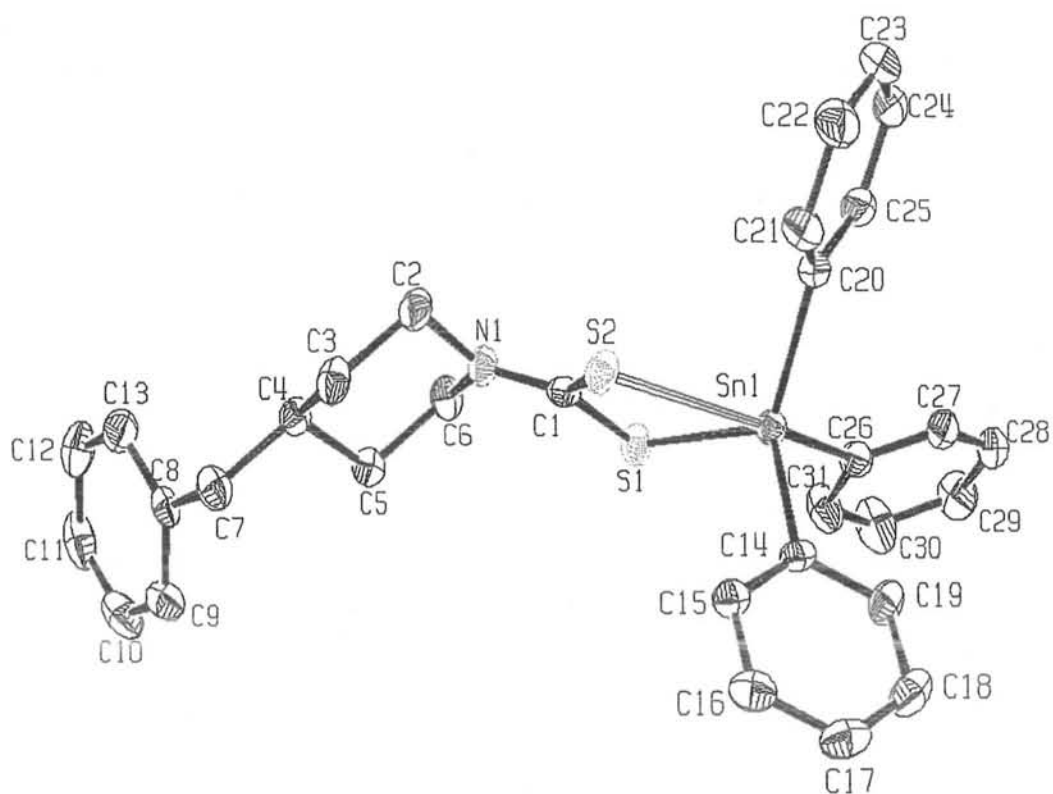


Fig 4.13: ORTEP drawing of Ph_3SnL^d (52) with atomic numbering scheme

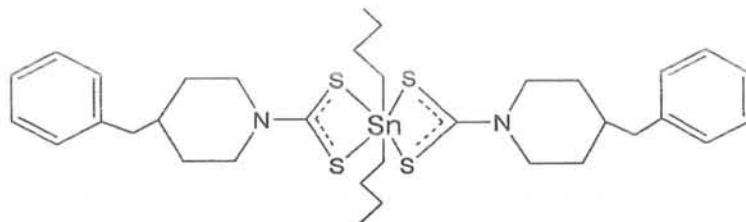
Table 4.25: Crystal data and structure refinement parameters for Ph₃SnL^d (52)

Empirical formula	C ₃₁ H ₃₁ NS ₂ Sn
Formula mass	600.38
Crystal system	Triclinic
Space group	P -1
<i>a</i> (Å)	9.2531(8)
<i>b</i> (Å)	10.7273(9)
<i>c</i> (Å)	14.4044(12)
α (°)	95.313(10)
β (°)	101.880(10)
γ (°)	94.328(10)
<i>V</i> (Å ³)	1386.6(2)
<i>Z</i>	2
Crystal habit/size (mm)	Block/ 0.50 x 0.45 x 0.40
<i>T</i> (K)	173(2)
Total reflections	10780
Independent reflection	4936
R indices (all data)	R1 = 0.0278, wR2 = 0.0750
Final R indices [<i>I</i> >2sigma(<i>I</i>)]	R1 = 0.0228, wR2 = 0.0530
Goodness-of-fit	1.197
θ range for data collections (°)	2.41- 25.93
Data/restraints/parameters	4936/0/316

Table 4.26: Selected bond lengths (Å) and bond angles (°) for Ph₃SnL^d (52)

S1-Sn1	2.4892(8)	Sn1-S2	2.935
C14-Sn1	2.144(3)	C20-Sn1	2.156(3)
C26-Sn1	2.173(3)	C1-S2	1.696(3)
C1-S1	1.758(3)		
C14-Sn1-S1	115.38(8)	C20-Sn1-S1	119.21(9)
C26-Sn1-S1	93.88(9)	C14-Sn1-S2	89.50
C20-Sn1-S2	83.72	C26-Sn1-S2	158.88
C14-Sn1-C20	115.43(11)	C14-Sn1-C26	104.96(11)
C20-Sn1-C26	103.11(11)	C1-S1-Sn1	94.00(10)
C1-S2-Sn1	80.75	S2-C1-S1	118.35(18)
S1-Sn-S2	65.70		

4.14 X-Ray Structure of $n\text{-Bu}_2\text{SnL}^d_2$ (**54**)



Crystal data and selected interatomic parameters are collected in Tables 4.27 and 4.28, respectively. An ORTEP view of the molecule including numbering scheme is shown in Fig. 4.14. The Sn atom in **54** is coordinated by two butyl groups and two 4-benzylpiperidine-1-carbodithioate ligands, with the latter adopting different asymmetric coordination modes. The first dithiocarboxylate ligand is chelating but forms asymmetric Sn-S bond distances of 2.5315(14) Å and 2.9574(15) Å, respectively while for the second ligand, Sn-S bond lengths are 2.5470(14) Å and 2.8970 (16) Å. The weaker Sn-S distances are well within the sum of the van der Waals radii for the Sn and S atoms of 4.0 Å. The overall geometry at Sn is, however, highly distorted from the *trans* octahedral: the C27-Sn-C31 angle is only 137.3(2)° which is intermediate between *cis* and *trans*, the Sn and the four S atoms of the ligands are nearly coplanar but distorted from square-planar geometry, so that the *cis* S2-Sn-S4 angle is only 83.89(4)° and the *cis* S1-Sn-S3 angle is 145.29(4)°. In both anisobidentate ligands, each shorter Sn-S bond is associated with a longer C-S bond and vice versa; this is in consonance with the bonding asymmetry of the ligands. The bond angles subtended at the Sn atom by the methylene carbons and S2 and S4 atoms range from 104.45(14)° to 107.05(18)° demonstrating that the Sn-C bonds are bent toward the longer Sn-S bonds. This obviously a consequence of repulsion between the bonding electron pairs around the central Sn atom. Electronic and steric arguments have also been invoked to account the distortion of the similar structures from the regular octahedral geometry. Thus, the coordination geometry about the Sn atom in compound **54** is best described as being distorted skew trapezoidal-bipyramidal.

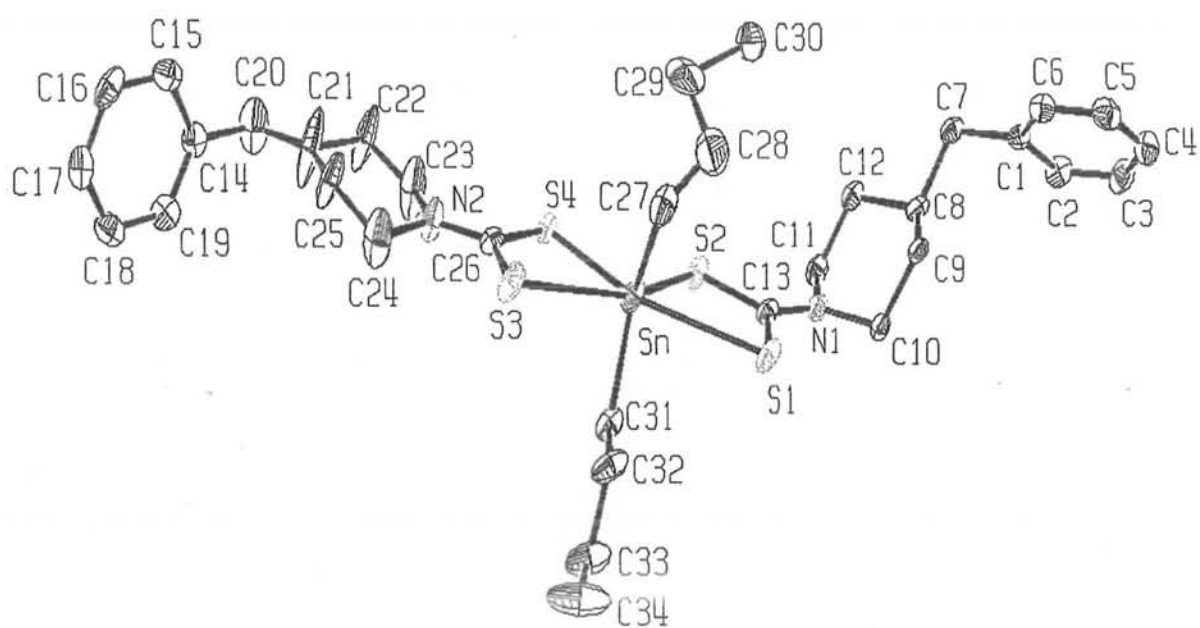


Fig 4.14: ORTEP drawing of $n\text{-Bu}_2\text{SnL}^d_2$ (54) with atomic numbering scheme

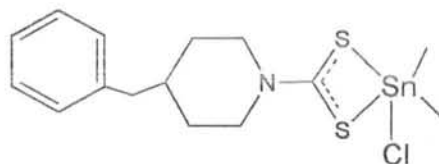
**Table 4.27: Crystal data and structure refinement parameters for n-Bu₂SnCIL₂^d
(54)**

Empirical formula	C ₃₄ H ₅₀ N ₂ S ₄ Sn
Formula mass	735.73
Crystal system	Triclinic
Space group, no.	<i>P</i> -1, 2
<i>a</i> (Å)	9.7767(13)
<i>b</i> (Å)	10.9801(15)
<i>c</i> (Å)	17.105(2)
α (°)	89.8273(19)
β (°)	79.0265(18)
γ (°)	80.4534(19)
<i>V</i> (Å ³)	1776.9(4)
<i>Z</i> (<i>Z'</i>)	2 (1)
Crystal habit/size (mm)	block/0.49 x 0.23 x 0.14
<i>T</i> (K)	100(1)
μ(Mo Kα [−]) (cm ^{−1})	11.92
Total reflections	20874
Independent reflections	10225
All	
For <i>F_o</i> ≥ 4.0 σ (<i>F_o</i>)	7585
$R(F) = \sum (F_o - F_c) / \sum F_o $	0.0528
For <i>F_o</i> > 4.0 σ (<i>F_o</i>)	
$wR(F^2) = [\sum [w(F_o^2 - F_c^2)^2] / \sum [w(F_o^2)^2]]^{1/2}$	0.1302
Goodness-of-fit	1.034
θ range for data collections (°)	2.51-25.68
Data/restraints/parameters	10225/0/581

Table 4.28: Selected bond lengths (Å) and bond angles (°) for n-Bu₂SnL^d₂ (54)

Sn-S1	2.9574(15)	Sn-S2	2.5315(14)
Sn-S3	2.8970(16)	Sn-S4	2.5470(14)
Sn-C27	2.141(7)	Sn-C31	2.135(5)
S1-C13	1.701(5)	S2-C13	1.743(5)
S3-C26	1.695(6)	S4-C26	1.731(5)
S1-Sn-S2	64.95(4)	S1-Sn-S3	145.29(4)
S1-Sn-S4	148.84(4)	S1-Sn-C27	84.57(18)
S1-Sn-C31	84.61(14)	S2-Sn-S3	149.76(5)
S2-Sn-S4	83.89(4)	S2-Sn-C27	107.05(18)
S2-Sn-C31	105.35(15)	S3-Sn-S4	65.87(4)
S3-Sn-C27	82.93(18)	S3-Sn-C31	82.95(14)
S4-Sn-C27	106.03(19)	S4-Sn-C31	104.45(14)
C27-Sn-C31	137.3(2)	Sn-S1-C13	81.33(18)
Sn-S2-C13	94.39(16)	Sn-S3-C26	81.43(18)
Sn-S4-C26	92.06(18)	S1-C13-S2	119.1(3)
S3-C26-S4	120.5(3)		

4.15 X-Ray Structure of $\text{Me}_2\text{SnClIL}^d$ (**57**)



The asymmetric unit of **57** contains two different molecules; The ORTEP diagram for one of these, molecule (1), together with an example of the atom numbering scheme used here is shown in Fig. 4.15, and crystal data and selected interatomic parameters are collected in Tables 4.29 and 4.30, respectively. The Sn atom is five-coordinated being chelated by an asymmetrically coordinating 4-benzylpiperidine-1-carbodithioate ligand, a chloride and two methyl substituents. The configuration about the tin atom is five-coordinate, with distorted trigonal-bipyramidal geometry at the central Sn atom. The sum of the equatorial angles involving the two α -carbons of the methyl groups and a S atom [S11, S22] : 358.7° , show little deviation from the ideal angle of 360° . For each molecule, the Cl atom occupies one of the apical positions of the trigonal-bipyramid with the Cl1-Sn1-S11 and Cl2-Sn2-S22 angles of $86.57(3)^\circ$ and $86.49(3)^\circ$, respectively. The quasi-axial S12 and S21 atoms cannot occupy exactly the position *trans* to Cl and Cl1-Sn1-S12 and Cl2-Sn2-S21 angles are $155.58(3)^\circ$ and $155.38(3)^\circ$. Thus, the dithiocarboxylate groups in both molecules are asymmetrically coordinated, and in each molecule Sn-S [Sn1-S12 = $2.6765(11)$ Å, Sn2-S21 = $2.6961(11)$ Å] bond distance approximately *trans* to the chloride is longer than the other Sn-S [Sn1-S11 = $2.4908(9)$ Å and Sn2-S22 = $2.4866(9)$ Å] bond distance. The S-C bond lengths [(Sx1-Cx13 = $1.745(5)$ and $1.706(3)$ Å) and (Sx2-Cx13 = $1.711(3)$ and $1.763(5)$ Å)] also illustrate the asymmetric nature of the dithiocarboxylate group in each molecule.

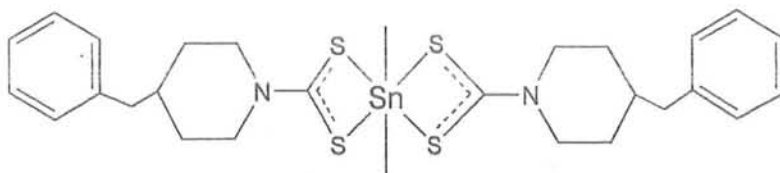
Table 4.29: Crystal data and structure refinement parameters for Me₂SnCIL^d (57)

Empirical formula	C ₁₅ H ₂₂ NS ₂ SnCl
Formula mass	435.63
Crystal system	Monoclinic
Space group, no.	<i>P</i> 2 ₁ , 4
<i>a</i> (Å)	13.2495(12)
<i>b</i> (Å)	9.7868(9)
<i>c</i> (Å)	13.6949(12)
β (°)	90.7045(11)
<i>V</i> (Å ³)	1775.7(3)
<i>Z</i> (<i>Z'</i>)	4 (2)
Crystal habit/size (mm)	Cut fragment/0.55 x 0.50 x 0.42
<i>T</i> (K)	100(1)
μ(Mo Kα [−]) (cm ^{−1})	18.17
Total reflections	14351
Independent reflections	
All	8608
For <i>F</i> _o ≥ 4.0 σ (<i>F</i> _o)	8251
$R(F) = \sum (F_o - F_c) / \sum F_o $	0.0302
For <i>F</i> _o > 4.0 σ (<i>F</i> _o)	
$wR(F^2) = [\sum [w(F_o^2 - F_c^2)^2] / \sum [w(F_o^2)^2]]^{1/2}$	0.0780
Goodness-of-fit	1.026
θ range for data collections (°)	2.56-28.28
Data/restraints/parameters	8608/0/365

Table 4.30: Selected bond lengths (Å) and bond angles (°) for Me₂SnCIL^d (57)

	x = 1	x =2		x = 1	x =2
Snx-Clx	2.5024(10)	2.4976(10)	Snx-Sx1	2.4908(9)	2.6961(11)
Snx-Sx2	2.6765(11)	2.4866(9)	Snx-Cx14	2.122(3)	2.123(3)
Snx-Cx15	2.123(4)	2.131(4)	Sx1-Cx13	1.745(5)	1.706(3)
Sx2-Cx13	1.711(3)	1.763(5)			
Clx-Snx-Sx1	86.57(3)	155.38(3)	Clx-Snx-Sx2	155.58(3)	86.49(3)
Clx-Snx-Cx14	96.86(16)	97.38(13)	Clx-Snx-Cx15	96.32(16)	96.38(13)
Sx1-Snx-Sx2	69.18(4)*	69.08(4)	Sx1-Snx-Cx14	112.38(10)	95.20(13)
Sx1-Snx-Cx15	114.86(11)	92.02(13)	Sx2-Snx-Cx14	95.12(16)	113.47(10)
Sx2-Snx-Cx15	91.51(13)	116.36(11)	Cx14-Snx-Cx15	131.48(15)	128.86(15)
Snx-Sx1-Cx13	89.76(11)	84.63(17)	Snx-Sx2-Cx13	84.50(17)	90.16(11)
Sx1-Cx13-Sx2	116.4(3)	116.1(2)			

4.16 X-Ray Structure of $\text{Me}_2\text{SnL}^{\text{d}}_2$ (**58**)



The structure of **58** is composed of a discrete monomeric molecule, in which the Sn atom exists in a skew-trapezoidal planar geometry. The equatorial plane is defined by four S atoms from two chelating dithiocarboxylate ligands. The Sn atom is 0.016(1) Å out of the least-squares plane formed by the four S atoms, and on the same side as atom C28. The two remaining octahedral sites are occupied by two methyl groups which lie over the weaker Sn-S bonds and define a C27-Sn-C28 angle of 135.64(7)°. The angle between the Sn-C27 bond and the least-squares plane is 69.92(5)°, and that between the Sn-C28 bond and the least squares plane is 65.71(5)°. The degrees of asymmetry in the modes of coordination of each dithiocarboxylate ligand, while comparable, are not equivalent. The first ligand forms Sn-S1 and Sn-S2 bond distances of 2.5190(4) Å and 2.9779(5) Å, respectively, while the other forms Sn-S3 and Sn-S4 bonds of 2.5240(4) Å and 2.9715(4) Å, respectively; the shorter bond lengths are close to the sum of the covalent radii of Sn and S and the longer distances are significantly less than the sum of their van der Waals radii (4.0 Å). The C-S bond distances [S1-C13 = 1.7548(16) Å and S3-C26 = 1.7496(16) Å] for the S atoms bound strongly to the Sn centre are longer than the C-S bonds [S2-C13 = 1.6902(16) Å and S4-C26 = 1.6990(15) Å] involving the S atoms forming the weaker bonds to the Sn atom.

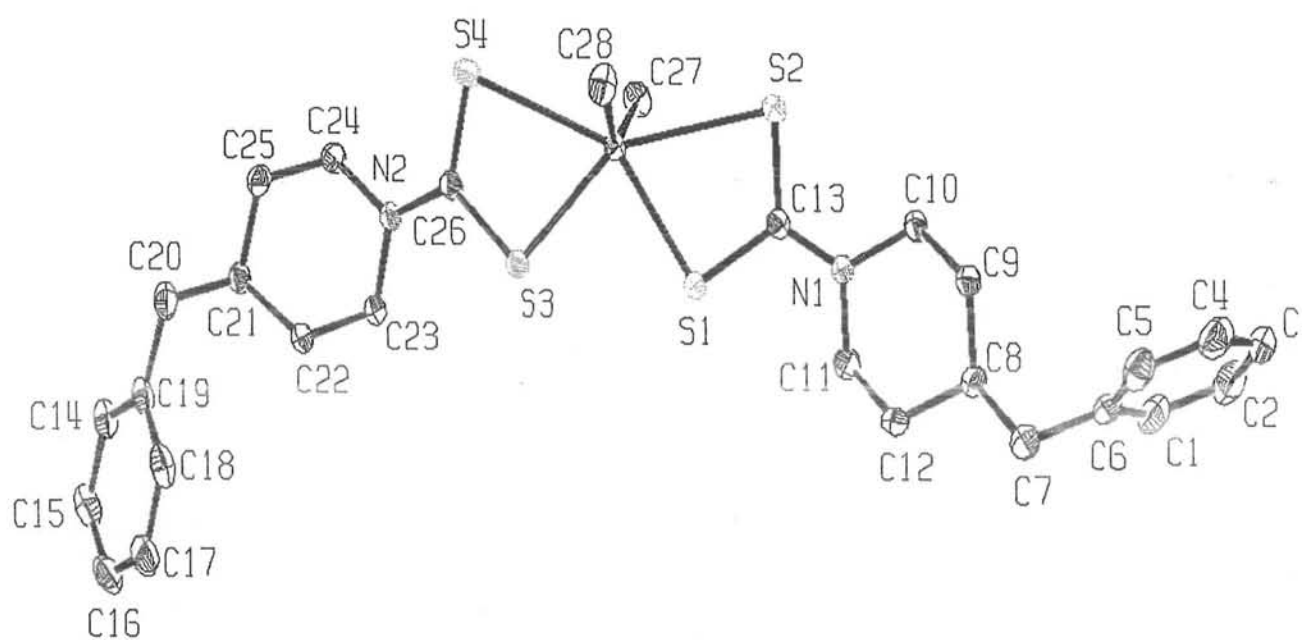


Fig 4.16: ORTEP drawing of $\text{Me}_2\text{SnL}^d_2$ (58) with atomic numbering scheme.

Table 4.31: Crystal data and structure refinement parameters for $\text{Me}_2\text{SnL}^{\text{d}}_2$ (58)

Empirical formula	$\text{C}_{28}\text{H}_{38}\text{N}_2\text{S}_4\text{Sn}$
Formula mass	649.60
Crystal system	Triclinic
Space group, no.	$P\bar{1}$, 2
a (Å)	9.8937(6)
b (Å)	11.4658(7)
c (Å)	14.2179(8)
α (°)	99.811(1)
β (°)	108.859(1)
γ (°)	96.158(1)
V (Å ³)	1480.99(15)
Z (Z')	2(1)
Crystal habit/size (mm)	Block/0.49 x 0.43 x 0.41
T (K)	100(1)
$\mu(\text{Mo K}\alpha^-)$ (cm ⁻¹)	11.64
Total reflections	11332
Independent reflections	6972
All	
For $F_o \geq 4.0 \sigma(F_o)$	6620
$R(F) = \sum (F_o - F_c) / \sum F_o $	0.0202
For $F_o > 4.0 \sigma(F_o)$	
$wR(F^2) = [\sum [w(F_o^2 - F_c^2)^2] / \sum [w(F_o^2)^2]]^{1/2}$	0.0510
Goodness-of-fit	1.042
θ range for data collections (°)	2.64-28.28
Data/restraints/parameters	6972/0/468

Table 4.32: Selected bond lengths (Å) and bond angles (°) for Me₂SnL^d₂ (58)

Sn-S1	2.5190(4)	Sn-S2	2.9779(5)
Sn-S3	2.5240(4)	Sn-S4	2.9715(5)
Sn-C27	2.1253(18)	Sn-C28	2.1103(19)
S1-C13	1.7548(16)	S2-C13	1.6902(15)
S3-C26	1.7496(16)	S4-C26	1.6990(15)
S1-Sn-S2	64.64(1)	S1-Sn-S3	82.41(1)
S1-Sn-S4	146.94	S1-Sn-C27	103.06(5)
S1-Sn-C28	108.78(5)	S2-Sn-S3	146.97(1)
S2-Sn-S4	148.33(1)	S2-Sn-C27	84.67(5)
S2-Sn-C28	82.01(6)	S3-Sn-S4	64.71(1)
S3-Sn-C27	106.16(5)	S3-Sn-C28	107.93(6)
S4-Sn-C27	83.98(6)	S4-Sn-C28	85.70(5)
C27-Sn-C28	135.64(7)	Sn-S1-C13	94.81(5)
Sn-S2-C13	81.09(6)	Sn-S3-C26	94.59(5)
Sn-S4-C26	81.01(6)	S1-C13-S2	118.74(10)
S3-C26-S4	118.58(9)		

References

- [1] A. W. Addison, T. N. Rao, J. Reedijk, J. Van Rijn, G. C. Verschoor, *J. Chem. Soc., Dalton Trans.* (1984) 1349.
- [2] M. N. Xanthopoulou, S. K. Hadjikakou, N. Hadjiliadis, M. Kubicki, S. Karkabounas, K. Charalabopoulos, N. Kourkouvelis, T. Bakas, *J. Organomet. Chem.* 691 (2006) 1780.
- [3] A. T. Kana, T. G. Hibbert, M. F. Mahon, K. C. Molloy, I. P. Parkin, L.S. Price, *Polyhedron* 20 (2001) 2989.
- [4] G. M. Sheldrick, W. S. Sheldrick, *J. Chem. Soc A* (1970) 490.
- [5] E. I. Stiefel, K. Matsumoto, *Transition Metal Sulfur Chemistry*, ASC Symposium Series, 653 (1995) 2, Washington, DC: American Chemical Society.
- [6] E. R. T Tiekink, *Main Group Met. Chem.* 15 (1992) 161.
- [7] M. I. Mohamed-Ibrahim, S. S. Chee, M. A. Buntine, M. J. Cox, R. T. Tiekink, *Organometallics* 19 (2000) 5410.
- [8] Z. Rehman, S. Ali, N. Muhammad, A. Meetsma, *Acta Cryst. E* 63 (2007) m431.
- [9] O. S. Jung, J. H. Jeong, Y. S. Sohn, *Organometallics*, 10 (1991) 2217.

CONCLUSIONS

- New tri-, chlorodi- and diorganotin(IV) dithiocarboxylates were synthesized in quantitative yields by the metathesis reaction of tri and diorganotin(IV) chlorides with aryl substituted piperazinium/piperidinium salt of the dithiocarboxylates in dry methanol.
- The appearance of new peaks for Sn-S, Sn-C and Sn-Cl (in case of chlorodiorganotin(IV) derivatives) in the Raman spectra indicated the formation of organotin(IV) dithiocarboxylates. In the IR spectra, peak pattern of C-S and C-N vibration modes put forward the bidentate nature of ligands in solid state, in most complexes.
- Multinuclear NMR (^1H , ^{13}C and ^{119}Sn) data revealed that chlorodiorganotin(IV) derivatives maintained their solid state trigonal bipyramidal geometry even in solution. The same is true for triphenyltin(IV) complexes while the coordination number of Sn changed from five to four in almost all other triorganotin(IV) derivatives and from six to five in diorganotin(IV) compounds.
- Mass spectral data are compatible with the structures confirmed by other spectroscopic techniques.
- X-ray analysis illustrated that the 1,1-dithioate moiety chelate the Sn atom in anisobidentate fashion with one short Sn-S bond and one long Sn-S bond. The bond length value for Sn-S_{short} fall in the range 2.441-2.536 Å while for Sn-S_{long} bond the range 2.676-3.179 Å was observed. The crystal structures confirmed trigonal bipyramidal geometry for tri- and chlorodiorganotin(IV) dithiocarboxylates while diorganotin(IV) derivatives demonstrate octahedral geometry in solid state. Furthermore, the asymmetric nature of the two bonded ligands, in case of diorganotin(IV) dithiocarboxylates, is either identical or dissimilar.
- The CV results revealed the following increasing order of binding strength of complex-DNA adduct: $(\text{C}_6\text{H}_{11})_3\text{SnL}$ (2.4×10^3) < $(\text{C}_6\text{H}_5)_3\text{SnL}$ (3.6×10^3) < $(n\text{-C}_4\text{H}_9)_2\text{SnCIL}$ (5.4×10^3) < $(n\text{-C}_4\text{H}_9)_3\text{SnL}$ (6.9×10^3) < $(\text{C}_6\text{H}_5)_2\text{SnL}$ (8.4×10^3) < $(\text{C}_2\text{H}_5)_2\text{SnCIL}$ (1.24×10^4) M^{-1} . The UV-Vis spectroscopic data also signify the same order of binding strength. The negative values of ΔG designate the spontaneity of complex-DNA binding.

- The positive peak potential shift in CV evidenced intercalative mode of interaction except for $(n\text{-C}_4\text{H}_9)_2\text{SnCIL}$ complex where electrostatic interaction was observed.
- The complexes screen for antibacterial activity show high activity than the corresponding ligand against different strains of bacteria. In general, the triorganotin(IV) complexes display high antibacterial action than the chlorodi- and diorganotin(IV) complexes. Most of the tested complexes show comparable activity to streptomycin. Zone of inhibition of compounds 42 and 43 is higher than that of standard drug against *Salmonella typhi*, and may be used as bactericides.
- The complexes with 4-(2-methoxyphenyl)piperazine-1-carbodithioate ligand have a good fungicidal action in comparison to the complexes of the other two ligands.

PUBLICATIONS

Years 2006, 2007

1. **Zia-ur-Rehman**, Saira Shahzadi, Saqib Ali, Guo-Xin Jin, *Tur. J. Chem.* 31 (2007) 435-442.
2. **Zia-ur-Rehman**, Niaz Muhammad, Saqib Ali, Auke Meetsma, *Act. Cryst.* E63 (2007) m-89-m90.
3. **Zia-ur-Rehman**, Niaz Muhammad, Saqib Ali, Auke Meetsma, *Act. Cryst.* E63 (2007) m431-m432.
4. **Zia-ur-Rehman**, Niaz Muhammad, Saqib Ali, Auke Meetsma, *Act. Cryst.* E63 (2007) o632-o633.
5. Niaz Muhammad, **Zia-ur-Rehman**, Saqib Ali, Auke Meetsma, *Act. Cryst.* E63 (2007) o634-o635.
6. Niaz Muhammad, **Zia-ur-Rehman**, Saqib Ali, Auke Meetsma, *Act. Cryst.* E63 (2007) o2174-o2175.
7. Niaz Muhammad, **Zia-ur-Rehman**, Saqib Ali, Auke Meetsma, *Act. Cryst.* E63 (2007) o2557-o2558.
8. **Zia-ur-Rehman**, Saira Shahzadi, Saqib Ali, Amin Badshah, Guo-Xin Jin, *J. Iran.Chem. Soc.* 3 (2006) 157-160.
9. **Zia-ur-Rehman**, Niaz Muhammad, Saqib Ali, Auke Meetsma, *Act. Cryst.* E63 (2006) m3560-m-3561.

Year 2008

10. **Zia-ur-Rehman**, Mirela Barsan, I. Wharf, Niaz Muhammad, Saqib Ali, A. Meetsma, Ian S. Butler, *Inorg. Chim. Act.* 361 (2008) 3322-3236.
11. Niaz Muhammad, Muhammad Nawaz Tahir, **Zia-ur-Rehman**, Saqib Ali and Farkhanda Shaheen, *Acta Cryst.* E64 (2008) o1542.
12. Niaz Muhammad, M. Nawaz Tahir, **Zia-ur-Rehman**, Saqib Ali, *Acta Cryst.* E64 (2008) o1458.
13. Niaz Muhammad, M. Nawaz Tahir, Saqib Ali, **Zia-ur-Rehman**, Muhammad Akram Kashmiri, *Acta Cryst.* E64 (2008) o1456.
14. Niaz Muhammad, Saqib Ali, M. Nawaz Tahir, **Zia-ur-Rehman**, *Acta Cryst.* E64 (2008) o1373.

15. Niaz Muhammad, M. Nawaz Tahir, Saqib Ali, **Zia-ur-Rehman**, *Acta. Cryst.* (2008).
16. Niaz Muhammad, M. Nawaz Tahir, Saqib Ali, **Zia-ur-Rehman**, *Acta. Cryst.* E64 (2008) m946-m947.
17. Muhammad Niaz, M. Nawaz Tahir, **Zia-ur-rehman**, Saqib Ali, Islam Ullah Khan, *Acta Cryst.* E64 (2008) o733.
18. Muhammad Niaz, M. Nawaz Tahir, **Zia-ur-rehman**, Saqib Ali, *Acta Cryst.* E64 (2008) o1717-o1718.

Year 2009

19. **Zia-ur-Rehman**, M. Nawaz Tahir, Muhammad Danish, Niaz Muhammada, Saqib Ali, *Acta Cryst.* E65 (2009) o503.
20. **Zia-ur-Rehman**, Afzal Shah, Niaz Muhammad, Saqib Ali, Rumana Qureshi, Ian Sydney Butler, *J. Organomet. Chem.* (Accepted).
21. Niaz Muhammad, **Zia-ur-Rehman**, Saqib Ali, A. Meetsma, F. Shaheen, *Inorg. Chim. Act.* (Accepted).
22. **Zia-ur-Rehman**, Afzal Shah, Niaz Muhammad, Saqib Ali, Rumana Qureshi, Ian Sydney Butler, *Europ. J. Med. Chem.* (accepted).
23. Niaz Muhammad, Afzal Shah, **Zia-ur-Rehman**, Shaukat Shuja, Saqib Ali, Rumana Qureshi, Auke Meetsma, Muhamma, Nawaz Tahir, *J. Orgmet. Chem.* (accepted).
24. **Zia-ur-Rehman**, Niaz Muhammad, Saqib Ali, Ian S. Butler, Auke Meetsma, Momin Khan, *Polyhedron* (Submitted).
25. **Zia-ur-Rehman**, Niaz Muhammad, Shaukat Shuja, Saqib Ali, Ian S. Butler, Auke Meetsma, *Spectrochim. Acta* (Submitted).
26. **Zia-ur-Rehman**, Niaz Muhammad, Saqib Ali, Ian S. Butler, Auke Meetsma, *Inorg. Chim. Acta* (Submitted).